Multi-Modelling of the Managed Aquifer Recharge Systems for Sustainable Groundwater Development in Beijing Plain, China

Liu, S.

DOI
10.4233/uuid:8a8bb162-9a18-4345-ad1e-2a9b9d8eb3e1

Publication date
2024

Document Version
Final published version

Citation (APA)
Liu, S. (2024). *Multi-Modelling of the Managed Aquifer Recharge Systems for Sustainable Groundwater Development in Beijing Plain, China*. [Dissertation (TU Delft), Delft University of Technology, IHE Delft Institute for Water Education]. IHE Delft Institute for Water Education.
https://doi.org/10.4233/uuid:8a8bb162-9a18-4345-ad1e-2a9b9d8eb3e1

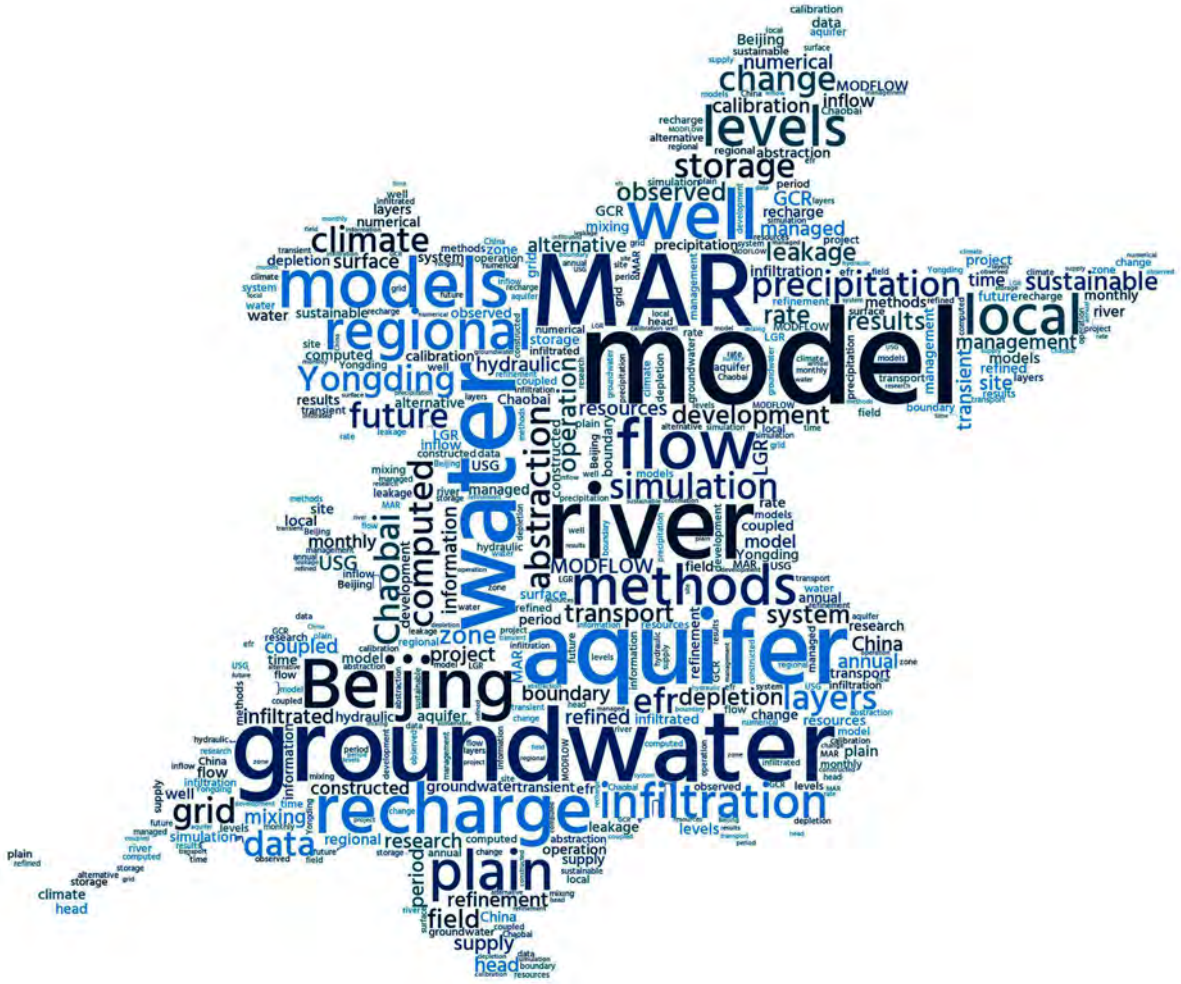

Multi-Modelling of the Managed Aquifer Recharge Systems for Sustainable Groundwater Development in Beijing Plain, China

Sida Liu

MULTI-MODELLING OF THE MANAGED AQUIFER RECHARGE SYSTEMS FOR SUSTAINABLE GROUNDWATER DEVELOPMENT IN BEIJING PLAIN, CHINA

Sida Liu

Multi-Modelling of the Managed Aquifer Recharge Systems for Sustainable Groundwater Development in Beijing Plain, China

DISSERTATION

for the purpose of obtaining the degree of doctor
at Delft University of Technology
by the authority of the Rector Magnificus Prof.dr.ir. T.H.J.J. van der Hagen,
chair of the Board for Doctorates
and
in fulfilment of the requirement of the Rector of IHE Delft
Institute for Water Education, Prof.dr. E.J. Moors,
to be defended in public on
Thursday, 25 April 2024 at 15:00 hours

by

Sida LIU
Master of Science, UNESCO-IHE Institute for Water Education
born in Beijing, China

This dissertation has been approved by the (co)promotor.

Composition of the doctoral committee:

Rector Magnificus TU Delft	chairperson
Rector IHE Delft	vice-chairperson
Prof.dr. M.E. McClain	IHE Delft / TU Delft, promotor
Dr. Y. Zhou	IHE Delft, copromotor

Independent members:

Prof.dr.ir. M. Bakker	TU Delft
Prof.dr. W. Wang	Chang'an University, China
Dr. V.F. Bense	Wageningen University & Research
Dr. G.H.P. Oude Essink	Utrecht University
Prof.dr.ir. P. van der Zaag	TU Delft / IHE Delft, reserve member

This research was conducted under the auspices of the Graduate School for Socio-Economic and Natural Sciences of the Environment (SENSE)

Published by IHE Delft Institute for Water Education
www.un-ihe.org
ISBN 978-90-73445-59-8

ACKNOWLEDGEMENTS

As I stand on the threshold of completing my PhD journey, I am filled with profound gratitude for the individuals who have been the cornerstone of my academic and personal growth.

First and foremost, I extend my heartfelt gratitude to Professor Michael McClain, my promotor. His steady encouragement and confidence in my abilities provided the foundation for my successful completion of this journey. His guidance and trust in my independent research direction were invaluable.

To my co-promotor, Dr. Yangxiao Zhou, I owe a debt of gratitude for his unwavering support both in the realm of academia and personal life. His infectious passion for research and his compassionate, patient approach to mentoring have left an indelible mark on my academic journey. During moments of self-doubt and struggle, his steadfast presence and understanding provided the strength I needed to persevere. I consider myself fortunate to have had such a mentor by my side.

To my supervisor Prof. Xusheng Wang, I also extend my heartfelt appreciation. Despite the geographical distance that separates us, Prof. Wang's dedication to my academic progress and his willingness to provide insightful scientific insights have been instrumental in shaping the quality of my research. I am truly grateful for his contributions to my academic journey, which have enriched my experience and expanded my horizons.

Gratitude extends to my esteemed colleagues - Zhi Yang, Chuan Tang, Mingzhao Xie, Feiran Wang, Weijia Luo, Yining Zang, and Fatima Eiman - whose collective efforts, insights, and collaboration fortified the bedrock upon which this dissertation stands. The exchange of ideas and the unity of purpose we shared have enriched my academic exploration beyond measure. To my friends – Tiago Huang, Ruiying Xu, Xiuhan Chen, Yifan Gou, Sien Liu, Xuan Zhu, Jingya Tian, Qiushi Zhang, He Zhu, Zengrui Chen, Xingyu Zhou, Yiran Cui, Xueyue Wang, Jingwen Cao, Chuansheng Cheng, Han Chen, Miao Wu, Jie Li, Jiaqi Liu, Alberto Casillas, Lei Zhong, Leng-Hsuan Tseng, Aftab Nazir, Jiaxin Wen, Zhechen Zhang, Qilong Li, Min Lu - your companionship has been a constant source of joy and strength. Your unwavering support and camaraderie have made this journey richer, reminding me that the connections we forge are as important as the academic milestones we achieve.

I’d also like to extend my gratitude to colleagues in Wageningen University that I’ve been working with for more than one year now. Dr. Inge de Graaf provided me this great opportunity to work on a wonderful research and meet all those wonderful and lovely people.

Finally, I reserve the most profound gratitude for my parents. Their unwavering love, support, and encouragement have been the cornerstone of my accomplishments. My mother's boundless kindness and my father's unyielding determination have profoundly shaped my character. Their unwavering faith in my choices provided me the courage to face challenges head-on. Their presence has been my guiding star, allowing me to overcome obstacles with unwavering determination.

To each individual who has played a part in this journey, whether through guidance, camaraderie, or silent encouragement, your collective impact has transformed this pursuit into an odyssey of self-discovery and growth.

SUMMARY

Groundwater depletion has become a worldwide problem, especially in heavily irrigated agricultural basins, such as High Plains Aquifer in the United States and North China Plain (NCP). Active measures have been taken to reverse the trend, namely reducing groundwater abstraction, and increasing groundwater recharge with Managed Aquifer Recharge (MAR) methods.

Groundwater depletion has become a critical issue in the Beijing Plain, located in the northwest corner of NCP, driven by the rapid socio-economic development since the 1980s. Groundwater is a vital resource, supporting life, human activities, and the ecosystem in Beijing City. However, groundwater over-exploitation has led to continuous groundwater level declines, posing severe threats to water security and other groundwater related environmental issues in the city.

To reverse the trend of groundwater level decline, restore depleted groundwater storage and achieve sustainable groundwater development, the Beijing municipality has taken several measures. Groundwater abstraction has been reduced by reducing the industrial water demand and replacing the urban water supply with the transferred surface water via the South-to-North (S2N) Water Transfer Project. In addition, the government initiated the Managed Aquifer Recharge (MAR) and Environmental Flow Release (EFR) operation at the two major rivers, Chaobai River and Yongding River, to enhance artificial groundwater recharge and recover the depleted groundwater storage.

Despite the progress in groundwater recharge projects in Beijing, there are several key scientific challenges. Quantitatively assessing the ongoing MAR operations, predicting the future impacts of various recharge scenarios in relation to sustainable groundwater development, and addressing potential long-term environmental concerns present significant challenges. This PhD research aims to develop numerical groundwater models and serve as a powerful tool to evaluate the effectiveness of the proposed measures in the Beijing Plain and their potential to ensure sustainable groundwater development in the long term. The research consists of several key components.

Firstly, various alternative groundwater conceptual models were examined to gain a comprehensive understanding of the groundwater system. These models aimed to provide insights into the complex dynamics of groundwater system. Among these alternatives, a suitable groundwater conceptual model was carefully selected, ensuring it aligns effectively with the objectives of the modelling process. The evaluation of three alternative regional groundwater flow models for the Beijing Plain revealed important insights. Among the models assessed, the AM3 model, constructed using a "true layer approach" demonstrated the highest level of hydrogeological realism. This model is capable for regional groundwater resources management and monitoring and for local

applications in delineating the capture zones of well fields and simulating MAR schemes. In contrast, the AM1 model, constructed using a “think layer approach”, with its fictitious presence of deep aquifers and improper allocation of abstractions, exhibited limitations in depicting contour maps, computing water balance, and delineating capture zones accurately. The AM2 model, with the “quasi-3D approach”, which neglected the flow process in aquitards and conceptualized the groundwater system as five continuous aquifers, showed applicability for groundwater resources assessment but fell short in particle tracking and contaminant transport simulations.

Secondly, different methods for refining the model grid were assessed. These methods included the conventional grid refinement (CGR) method, local grid refinement (LGR) method, and unstructured grid (USG) method. The primary objective of this assessment was to identify the refinement method that possesses the utmost capability to accurately simulate the MAR and EFR operations. The CGR and USG methods proved effective in constructing coupled regional and local models for flow and solute transport simulations. The LGR method has limited applications due to the absence of a corresponding transport model code. The choice of method should consider the local model requirements, hydrogeological conditions, and available user interface.

Thirdly, a monthly transient groundwater model based on the “true layer approach” was developed and calibrated to simulate the groundwater level and groundwater balance from 1995 to 2020. This model was then refined with the CGR method and used for simulating the MAR operation in the Chaobai River and the EFR operation in the Yongding River. The simulations of regional groundwater flow revealed a significant decline in groundwater levels and storage since 2000. Severe depletion was exacerbated by consecutive droughts and increased abstraction from 2000 to 2014. Since 2015 transferred water from the S2N Transfer Project substituted a large amount of groundwater abstractions and MAR and EFR operations increased groundwater recharge. In Chaobai River, the pilot MAR system has successfully enhanced groundwater recharge and recovered aquifer storage since 2015. Transport simulation of numerical tracers assigned in the MAR tracked the movement of the recharged water and determined the capture of the recharge water by the nearby wells. In the Yongding River area, it was observed that groundwater levels increased significantly near the river channel during EFR events from 2019-2020. These releases contributed to groundwater recharge and ecosystem recovery. The study also demonstrated the importance of considering operational and physical factors in controlling the river leakage rate and highlighted the potential of EFR in improving riverine ecosystems and groundwater-dependent ecosystems.

Lastly, the future perspective of groundwater resource development under climate change in Beijing Plain was evaluated with a transient prediction model. The calibrated transient flow model was extended until 2050 to simulate the long-term impacts of measures taken in Beijing Plain under climate change from 2021 to 2050. Model simulations have shown that sustainable groundwater development could be attained by controlling abstraction

and implementing large-scale MAR in the Chaobai River and continuous EFR in the Yongding River. The results emphasize the importance of groundwater abstraction reduction for reversing groundwater level decline and the effectiveness of MAR and EFR operations in restoring groundwater depletion in shallow aquifers and maintaining groundwater abstraction in these areas. Sustainable groundwater resource development in Beijing Plain is achievable with these combined measures.

The modelling approaches developed in this study provide a robust framework that can be adapted and applied to different regions. While data availability may sometimes be limited, several alternative conceptual models with different hydrogeological interpretations can be constructed to test their model accuracy and the model capabilities in steady-state simulation. This enabled the suitability of these models to be determined and the selection of the proper model conceptualization that achieved the modelling objectives for the transient numerical simulations. Once the models' ability to faithfully replicate historical fluctuations in groundwater levels was ensured, they were confidently employed to simulate the performance of MAR operations and predict the impact of different future MAR schemes on local and regional groundwater flow systems under different scenarios. This approach also allows for continuous model refinement, updating, and extension based on new data availability or the introduction of extra MAR schemes, which provides future perspective of the groundwater resources development in a regional scale.

Experiences of groundwater resource development in Beijing provide lessons for other large cities in the world. Long-lasting groundwater depletion had taken place due to the lack of proper management. The crisis of droughts had negative effects on groundwater depletion since the response to drought management was always increasing groundwater abstraction. Once the authority realises that negative environmental impacts such as land subsidence were caused by groundwater over-exploitation, control measures were implemented. Reduction of groundwater abstraction was more effective in reversing the trend of groundwater level decline and was possible when the alternative resource was in place. The increase of groundwater recharge with MAR and EFR has a rapid effect on replenishing groundwater in the shallow aquifer and sustaining important well fields. Long-term sustainable groundwater resources development can be achieved with restricted abstraction control and continuous operation of large-scale MAR and EFR systems.

SAMENVATTING

De uitputting van grondwater is een wereldwijd probleem geworden, vooral in zwaar geïrrigeerde landbouwbekkens zoals de High Plains Aquifer in de Verenigde Staten en de Noord-Chinese Laagvlakte (NCP). Er zijn actieve maatregelen genomen om de trend om te keren, zoals het verminderen van grondwateronttrekking en het extra aanvullen van het grondwater met Managed Aquifer Recharge (MAR) methoden

Grondwateruitputting is een kritiek probleem geworden in de vlakte van Peking, gelegen in de noordwesthoek van de NCP, aangedreven door de snelle sociaal-economische ontwikkeling sinds de jaren 80. Grondwater is een vitale hulpbron die het leven, menselijke activiteiten en het ecosysteem in de stad Beijing ondersteunt. Echter, overmatige exploitatie van grondwater heeft geleid tot een continue daling van het grondwaterniveau, wat ernstige bedreigingen vormt voor de waterveiligheid en andere aan grondwater gerelateerde milieuproblemen in de stad.

Om de trend van dalende grondwaterstanden te keren, de uitgeputte grondwateropslag te herstellen en duurzame ontwikkelingsstrategieën van grondwaterbronnen te promoten, heeft de gemeente Beijing verschillende maatregelen genomen. Grondwateronttrekking is verminderd door de industriële watervraag te verminderen en de stedelijke watervoorziening te vervangen met oppervlaktewater overgebracht door het Zuid-Noord-waterproject (S2N).. Daarnaast is de overheid begonnen met Managed Aquifer Recharge (MAR) en Environmental Flow Release (EFR) projecten in de twee grote rivieren, de Chaobai rivier en de Yongding rivier, Om de kunstmatige aanvulling van het grondwater te verbeteren en de uitgeputte grondwateropslag te herstellen.

Ondanks de vooruitgang in grondwateraanvulling projecten in Beijing, zijn er verschillende belangrijke wetenschappelijke uitdagingen. Het kwantitatief beoordelen van de lopende MAR-operaties, het voorspellen van de toekomstige impact op aanvulling van het grondwater in verschillende scenario’s van duurzaam grondwater gebruik. en het aanpakken van potentiële milieuproblemen op de lange termijn vormen belangrijke uitdagingen. Dit promotieonderzoek streeft ernaar numerieke grondwatermodellen te ontwikkelen en te dienen als een krachtig hulpmiddel om de effectiviteit van de voorgestelde maatregelen in de vlakte van Beijing en hun potentieel om duurzame grondwaterontwikkeling op de lange termijn te waarborgen te evalueren. Het onderzoek bestaat uit een aantal belangrijke componenten.

Ten eerste werden alternatieve conceptuele grondwatermodellen onderzocht om een uitgebreid begrip van het grondwatersysteem te verkrijgen. Deze modellen zijn bedoeld om inzichten te bieden in de complexe dynamiek van het grondwatersysteem. Onder deze alternatieven werd een geschikt conceptueel grondwatermodel geselecteerd, ervoor

zorgend dat het effectief aansluit bij de doelstellingen van het modelleringsproces. De evaluatie van drie alternatieve regionale grondwaterstromingsmodellen voor de vlakte van Beijing onthulde belangrijke inzichten. Van de beoordeelde modellen toonde het AM3-model, opgebouwd met behulp van een "echte laag benadering", het hoogste niveau van geohydrologisch realisme. Dit model is geschikt voor het beheer en de monitoring van regionale grondwatervoorraden en voor lokale toepassingen bij het afbakenen van de vangzones van putvelden en het simuleren van MAR-schema's. Daarentegen vertoonde het AM1-model, opgebouwd met behulp van een "dunne laag benadering", met zijn fictieve aanwezigheid van diepe aquifers en onjuiste toewijzing van onttrekkingen, vertoonde beperkingen in het weergeven van contourkaarten, het berekenen van de waterbalans en het nauwkeurig afbakenen van vangzones. Het AM2-model, met de "quasi-3D-benadering", die het stromingsproces in aquitards negeerde en het grondwatersysteem conceptualiseerde als vijf doorlopende aquifers, toonde toepasbaarheid voor de beoordeling van grondwaterbronnen maar schoot tekort in deeltjestracering en Simulaties van het transport van verontreinigingen.

Ten tweede werden verschillende methoden voor het verfijnen van het modelrooster beoordeeld. Deze methoden omvatten de conventionele rooster verfijning methode (CGR), lokale rooster verfijning methode (LGR), en ongestructureerde rooster methode (USG). Het primaire doel van deze beoordeling was om de verfijningsmethode te identificeren die de grootste capaciteit bezit om de MAR- en EFR-operaties nauwkeurig te simuleren. De CGR- en USG-methoden bewezen effectief te zijn in het construeren van gekoppelde regionale en lokale modellen voor simulaties van stroming en transport van opgeloste stoffen. De LGR-methode heeft beperkte toepassingen vanwege de afwezigheid van een bijbehorende transportmodelcode. De keuze van methode moet rekening houden met de lokale modelvereisten, hydrogeologische omstandigheden en beschikbare gebruikersinterface.

Ten derde werd een maandelijks tijdsafhankelijk grondwatermodel op basis van de "echte laag benadering" ontwikkeld en gekalibreerd om het grondwaterniveau en de grondwaterbalans van 1995 tot 2020 te simuleren. Dit model werd vervolgens verfijnd met de CGR-methode en gebruikt voor het simuleren van de MAR-operatie in de Chaobai-rivier en de EFR-operatie in de Yongding-rivier. Uit de simulaties van de regionale grondwaterstroming bleek dat de grondwaterniveaus en -opslag sinds 2000 aanzienlijk waren gedaald. . Ernstige uitputting werd verergerd door opeenvolgende droogtes en verhoogde onttrekking van 2000 tot 2014. Sinds 2015 heeft oppervlaktewater aangevoerd door het S2N-kanaal een groot deel van de grondwateronttrekkingen vervangen een hebben MAR- en EFR-operaties de grondwateraanvulling verhoogd. In de Chaobai rivier heeft het MAR pilotsysteem sinds 2015 met succes de aanvulling van het grondwater verbeterd en de opslag in de aquifer hersteld. Transportsimulaties van numerieke tracers die in het MAR-systeem werden gebruikt, volgden de beweging van het aangevulde water en bepaalden de opvang van het aangevulde water door de

nabijgelegen putten. In het gebied van de Yongding-rivier werd waargenomen dat de grondwaterniveaus aanzienlijk stegen in de buurt van het rivierkanaal tijdens EFR-gebeurtenissen van 2019-2020. Deze debieten droegen bij aan grondwateraanvulling en ecosysteemherstel. De studie toonde ook aan hoe belangrijk het is om operationele en fysieke factoren te overwegen om de infiltratiesnelheid van het rivierwater naar het grondwater te beheersen en benadrukte het potentieel van EFR bij het verbeteren van fluviale en grondwaterafhankelijke ecosystemen.

Tot slot werd het toekomstperspectief voor de ontwikkeling van grondwatermiddelen onder klimaatverandering in de vlakte van Beijing geëvalueerd met een tijdsafhankelijk voorspellingsmodel. Het gekalibreerde tijdsafhankelijke stroommodel werd verlengd tot 2050 om de langetermijneffecten van de maatregelen genomen in de vlakte van Beijing onder klimaatverandering van 2021 tot 2050 te simuleren. Modelsimulaties hebben aangetoond dat duurzame ontwikkeling van grondwatermiddelen bereikt kan worden door de onttrekking te beheersen en grootschalige MAR in de Chaobai-rivier en continue EFR in de Yongding-rivier uit te voeren. De resultaten benadrukken het belang van het verminderen van grondwateronttrekking, voor het omkeren van de daling van het grondwaterniveau en de effectiviteit van MAR- en EFR-operaties bij het herstellen van grondwateruitputting in ondiepe aquifers en het handhaven van grondwateronttrekking in deze gebieden. Met deze gecombineerde maatregelen is een duurzame ontwikkeling van de grondwatervoorraden in de vlakte van Peking haalbaar.

De modelleringsbenaderingen die in deze studie zijn ontwikkeld, bieden een robuust kader dat kan worden aangepast en toegepast in verschillende regio's. Hoewel de beschikbaarheid van gegevens soms beperkt kan zijn, kunnen verschillende alternatieve conceptuele modellen met verschillende geohydrologisch interpretaties worden geconstrueerd de modelnauwkeurigheid en de modelcapaciteiten in steady-state simulatie te testen Hierdoor kon de geschiktheid van deze modellen worden bepaald en kon het juiste modelconcept worden geselecteerd waarmee de modelleringsdoelen voor de tijdsafhankelijk numerieke simulaties konden worden bereikt. Zodra de modellen in staat waren om historische fluctuaties in grondwaterniveaus getrouw na te bootsen, werden ze vol vertrouwen gebruikt om de prestaties van MAR-operaties te simuleren en de impact van verschillende toekomstige MAR-schema's op lokale en regionale grondwaterstroomsystemen onder verschillende scenario's te voorspellen. Deze aanpak maakt het ook mogelijk om het model voortdurend te verfijnen, bij te werken en uit te breiden op basis van de beschikbaarheid van nieuwe gegevens of de introductie van extra MAR-systemen, wat een toekomstperspectief biedt voor de ontwikkeling van grondwaterbronnen op regionale schaal.

De ervaringen met de ontwikkeling van grondwatervoorraden in Beijing zijn leerzaam voor andere grote steden in de wereld. Langdurige uitputting van grondwater had plaatsgevonden door gebrek aan goed beheer. De droogtecrisis had negatieve gevolgen voor de uitputting van het grondwater, omdat de reactie op droogtebeheer altijd een

toename van de grondwateronttrekking was. Zodra de autoriteiten zich realiseerden dat negatieve milieueffecten zoals bodemdaling werden veroorzaakt door overexploitatie van grondwater, werden er controlemaatregelen geïmplementeerd. Vermindering van de grondwateronttrekking was effectiever in het omkeren van de trend van dalende grondwaterstanden en was mogelijk toen alternatieve waterbronnen beschikbaar waren. De toename van grondwateraanvulling met MAR en EFR heeft een snel effect op het aanvullen van grondwater in de ondiepe watervoerende laag en het in stand houden van belangrijke putvelden. Duurzame grondwatervoorraadontwikkeling op lange termijn kan worden bereikt met beperkte onttrekkingscontrole en continue werking van grootschalige MAR- en EFR-systemen.

CONTENTS

1

INTRODUCTION

1.1 BACKGROUND

1.1.1 Worldwide groundwater depletion

Groundwater, as a precious natural resource, accounts for as much as 33% of total water withdrawals worldwide. Over two billion people rely on it as their primary water source, particularly in arid and semi-arid regions, where it often serves as the dominant source of fresh water (Famiglietti 2014). However, the rapid development and increasing demands of human populations have led to the overexploitation of groundwater on a global scale (Howard and Gelo 2001). This has caused significant depletion in many aquifers, including well-known examples such as the High Plain Aquifer in the United States (Scanlon et al. 2012), the Indus Basin Aquifer in Pakistan and India (Basharat 2019), the North China Plain Aquifer (Yang and Zehnder 2001), and the Arabian Aquifer System in Saudi Arabia (Mazzoni et al. 2018). According to global modelling studies, the global groundwater storage loss from 1960 to 2010 is estimated as 7013 km^3 , with an increasing depletion rate (de Graaf et al. 2017).

Groundwater depletion leads to negative impacts on the environment, such as land subsidence, saltwater intrusion, reduced streamflow, and the degradation of groundwater-dependent ecosystems (Wada et al. 2010). It can also affect human well-being, such as food security, health, livelihoods and socio-economic development (Konikow and Kendy 2005).

Solving the groundwater depletion problem requires collaboration between policymakers and researchers. These issues have gained attention from policymakers and researchers. Investing in research and technological innovations is essential to better understand and mitigate the impacts of groundwater depletion (Jia et al. 2020). Furthermore, there is a need for improved governance and management of groundwater resources at local, national, and international levels (Megdal 2018).

1.1.2 Managed Aquifer Recharge as an effective solution for groundwater depletion

The term “Managed Aquifer Recharge” (MAR) gained widespread acceptance as an effective approach to address groundwater depletion, particularly in arid and semi-arid regions (UNESCO 2005). The definition of MAR was explained by Dillon in 2005 as the intentional banking and treatment of water in aquifers, containing a wide range of methods. Before 2005, it was also referred to as “artificial recharge”, “enhanced recharge” or “water banking”. The implementation of MAR began in western countries in the mid-20^{th} century, driven by the rapid urbanization and industrialization after World War II (Zhang et al. 2020). For instance, in the Netherlands, the large-scale MAR project, the sand dune filtration was initiated in the 1950s to address groundwater over-exploitation and seawater intrusion issues in coastal dunes (Olsthoorn and Mosch 2002). In the United

States, Aquifer Storage and Recovery (ASR) was first introduced in 1968 to prevent salinity intrusion and ensure water supply (Pyne 1995). Australia utilized infiltration basins to recharge groundwater storage in the Burdekin Delta (Charlesworth et al. 2020). However, it was in the 1990s that the global thriving of MAR began, as the water demand and the water shortage challenge intensified globally. Not only developed countries have been steadily increasing the extent and scale of their MAR operations, but developing countries like India, China and South Africa have also started planning and initiating MAR techniques.

MAR can be separated into two major categories based on the techniques employed: those focusing on infiltrating water (including spreading methods, induced bank filtration, and well recharge) and those focusing on intercepting water (including in-channel modification and runoff harvesting) (IGRAC 2007). MAR has been recognized as a solution for recovering depleted groundwater storage and combating declining groundwater levels. It replenishes depleted aquifers by intentionally recharging different water sources during the period with abundance, which can be used during dry periods. MAR also improves water quality through natural infiltration processes and benefits groundwater-dependent ecosystems. Furthermore, MAR plays a crucial role in ensuring water security by providing a reliable water supply for agricultural, industrial, and domestic use, thereby reducing the risk of water shortages, and contributing to the sustainable development of groundwater resources.

1.1.3 Numerical Modelling as a tool for assessing the effectiveness of MAR operation

Numerical modelling has emerged as a valuable tool for evaluating the effectiveness of MAR operations (Kloppmann et al. 2012; Ringleb et al. 2016). It allows researchers and practitioners to simulate and analyse complex hydrological processes and provides insights into the change of aquifer systems in response to the operation of MAR. By using numerical models, various aspects of MAR, such as recharge rates (Ganot et al. 2017; Niswonger et al. 2017), water movement (Xanke et al. 2016), recovery efficiency (Ward et al. 2009; Guo et al. 2010) and mixing process (Vandenbohede et al. 2013; Bahar et al. 2021), can be assessed in a cost-effective and time-efficient manner.

Another advantage of numerical modelling is its capability to simulate different scenarios and assess the impact of various factors on MAR operations. By adjusting input parameters such as recharge rates, aquifer properties, and pumping rates, the performance of MAR systems can be evaluated under different hydrological conditions (Karimov et al. 2015; Yaraghi et al. 2019). This information is crucial for designing and optimizing MAR projects, as it helps in identifying potential challenges and selecting the most suitable techniques for specific hydrogeological settings.

In summary, numerical modelling greatly enhances our understanding of MAR processes. By facilitating informed decision-making for sustainable groundwater management, numerical modelling contributes significantly to the successful implementation and optimization of MAR projects.

1.1.4 Towards sustainable groundwater development in Beijing Plain

Beijing Plain is one of regions facing severe groundwater depletion problem. Figure 1-1 shows the map of the Beijing Plain. The total plain area is around 6400 km^2. Before 2014, groundwater accounted for more than 60% of the water supply in Beijing City. During the 10-year consecutive drought, which started from 1999, the annual groundwater abstraction was up to 2.5 billion m^3/year. Groundwater was heavily over-exploited, which caused depletion and also led to other related environmental problems such as drying up of surface water bodies (Jiang et al. 2014), land subsidence (Zhang et al. 2014) and water quality degradation (Zhang et al. 2008).

A turning point came in 2014 when water from the South-to-North (S2N) Water Transfer Project was delivered to Beijing (Liu and Zheng 2002). Through this water transfer project, approximately 1.2 billion m^3 of water is annually conveyed to Beijing, providing an alternative water source to replace groundwater extraction for urban water supply (Gao and Yu 2018). The operation of this project has significantly alleviated pressure on groundwater resources and reduced the pressure on the aquifer system (Long et al. 2020).

The availability of additional water from the S2N Water Transfer project presents a unique opportunity to utilize it as a viable source for implementing MAR in the Beijing Plain (Zhou et al. 2021). In Chaobai River, the dry river channel offered the opportunities for infiltrating the water through the riverbed and replenishing the depleted shallow aquifers (Figure 1-1). Since 2015, a pilot MAR operation in Chaobai River has been implemented near the No.8 Well Field. And it is expected that the operation of the full-scale MAR scheme will gradually restore the groundwater depletion in the Chaobai River region.

In addition, the Yellow River water diversion project also provides extra water for an Environmental Flow Release (EFR) project in Yongding River in Beijing Plain (Figure 1-1) since 2019, which has substantially improved the riverine ecosystem and enhanced groundwater recharge in the west part of Beijing Plain (Xu et al. 2022). By releasing water into the dry river channel, each year's water release has led to a noticeable increase in the groundwater level.

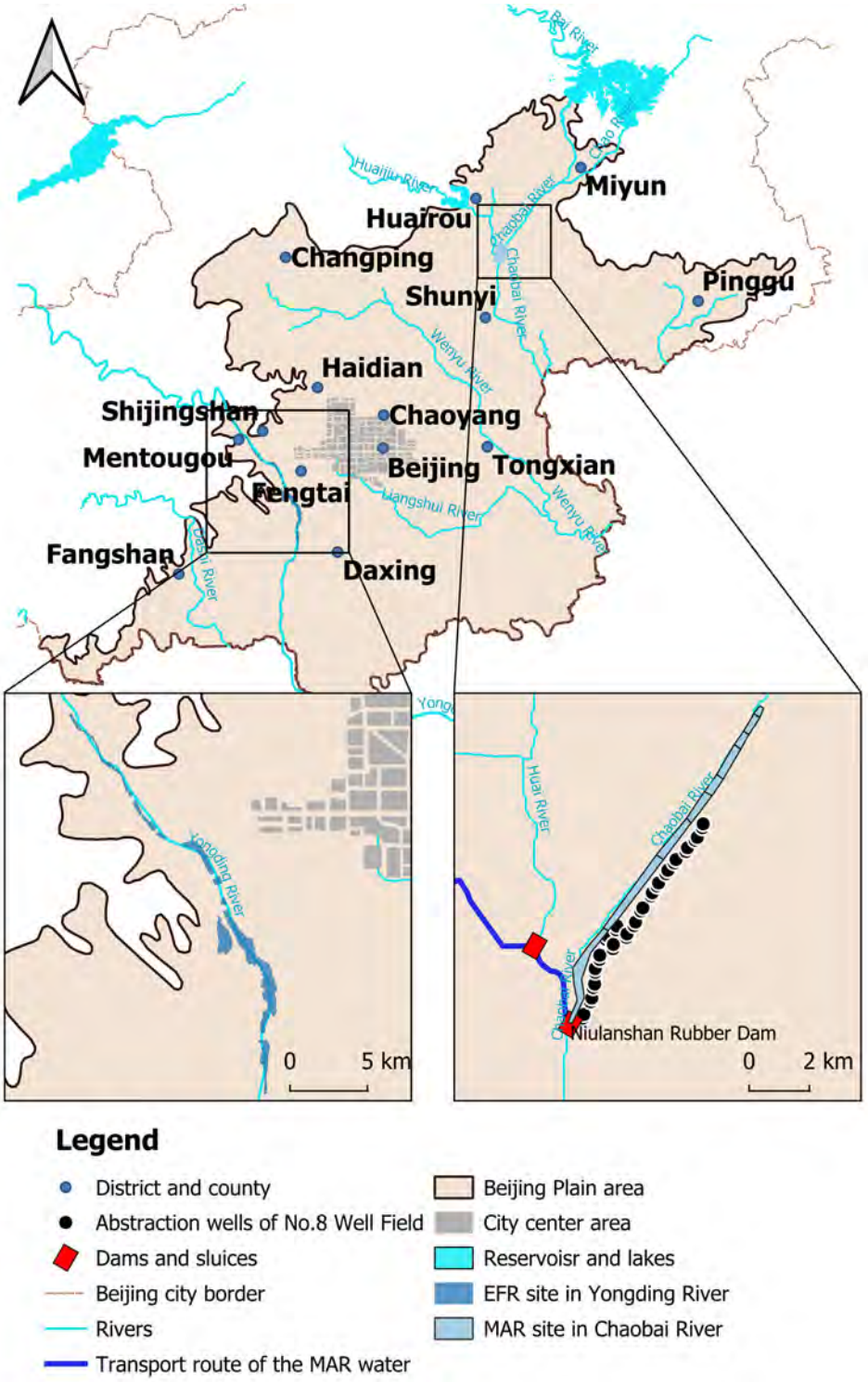

Figure 1-1 Map of the Beijing Plain and locations of the MAR and EFR projects in Chaobai and Yongding River

Details of the MAR and EFR projects are described in the following chapters. Overall, by combining the measures of reducing groundwater extraction and implementing MAR

and EFR in Beijing Plain, the city is working to achieve sustainable water development in the near future (Zhou et al. 2012).

1.2 RESEARCH QUESTIONS AND OBJECTIVES

The general objective of the research is to develop a comprehensive modelling framework of numerical groundwater models and apply the models to evaluate the effectiveness of proposed measures for achieving long-term sustainable groundwater development in the Beijing Plain. The research provides science-based recommendations for improving groundwater resource management in the Beijing City. Here follows the specific research questions and objectives.

1.2.1 Research Questions

- Which alternative conceptual and numerical groundwater models are capable of simulating regional groundwater flow and can be easily refined to assess managed aquifer recharge and river leakage at a local scale?
- What are the strengths, limitations, and applicability of three different methods for coupling regional and local groundwater flow models in the context of MAR simulations?
- How was the historical change of groundwater levels and water budget in response to human activities and climate variability (especially droughts)?
- How effective can the MAR replenish the depleted storage and sustain the well field in the Chaobai River area of Beijing Plain?
- What are the benefits of implementing EFR in Beijing's Yongding River, and what factors influence the efficiency of the groundwater recharge through EFR?
- Can sustainable groundwater development be achieved in Beijing Plain through measures including reducing groundwater abstraction and implementing MAR in major rivers under future climate change?

1.2.2 Research Objectives

- Construct and compare alternative groundwater models for the Beijing Plain to select a suitable model for designing and simulating MAR schemes and river leakages from EFR.
- Compare different methods for coupling regional and local groundwater flow models and select an efficient method for the MAR and EFR simulations.
- Construct and calibrate a long-term regional transient groundwater flow model to diagnose historical changes of groundwater levels and water budgets in response

to human activities and climate variability (specially droughts). Refine this model to simulate MAR and EFR.

- Use the refined transient groundwater flow model to simulate the recovery of groundwater levels and storage, and to predict long-term effects in sustaining the wells with the implementation of MAR schemes in the Chaobai River area.
- Use of the refined transient groundwater model to estimate enhanced groundwater recharge from river leakage and to determine the restoration of groundwater and surface water connectivity with the implementation of EFR in the Yongding River area.
- Construct a long-term transient prediction model including future climate change to assess the feasibility of sustainable groundwater development in the Beijing Plain with continuation of measures of reduced groundwater abstraction and MAR and EFR operations in major rivers.

1.3 RESEARCH METHODOLOGY

This section provides an overview of the research methodology employed in this study, and outlines the methods and main procedures used to address each research objective. In general, the research can be split into six aspects, aiming to answer the six research questions defined. Detailed methods can be found in the material and methods section of the associated chapters.

- **Constructing a suitable conceptual and numerical model for simulating the groundwater flow system and the MAR implementation in Beijing Plain**

Three alternative conceptual models (AM1, AM2, and AM3) were developed based on different hydrostratigraphic interpretations, with variations in aquifer representation and model layer discretization. Borehole data were analysed to classify Quaternary sediments into hydrogeological formations and conceptualise aquifers and aquitards. AM1 model was constructed with a “thin-layer approach” so that a thin model was extended in the areas where aquifers and aquitards were seamed out. AM2 model was constructed with a quasi-3D approach so that the subsequent aquifer and aquitard were combined into one model layer. AM3 model was constructed with a “true-layer approach” so that aquifers and aquitards were truncated with the bedrock. The steady-state groundwater flow models were constructed and calibrated for these three models. The multi-model analysis method was used to evaluate the models' performance with information criteria. The capture zone of a large well field was delineated with three alternative models as additional evaluation criterion. As a result, AM3 model was identified as most suitable model for the purpose of this study.

- **Refinement of the regional groundwater flow model in the area of interest for the detailed simulation of MAR scheme**

Three methods of model grid refinement were applied to create a local refined groundwater model for MAR simulation in conjunction with the regional flow model constructed with AM3 model. These methods include the conventional grid refinement (CGR), the local grid refinement (LGR), and the unstructured grid refinement (USG). These three methods were tested and compared for the simulation of MAR in Chaobai River and for the transport simulation of a numerical tracer to track the movement of the recharge water and mixing process at pumping wells. Although CGR was computationally less effective, it is readily run with the same computer codes of the regional model. LGR can create a child model for the local area for the flow simulation, but the corresponding particle tracking, and transport simulation still have some issues. USG is very flexible to create local model grid and has the advantage to account for complex local features, but the regional model constructed with the structured grid must be run with the new computer codes. The comparison of simulation results of MAR schemes from these three refinement methods shows that CGR is sufficient for the purpose of this research.

- **Diagnosing historical changes of groundwater levels and water budget in response to human activities and climate variability**

Continuous decline of groundwater levels was observed from groundwater level measurements in a large number of observation wells. A long-term transient regional groundwater model was constructed using AM3 model and calibrated with measurements from 1995 to 2020. The month was used as stress period so that seasonal variations of groundwater levels and budget can be simulated. The model inputs include monthly recharge from precipitation infiltration, lateral inflow from the mountainous area, river leakage, groundwater abstraction from different sectors, and evapotranspiration. The model reveals that continuous declines of groundwater levels were mainly caused by increases in groundwater abstractions. Consecutive droughts accelerated groundwater level decrease and storage depletion with double impacts of recharge reduction and installation of emergency well fields to combat droughts. The calibrated regional transient flow model served as a basic tool for the simulation of MAR and EFR.

- **Simulating the effects of the MAR scheme in Chaobai River area**

The transient regional flow model was refined with CGR method for MAR simulation in the Chaobai River area. The local model was refined with a grid of 20m cell size and re-calibrated with groundwater level measurements around MAR during a pilot MAR test from 2015 to 2018. The pilot MAR had already a positive effect on increasing groundwater levels. A large-scale MAR was designed and long-term effects on recovery of groundwater storage were predicted until 2050. Transport simulation of a numerical

tracer assigned in the MAR computed the mixing percent of MAR water at pumping wells in the nearby well field. The results indicate that with the operation of the large-scale MAR, depleted groundwater storage can be largely restored and the large well field nearby can be sustained with MAR recharge.

Simulating the effects of EFR in the Yongding River area

The transient regional flow model was refined with CGR method for EFR simulation in the Yongding River area. The local model was refined with a grid of 20m cell size and re-calibrated with groundwater level measurements around the river in 2019 and 2020. Leakage from the EFR had a positive effect on increasing groundwater levels along the river. The long-term effect of EFR was predicted until 2050. Transport simulation of a numerical tracer assigned in the river tracked the movement of leakage water in the aquifer. The results show that the continuous operation of EFR will restore the depleted groundwater storage and groundwater/surface water connectivity in the near future.

- **Assessing the feasibility of sustainable groundwater development with the continuation of the proposed measures under future climate change**

A long-term prediction model was constructed and used to assess the feasibility of sustainable groundwater development. The transient model prediction was from 2021 to 2050. The model included the groundwater abstraction rate at year 2020, large scale MAR operation in Chaobai River, and continuous EFR in Yongding River. Groundwater recharge was computed from the projected monthly rainfall from the regional climate models (RCMs).

Three prediction models were constructed to analyse the changes in groundwater levels and water budgets. The first model, Pav, used historical mean monthly rainfall. The second model, Prcp45, used projected monthly rainfall from the RCP4.5 scenario. Lastly, the third model, Prcp85, used projected monthly rainfall from the RCP8.5 scenario.

By simulating the groundwater level and budget changes using these three models, the study aimed to assess the potential of achieving groundwater sustainability in the Beijing Plain in the near future. The results of the analysis would provide valuable insights into the effectiveness of the planned MAR implementation and EFR operation, as well as the influence of future climate change on the groundwater system.

1.4 INNOVATION AND CHALLENGES

A comprehensive modelling framework was developed and applied to simulate MAR at local scale in conjunction with groundwater at regional scale in Beijing Plain. Constructing the groundwater flow model requires a clear understanding of the modelling objectives and the selection of an appropriate conceptual model that accurately represents the intricacies of the groundwater flow system. The development of the transient flow

model also requires the ability to interpolate the limited available data and information into the model inputs while ensuring model accuracy. The model also should consider both human-induced changes (including the groundwater exploitation and MAR implementation) and also the natural fluctuations (including the natural groundwater recharge variations due to the climatic change). The research innovation lies in two key aspects. Firstly, this study addresses the scientific challenge of accurately predicting and assessing the impact of MAR projects on the groundwater system by proposing an optimized modelling approach for multi-scale groundwater flow simulation. Secondly, this study presents a pioneering application of numerical simulation methods to systematically investigate the combined impacts of two MAR projects in Yongding River and Chaobai River under future regional climate scenarios in Beijing.

Furthermore, the proactive measures undertaken in Beijing have made it a leading example of rapid and successful progress towards achieving sustainable groundwater development for a mega city. This study not only generates science-based assessment for Beijing municipality but also offers a methodological framework that can be applied in other regions facing similar groundwater management issues. This research makes a valuable and significant contribution to the broader scientific and policy-making community involved in sustainable water management, offering innovative insights and practical implications for addressing groundwater challenges.

1.5 THESIS OUTLINE

This thesis consists of seven chapters.

Chapter 1 defines the context of the research.

Chapter 2 compares three alternative groundwater models for the Beijing Plain, assessing their performance and suitability for groundwater management and monitoring. It evaluates different modelling approaches' accuracy and applicability in representing the aquifer system and informing groundwater resource management decisions.

Chapter 3 focuses on comparing three methods for coupling regional and local groundwater flow models for MAR simulations. It discusses the construction, limitations, and suitability of each method (CGR, LGR, and USG) based on model complexity and available graphical user interfaces.

Chapter 4 provides a detailed analysis of MAR implementation in the Chaobai River of Beijing Plain, utilizing a numerical model. It presents findings related to groundwater level recovery, storage change, MAR operation effectiveness, the mixing of the infiltrated water with the native groundwater, and long-term impacts on the aquifer storage and water supply.

Chapter 5 evaluates the implementation of EFR in Beijing's Yongding River. It assesses observed EFR events, predicts long-term effects, and explores factors influencing groundwater recharge efficiency.

Chapter 6 assesses the potential for long-term sustainable groundwater development in the Beijing Plain. It explores the effects of measures such as reducing groundwater abstraction and implementing managed aquifer recharge in major rivers. The chapter provides a comprehensive analysis using a groundwater flow model and climate scenarios, aiming to inform groundwater management strategies for the region.

Chapter 7 summaries conclusions and indicates future research directions.

2

ASSESSMENT OF ALTERNATIVE GROUNDWATER FLOW MODELS FOR BEIJING PLAIN, CHINA

Corresponding paper: Liu, **S**., Zhou, Y., Tang, C., McClain, M., & Wang, X. S. (2021). Assessment of alternative groundwater flow models for Beijing Plain, China. Journal of Hydrology, 596, 126065.

ABSTRACT

Three alternative groundwater flow models were evaluated for Beijing Plain, China. The first model (AM1) was constructed with the "thin layer approach" in which all 9 model layers, including five aquifers separated by four aquitards, are continuously present in the same model area. The second model (AM2) was constructed with the "quasi-3D approach" in which the hydrogeological formations were classified into five aquifer units consisting of mixed permeable and semi-permeable layers at different depth ranges. The third model (AM3) was constructed with the "true layer approach" in which aquifers and aquitards were defined according to hydrostratigraphic properties, and model layers are absent in the area where corresponding hydrogeological formations intersect bedrocks. All 3 models were calibrated with the parameter optimization method under the steady state flow condition with the same hydrological stresses and observation data. All three models fit to observations well with the similar calibration criteria values. Furthermore, AIC and BIC information criteria could not distinguish three alternative models. Only KIC could identify AM3 as the best model. Major differences of the three alternative models were identified from a hydrogeological perspective. The AM1 model depicted an illusion through contour maps that groundwater was present everywhere in the deep aquifers. The model computed larger vertical leakages because more abstraction rates were assigned improperly in deep aquifers. The AM2 model was able to compute regional groundwater balances and depicted spatial groundwater level variations. However, the AM2 model computed longer groundwater travel times around the wellfield and should not be used for the delineation of the well field protection zones and contaminant transport simulation. The AM3 model could not only compute the regional groundwater balances and describe spatial groundwater distribution in deep confined aquifers, but also delineate the capture zone of the wellfield. It can therefore be used for simulating contaminant transport. Furthermore, the AM3 model is suitable to construct a coupled regional and local flow model for simulating a managed aquifer recharge scheme.

2.1 INTRODUCTION

Groundwater is the major source of the water supply in many mega-cities, especially in arid and semi-arid regions (Howard and Gelo 2001; Wheater et al. 2010; Vaux 2011). As one of the biggest cities in the world, with a population of more than 20 million, Beijing, China, has suffered from serious water shortages since the end of the last century (Wei 2005). The annual water consumption in the city is higher than 3.8 billion m^3(Yang and Zehnder 2001) , and more than 60% is supplied from groundwater exploitation (Beijing Water Authority 2019). Because of the continuous drought since 1999, emergency well fields were constructed and operated, leading to a significant increase in the groundwater pumping rate. The over-exploitation of groundwater has depleted the groundwater storage and caused a series of environmental problems: the continuous decline of groundwater

levels, drying streams and drying shallow wells (Zhou et al. 2013). Moreover, the city still suffers from water shortages and other environmental problems such as ecosystem degradation and land subsidence (Chen et al. 2011; Zhu et al. 2015). To mitigate the groundwater depletion and improve the security of the urban water supply, a Managed Aquifer Recharge (MAR) project in the northeast area of Beijing was planned. The Chaobai River channel, near the largest groundwater pumping site in Beijing, will be used to construct infiltration basins to replenish the shallow aquifer. It is necessary to construct an effective groundwater flow model with respect to the MAR site for assessing and optimizing the project. However, this is a challenge because of the complexity in hydrogeological conditions and human activities in the Beijing Plain. Furthermore, the boundaries of the local model must be linked to the regional flow conditions. A plausible solution is to construct a local groundwater model coupled with a regional model, from which the boundary conditions of the local model can be obtained. Moreover, coupling models of different spatial scales provides the two-way iterative feedback between them, which also helps to analyse the influence of water use change at local scale on the larger region.

Uncertainties of groundwater modelling come from (1) conceptual hydrogeological framework; (2) boundary conditions; (3) hydrogeological parameters; and (4) hydrological stresses. A large amount of literature deals with uncertainties originated from hydrogeological parameters (Wu and Zeng 2013). The generalized likelihood uncertainty estimation (Beven and Binley 1992) and Monte Carlo simulation (Hassan et al. 2009; Alberti et al. 2018; Moeck et al. 2020) were mostly used methods for quantifying model uncertainties from uncertain parameters. Problems in the conceptualisation of groundwater systems was recognised some time ago (Bredehoeft 2005). In recent years, development and assessment of alternative conceptual models have been received increasing attention (Enemark et al. 2019). Rojas et al. (2008) developed a method by combining generalized likelihood uncertainty estimation and Bayesian model averaging to quantify conceptual model uncertainties and illustrated this with a hypothetical case. Different classifications of the aquifer systems and boundary conditions can result in alternative conceptual models (Anderson et al. 2015; Beven 2018). It is preferred to have different ways of conceptualizing physical structures, flow processes and spatial variabilities (Neuman and Wierenga 2003; Anderson et al. 2015) to reduce the model uncertainty. The physical structures could be conceptualized in different levels of complexity and with alternative interpretations (Foglia et al. 2013; Elshall and Tsai 2014; Aphale and Tonjes 2017). Flow processes especially groundwater recharge or boundary conditions can also be determined and depicted by different approaches (Ye et al. 2010). Spatial variabilities can be conceptualized differently by considering the level of complexity (Foglia et al. 2007; Schöniger et al. 2014).

Conceptual models could be evaluated by different criteria and rank methods. The selection of models is generally guided by three principles: parsimony, maximum

likelihood and hydrologic consistency. The parsimony principle favours model simplicity whereas the maximum likelihood principle favours models having a better fit with the observations (Enemark et al. 2019). The hydrologic consistency principle is applied by researchers to evaluate the suitability of the model structures for the modelling objectives (Martinez and Gupta 2011; Shafii and Tolson 2015). The models can be ranked by different techniques. The most commonly used techniques are Information Criteria (IC) (Poeter and Hill 2007) and Generalized Likelihood Uncertain Estimation (GLUE) (Beven and Binley 1992). The IC is to assess the bias of the models to the observations and the model complexity. Akaike's Information Criterion (AIC) (Akaike 1973, 1974), corrected AIC (AICc) (Sugiura 1978), Bayesian Information Criterion (BIC) (Schwarz 1978) and Kashyap Information Criterion (KIC) (Kashyap 1982) are mostly used in the model ranking. A model with lower AIC, AICc, BIC, and KIC is preferred (Emiliano et al. 2014).

In this study, we assessed three alternative models of simulating regional groundwater flow in the Beijing Plain, China. The objectives of the study were to compare three alternative models from both the model calibration perspective and hydrogeological perspective. Although all three models were calibrated to the observed groundwater heads equally well, they differ largely in estimating vertical leakages cross the model layers, representing spatial distribution of groundwater resources, and delineating the capture zone of the wellfield. The results from this study enrich the literature on real world case studies for alternative groundwater model development and assessment. They also provide guidelines for developing a proper conceptual model for a specific groundwater resources management objective.

2.2 MATERIAL AND METHODS

2.2.1 Study area

Beijing City (39˚28′~41˚05′N, 115˚25′~117˚30′E) is located in the north-eastern part of China (Figure 2-1a), surrounded by Hebei Province and Tianjin City. The total area of Beijing is 16,800 km^2, with 62% mountainous area and 38% plain area. With the temperate monsoon climate, summer is hot and humid while winter is cold and dry. The average annual temperature is 12 °C. The average annual precipitation and open pan water evaporation are 593 mm and 1728 mm, respectively. The temporal distribution of rainfall is uneven. On average, 75% of rainfall occurs in the rainy season (from June to September). There are two main rivers in the plain, Yongding River and Chaobai River, which together count for more than 90% of the surface runoff in the area (Zhou et al. 2012).

In geology, the Beijing Plain consists of several alluvial fans and plains formed by the two main rivers and several small streams. The thickness of the Quaternary deposits varies from 30 m to more than 500 m (Zhang et al. 2008). The plain is surrounded by

mountains on the west and north and has the characteristic of a piedmont plain. As shown in Figure 2-1b, in each river basin the aquifer system transits from an unconfined single layer aquifer with gravel sands near the mountain front to semi-confined multi-layer aquifers with fine sands and clays in the lowland area.

Groundwater is recharged from several sources. Precipitation infiltration into the top aquifer accounts for more than half of the total groundwater recharge in the plain area. Other sources include surface water leakage, lateral flow from the mountain area, irrigation return flow in the suburb area and pipe leakage in the urban area. There are also several ways of groundwater discharge, including evapotranspiration, drainage along lower streams and abstraction for domestic, agricultural and industrial purposes.

2.2.2 Three alternative models

Alternative models can be formed either by different hydrostratigraphic interpretations of geological formations (Enemark et al. 2019) or by different discretisation of numerical model layers (Rojas et al. 2008; Zhou and Herath 2017). Hydrostratigraphic classifications of borehole logs are the basis for developing alternative models.

A regional groundwater flow model of the Beijing plain was developed and used for scenario analysis of sustainable groundwater resources development (Zhou et al. 2012). The alluvial aquifer system was classified into 5 aquifers separated by 4 aquitards based on limited borehole logs from about 500 boreholes. Nine model layers were used to represent every aquifer and aquitard. In the areas where some aquifer or aquitard is absent, a thin model layer extends. This approach is termed as the “thin layer approach” and the resulting numerical model is named the first alternative model (AM1). In the AM1 model, all model layers continuously present in the same model area.

In this study, a total of more than 1800 well-documented borehole logs were collected and analysed. Most boreholes were drilled in the last 10 years for implementing a national groundwater monitoring programme. Figure 2-2a shows the spatial distribution of geological boreholes in the Beijing Plain. Boreholes that penetrate the bedrocks were used to determine the basement elevation of the aquifer system. Deep boreholes with a depth of more than 200 meters were used as primary boreholes for hydrostratigraphic classifications. The Quaternary sediments were classified into 33 soil types with different properties in the grain size, roundness, and sorting. These 33 soil types were further categorized into eight hydrogeological formations by merging the soil types with similar permeability. For each borehole log, adjacent sandy formations with high permeability were grouped as aquifers; and those clayey sediments including discontinuous find sands with lower permeability were grouped as aquitards. For the deepest borehole logs, five aquifers alternating with four aquitards were identified. Two typical primary borehole profiles are displayed in Figure 2-2b.

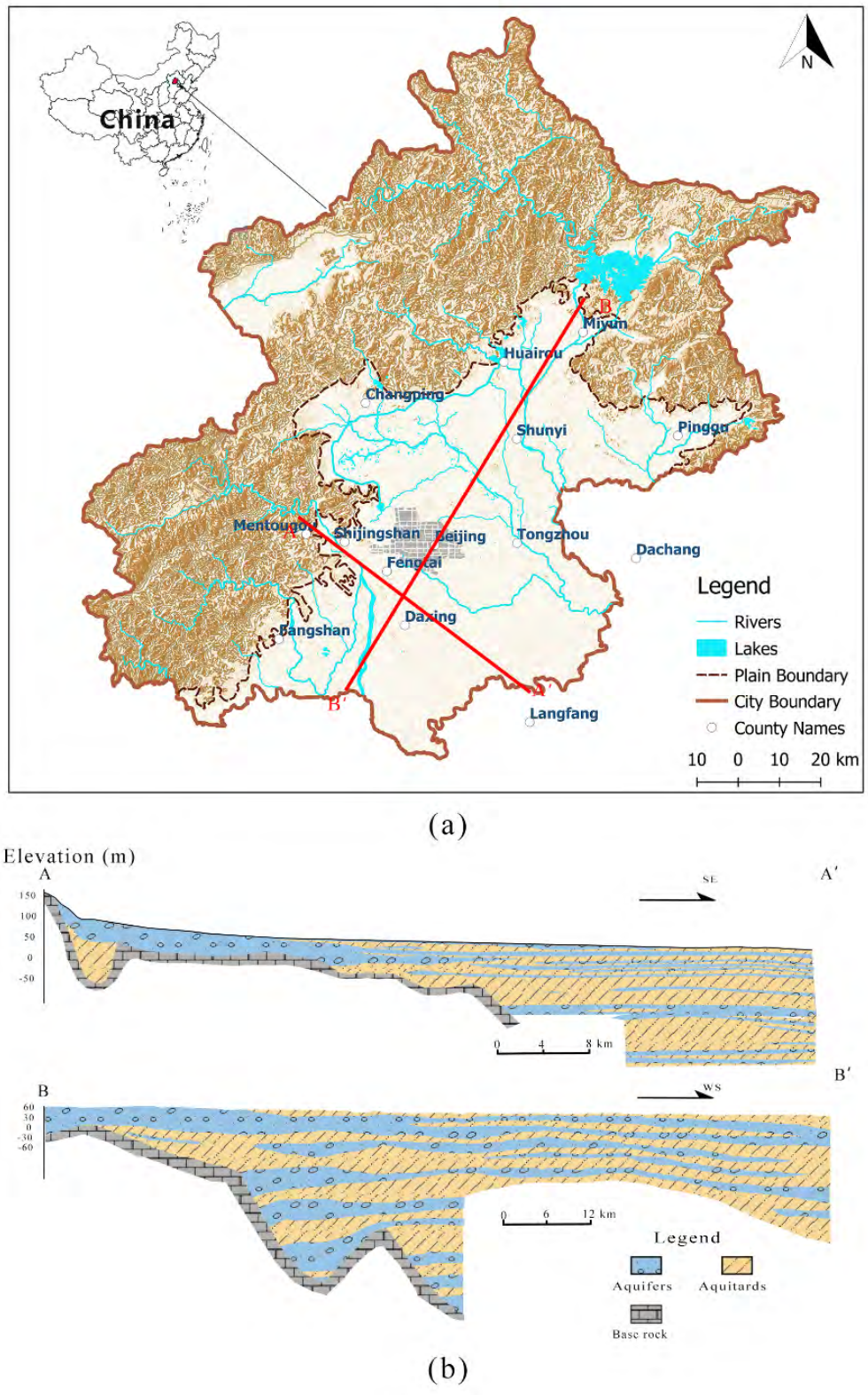

Figure 2-1(a) Study area. The solid brown borderline is the administrative border of Beijing City including both mountain and plain areas. The dashed brown borderline is the modelling area of the Beijing Plain. (b) Two typical cross-sections of the plain area.

By projecting the hydrostratigraphic classifications of the borehole data in the plain, three hydrogeological zones can be distinguished: the single-layer zone, the transition zone, and the multi-layered zone. As is shown in Figure 2-2a, the single-layer zone exists at the edge of the west and north plain. The aquifer in this zone exists in the entire plain and consists of mainly poorly sorted cobbles and gravels with very high permeability. The horizontal hydraulic conductivities of this aquifer can be up to 200 m/d. The multi-layered zone covers a large part of plain area. Alternating permeable and semi-permeable formations were grouped into five aquifers and separated by four aquitards. The aquifers consist of multiple medium to coarse sand layers and the aquitards consist of multiple silt and clayey sand layers. A narrow belt of the transition zone exists between the single-layer and multi-layered zones. The transition zone contains 2-3 aquifers varying spatially. Deposits gradually change from gravels to a mixture of sands and gravels. Clayey sand and silt layers also exist, forming several continuous aquifers and aquitards.

Conventionally, the aquifer systems were distinguished into four aquifer groups according to their depths for groundwater resources development, monitoring, and management in the Beijing plain. In general, the first aquifer group is the phreatic aquifer in the single-layer zone and the semi-confined aquifers less than 50 meters below the surface in other zones. The second, third and fourth aquifer groups are the semi-confined aquifers in the depth of 50-100 m, 100- 180 m, 180-300 m and deeper than 300 m below the ground surface. In this study, a fifth aquifer group was defined below the depth of 400 m in agreement with the hydrostratigraphic classifications (Figure 2-3a). Groundwater abstractions are mainly for agricultural use in the first aquifer group, for domestic water supply in the second and third aquifer groups, and for industrial water supply in the fourth and fifth aquifer groups. A groundwater model consisting of five model layers corresponding to these five aquifer groups was developed as the second alternative model (named as AM2). The objective of the AM2 model is to test whether the conventional conceptualisation of the aquifer systems is sufficient for the purposes of groundwater resources management and monitoring. The physical structure of the AM2 model is shown in Figure 2-3b. The computational cost of AM2 is the lowest, because the numbers of model layers and active cells are the smallest among the three models.

A third alternative conceptualisation of the hydrostratigraphic classifications is shown in Figure 2-3c. In the deepest plain area, the aquifer systems consist of five aquifers separated by four aquitards. The deeper aquifers and aquitards are truncated with the bedrock towards the mountains. In the numerical model discretisation, a model layer terminates in the area where the representing aquifer or aquitard intersects with bedrock. This approach is termed as the “true layer approach” and the resulting numerical model is the third alternative model (AM3). In the AM3 model, model layers are absent in the area where the corresponding aquifer and/or aquitards are absent. Therefore, the model areas differ in different model layers.

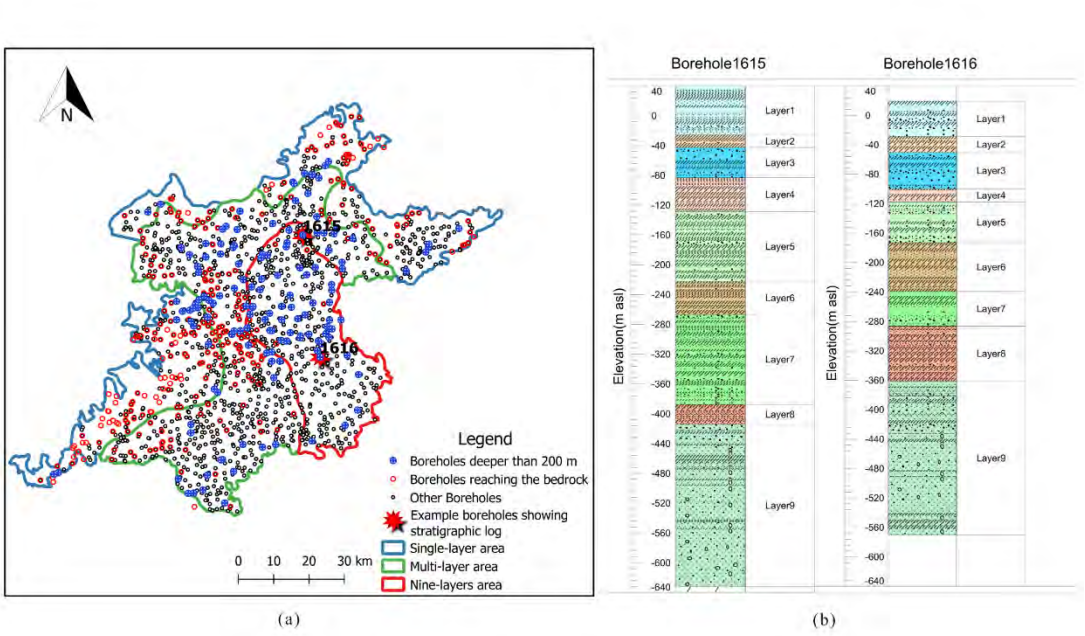

Figure 2-2 Geological data source in the Beijing Plain: (a) Borehole locations; (b) Typical borehole profiles with sediments grouped into aquifer-aquitard layers.

The top and bottom elevations of the model are the same for three alternative models. The top elevation was taken from the Digital Elevation Model (DEM) of 90 m resolution. The bottom elevation was the basement of the bedrock and which was treated as a no-flow boundary for all models. The top and bottom elevations of other model layers were interpolated from borehole log classifications.

There are two different types of lateral boundary conditions for models. The plain is receiving lateral inflow from the mountain area in the west and north, which was estimated from previous hydrogeological surveys and was treated as a specified flow boundary in this study. The other side is the administrative boundary of Beijing and simulated as head dependent flow boundaries.

All models consist of similar parameter zones. However, the parameterization of AM2 is different from the AM1 and AM3 models. The horizontal (K_h) and vertical (K_v) hydraulic conductivity parameter zones for AM1 and AM3 were actual values determined by the lithological types combined with structural geological maps. Initial values were obtained by the results of pumping tests and empirical values. However, model layers in the AM2 model consist of the mixed aquifer and aquitard. The vertical hydraulic conductivity values were obtained by calculating an equivalent hydraulic conductivity value as the harmonic mean of the vertical hydraulic conductive values of the aquifer and aquitard for each parameter zone.

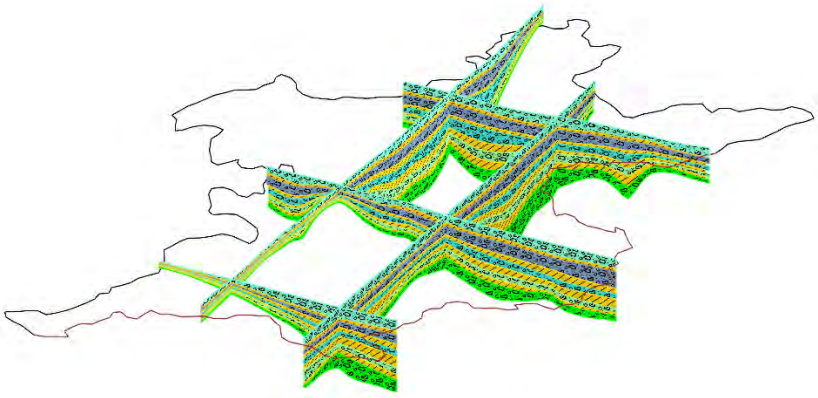

(a) AM1

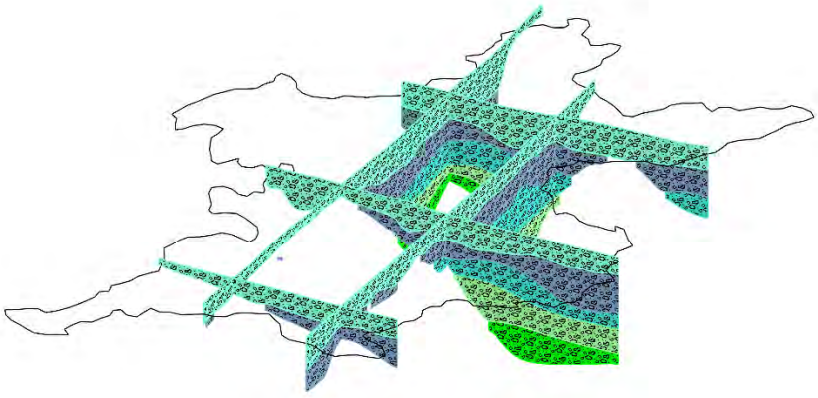

(b) AM2

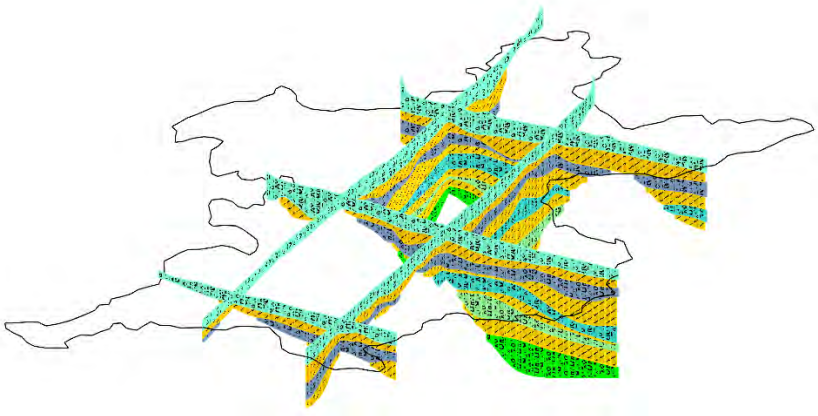

(c) AM3

Figure 2-3 Conceptualization of the aquifer systems: (a) the conceptualisation of the five aquifers separated with four aquitards with the thin layer approach in AM1; (b) the conventional conceptualisation of five aquifer groups for AM2; and (c) the conceptualisation of the five aquifers separated with four aquitards with the true layer approach for AM3

Beijing plain went through a long-term relatively wet period from 1985 to 1998 (14 years) and observed monthly groundwater levels varied in stationary state. Groundwater flow can be considered to be in a steady state condition in this period. In the year of 1995, a groundwater resources assessment project was carried out in the Beijing plain. Groundwater recharges and discharges were estimated and were made available for the construction of the steady state groundwater flow models. Hydrological stresses and their simulations were kept the same for all three models (Table 2-1). The Groundwater Modelling System (GMS10.4, Aquaveo, 2017) was used to create the conceptual model of inflow and outflow components and then converted to MODFLOW packages (MODFLOW-2005, Harbaugh, 2005) for flow simulation. Recharge from precipitation infiltration was estimated for different zones based on spatial distribution of precipitations and infiltration coefficients. Irrigation return flow and pipe leakage were specified for different districts as areal recharge. All areal recharges were converted to MODFLOW Recharge package. Lateral inflow coming from the mountain area was defined as specified flow boundary and was simulated with MODFLOW Well package (injection rates). Rivers and canals were delineated and conceptualized as a specified inflow source and were also simulated with MODFLOW Well package (injection rates). Evapotranspiration in the shallow groundwater areas was simulated with MODFLOW EVT package. Groundwater abstractions were categorised as domestic water supply wells, agricultural wells and industrial wells. Agricultural wells were pumping groundwater in the shallow aquifer (located in the top modelling layer). Industrial wells were pumping groundwater in deeper aquifers. There are two different types of domestic water supply wells, distributed wells operated in small towns and centralized wells operated by drinking water supply companies. All groundwater abstractions were merged in MODFLOW Well package for the simulation. Lateral flow from the administrative boundary was defined as head-dependant flow boundary and simulated with MODFLOW General Head Boundary package.

In total there are 202 observation wells in the plain with different depths. Most of the observation wells penetrate the shallow aquifers. All the observation wells were assigned to the corresponding model layers according to their depths.

Table 2-1 Summary of sources and sinks in the conceptual model.

	Stresses	GMS coverage	MODFLOW packages
Inflow	Recharge from rainfall	Areal recharge	Recharge (RCH)
	Pipe leakage	Areal recharge	Recharge (RCH)
	Irrigation return flow	Areal recharge	Recharge (RCH)
	Lateral flow from the mountain	Specified flow	Well (WEL)
	Rivers and canals	Specified flow	Well (WEL)
Outflow	Evapotranspiration	Evaporation	Evapotranspiration (EVT)
	Domestic water supply wells	Wells	Well (WEL)
	Agricultural wells	Wells	Well (WEL)
	Industrial wells	Wells	Well (WEL)
	Lateral flow from the administrative boundary	Head dependent flow	General Head Boundary (GHB)

2.2.3 Set-up of the numerical models

The first model layer covers the same model area for all three models. The finite difference grid for MODFLOW model consists of 116 rows and 138 columns with a regular cell size of 1000m x 1000m. The AM1 model consists of 9 model layers corresponding to 5 aquifers and 4 aquitards. All 9 model layers cover the same model area since a thin model layer was extended to the same model boundary in areas where aquifer or aquitard is absent. The AM2 model consists of 5 model layers corresponding to five aquifer groups. The AM3 model consists of 9 model layers, but the model layer stops in areas where aquifer or aquitard is absent. The GMS utility of truncation was used to cut off model areas with the basement elevation. The grid cells outside the aquifer or aquitard areas were made inactive. Figure 2-4 shows the model grid in the same row for three models and their differences can be clearly seen.

The same MODFLOW packages were used for all three models (Table 2-1). The layer property package (LPF) was used to represent hydraulic properties of the aquifers and aquitards. The horizontal and vertical hydraulic conductivity values were specified for every parameter zone. Input data for MODFLOW packages were converted from GMS conceptual model coverages systematically.

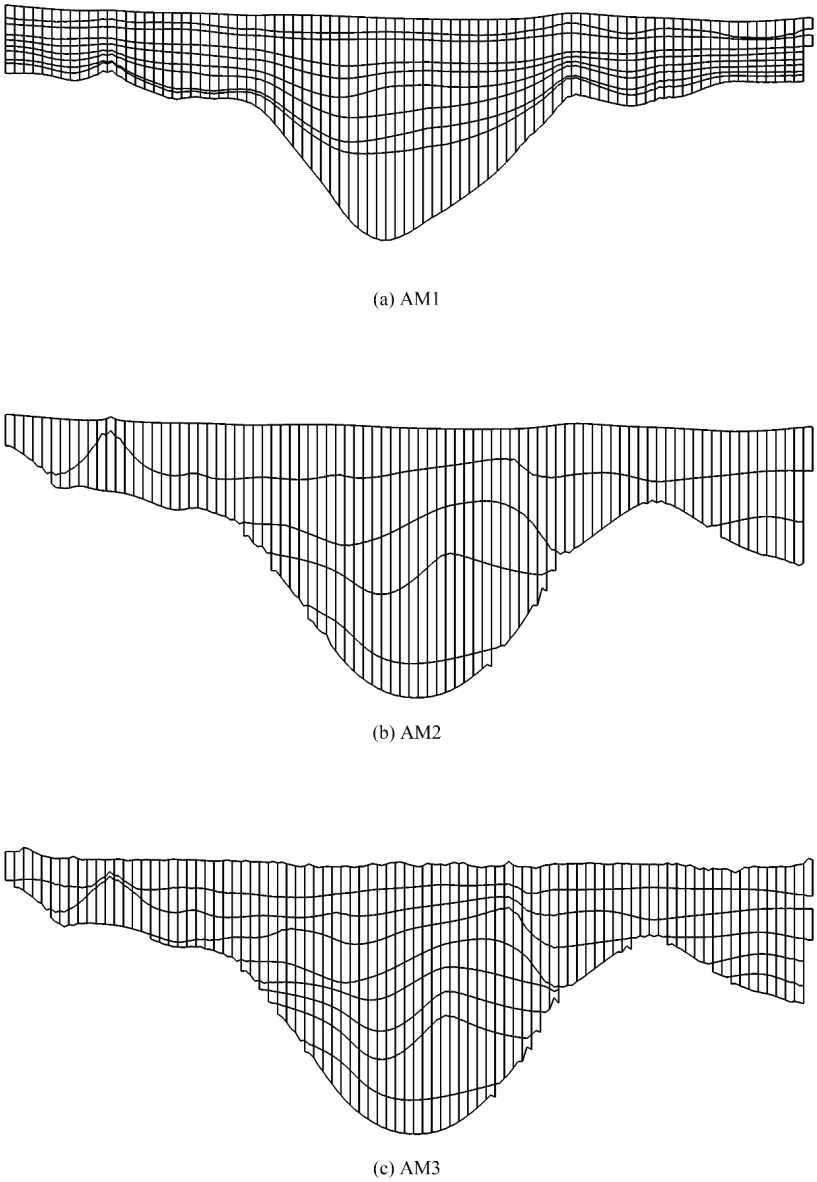

Figure 2-4 Numerical model grids in the row number 46: (a) AM1 consists of 9 model layers with the same boundary; (b) AM2 consists of 5 model layers; and (3) AM3 consists of 9 model layers with different boundary.

2.2.4 Model calibration and sensitivity analysis

All three models were calibrated to observed groundwater heads in 202 observation wells.

Firstly, manual calibration with the traditional trial and error method was applied. Hydraulic conductivities, groundwater recharge and pumping depth of the distributed

water supply wells were adjusted to get a better fit to observed groundwater heads. PEST (Doherty 2010) was then applied to optimize the horizontal and vertical hydraulic conductivities and estimate the parameter sensitivities of the three models.

Important parameters and observations can be identified by statistics such as Composite Scaled Sensitivity (CSS) and leverage. CSS is calculated as:

$$CSS_j = \sqrt{\sum_{j=1}^{n} \frac{DSS_{ij}{}^2}{n}} \qquad (2\text{-}1)$$

where j denotes the j^{th} parameter in the model. n is the total number of observations. DSS_{ij} is the dimensionless scaled sensitivity, which is calculated as:

$$DSS_{ij} = \omega_i^{\frac{1}{2}} b_j \frac{\partial y_i}{\partial b_j} \qquad (2\text{-}2)$$

where $\omega_i$is the weight for observation i. In this case, all the observations have equivalent weight as 1. b_j is the value of parameter j, $\partial y_i / b_j$ is the derivative of the simulated value of observation y_i with respect to parameter b_j. A larger absolute DSS value indicates that the parameter b_j is more sensitive to the estimation of observation y_i.

The importance of observations to parameter estimation can be evaluated with the leverage of the observations calculated as:

$$L_i = \boldsymbol{x}_i{}^T (\boldsymbol{X}^T \boldsymbol{\omega} \boldsymbol{X})^{-1} \boldsymbol{x}_i \qquad (2\text{-}3)$$

Where **X** is a sensitivity matrix with elements equal to $\partial y_i / b_j$ and $\boldsymbol{x}_i$ is the ith row of **X,** $\boldsymbol{\omega}$ is the weight matrix on observations. It reflects the correlation between the parameters and observations. The range of leverage is from 0 to 1. The closer it is to 1, the higher the observation contributes to the parameter estimation.

2.2.5 Multi-model analysis

The three alternative models were evaluated using information criteria including the AIC, AICc, BIC and KIC. Akaike information criteria (AIC and AICc) are defined as:

$$AIC = n\, ln(\sigma^2) + 2k \qquad (2\text{-}4)$$

$$AICc = n \ln\left(\sigma^2\right) + 2k + \frac{2k(k+1)}{n-k-1} \qquad (2\text{-}5)$$

$$\sigma^2 = \frac{SWSR}{n} \qquad (2\text{-}6)$$

$$SWSR = \sum_{i=1}^{n} \omega_i \left[y_i - y_i'(b) \right]^2 \quad (2\text{-}7)$$

where:

$k = NPE+1$, NPE is the number of process model parameters. σ^2 is the mean square error. $SWSR$ is the sum of weighted squared residuals. $y_i'(b)$ is model calculated groundwater heads using calibrated parameter group b.

Bayesian information criterion is defined as:

$$BIC = n\, ln(\sigma^2) + k\, ln(n) \quad (2\text{-}8)$$

Kashyap information criterion is defined as (Schenk et. al., 2018):

$$KIC = n\, ln(\sigma^2) - (k-1)\, ln(2\pi) + ln|\boldsymbol{X}^T \omega \boldsymbol{X}| \quad (2\text{-}9)$$

where $\boldsymbol{X}$ **i**s the sensitivity matrix.

The model with smaller AIC, AICc, BIC and KIC values is considered the better model. UCODE (Poeter et al. 2014) was used to compute Akaike, Bayesian, Kashyap information criteria.

2.2.6 Delineation of wellfield capture zone

One of the main objectives of applying a regional groundwater flow model is to manage and protect well fields for drinking water supply. Delineation of the capture zone of a well field is very important for the protection of potable groundwater resources. One of the largest well fields in Beijing Plain, NO. 8 well field, is located in the Chaobai River alluvial fan in the northeast model area. The well field consists of pumping wells abstracting a total of 449,530 m^3/day. According to pumping well depths, abstraction rates were assigned in the first, third and fifth model layers in the AM1 model, first and second model layers in the AM2 model, and the first and third model layers in the AM3 model. One hundred particles were placed evenly in a circle around every well block at different model layers and tracked backwards until arriving at recharge areas. The area encircled by all pathlines forms the capture area. MODPATH (Pollock 1994) was used to compute pathlines based on the computed cell-by-cell flow components from MODFLOW model. With the endpoint mode of the MODPATH simulation, water particles entering the abstraction well cells can be traced backward until the points of recharge. The capture zones of the large well field in the model domain can be defined by the final locations of these water particles. With the pathline mode of the MODPATH simulation, groundwater traveling time can be obtained for each particle and cumulative groundwater travel time of all particles can be calculated for a well field.

2.3 RESULTS

2.3.1 Results of model calibration and sensitivity analysis

Figure 2-5 compares the model calibration of the three alternative models. In general, the performance of the three models is equally good. The mean differences between the simulated and observed groundwater levels for AM1, AM2 and AM3 are -0.80, -1.82 m and -2.22 m, respectively. AM2 and AM3 slightly underestimated groundwater levels on average, which can be seen from the greater number of points below the diagonal line in the scatter plots. The root means square errors are 7.02, 6.43, and 6.37, respectively, for three models. The coefficients of determination for the three models are 0.790, 0.832, and 0.838, respectively.

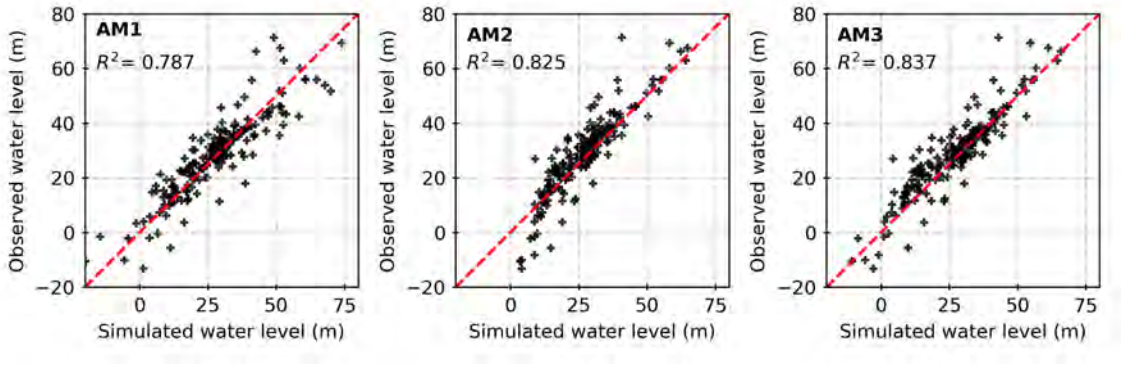

Figure 2-5 Scatter plots of the simulated and observed groundwater heads for AM1, AM2 and AM3 models.

The contour maps of groundwater levels in five aquifers from the three models are presented in Figure 2-6. There are distinct differences between contour maps. Firstly, only the extent of the first aquifer is the same for all the models. However, many dry model cells occur in AM1, because AM1 assumed a small thickness of the first aquifer so that the computed groundwater levels were below the bottom of the aquifer in the Yongding River alluvial fan. Secondly, the aquifer area becomes smaller with the increase of depth in the AM2 and AM3 models while the aquifer area remains the same in the AM1 model. Both AM2 and AM3 follow the actual extent of the aquifers so that the aquifer seams out towards the mountain front. However, the AM1 model used a thin layer approach so that the modelled aquifers extend to the same boundary with a very small thickness (1.0 m) in the area where the aquifers are absent. The AM1 model gives a false illusion that deep groundwater continuously presents everywhere in all aquifers.

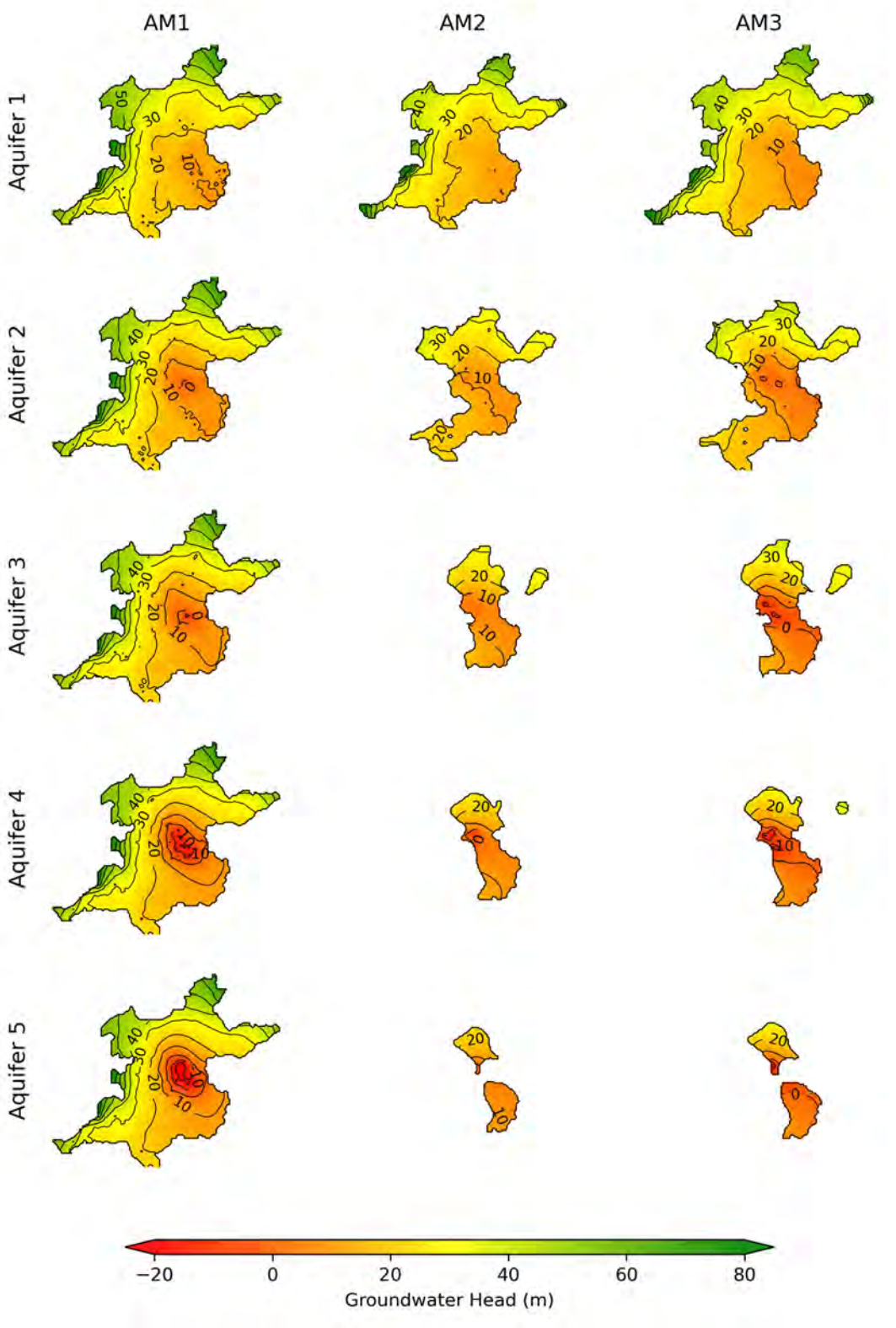

Figure 2-6 Contour maps of groundwater levels in 5 aquifers computed with three alternative models: (a) AM1, (b) AM2 and (c) AM3.

Computed groundwater balance components were checked **(**Table 2-2) and compared with the groundwater resources assessment of Beijing Plain in 1995. The total volume of the inflow and the outflow of the three alternative models are approximately the same. The areal recharge and abstraction are the same for all models. Small differences exist in the water exchange through GHB boundaries and evapotranspiration rate, which are caused by differences in computed groundwater levels from the three models. It shows that all three models can compute the same regional groundwater balance under steady-state conditions.

Figure 2-7 shows the composite scaled sensitivity (CSS) of parameter zones with the 30 most sensitive parameters. Large differences can be observed in most of the sensitive hydraulic conductivities from the three models. The most sensitive 30 parameters in the AM1 model include horizontal hydraulic conductivities in aquifer layers 3, 1, 5, 7 and 9; and several vertical hydraulic conductivities in aquitard layers 2, 6, 4 and 8. Sensitive parameters in the AM2 model consist of mostly horizontal hydraulic conductivities in aquifer layers 1 and 3; and some vertical hydraulic conductivities in aquitard layers 4 and 6. Several vertical hydraulic conductivities are also sensitive. The most sensitive hydraulic conductivities in the AM3 model consist of mostly horizontal hydraulic conductivities in aquifer layer1, a few in layer 3 plus some vertical hydraulic conductivities in aquitard layer 2. In all models, a number of vertical hydraulic conductivity parameters in the aquitards are sensitive, indicating that leakages through aquitards are important flow components for deep semi-confined aquifers.

Figure 2-8a shows 50 observations with the highest leverage (L_{ij}) values for the three models. All observations are important for the calibration of hydraulic conductivity parameter values. However, most important observations are found in the upper 3 aquifers in the AM2 and AM3 models, while observations in deep aquifers are also important for the AM1 model (Figure 2-8a). Furthermore, the observations with high leverage have different spatial distributions in the three models (Figure 2-8b). The pattern of spatial distribution and locations of aquifers of most important observations are similar in the AM2 and AM3 models. The major difference in AM1 is that the most important observations in the middle model area are located in deeper semi-confined aquifers 4 and 5 corresponding to the deepest cone of depression (Figure 2-8b).

Table 2-2 Computed groundwater balance from three alternative models.

Flow components		AM1		AM2		AM3	
		Rate (m^3/d)	Percentage	Rate (m^3/d)	Percentage	Rate (m^3/d)	Percentage
Inflow	Rivers and canals	1,437,623	19.41%	1,438,972	19.39%	1,438,992	19.43%
	Lateral inflow from mountain front	1,224,546	16.54%	1,224,546	16.50%	1,224,546	16.53%
	Inflow from GHB	96,994	1.31%	113,800	1.53%	98,110	1.32%
	Areal recharge	4,645,889	62.74%	4,644,155	62.58%	4,645,889	62.72%
Outflow	Abstraction	6,954,360	93.91%	6,954,274	93.70%	6,954,707	93.89%
	ET	199,110	2.69%	109,992	1.48%	133,735	1.81%
	Outflow from GHB	251,585	3.40%	357,208	4.81%	319,136	4.31%

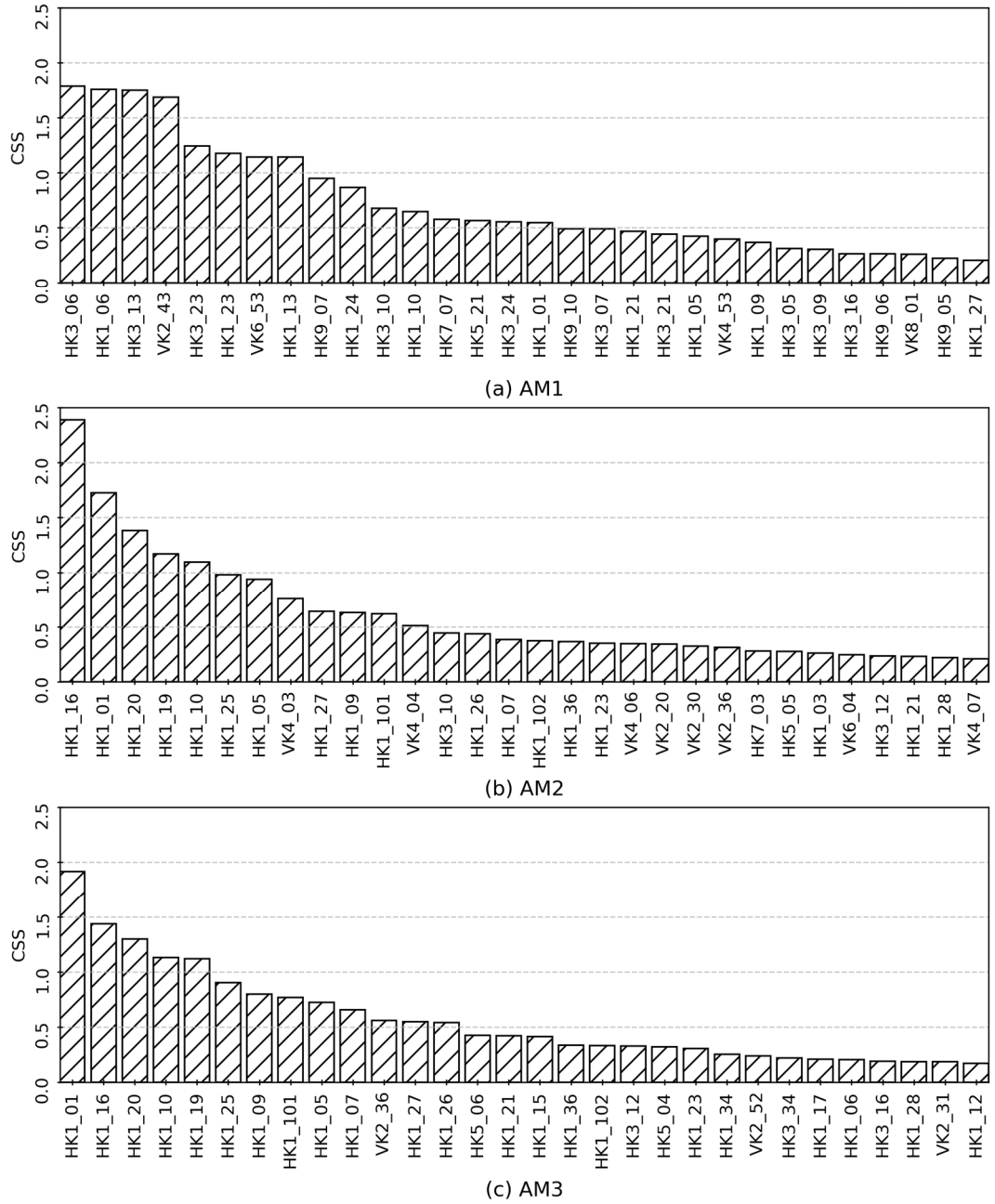

Figure 2-7 Composite scaled sensitivity (CSS) of parameters in three models: (a) AM1, (b) AM2, and (c) AM3. H refers horizontal hydraulic conductivity and V refers vertical hydraulic conductivity. The first number indicates model layers, last numbers indicate parameter zones.

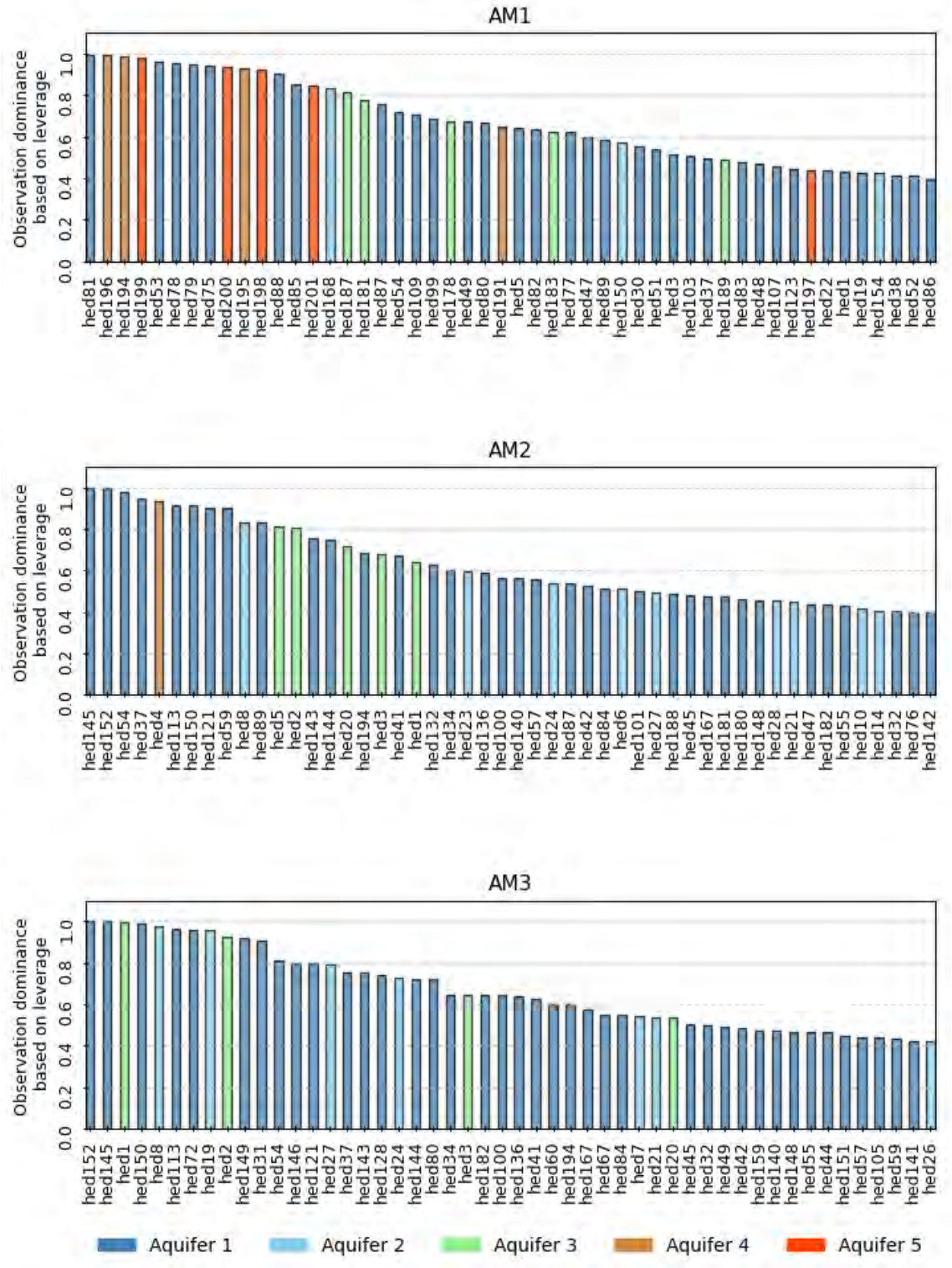

Figure 2-8(a) Computed leverage value of 50 observation wells.

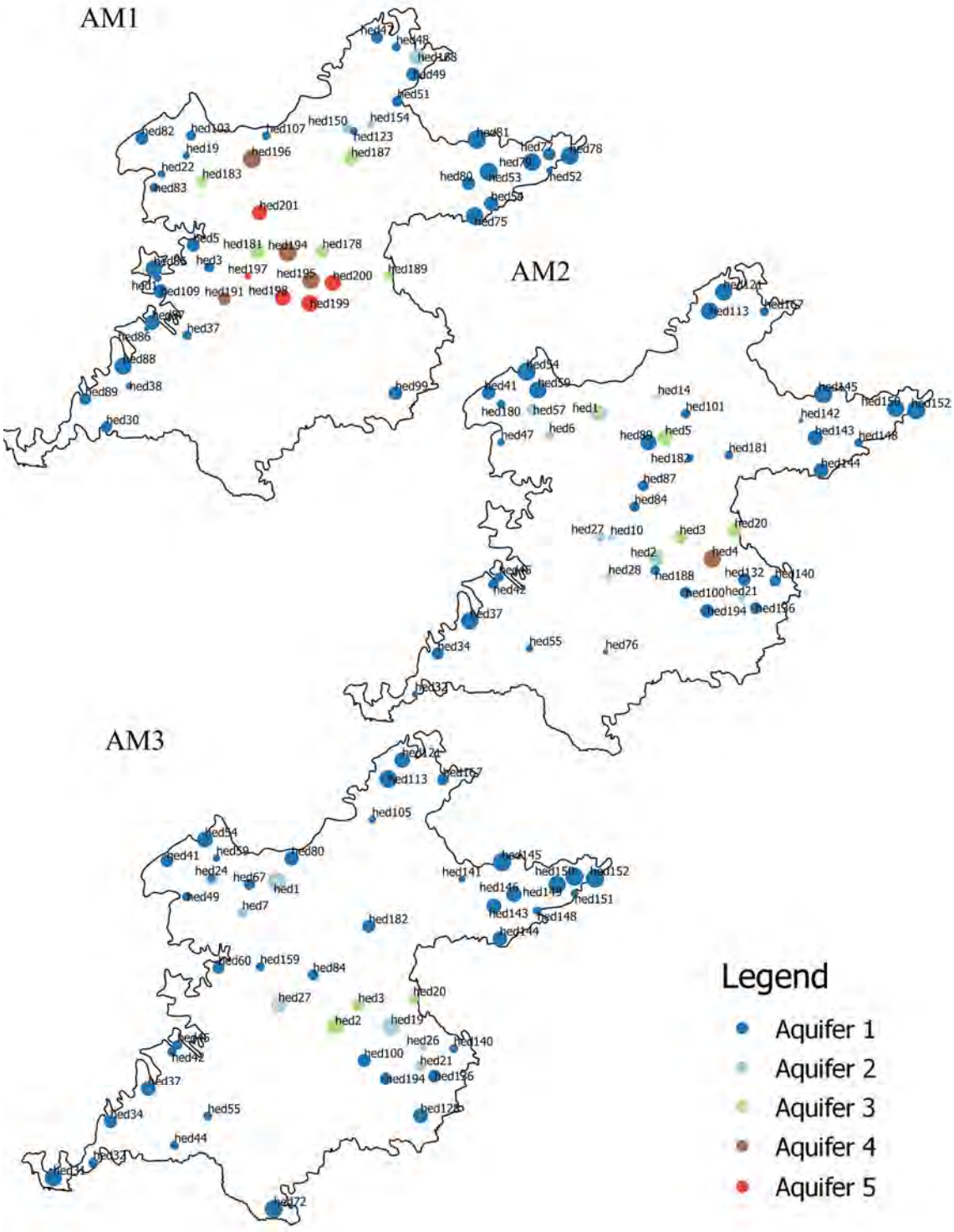

Figure 2-8 (b) The graduated size of the symbols indicates the magnitude of the leverage for each observation.

2.3.2 Results of Multi-Model Analysis

Table 2-3 presents the information criteria calculated by UCODE 2014 for the three models. In general, there is no significant difference in AIC, AICc and BIC values from the models. However, the KIC value from the AM3 model is much smaller than the AM1 and AM2 models. All models are informative for computing groundwater levels at locations of observation wells.

Table 2-3 Information Criteria values computed from UCODE 2014.

Models	Total number of parameters	Total number of observations	AIC	AIC_C	BIC	KIC
AM1	61	202	911.37	967.57	1,116.48	675.13
AM2	60	202	874.05	928.08	1,075.86	686.35
AM3	62	202	873.33	931.76	1,081.75	295.16

2.3.3 Computation of travel times and delineation of the capture zone

Figure 2-9 presents capture zones delineated by the alternative models. The shape of the capture zone indicates clearly the sources of water to the wells. Groundwater to the wells located at the top unconfined aquifer mainly comes from river leakage and areal recharge, while groundwater flowing to the wells located in the semi-confined aquifer comes from leakage and boundary inflow. Large differences can be observed from capture zones delineated by the three models. The capture areas of the wells in the first aquifer delineated by the AM1, AM2, and AM3 models are about 43.1 km^2, 51.7 km^2, and 65.1 km^2, respectively. The maximum areas of the capture zone for the well field delineated by AM1, AM2 and AM3 are about 334.7 km^2, 284.6 km^2, and 291.0 km^2, respectively. The AM1 model computed a small capture zone in the first aquifer because a small abstraction rate was assigned in this aquifer. However, the AM1 model computed the largest capture zone of the wellfield since large amount of abstractions were assigned in the deep aquifers.

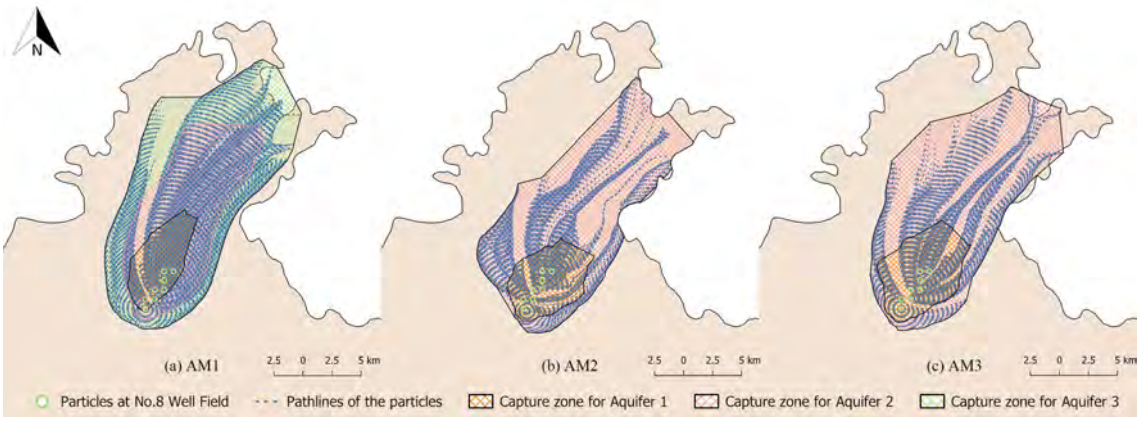

Figure 2-9 Capture zones delineated for the No.8 Well Field with 3 models: (a) AM1; (b) AM2, and (c) AM3.

The cumulative travel time distribution is usually used as an indicator for water quality of the well field (Moel et al. 2006). Particle travel times in Figure 2-9 were analysed statistically and cumulative travel time distributions were plotted in Figure 2-10. The cumulative travel time curves of the AM1 and AM3 models are similar while the curve of AM2 shows a significant delay effect. The mean travel times of all water particles from recharge areas to arrive at the well fields were about 33 years, 72 years, and 39 years, respectively, estimated from the AM1, AM2 and AM3 models. The AM2 model computed longer travel times for shorter pathlines (in aquifer 1).

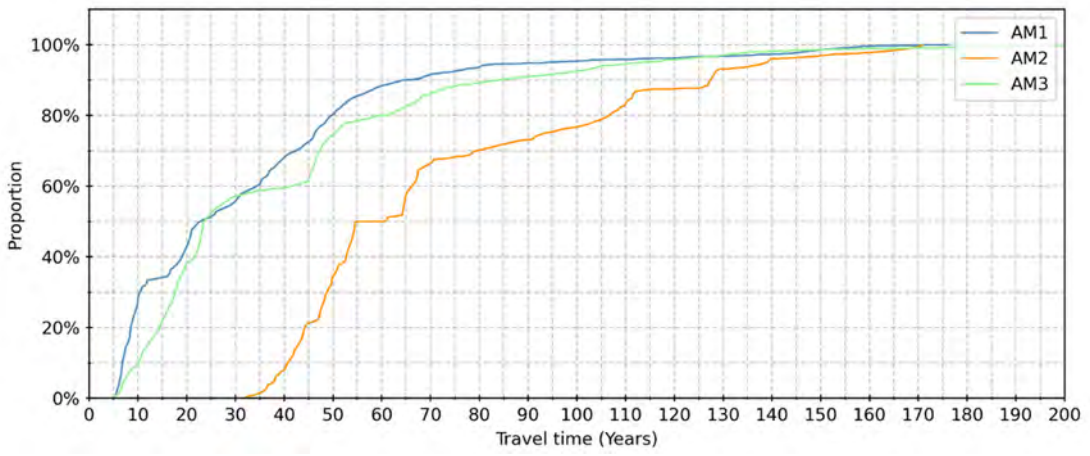

Figure 2-10 Cumulative distribution of travel times to the well field computed by three models, AM1, AM2, and AM3.

2.4 DISCUSSION

2.4.1 Statistical model comparisons

The conventional model calibration was evaluated using statistical criteria such as mean residual errors, root mean squared errors, and coefficient determination. Information criteria were introduced in recent years for multi-model comparisons. The commonly used information criteria are AIC, AICc, BIC and KIC.

From the model calibration statistics, all 3 models could fit to observed groundwater levels with very small differences. AM1 model is less biased with a small mean residual error, but slightly larger root mean squared error. AM2 and AM3 perform equally well with smaller root mean squared errors but lager mean residual errors, indicating underestimation of groundwater levels.

The information criteria not only consider the squared residual errors, but also the trade-off between the number of observed data and number of parameters estimated. The parametrisation for a proper model requires that the number of model parameters should be smaller than the number of observations (Hill and Tiedeman 2006). In all three alternative models for the Beijing plain, the number of parameters optimised by UCODE is much smaller than the number of observations. The same number of observations were used for computing information criteria with more less the same number of parameters. Therefore, larger values in AIC, AICc and BIC from AM1 model are mainly attributed to larger mean squared residual errors. There are no differences in these values between the AM2 and AM3 models since their mean squared residual errors are almost the same. A number of researchers are in favour of using KIC for multi-model comparison (Schenk et al. 2018) since KIC is the only criterion including the Fisher information term, which considers the quality of observations and parameter estimates (Ye et al. 2008). The KIC value of the AM3 model is less than half of those of the AM1 and AM2 models, which is caused by the Fisher information term. Therefore, AM3 can be considered as a relatively better model according to KIC criterion.

2.4.2 Hydrogeological interpretations

The three alternative models for the Beijing Plain differ largely on the conceptualization of aquifers and aquitards and their areal extents. Since the bedrock of the Beijing Plain undulates and uplifts towards the mountain front, the area extents of aquifers and aquitards differ. The AM1 model used the same model area for nine model layers and assumed a thin model layer extending to the whole model area when the actual aquifers and aquitards are absent. The AM2 and AM3 models used the actual extent of hydrogeological units so that the model areas are different for each model layer. Unlike the AM3 model that classifies the stratigraphic formations into five aquifers separated by 4 aquitards, the AM2 model groups the stratigraphic formations into 5 aquifer units.

Therefore, differences in vertical discretisation may result in differences in vertical leakages.

Table 2-4 presents the results of computed vertical flow from a top model layer to an adjacent lower model layer as vertical leakage. AM2 and AM3 computed similar downward leakage since they used the same hydrostratigraphic classifications. Downward leakages computed from the AM1 model are in general larger than the AM2 and AM3 models. The hydrostratigraphic classifications in the AM1 model is different from other 2 models. The AM1 model assumed a thin top unconfined aquifer (less than 50m) and more abstractions were located in aquifers 2, 3 and 4. Since groundwater in the deeper semi-confined aquifer originates only from vertical leakage from top aquifers, larger groundwater abstractions in deeper aquifers were fed by larger leakages in AM1 model.

Hydrogeologically, the AM1 model provided an illusion that deep groundwater presents everywhere in the Beijing plain and computed a large amount of vertical leakage due to inaccurate vertical classification of aquifers and aquitards based on limited borehole data. The AM2 and AM3 models improved vertical classifications of hydrostratigraphic formations with much more borehole data and placed abstraction wells in proper aquifers. These two models conceptually represent more realistically hydrogeological structures in the Beijing plain.

Table 2-4 Downward vertical leakage from model layers computed by the AM1, AM2 and AM3 models.

Model layer	AM1(m^3/d)	AM2(m^3/d)	AM3(m^3/d)
Aquifer 1	5,276,193	2,151,686	2,418,669
Aquitard 1	5,247,549		2,368,022
Aquifer 2	2,149,085	542,147	450,272
Aquitard 2	2,116,913		445,773
Aquifer 3	892,784	247,656	252,427
Aquitard 3	879,806		249,755
Aquifer 4	494,336	14,819	76,756
Aquitard 4	483,045		60,825
Aquifer 5	-	-	-

From groundwater resources management and monitoring perspectives, the AM2 model can perform equally well compared to the AM3 model since both models produced similar contour maps of groundwater levels (Figure 2-6), computed the same regional water balance (Table 2-2) and vertical leakage (Table 2-4). However, the AM2 model has a larger aquifer thickness (layer 1 and 2 combined comparing to AM3) and therefore larger transmissivity values, it computed a flatter hydraulic gradient around the wellfield compared to the AM3 model. Concerning the calculation of the groundwater travel times, particles were placed in a circle around the well at the middle of the aquifer height, travel

distances from the well location to surface recharge area are also longer. Thus, the AM2 model should not be used to compute travel time and delineate the capture zone due to the shortcomings in the conceptual model structure. However, from the principle of parsimony (Hill and Tiedeman, 2007), the AM2 model can be considered for groundwater resources management and monitoring in the Beijing plain since the model has a simpler structure. The AM3 model can adequately represent vertical flow velocities through the aquitards which are required to delineate wellfield protection areas and simulate contaminant plume movement. For these purposes, the AM3 model must be used.

2.4.3 Perspective for further applications

Another important objective of groundwater modelling in the Beijing plain is to investigate the feasibility of using managed aquifer recharge (MAR) as a management tool to sustain groundwater resources development, especially for drinking water supply. Potential sites for MAR are alluvial fans in the Yongding River and Chaobai River catchments. For this purpose, a locally refined groundwater model in which the model cell size is much smaller than the infiltration pond should be used to simulate the MAR scheme. The boundaries of the local model should be linked to the regional model so that interactions between the local and regional models are assured. The methods for coupling regional and local models are the newly developed local grid refinement (LGR) method (Mehl and Hill 2006) and the unstructured grid method (USG) method (Panday et al. 2013). MODFLOW-LGR can simulate the groundwater flow in a block-shaped high-resolution local model (a child model) coupled with the coarser regional model (a mother model). The child model and the mother model can be simultaneously run for the coupled interactions. The MODFLOW-USG is flexible to refine grids for a local area and more model layers to better represent the MAR scheme. For both methods, a functional regional model is required. The regional model AM3 constructed with “true layer approach” is suitable for simulating the MAR scheme with the coupled regional and local models. On-going research on testing MODFLOW-LGR and MODFLOW-USG for the design and simulation of the MAR scheme in the Chaobai River catchment is undertaken with the AM3 model. However, detailed hydrogeological data are necessary.

2.5 CONCLUSIONS

Three alternative regional groundwater flow models for the Beijing Plain were evaluated in this study. The first alternative model AM1 was constructed with the “thin layer approach” so that all model layers are continuously distributed in the same model area. The AM2 model was constructed by a “quasi-3D approach”, which neglected the existence of aquitards in the system and conceptualized the groundwater system as five continuous aquifers. The AM3 model was constructed with the “true layer approach” so that aquifers and aquitards are separated and model layers are absent in the area where

corresponding hydrogeological units intersect bedrock. The parameter optimization method was used to optimize hydraulic conductivity values for all models and the multi-model analysis was used to compare the relative performance of the three models. The differences in depicting contour maps, computing water balance and leakages, delineating capture zones together with travel times were analysed.

Statistically, the AM1 model can fit observations equally well and produce similar information criteria values compared to the AM2 and AM3 models. The major deficits of the AM1 model include: (a) fictitious presence of deep aquifers with thin model layers, (b) a very thin top unconfined aquifer, and (c) improper allocations of more abstractions in deeper aquifers. Due to these deficits, the AM1 model depicts false contour maps in deep aquifers, computes larger vertical leakages, and delineates a smaller capture area in the top aquifer.

The AM2 model produces satisfactory model calibration statistics and provides similar information criteria values. The AM2 model can also compute regional groundwater balances and vertical leakages. However, the AM2 model computes longer travel times around the wellfield since it assumes much thicker aquifers and neglects aquitards. Therefore, the AM2 model can be used for groundwater resources management and monitoring purposes, but is inadequate to perform particle tracking and contaminant transport simulations.

AM3 is a more realistic groundwater model for the alluvial aquifer system in Beijing plain. AM3 gives the smallest root mean squared error for the model calibration and a much smaller KIC value for information model comparison. Hydrogeologically, AM3 can fulfil all tasks of groundwater resources management, monitoring and wellfield capture zone delineation. AM3 is suitable for contaminant transport simulation and simulation of managed aquifer recharge in future studies.

In conclusion, statistical and information criteria alone might not be sufficient to identify best alternative groundwater models due to the limitation of observations. Hydrogeological interpretation is equally important for assessing multiple alternative models. A simplified quasi-3D model may be sufficient for regional groundwater resources planning and management, but a multiple aquifer-aquitard conceptual model is more accurate to perform particle tracking and contaminant transport simulations.

3

COMPARATIVE ASSESSMENT OF METHODS FOR COUPLING REGIONAL AND LOCAL GROUNDWATER FLOW MODELS

Corresponding paper: Liu, S., Zhou, Y., Xie, M., McClain, M. E., & Wang, X. S. (2021). Comparative Assessment of Methods for Coupling Regional and Local Groundwater Flow Models: A Case Study in the Beijing Plain, China. Water, 13(16), 2229.

ABSTRACT

A coupled regional and local model is required when groundwater flow and solute transport are to be simulated in local areas of interest with a finer grid while regional aquifer boundary and major stresses should be retained with a coarser grid. The coupled model should also maintain interactions between the regional and local flow systems. In the Beijing Plain (China), assessment of managed aquifer recharge (MAR), groundwater pollution caused by rivers, capture zone of well fields, and land subsidence at the cone of depression requires a coupled regional and local model. This study evaluates three methods for coupling regional and local flow models for simulating MAR in the Chaobai River catchment in the Beijing Plain. These methods are the conventional grid refinement (CGR) method, the local grid refinement (LGR) method and the unstructured grid (USG) method. The assessment included the comparison of the complexity of the coupled model construction, the goodness of fit of the computed and observed groundwater heads, the consistency of regional and local groundwater budgets, and the capture zone of a well filed influenced by the MAR site. The results indicated that the CGR method based on MODFLOW-2005 is the easiest to implement the coupled model, capable of reproducing regional and local groundwater heads and budget, and already coupled with density and viscosity dependent model codes for transport simulation. However, the CGR method inherits shortcomings of finite difference grids to create multiple local models with inefficient computing efforts. The USG method based on MODFLOW-USG has the advantage of creating multi-scale models and is flexible to simulate rivers, wells, irregular boundaries, heterogeneities and the MAR site. However, it is more difficult to construct the coupled models with the unstructured grids, therefore, a good graphic user interface is necessary for efficient model construction. The LGR method based on MODFLOW-LGR can be used to create multiple local models in uniform aquifer systems. So far, little effort has been devoted to upgrade the LGR method for complex aquifer structures and develop the coupled transport models.

3.1 INTRODUCTION

Groundwater models are widely applied for groundwater management purposes. The finite-difference computer program MODFLOW is the most commonly applied code to analyse groundwater flow system, predict groundwater level changes, and calculate water balance components. The high capacity of the modern computers makes groundwater studies on large basin-scale much easier in recent decades. Regional groundwater models provide insights into the groundwater system on large scale and decision-makers can consider the bigger picture when choosing a good pathway towards the long-term groundwater sustainability of the region (Zhou and Li 2011). However, as local scale groundwater problems increase, a finer grid resolution is required to investigate problems

like analysing well fields (Ebraheem et al. 2004), tracing groundwater contaminants (Gedeon and Mallants 2012), delineating the capture zones of pumping wells, etc. The complexity of regional groundwater models is normally insufficient to represent the local heterogeneity (Huang et al. 2008). Using a large scale regional model to simulate the local scale groundwater problems can be inaccurate and not cost-beneficial (Zeng et al. 2017) and it is common that the natural hydraulic boundary is located far from to the target local study area so that the extent of the model area becomes much larger than the area of interest (Leake 1998). In these situations, using unified global refined grids would be computationally expensive (Mehl et al. 2006). This issue can be solved using the emerging regional and local model coupling technique, which allows various grid size in one model domain. Finer grids in the target research area can be embedded into the regional model with coarser grids (Leake and Claar 1999; Feinstein et al. 2010).

In general, the coupling of regional and local models can be achieved by three schemes: full coupling, one-way coupling and two-way coupling (Zeng et al. 2017). The conventional grid refinement method (hereafter referred to as the CGR method) in MODFLOW is the most stable and viable fully coupling scheme (Harbaugh et al. 2000). It integrates the regional and local model in one assembled matrix. The implementation of the CGR method is the most straightforward method and requires the least modification of the original structured regional model. However, the CGR method loses its advantage when there is more than one local model embedded with the regional model because it requires the refinement of entire rows and columns where the local model is located.

A typical one-way coupling scheme in MODFLOW is the telescopic mesh refinement (TMR) method (Leake and Claar 1999). The TMR method is usually numerical stable and computationally efficient, and compatible to operate some independently developed computer codes (Khan et al. 2007; Lin and Zheng 2008). However, the drawback of this method is the lack of numerical rigor (Feinstein et al. 2010). It only uses flux or heads information from the regional model as the local model boundary conditions. Without a feedback mechanism between regional and local grids, huge sub-model error can be introduced when local parameters or stresses are different from the regional scale.

The two-way coupling scheme links the regional grid and local refined grid and provides feedbacks between the two grids. The local grid refinement (LGR) method was developed based on the MODFLOW-2005 code as a two-way coupling scheme. MODFLOW- LGR allows to extract local model boundary condition from the regional model (Michael and Khan 2016; Appels et al. 2017; Huang and Chiu 2018) and it can keep consistent groundwater heads at shared nodes but requires block-shaped refined area and normally requires a longer simulation time for convergence. There are also case studies combining the TMR and LGR method for multi-scale modelling (Hoard 2010). However, LGR method is not suitable when the target refined area is not a centralized area, for example,

when an aquifer storage recovery wells system is distributed over a large area (Forghani and Peralta 2017).

In recent years, the unstructured grid method (hereafter referred to a USG) in MODFLOW-USG was applied by many studies. The USG method is a fully coupling method that generates a more flexible mesh (Panday et al. 2013). The USG method is numerically rigorous and has been applied for different kinds of modelling purposes. Since the design of the grid is very flexible, the grid refinement is no longer restricted by the shape grid and refinement area. Multi-scale models can be constructed by the USG method either when the boundary of the local model area is irregular or the hydrological stresses change in the local area might have a significant influence on the larger region (Hayes et al. 2020; Sun et al. 2020). Finer grid resolution can be used to refine the area near river channels (Božović et al. 2020; Yang and Tsai 2020) or only on the model top layer (Feinstein et al. 2016) to investigate surface and groundwater interaction. Except for the ortho-grid, the Voronoi grid can be applied to simulate the area of interest with higher resolution (Eshtawi et al. 2015; Sreekanth and Moore 2018; Gonzalez et al. 2020). The USG method can also be used to simulate axisymmetric problems by using coaxial cylindrical cells (Memari et al. 2020). The USG method potentially results in asymmetry and irregular banding matrix in solving equations. It also requires more complex discretization files so that the model construction can be arduous.

Few studies have systematically compared these methods. Sbai (2020) evaluated the improvement of the performance of using USG to represent the aquifer heterogeneity and compared it with the homogeneous coarser grid model. Lux (2016) analysed the difference between using the structured grid and the unstructured grid to simulate the multi-lateral wells. The unstructured grid could provide higher resolution keeping cell numbers relatively low by only refining around the wells. Some synthesis cases were analysed to evaluate the accuracy and process time (Mehl et al. 2006; Vilhelmsen et al. 2012)

In this study, the regional groundwater flow model of the Beijing Plain was coupled with a local refined grid model in the target area for MAR simulation. Like all the other mega-cities, with rapid urbanization and population growth, the city of Beijing is facing many environmental problems, such as a continuous groundwater level decline (Zhou et al. 2012), land subsidence (Zhu et al. 2015) and groundwater contamination. To evaluate the impact of those problems, a coupled local groundwater model with higher resolution is required. We applied the CGR method, the LGR methods and the USG method to refine the area with a planned MAR project and a large groundwater well field. The refined local models will be used to design and simulate the MAR scheme and evaluate the effectiveness of groundwater storage recovery at a groundwater well field near the MAR site. Three refinement methods were compared in terms of the goodness of fit of the computed and observed groundwater heads, the consistency of regional and local

groundwater budgets, and the capture zone of the well filed. The advantages and limitations of three methods were discussed. The results of this study are helpful for the modelers to select a suitable refinement method according to the complexity of the study area and processes to be simulated.

3.2 MATERIALS AND METHODS

3.2.1 The Regional Groundwater Flow Model

Beijing city (39°28′~41°05′N, 115°25′~117°30′E) is located in the northwest corner of the North China Plain. The total area of the city is 16,800 km^2 with 62% of mountainous area and 38% of plain area. With the rapid development and the increasing population of Beijing city, the water shortage has become one of the most important environmental problems. To assist in managing the groundwater resources in the Beijing Plain, a regional groundwater flow model has been constructed, which aims to simulate the alluvial groundwater system (Liu et al. 2021a). In this study, the grid orientation of the regional model has been rotated 33 degrees clockwise toward the north-east to minimize the number of column and rows to be refined in the CGR method and at the same time maximize the refined area of the LGR method, which will be described in the next session.

Figure 3-1 shows the physical structure, boundary conditions, and flow processes of the hydrogeological conceptual model and the regional numerical model grid. Four aquitards were included in the model to represent the leakage between the five major aquifers. The top aquifer is distributed in the whole plain area while the extents of the lower aquifers are truncated by the bedrock. Hydraulic properties for nine model layers were assigned to parameter zones. The mountain front boundary in the west and north were defined as lateral inflow boundary while the administrative boundary in the south and east was simulated with the general head boundary. The hydrological stresses include areal recharge, river and canal leakage, ET and abstractions.

Grid cell size of the regional model were designed as 1000 m by 1000 m. A steady-state groundwater flow was simulated and calibrated with average fluxes in a long period of wet years, using MODFLOW-2005 (Harbaugh 2005). In this study, Groundwater Modeling System (GMS) version 10.4 (Aquaveo 2019) was used to create the coupled models. With the conceptual model approach in GMS10.4, boundary conditions, parameters and stresses were created and stored in coverages, which are independent from the numerical model grid. When a coupled regional and local model grid was designed, data in the conceptual model were transferred automatically to the numerical model. In this way, three different coupled models were created more efficiently.

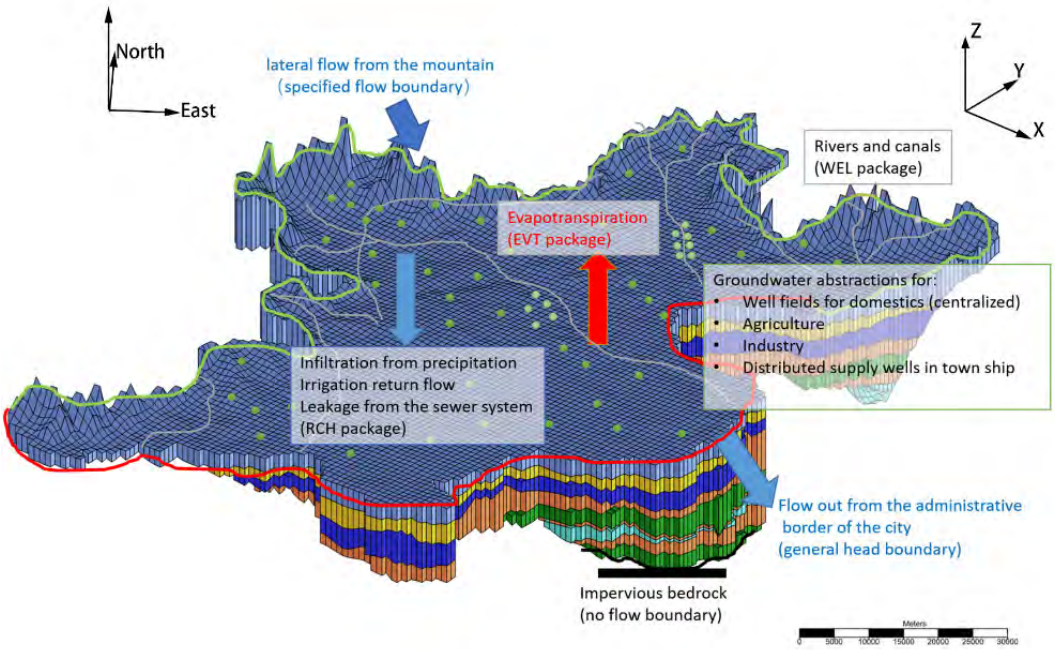

Figure 3-1 The conceptual model and the grid discretization of the regional groundwater flow model. (Location of the line and point representing the sources and sinks are not genuine, display purpose only).

3.2.2 Coupling Regional and Local Models

Different local grid refinement methods were applied on the basis of this regional model, to incorporate a coupled local groundwater flow model the planned MAR site in the Chaobai River catchment. The location of the MAR site is close to the No.8 Well Field, where groundwater has been over-exploited since the continuous drought in 1999. To evaluate the change in the local groundwater flow system in response to the MAR project implementation, CGR method, LGR method and USG method were applied to create a local refined model in the MAR area coupled in the regional steady-state flow model. The area of the local model is around 240 km^2 and defined as the area in the vicinity of the MAR site and along the direction of the Chaobai River.

- Conventional Grid Refinement (CGR) method

The CGR method refines the local model area using a variably spaced grid, which can be realized by further dividing the rows and columns into smaller cells in the local model area. In this study, each model row and column of the regional model grid was divided into 10 rows and columns, so that the local grid resolution became 100 m by 100 m in the local model area. The refined model grid by the CGR method is shown in Figure 3-2. The

refined grids go through rows and columns of the entire mode area and cut through all model layers. After mapping the conceptual model to the CGR model grid, the model was executed by MODFLOW-2005.

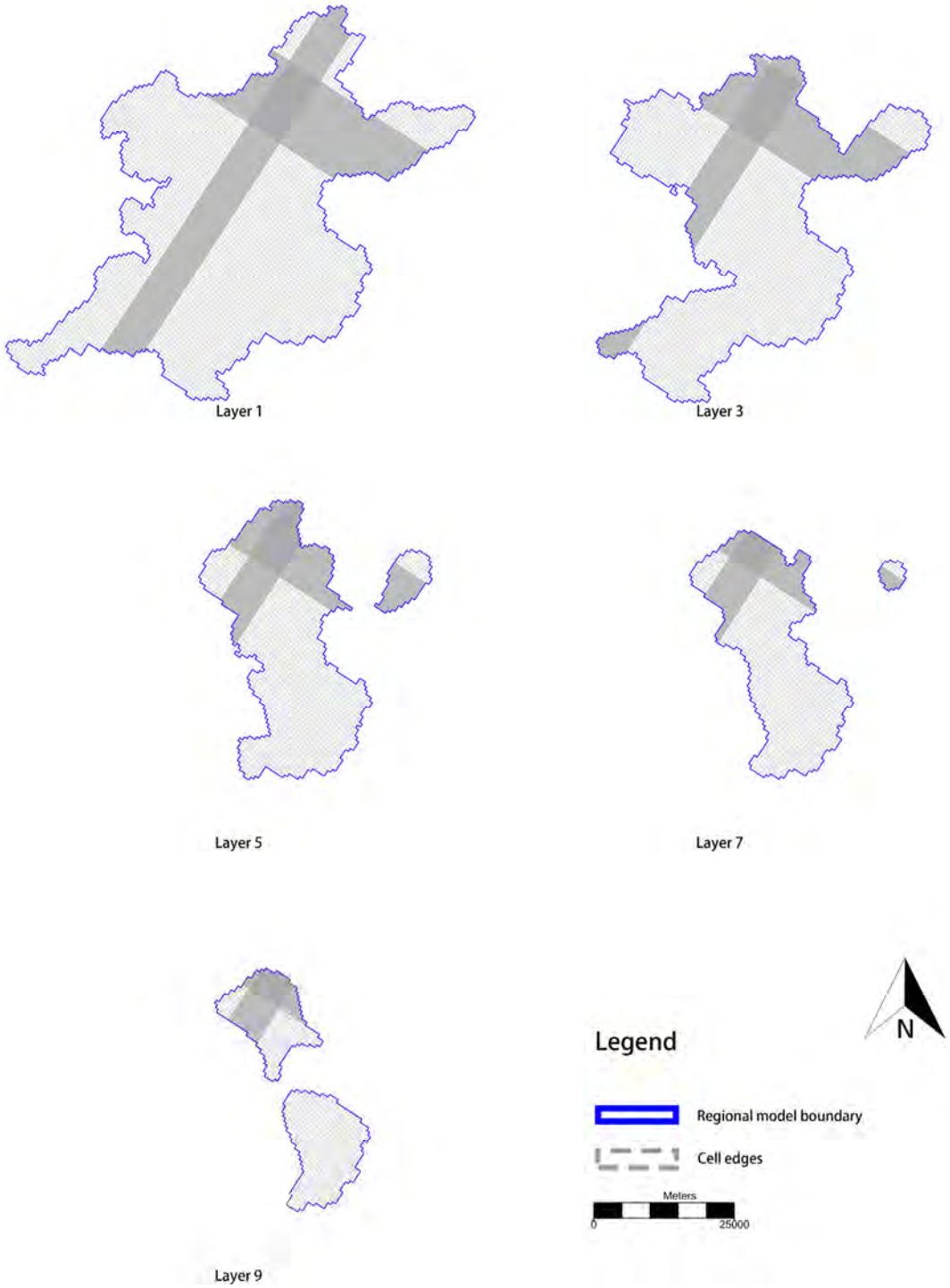

Figure 3-2 Grid refinement with the CGR method. The refined grids extend to the entire model area and all model layers.

- Local Grid Refinement (LGR) method

LGR method can be realized by the computer program MODFLOW-LGR share node (Mehl and Hill 2006) method developed by USGS, which refines the local model area both horizontally and vertically. The number of layers to be refined can also be specified by the user. However, the shape of the local model is restricted to a blocked-shaped area and needs to be unified through all the refined model layers. The horizontal refinement factor of the local model must be an odd integer so that the edges of the local model grid can be located inside the shared nodes of the regional grid. Cells in the regional model that overlapped with the local model are abolished. However, some data input (that depends on the model cell area directly or indirectly) needs to be modified for the cells at the interface of the regional and local grids to prevent the double-counted sources and sinks. In this study, due to the decreasing layer extent of the lower model layers, only the first three layers of the regional model were refined. Figure 3-3 shows the shape of the refined local model of the LGR method.

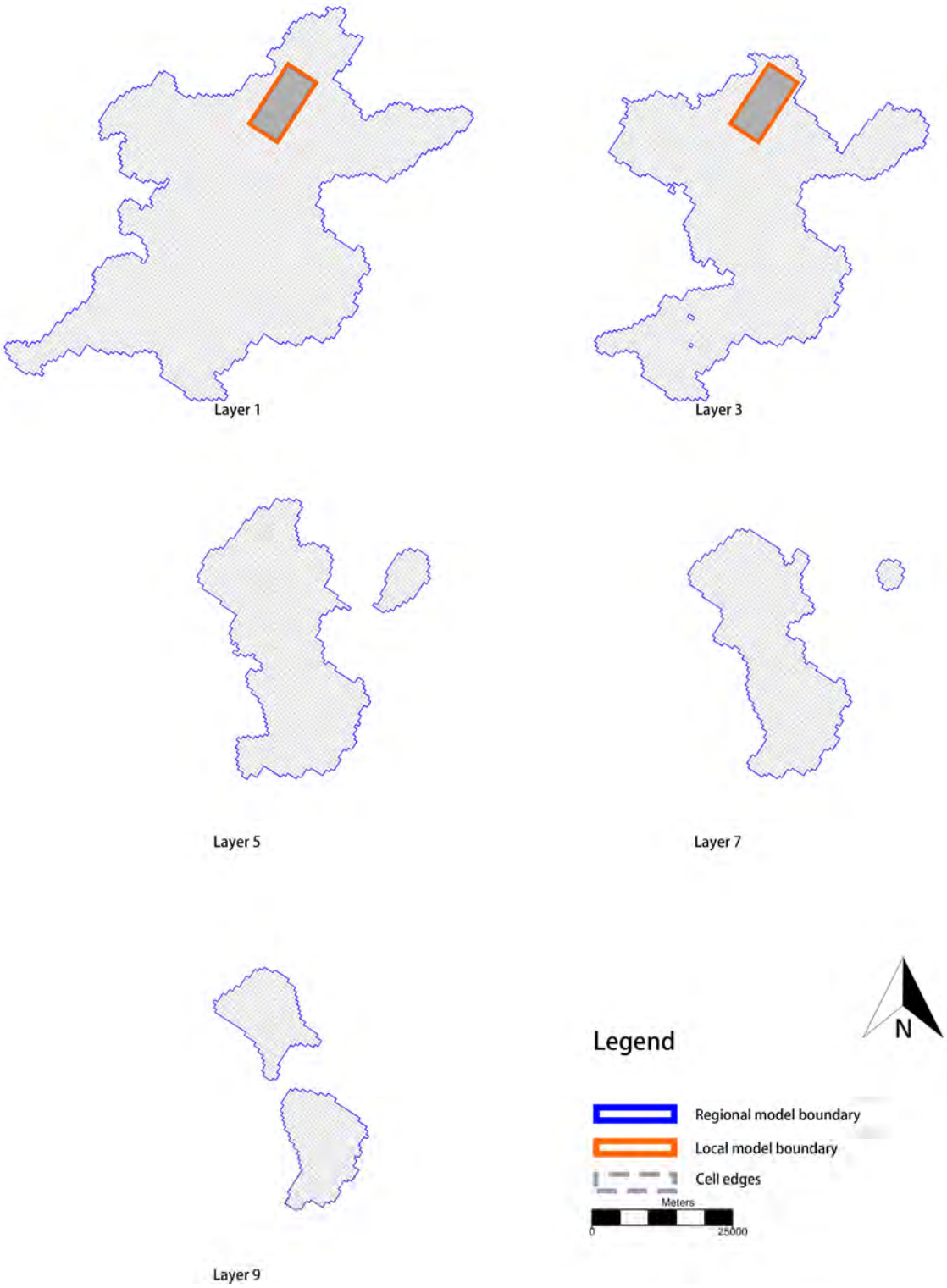

Figure 3-3 Grid refinement with the LGR method. The refined grids are located only in the local model area and in the five model layers.

The refinement factor was set as 9 so that the size of the local grid is 111.11 m. The regional model cells that overlapped with the local model area were inactivated only in the first two layers. The local grid's layer bottom replaces 1/2 of the thickness of the regional model layer. Thus, the overlapped cells in the third layer of the regional model were remained active to allow the communication between the regional and local grids. When transferring the conceptual model data to the refined local grids using GMS 10.4, the sources and sinks of the local model area in layer 3 were also transferred to the regional grid, which were removed manually to avoid double account of those stresses. The cells on the interface of the regional and local models were defined as specified head boundary for the local model and the head values were obtained from the computed heads from the regional model. The LGR model can be run separately or jointly with the regional model. The simultaneous solution scheme provides feedback between the regional and local models (Mehl et al. 2006), keeping consistent groundwater heads on the adjoining interface of the two models.

- Unstructured Grid Refinement (USG) method

The USG method can be applied by using the MODFLOW-USG version 1 (Panday et al. 2013) to simulate the groundwater flow that supports various structured and unstructured grid types. As a fully coupling refinement method, the USG method is the most flexible grid refinement scheme among the three methods. It does not have restrictions on the shape of the refined area and is also very flexible for vertical refinement. It only requires faces of horizontal top and bottom cells. The discretization can be the combination of an arbitrary number of nested grids or grids with other irregular shapes. And the flexible vertical refining capability of USG makes it easier to delineate the discontinuous confining units in the model domain. In this case, the refinement factor of the USG method can only be an even integer because the finer and coarser grids are embedded by shared faces. Thus, to acquire a relatively similar refined level with other methods in this study, the refinement factor of the local model by the USG method was chosen as 8. The quadtree grids used to create the local model have a 125 m grid size (Figure 3-4). All the model layers have been refined in the area of interest. Due to the decreasing layer extent of the deeper layers, the numbers of refined grids are less in the lower layers.

To evaluate the planned MAR system in the Chaobai River, it is necessary to compare the groundwater travel time computed by local models. MODPATH version 3.0 (Pollock 1994) and Mod-PATH3DU (Craig et al. 2020) were applied to the CGR, and USG models to calculate groundwater travel times and delineate the well field capture zones. In each refined local model, 100 particles were placed in each extraction wells at the No.8 well field near the MAR site for backward particle tracking. The pathlines report provided information on the groundwater capture zone and travel time from the recharge area to the well field.

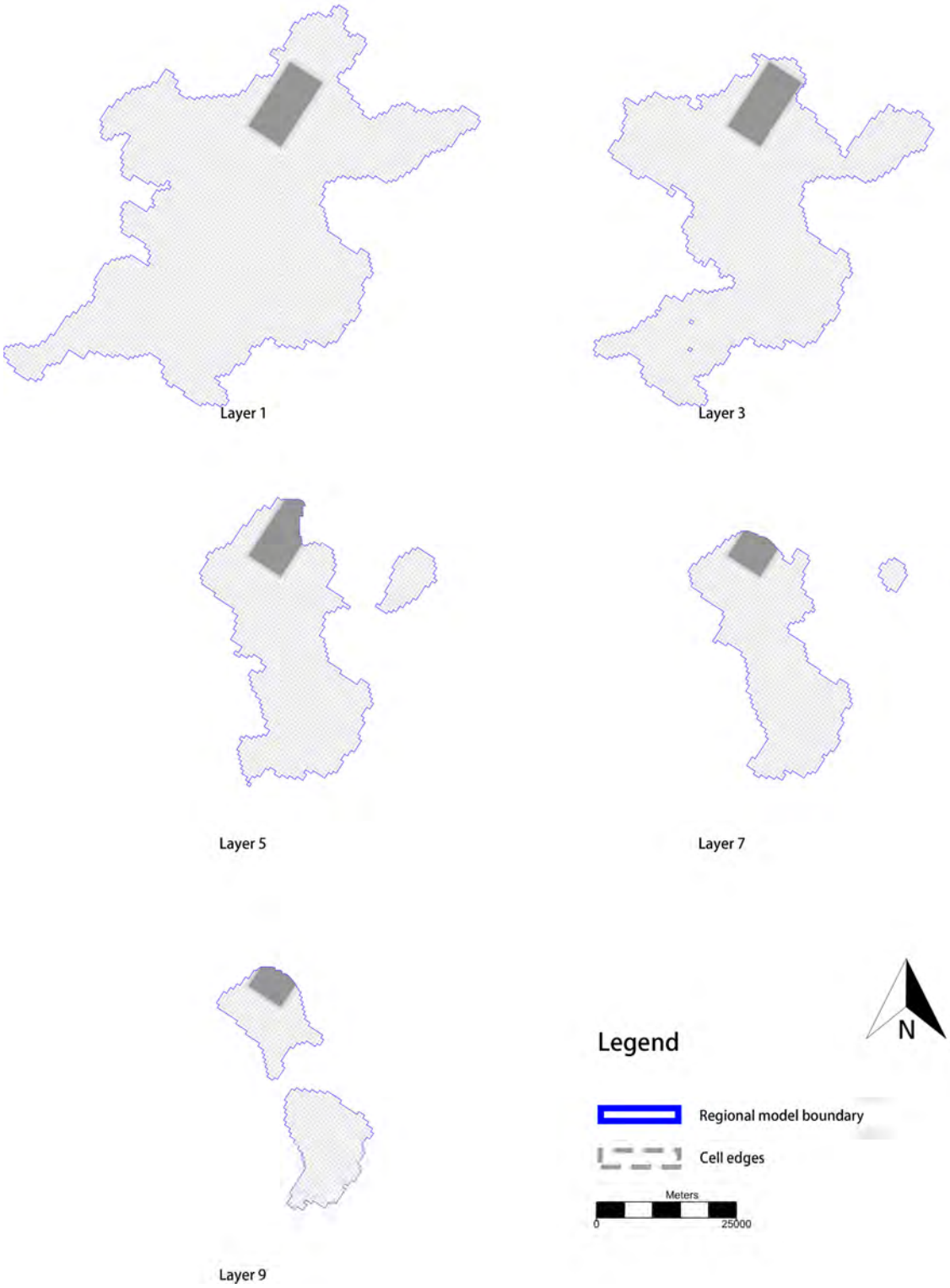

Figure 3-4 Grid refinement with the USG method. The refined grids are located only in the local model area and in all model layers.

3.3 RESULTS

The regional groundwater flow model was constructed and calibrated with alternative model method (Liu et al. 2021a). The model created with the true-layer approach was found most suitable for the simulation of MAR scheme. This model was used in this study to develop the coupled regional and local models.

3.3.1 Comparison of Computed and Observed Heads

First, three coupled models with CGR, LGR and USG methods were compared with the original regional model (Liu et al. 2021a). Figure 3-5 shows the scatter plots of the computed groundwater heads versus the observed heads from three coupled models. The coefficient of determinations of the original regional model was 0.830 for the entire model domain and 0.693 for the observation wells in the local model area (Liu et al. 2021a). The coefficient of determinations of three coupled models are similar with the original model while the coefficients of determinations of three local models are higher than the original regional model, indicating that the calibration accuracy of the original regional model is maintained by three coupled models. Table 3-1 lists statistics of three coupled models which show that both the mean error (ME) and the root mean squared errors (RMSE) of the local models are much smaller than the regional models, which confirm the necessity to create a local refined model for MAR simulation with high accuracy. Although the LGR model gives the lowest errors of the local model, other models are also acceptable for MAR simulation.

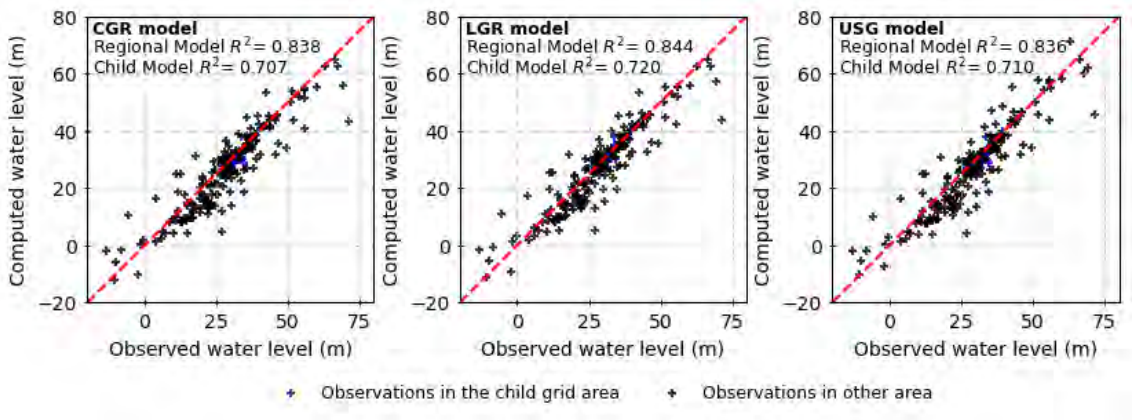

Figure 3-5 The scatter plots of the computed and observed groundwater heads from the CGR, LGR and USG models.

Table 3-1 Statistics of computed and observed groundwater levels for the three models.

	Original	CGR Model		LGR Model		USG Model	
	Regional Model	Regional Model	Local Model	Regional Model	Local Model	Regional Model	Local Model
ME	−2.22	−2.24	−1.14	−1.64	−0.42	−2.17	−1.30
RMSE	6.37	6.37	2.26	6.31	1.85	6.91	2.79

3.3.2 Comparison of Computed Groundwater Budgets

The groundwater balance components of three coupled models are shown in Table 3-2. In general, all major inflow and outflow components are the same as the original regional flow model, no changes were found comparing with the original regional model. Only very small differences were found in the areal recharge due to a small change in the model area by grid refinement. Some comparatively large differences were found in flows through general head boundary (GHB) and ET values since they are head dependent. However, both flow components are relatively small and do not influence the total groundwater budget.

Table 3-2 Groundwater balance results of three coupled models.

	Flow component	CGR model		LGR model		USG model	
		Rate (m^3/d)	Changes	Rate (m^3/d)	Changes	Rate (m^3/d)	Changes
Inflow	Rivers and canals	1,438,992	0%	1,438,992	0%	1,438,992	0%
	Mountain front inflow	1,223,699	0%	1,223,699	0%	1,223,699	0%
	Inflow from GHB	95,448	−2.71%	92,035	−6.19%	108,789	10.88%
	Areal recharge	4,643,656	−0.05%	4,661,764	0.34%	4,646,976	0.02%
Outflow	Abstraction	6,954,707	0%	6,954,767	0.001%	6,954,707	0%
	ET	125,401	0.04%	143,898	14.80%	154,983	23.65%
	Outflow from GHB	321,673	−0.13%	330,184	2.51%	309,516	-3.91%

The groundwater balance components of three local models are shown in Table 3-3. The computed flow components in the local model area (239.75 km^2) from the CGR and USG methods are very close. The LGR model computed relatively smaller water budget since the local model area from LGR refinement is smaller (212.19 km^2). During the LGR grid refinement, cells in the regional model that overlapped with the local model were inactivated. However, the local model area is smaller than the inactivated area because the local model is embedded with the regional grid by shared-nodes (centroid of the cell).

Thus, some recharge and abstractions located at the interfaces of the regional and local models were not counted in the local model. Differences in other head-dependent flow components are the consequences of smaller recharge and abstractions.

Table 3-3 Computed groundwater balance from three local models.

	Flow Component	CGR Model (m^3/d)	LGR Model (m^3/d)	USG Model (m^3/d)
Inflow	Rivers and canals	181,442	168,315	179,586
	From regional model	403,673	396,699	424,061
	Areal recharge	189,917	143,369	168,449
	Total	775,032	708,384	772,096
Outflow	Abstraction	699,331	638,155	687,999
	ET	358	3,200	2,590
	To regional area	75,340	67,031	81,446
	Total	775,028	708,385	772,035

3.3.3 Comparison of Computed Contour Maps

Figure 3-6 shows the computed groundwater head contour maps in layer 1 and layer 3 of the local model area from three coupled models.

Generally, the computed groundwater head contour lines are similar from three local models. The shape of the contour lines of the USG model is smoother than the other two models. All three models computed a cone of depressions at the local model area, which is caused by the No.8 well field. Small differences in the computed heads were found at the centre of the cone of the depression. In the first model layer, the computed minimum groundwater heads of the CGR, LGR and USG model are 25.79 m, 26.50 m and 25.48 m, respectively. On the third layer, the computed minimum heads are 19.18 m, 20.29 m and 17.68 m, respectively.

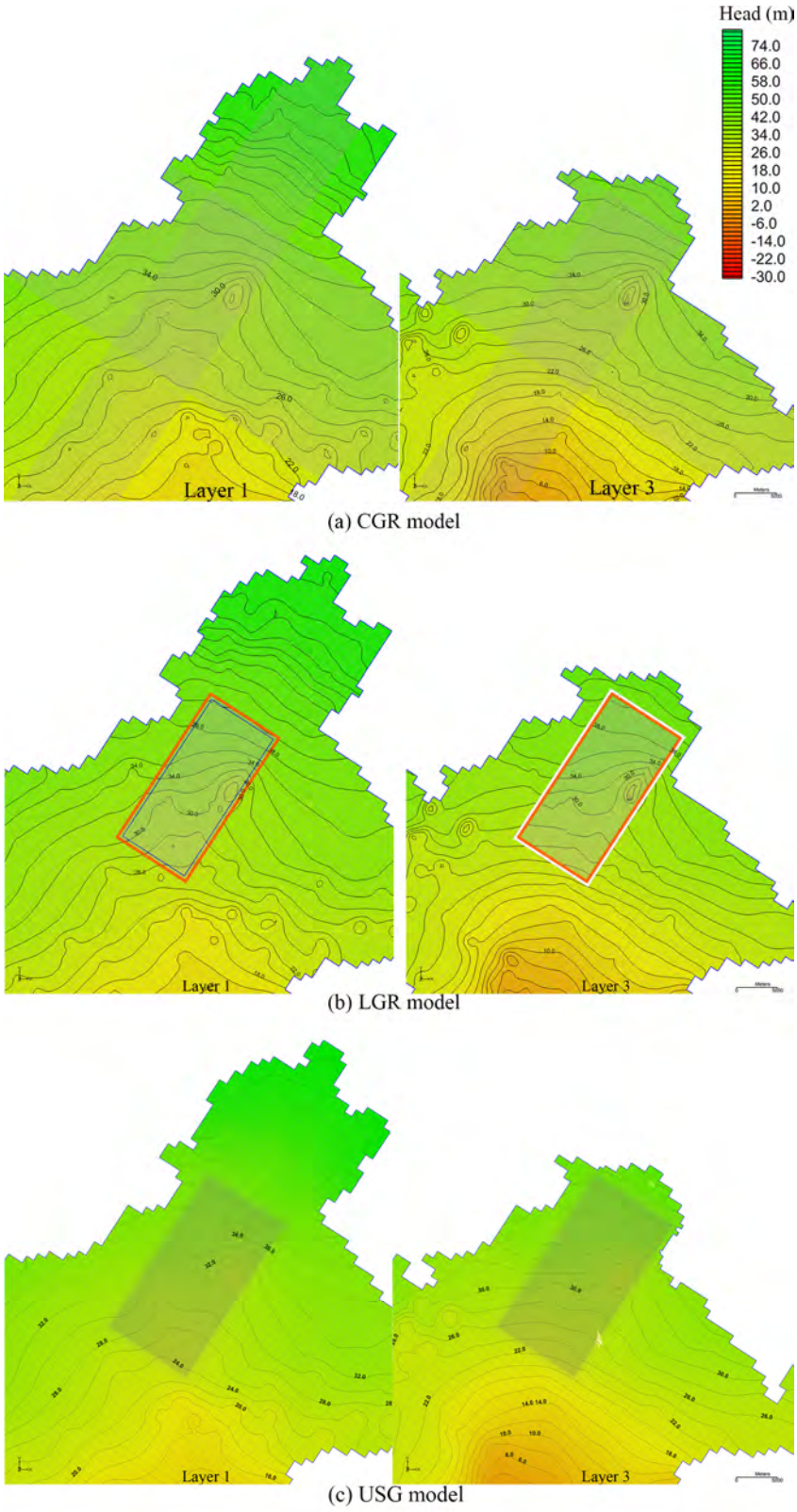

Figure 3-6 Contour maps of the local model area computed by a) CGR model, b) LGR model, and c) USG model.

3.3.4 Comparison of Computed Capture Zones

As shown in Figure 3-7, the capture zones of the No.8 Well Field were delineated separately for the shallow (layer 1) and deeper (layer 3) aquifers, which shows the maximum size of the catchment area in which the groundwater could be captured. The areas of the capture zone delineated by the CGR method and USG method in layer 1 are 63.9 km^2 and 53.2 km^2, which are 2% and 18% smaller than the capture zone generated by the original regional model (65.1 km^2). The capture zone delineated by the CGR method and the USG method in layer 3 are 310 km^2 and 296 km^2, which are 27% and 1.7% larger than the capture zone generated by the original regional model (291 km^2). However, the shape of the capture zone generated the CGR and USG models are quite different.

Groundwater in wells located in the shallow aquifer mainly comes from river leakage and precipitation recharge. Groundwater abstracted from the deeper aquifer comes mainly from leakage of the shallow aquifer. It appears that the river leakage has a larger influence on the capture zone delineation in the shallow aquifer with the particle tracking model mod-PATH3DU linked to the USG model. The pathlines generated with mod-PATH3DU are restricted from crossing the river, suggesting a potential limitation in the model's handling of river-aquifer interactions. Conversely, MODPATH linked to the CGR model treats the river as a weak source, allowing generated pathlines to cross the river. This discrepancy raises questions about the accuracy of the USG model in delineating the full extent of the capture zone, particularly in the shallow aquifer where river-aquifer interactions are crucial. Thus, the CGR model appears the better of the two in delineating the capture zone for the shallow aquifer (Layer 1). For the deeper aquifer (Layer 3), pathlines generated with mod-PATH3DU ended up at the water table while pathlines generated with MODPATH reached inflow boundary as source water. It is not possible to determine which of these two is more correct. MODPATH (version 3) did not work with the LGR model so that it was not possible to delineate the capture zone with the LGR model.

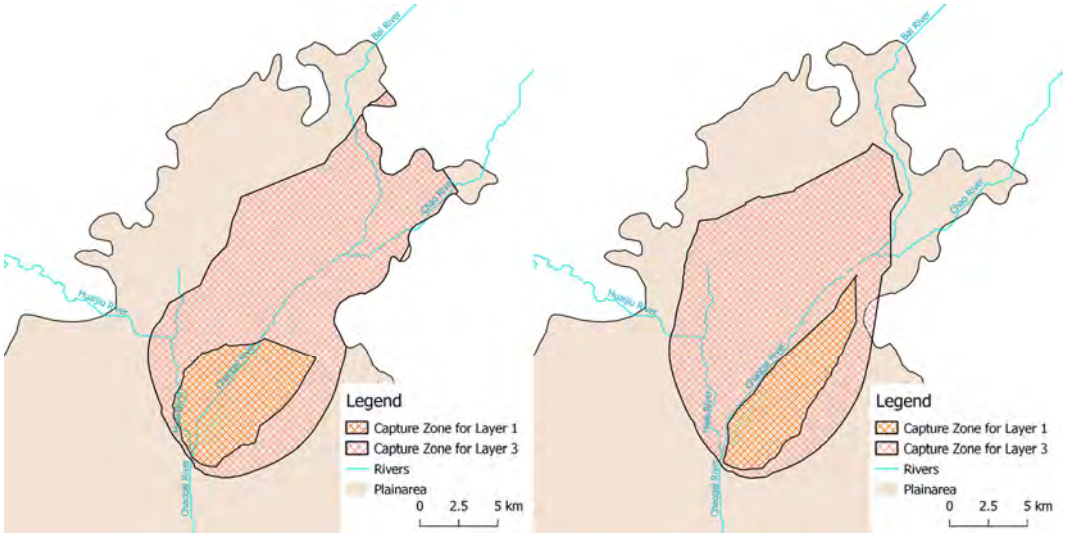

Figure 3-7 The capture zones delineated with CGR (left) and USG (right) models.

3.4 DISCUSSION

Based on the results shown above, we summarize the pros and cons of the different methods with regards to the following aspects: the complexity of model construction, the limitations and the conditions for application, and the shortcomings of the current version of GMS interface (GMS10.4).

Among the three refinement methods, the CGR method is the easiest and most straightforward to implement and requires the least modification to an existing regional model. No extra data or model input files need to be prepared. Under the GMS environment, each row and column of the regional model grid in the local model area can be selected and divided into a number of sub-grids to create a coupled regional and local model grid. Afterwards, coverages in the conceptual model can be mapped and transferred to MODFLOW packages to establish a coupled regional and local flow model. With the same convergence criteria as the regional model, the CGR coupled model can reproduce the same results as the original regional model. Moreover, the CGR method is very flexible to modify the existing local model and to add a new local model. Like in this study, the cone of depression around the No. 8 well field has been expanded larger and deeper with further over-exploitation. Thus, it is necessary to enlarge the local model area to include the enlarged cone of the depression for a transient simulation. This modification can be easily implemented in the transient model construction. Furthermore, the coupled model was developed from an existing regional model in this study, elevations of all model layers were re-interpolated to have more accurate elevations for the refined grids. However, the refined grids with the CGR method extends over the entire model area and cut through all model layers, a coupled model with much larger number

of model cells is created resulting in longer computation time. Although the extra simulation time for a steady-state flow model is negligible, the computation time might increase a lot with transient model simulation, especially when coupled with solute and heat transport simulation. Another shortcoming is that the CGR method cannot refine model layers in the local model area. Thus, the CGR method is more efficient when there is only one local model, the local model area is relatively small, and no vertical refinement is required. By far, the CGR method is still widely used for the coupled modelling of groundwater flow, solute and heat transports since all standard model codes such as MODFLOW, MODPATH, MT3DMS and SEAWAT can be run with the CGR girds without any modifications.

The construction of the LGR model needs more modifications than the CGR model. Similar to the CGR method, the local model was constructed based on the regional model in this study. Thus, the top and bottom elevations of local model layers were interpolated again to obtain more accurate model structure. The advantage of the LGR method is that a number of the local models with desired refinements can be created and embedded into the regional model so that the regional model grid is not changed. The coupled LGR model can be run jointly or sequentially from the regional model to the local model. Thus, computation efficiency can be achieved by only running the local model while the regional model is not influenced by the local model. However, the construction of the LGR model has a number of restrictions. Firstly, the LGR method requires a blocked-shape of the local model area with the same horizontal refinement for selected model layers. A problem occurs when the local model area covers the irregular boundary or the areal extents of the model layers are different. Like in this study, the local model area is located in the upstream of the Chaobai River where the model boundary is irregular and the extent of the model layer decreases with an increase of the depth as the basement uplifting towards the boundary. Under this circumstance, the extent of the local model area was not able to cover the entire influence area of the No. 8 well field. Secondly, the hydrological stresses at the interface of the local and regional grid may be double counted and need to be checked and revised manually by the user. If there are large number of sources and sinks located in the interface cells, a large discrepancy of the groundwater balance can be expected. Thirdly, MODFLOW-LGR couples the regional and local model at the interface cells. The interface cells at the edge of the local model were simulated as specified head cells with the heads being computed by the regional model. In the regional model, the interface cells are treated as specified flow cells with the flows being computed by the local model. Therefore, a large number of iterations might be required to achieve consistence of computed heads and flows at the interface cells. For coupled models with complex hydrogeological conditions, it is more difficult to meet the convergence criteria in the MODFLOW-LGR. So far, only MODPATH version 5 is coupled with MODFLOW-LGR to perform particle tracking, which has not been accommodated to the GMS 10.4. No solute, salt and heat transport models have been

developed for coupling with MODFLOW-LGR. Thus, the application of LGR method is still limited to the coupled regional and local groundwater flow simulations in less complex hydrogeological conditions.

Although the USG method supports a wide variety of structured and unstructured grid types, including nested grids and grids based on prismatic triangles, rectangles, and hexagons shapes, to simulate rivers and wells with flexible refined grids, the construction of the USG model requires a big effort. The unstructured grid needs to be set up separately from the regional model grid. For a large regional groundwater model, creating a desirable unstructured grid local model takes a lot of time and effort and once it is constructed, further modification is not possible. At the same time, pre-processing of the model input data also requires that the modeller has a deeper understanding of the MODFLOW-USG software. However, the USG model is the most flexible method that can accommodate a variety of demands. The shape and location of the local model area have fewer restrictions compared with the LGR method. Especially with the problems that require multi-scale model simulation simultaneously, the USG model does not have any restriction on the number of embedded local models and the interested model area can be refined into different levels of resolution. In this study, the characteristics of the USG model provide great convenience to the simulation of the MAR system in the Chaobai River catchment. A multi-scale model can be created which couples the regional scale, local scale and MAR site scale models and they interact with each other simultaneously. However, with the currently USG version 1, some flow packages are not supported yet. The ability to simulate the unsaturated zone flow in the USG model is relatively weak. Only the SRF2 package is currently supported, which can simulate the unsaturated flow beneath a hydraulically disconnected stream and aquifer. Furthermore, a particle racking code (mod-PATH3DU) and a solute transport model code (MODFLOW-USG Transport) have been developed for coupling MODFLOW-USG model. These coupled models enable the USG models to simulate flow and solute transport with coupled multiple scale models. Thus, the USG method has good potential for a wide range of applications in simulation of flow and solute transport in multiple scales.

Since all of the abovementioned models require text input files and save model results in data files, a good graphical user interface (GUI) for the model construction and results analysis is required. GMS10.4 is one of better commercial modelling environments and was used in this study. The conceptual model approach in GMS is well suited to construct the coupled regional and local models. GMS supports all available models (MODFLOW, MODPATH, MT3DMS, RT3D, and PHT3D) with the CGR method. GMS also supports flow and transport models (MODFLOW-USG, mod-PATH3DU, and MODFLOW-USG Transport) with the USG method. In the current GMS 10.4 version, only MODFLOW-LGR is supported for coupled flow simulation with the LGR method. A latest particle tracking code MODPATH version 5 was not supported yet so that particle tracking cannot

be performed in GMS10.4. Furthermore, some sources and sinks were double counted at interface cells with the LGR method and have to be removed manually.

3.5 CONCLUSIONS

Based on the regional groundwater flow model of the Beijing Plain, a coupled local groundwater flow model with finer grid resolution was constructed with three different refinement methods: the conventional grid refinement (CGR) method based on MODFLOW-2005, the local grid refinement (LGR) method based on MODFLOW-LGR, and the unstructured grid (USG) method based on MODFLOW-USG. All three methods were able to create a coupled local model for the MAR site in the Chaobai River. The computed regional groundwater contour maps and flow budgets from three methods are very close to the original regional flow model. However, the LGR model produced a slightly smaller flow budget from the local model since a smaller local model area was created with the refinement and coupling method. Large differences were found in capture zone delineation for the No. 8 well field. These differences may be caused by using different particle tracking codes. MODPATH in the CGR method can track pathlines across weak sources and sinks. mod-PATH3DU coupled with MODFLOW-USG in the USG method terminates pathlines at weak sources and sinks, which is not suitable for application in areas with significant groundwater-surface water interactions. It was not possible to delineate the capture zone with the LGR method since a latest MODPATH code was not linked in GMS 10.4.

The comparative assessment of the three methods found that the CGR method is capable of constructing coupled regional and local models for flow, solute, salt and heat transport simulations, but inherits the shortcomings of regular finite difference grids. The USG method is very flexible to construct multi-scale models with unstructured grids fitting to rivers, wells, irregular boundaries, and heterogeneities. So far, the USG method can be used to simulate flow and solute transport. A good graphic interface is very important for the USG model construction and result analysis due to the complexity to create unstructured grids and prepare model inputs. The LGR method has limited applications because the corresponding transport model code has yet to be developed and the interfacing problem is still to be solved. Thus, the selection of a method should consider the requirement of the local model, complexity of the hydrogeological conditions, flow and transport processes to be simulated, and the available graphic user interface.

4

NUMERICAL ASSESSMENT ON THE MANAGED AQUIFER RECHARGE TO ACHIEVE SUSTAINABLE GROUNDWATER DEVELOPMENT IN CHAOBAI RIVER AREA

Corresponding paper: Liu, S., Zhou, Y., Luo, W., Wang, F., McClain, M. E., & Wang, X. S. (2022). A numerical assessment on the managed aquifer recharge to achieve sustainable groundwater development in Chaobai River area, Beijing, China. Journal of Hydrology, 613, 128392.

ABSTRACT

Intensive groundwater exploitation has depleted groundwater storage and led to a series of geo-environmental problems in Beijing Plain, China. Managed Aquifer Recharge (MAR) has been endorsed to mitigate groundwater storage depletion and achieve groundwater sustainability. A pilot MAR has been tested in the Chaobai River catchment since 2015. An innovative large-scale MAR consisting of 9 cascade terraced infiltration ponds was proposed and its effectiveness was assessed in this study using an integrated modelling approach. The integrated model coupled the regional and local transient flow and transport processes. The transient regional flow model simulated historical groundwater level declines and storage depletion in the Beijing Plain from 1995 to 2018. The coupled regional and local flow model was used to simulate the pilot MAR test in the Chaobai River from 2015 to 2018. A significant groundwater level increase was observed nearby the pilot MAR since 2015. The transport model results indicate that approximately 40% of the infiltrated water was captured by pumping wells in the No.8 well field. The models were further used to assess the long-term effects of the large-scale MAR from 2020 to 2050. The simulation results show that the groundwater system will reach a new equilibrium state under the implementation of the large-scale MAR scheme. Almost 91% of the abstracted water in the No. 8 well field will come from the MAR infiltration. The proposed large-scale MAR is very effective in restoring the depleted aquifer storage and maintaining the groundwater abstraction in the No.8 well field. However, with the increase of the groundwater level, the infiltration rate of several ponds will decrease. Therefore, it is important to maintain a dynamic balance between artificial recharge and groundwater abstraction in order to achieve a sustainable long-term MAR operation in the region.

4.1 INTRODUCTION

Groundwater storage depletion has become a global issue that threats the sustainable water development (Aeschbach-Hertig and Gleeson 2012; Famiglietti 2014). Despite the impact of climate change, the long-term groundwater depletion is always resulted from intensive groundwater abstraction (UN-water 2022). The Managed Aquifer Recharge (MAR) systems, which are widely applied globally, could help to enhance the groundwater recharge artificially and recover the aquifer storage (Bouwer 2002; Dillon 2005; Gale 2005). The classification of MAR techniques has been summarized by IGRAC in the global MAR inventory report including the spreading methods, induced bank filtration, well and borehole recharge that focus on getting water infiltrated; and in-channel modifications and runoff harvesting technique that focus primarily on capturing the water (IGRAC 2007).

Among the techniques abovementioned, the spreading method in the river channel or by infiltration basin is a widely applied type of MAR globally, especially in the area with adequate land space and high permeable soil that allows water infiltration to the unconfined aquifer (Ghayoumian et al. 2005). The application of the spreading method usually combines with the source water capture system and recovery wells for water supply (IGRAC 2007). The stormwater spreading system is implemented to augment the groundwater storage and decrease the peak discharge of the river as a flood control structure in the area with uneven rainfall patterns (Hashemi et al. 2015; Yaraghi et al. 2019). In coastal area, reclaimed water is used to recharge the unconfined aquifer to prevent seawater intrusion (Abbo and Gev 2008; Evans and Arunakumaren 2012). Desalinated water has been used for injection without the concern of the clogging issue (Ganot et al. 2017). Lake or river water diverted from other regions can also be the source water for the water spreading for drinking water production (Olsthoorn and Mosch 2002; Mirlas et al. 2015) or increasing the groundwater storage during the dry season (Barber et al. 2009) and reduce the groundwater depletion in the pumping intensive area (Pliakas et al. 2005; Izbicki et al. 2008; Teatini et al. 2015).

Numerical modelling as an effective tool for the design of the MAR system and the optimization of the MAR scheme, has been widely applied (Maliva et al. 2015). Groundwater flow model is the most frequently applied model type for the simulation of the MAR system (Ringleb et al. 2016). The main modelling objectives of the groundwater flow model include 1) identifying the suitable site for the MAR structures (Rahman et al. 2013; Karimov et al. 2015; Russo et al. 2015; Sashikkumar et al. 2017) ; 2) assessing the MAR performance (Neumann et al. 2004; Barber et al. 2009; Niswonger et al. 2017; Ronayne et al. 2017); 3) evaluating the impact of the MAR operation on the groundwater recharge dynamic (Mirlas et al. 2015; Masetti et al. 2016); 4) estimating the infiltration capacity (Namjou and Pattle 2002; Hsieh et al. 2010; Ganot et al. 2017; Masetti et al. 2018) ; 5) optimizing the future MAR scheme (Zeelie 2002; Lacher et al. 2014; Teatini et al. 2015; Xanke et al. 2016). Combined with the groundwater flow model, solute transport modelling is also applied frequently to 1) investigate the mixing process of the infiltrated water with the natural groundwater (Vandenbohede et al. 2013; Bahar et al. 2021); 2) examine the recovery efficiency of the MAR implementation (Huang and Chiu 2018; Jarraya Horriche and Benabdallah 2020); 3) assess the clogging issues by the geochemical processes (Soleimani et al. 2009).

To cope with the continuous groundwater storage depletion and the uncertainty of the future climate change in Beijing, utilizing MAR infrastructures to replenish the depleted aquifer has been considered in the last several decades (Zhang et al. 2008). Several potential artificial recharge sites has been selected (Zhang et al. 2013; Yao 2014). The natural dry riverbed of the two main rivers in Beijing Plain have been recognized as ideal MAR sites for surface water infiltration and recharge of the shallow aquifer. Pilot MAR

project has been implemented since 2015 (Zhou et al. 2021; Cao et al. 2022). Modelling studies have also been carried out to evaluate the performance of the current MAR implementation and the potential of the future MAR operation in Beijing (Zhou et al. 2012; Hao et al. 2014; Nan et al. 2016; Hu et al. 2019a; Ma et al. 2020; Xu et al. 2022). However, most of these modelling studies were only dedicated to the local-scale simulation of MAR sites with relatively short simulation period, which lack the capability to evaluate the contribution of the MAR operation to restoring the groundwater depletion of the entire plain region and support the decision making for an integrated groundwater management of the city. In addition, the boundary conditions of local modelling studies are normally defined as no flow or constant head boundary based on the groundwater contour map. The uncertainty caused by the boundary conditions on the predicted result for the future scenarios has been addressed by different researchers (Liu et al. 2009; Rojas et al. 2010; Wu and Zeng 2013).

This paper aims at assessing the effectiveness of achieving sustainable groundwater development in the Chaobai River area by implementing a large-scale MAR in the riverbed. An innovative MAR system consisting of 9 cascade terrace infiltration basins was designed in the 12 km long riverbed for artificial groundwater recharge. With the multi-scale groundwater flow and solute transport models, the local MAR system in the Chaobai River and the regional groundwater flow in the Beijing Plain can be simulated simultaneously. Therefore, a unique modelling strategy was carried out in a number of steps. Firstly, a regional transient groundwater flow model was constructed from 1995 to 2018 to assess groundwater depletion in the Beijing Plain. Secondly, a local groundwater flow model was developed for the pilot MAR in the Chaobai River coupled with the regional flow model. The movement of the infiltrated water was tracked with a tracer transport model Thirdly, the long-term effect of the designed large-scale MAR was simulated with the coupled model from 2020 to 2050. The findings from the model simulations support the implementation of the large-scale MAR as an effective measure to achieve sustainable groundwater resources development in the area.

4.2 MATERIALS AND METHODS

4.2.1 A review of groundwater model development in Beijing Plain

The area of Beijing has the typical characteristic of a piedmont plain surrounded by mountains in the north and west (Zhou et al. 2013). The long-term average annual precipitation and open pan water evaporation are 593 mm and 1728 mm, respectively. The temporal distribution of the rainfall is very uneven throughout the year. 75% of the total rainfall occurs during the raining period from June to September. Two large rivers, Chaobai and Yongding, run dry most time since reservoirs were constructed at upstream.

In recent years, Beijing municipality started to rehabilitate these two rivers and implement pilot managed aquifer recharge. The aquifer system varies from an unconfined aquifer near the foot of the mountains to multi-layered semi-confined aquifers downstream of the plain. Groundwater provides almost two-thirds of the water supply for Beijing City. To manage the groundwater resources of the Beijing Plain, regional groundwater studies began in the 1990s. In 1995, an investigation of the groundwater resources in Beijing was carried out. Groundwater storage and water budget components were calculated and analysed, which provided solid information for the construction of a regional groundwater model of the Beijing Plain. A three-dimensional transient groundwater flow model was built to evaluate the groundwater resources from 1995 to 2005 using MODFLOW-2000 (Han 2007). This transient flow model was extended to 2010 to analyse options for sustainable groundwater resources development (Zhou et al. 2012). Based on the previous modelling study, an alternative model was constructed with the so-called “true-layer” model approach (Figure 4-1a) where model layers were truncated with the actual extension of aquifers and aquitards (Liu et al. 2021a). The conceptual model consists of five aquifers and four aquitards. Nine model layers were used to represent every aquifer and aquitard. This regional model was calibrated in the steady state using the recharge and discharge data of the year 1995, in which the total groundwater recharge and discharge are approximately balanced. Afterwards, coupled regional and local scale models with different refining methods were constructed and evaluated for the simulation of the MAR scheme in the Chaobai River catchment (Liu et al. 2021b).

4.2.2 Extension of the regional transient groundwater flow model

A new transient regional flow model was developed in this study to simulate groundwater flow changes in Beijing plain from the year 1995 to 2018 with a monthly stress period using the MODFLOW 2005 program in GMS modelling environment (Aquaveo, 2019). The total model area is 6,642 km^2 and was discretised with a uniform grid of 1000m by 1000m. The model consisted of 9 model layers corresponding to 5 aquifers and 4 aquitards. In total, 23,300 active cells were included in the model simulation. The transient inputs of the old transient model for 1995 to 2010 were adopted and the model was extended to 2018, including recent changes in the reduction of groundwater abstractions since the delivery of the new water source to Beijing from the South to North Water Diversion project by the end of 2014. The main sources and sinks of the flow model are depicted in Figure 4-1a. Monthly groundwater recharge series were extended using monthly meteorological data from 2011 to 2018 and simulated by the Recharge (RCH) package. Infiltration coefficients were assigned to recharge zones based on the characteristic of the land surface and soil type. Map of the infiltration coefficients can be found in Appendix A Figure A-1. Groundwater evaporation was simulated by the Evapotranspiration (EVT) package derived from the pan evaporation data. Abstraction was simulated by the Well (WEL) package and categorized into four types: industrial use,

agricultural use, township water supply, and urban water supply well fields. The annual groundwater abstractions for different usages were obtained from the Beijing Water Resource Bulletin (Beijing Water Authority 2021a). The total amount of abstraction was allocated to each district and mapped to the corresponding grid cells in the model. Irrigation return flow was calculated based on the annual agricultural groundwater use and simulated by RCH package. Pipeline leakage was simulated also by RCH package and specified as a constant value in the city centre area. Since the rivers are dry most time and have water only during raining periods. The amount of leakage was computed for raining periods and was simulated as injection rates in WEL package. Lateral boundary flow from the mountainous region was derived from the annual water balance calculation of the Beijing Plain and simulated as injection wells by WEL package. The administrative borders in the south and east were specified as head-dependent boundary simulated by General Head Boundary (GHB) package. Afterwards, these model inputs were examined and adjusted by an inverse modelling process to check the consistency of the computed and observed groundwater level time series. The hydraulic conductivities were optimised with PEST in the previous model study (Liu et al., 2021b). The specific yield and specific storage values were obtained from the previous transient model (Zhou et al. 2012) and manually adjusted for better model fit. This calibrated model was used for the evaluation of the groundwater level and storage changes in response to the reductions of groundwater abstraction and to couple a local flow model for the design and simulation of the MAR scheme in the Chaobai River.

4.2.3 Simulation of pilot MAR in Chaobai River with multi-scale transient models

To simulate the MAR operation in the Chaobai River catchment, the regional model grid was refined with the conventional grid refining method with variable spacing and the grid lines in each direction extends out to the model boundary Chaobai River area into a local model grid and a site model grid in MODFLOW-2005 (Figure 4-1b-d). The area of the local model is 561 km^2 and the uniform model grid size is 100 m. The area of the MAR site model is 26.6 km^2 with a uniform model grid of 20m by 20m. The determination of the local and site model boundary was tested iteratively which ensures the extents of the refined grid area are sufficient to capture the influence of the MAR operation on the local groundwater flow field.

The MAR site of the Chaobai River channel is dry most of the time throughout the year because the reservoir upstream captures most of the river discharge. The intense groundwater exploitation nearby the NO.8 Well Field has created a large cone of depression in the surrounding area. A feasibility study showed that this section of the river channel is an ideal place for the implementation of the MAR system. The pilot MAR test started in 2015. Source water from the South to North Water diversion project

(Webber et al. 2017) was transferred to the Niulanshan Rubber dam and spread to the 1.5 km river channel (Figure 4-2a). It has been verified that the quality of the source water reaches the standard of Category II based on the Chinese Standard of Groundwater Quality (AQSIQ and SAC 2017), which is better than the natural groundwater quality. Thus, the risk of clogging problem caused by the artificial recharge is minimal.

The groundwater flow model was designed to simulate the variation of the groundwater level during and after the pilot MAR test. The infiltration process was simulated with the River (RIV) package of the MODFLOW program. The 1.5-km river channel was divided into three polygons in the conceptual model (Figure 4-2b). The required input data include the head stage of the infiltration pond (H), the elevation of the pond bottom (H_b) and the conductance of the riverbed (C_b). The flow rate of the source water to the infiltration pond was obtained from Beijing Water Authority. The water depth of the infiltration pond was obtained from the inflow rate, water release duration and the pond area. The riverbed conductance was calibrated to match the infiltration rate of the pond equal to the measured rate. Detailed input data can be found in Appendix A Table A-1. In 2015, 33.7 million m^3 of water were infiltrated from the Chaobai riverbed between August and November. In 2016, 10.3 million m^3 of water were infiltrated in 15 days from July 20th. In 2017 and 2018, approximately 44 million m^3 of source water were infiltrated between May and November. The groundwater levels in the monitoring wells nearby showed a significant increase in response to the pilot MAR test. During the non-recharge period, the groundwater levels decreased because of the continued abstraction in the NO.8 Well Field. The head stage of the RIV package was set as the sum of the pond bottom elevation with the pond water depth during the recharge period. During the non-recharge period, the head stage was assigned the same as the pond bottom elevation so that no infiltration takes place. The conductance value was estimated based on the empirical value of the riverbed materials and calibrated by matching the computed river leakage with the inflow to the MAR site.

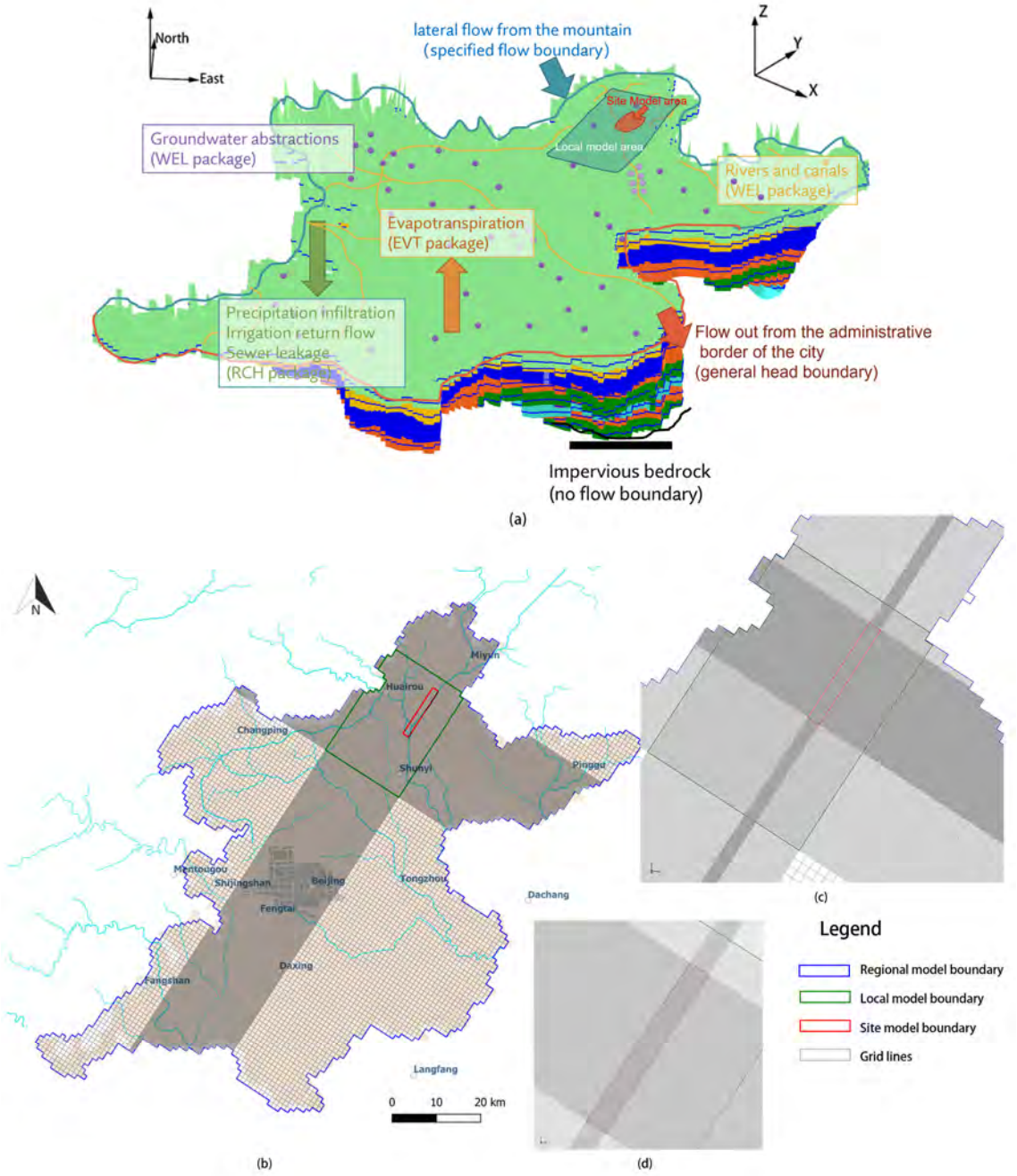

Figure 4-1(a) The conceptual model of the coupled regional and local groundwater flow model of the Beijing Plain (revised from Liu et al., 2021b)). Each colour represents one model layer. (b)-(d): Grid of the multi-scale models: (b) regional model (1000m x1000m); (c) local model (100m x 100m); and (d) site model (20m x 20m). The blue, green and red lines are the boundaries of the regional, local and site models, respectively.

4.2.4 Design and simulation of a full-scale MAR in Chaobai River

The pilot MAR test in the Chaobai River has shown the feasibility of the implementation of a full-scale MAR system. In this scheme, a total of 12.4 km dry riverbed was designed to be converted into nine terraced infiltration ponds with different lengths elevated from south to north (Zhou et al. 2021). As is shown in Figure 4-2c, the total recharge area is approximately 3.03 km^2. The layout of the full-scale MAR scheme is shown in Figure 4-2d. The source water is designed to flow into the MAR infiltration ponds from the inlet at the upstream infiltration pond (pond 9). The artificial recharge is planned from April to November each year with a 14 m^3/s inflow rate of the source water. The maintenance of the infiltration ponds will be done during the non-recharge period. In total, 1.121 million m^3 of water can be recharged daily to the unconfined aquifer beneath the MAR site. The estimated annual recharge capacity is about 290 million m^3.

For the simulation of this full-scale MAR operation, the terraced infiltration ponds were conceptualized into nine polygons. The bottom elevation of the pond and the conductance of the pond bottom were assigned to each polygon. The water depth in each pond was set as 0.4 m, which was derived from the designed inflow rate of the source water. The properties of these nine infiltration ponds are specified in Table 4-1. To simulate the long-term effect of the full-scale MAR operation, the simulation period was set from the year 2020 to 2050 with the monthly stress period. Other sources and sinks were kept the same as the current situation.

Table 4-1 The designed dimension of infiltration ponds for the long-term MAR operation.

Pond number	Width (m)	Length (m)	Pond bottom elevation (m)	Head stage of the infiltration pond during the recharge period(m)	Hydraulic conductance (m^2/d)
Pond 1	350	3400	31	31.4	360 for all ponds
Pond 2	250	2900	32	32.4	
Pond 3	270	1700	34	34.4	
Pond 4	260	1100	35	35.4	
Pond 5	250	690	37	37.4	
Pond 6	260	1200	39	39.4	
Pond 7	200	530	41	41.4	
Pond 8	215	620	42	42.4	
Pond 9	170	300	44	44.4	

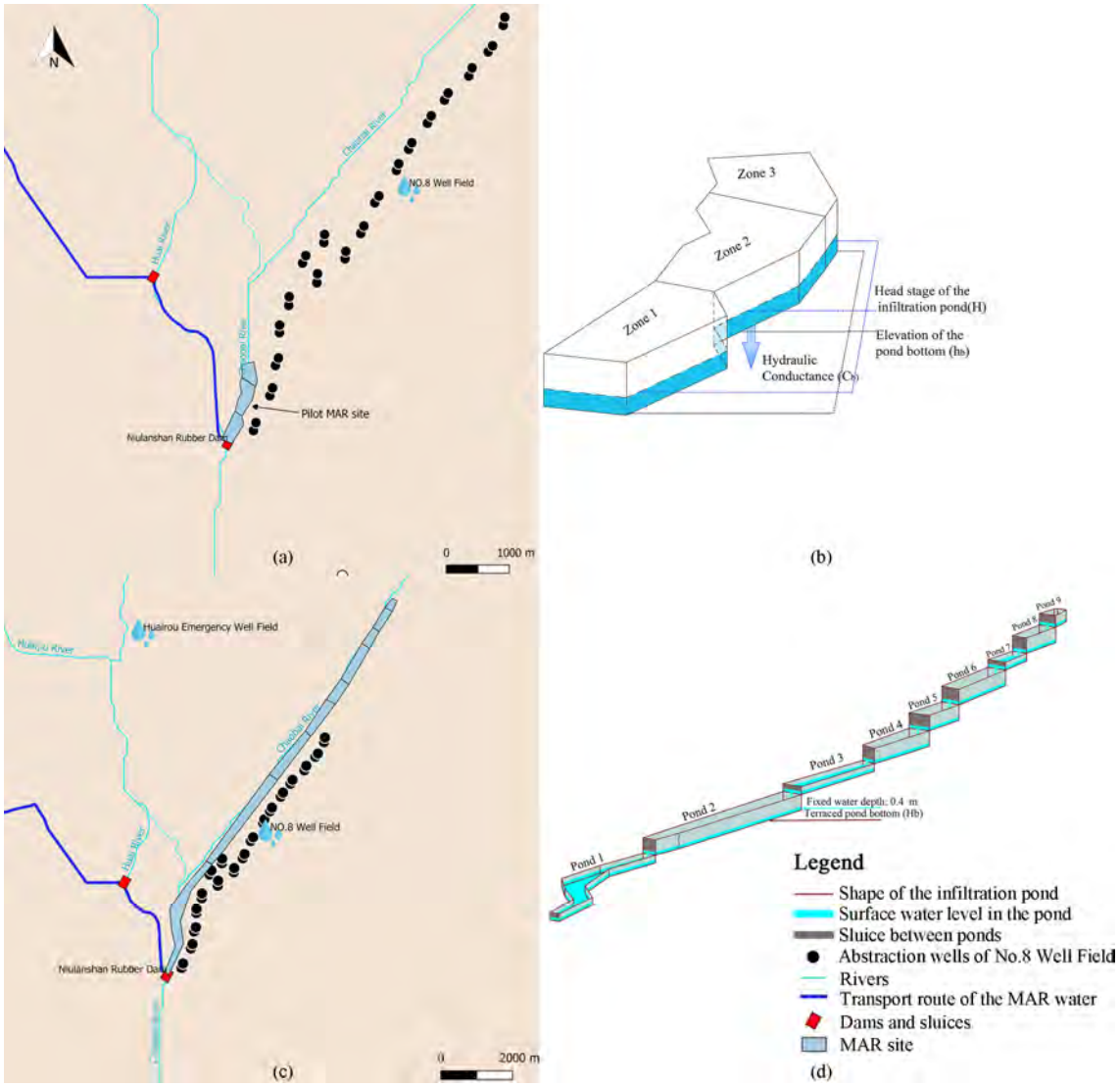

Figure 4-2 Location of the Pilot MAR site (a) and the diagram of the MAR infiltration simulation in the MODFLOW RIV package (b). Location of the full-scale MAR site (c) and the layout of the full-scale MAR scheme consisting of nine cascade terraced ponds simulated with MODFLOW RIV package (d).

4.2.5 Tracking the movement of infiltrated water with hypothetical tracer using transport model

The groundwater flow models of the MAR simulation can help to analyse and predict the recovery of the groundwater head and storage. The mixing process of the MAR infiltrated water with the native groundwater needs to be simulated by a solute transport model (Lautz and Siegel 2006; Ronayne et al. 2017; Ganot et al. 2018). In this study, we are interested to track water particles from the infiltration pond to arrival at pumping wells in the No.8 Well Field. So, the hypothetical tracer representing water particles was simulated

only with advective transport using M3TDMS (Zheng and Wang 1999). Because of the stable and continuous groundwater abstraction of the NO.8 Well Field, the infiltrated MAR water will partially be captured by the abstraction wells used for the urban water supply and partially stored in the aquifer as storage. The groundwater abstracted from the No.8 Well Field (Q_{abs}) is the summation of the groundwater from two sources: a) natural groundwater ($Q_{natural}$) and b) MAR infiltration (Q_{MAR}). A hypothetical tracer was created to simulate the transport of the infiltrated water by the MT3DMS program. The tracer concentration in the MAR infiltration ponds (C_{MAR}) was set as 100mg/L. Only advective transport with Method of Characteristics (MOC) method was considered in this case which means the tracer is conservative and only moves with groundwater flow. The concentration of the natural groundwater ($C_{natural}$) was defined as 0 mg/L. Thus, the concentration of the tracer at the No.8 Well Field (C_{abs}) can be computed by the solute transport model. The water balance and mass balance equations of the tracer can be written as follows:

$$Q_{natural} + Q_{MAR} = Q_{abs} \qquad 4\text{-}1$$

$$C_{natural} \times Q_{natural} + C_{MAR} \times Q_{MAR} = C_{abs} \times Q_{abs} \qquad 4\text{-}2$$

By dividing both equations with the well yield Q_{abs}, applying $C_{natural}$ =0 mg/L and C_{MAR} = 100 mg/L into Equation 4-3. The fractions of the MAR infiltrated water to the well (f_{MAR}) can be derived as Equation 4-4:

$$C_{naturral} \times \frac{Q_{naturaal}}{Q_{abs}} + C_{MAR} \times \frac{Q_{MAR}}{Q_{abs}} = C_{abs} \qquad 4\text{-}3$$

$$f_{MAR} = \frac{Q_{MAR}}{Q_{abs}} = \frac{C_{abs} - C_{natural} \times \frac{Q_{natural}}{Q_{abs}}}{C_{MAR}} = \frac{C_{abs}}{100} \qquad 4\text{-}4$$

Thus, the tracer concentration at the well field is equivalent to a mixing percentage of the MAR water with the natural groundwater. With this solute transport model, the mixing process was traced, and the movement of the MAR water was tracked. In addition, the contribution of the MAR water to the groundwater abstraction at the No.8 Well Field was quantified by checking the mass balance of the solute transport simulation result.

4.3 RESULTS

4.3.1 Transient model calibration

The transient regional groundwater flow model was calibrated by minimizing the residuals of the computed and observed groundwater head by trial and error. Detailed model calibration information can be found in Appendix A. The time-series of the computed and observed groundwater head in three wells in three typical locations are plotted in Figure 4-3. These fitting curves show that the computed heads mimic long-term variations of the observed heads. Groundwater levels in these 3 observation wells show a similar pattern of changes: a long-term trend of decrease and reversal of the decline in recent years. Observation well H01 is located in the shallow aquifer in the eastern plain area (Figure 4-3a). The groundwater level in this well dropped about 7 m from 1995 to 2016. Seasonal periodic fluctuations indicate groundwater recharge in raining seasons. The groundwater level in observation well H02 located near the Beijing urban area shows a larger decrease of about 12 m until 2000. There are several drinking water plants surrounding the urban area mainly supplied by groundwater abstraction. The rapid decrease of groundwater levels occurred in observation well H03 located in the Chaobai River catchment. The groundwater level dropped more than 40 m from 1995 to 2014. This large decline in groundwater levels was caused by intensive groundwater abstraction by the No.8 Well Field and Huairou Emergency Well Field. The annual abstraction during the continuous drought from 1999-2010 was more than 200 million m^3 in the No.8 Well Field. To cope with the groundwater shortage, Huairou Emergency Well Field was installed in 2003, which provided over 240 million m^3 of water every year during the drought period. In this period, an estimated 1.28 billion m^3 per year of groundwater was abstracted by these two well fields. The arrival of the “south water” from the South to North Water Diversion Project by the end of 2014 has reversed the trend of decrease. Since 2015, the Huairou Emergency Well Field has stopped operation, and the annual groundwater abstraction in the No.8 Well Field has been reduced to approximately 60% compared to the drought period. Combined with the artificial groundwater recharge in the Chaobai river channel, the groundwater level has recovered in recent years.

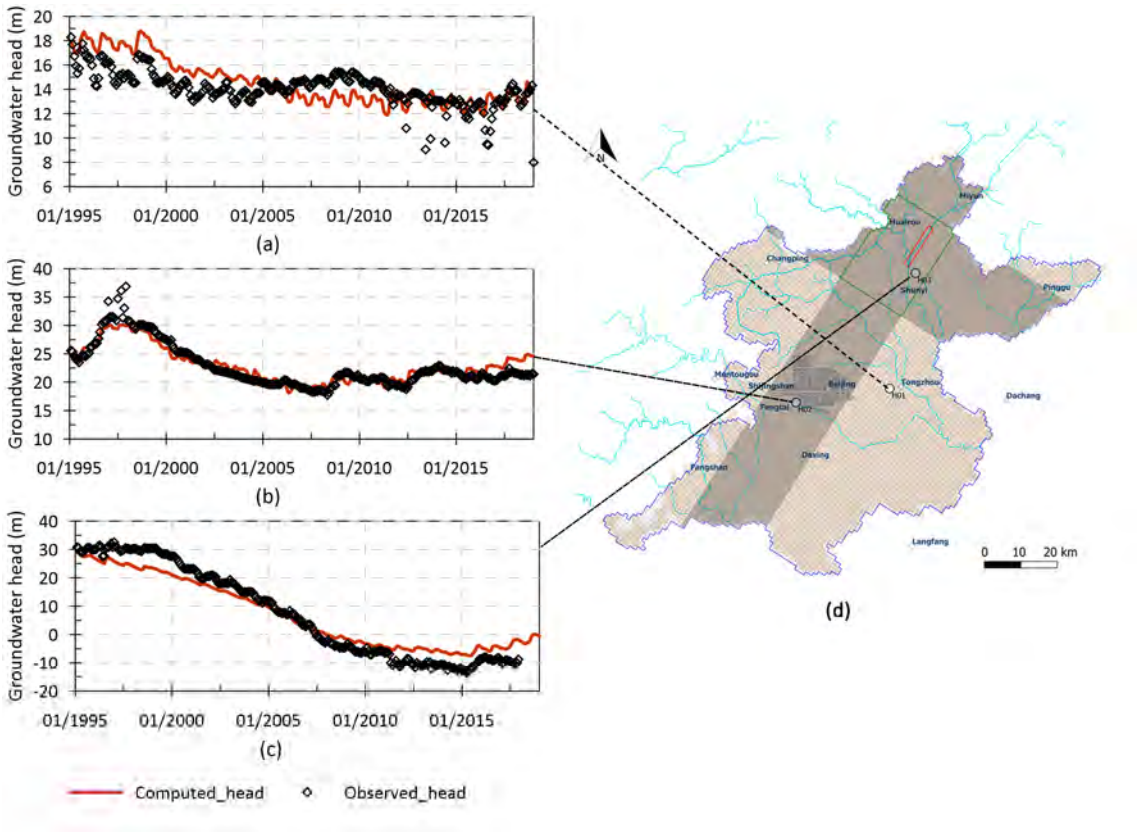

Figure 4-3 Computed and observed groundwater head time series in Tongzhou District (a), Beijing urban area (b), and Chaobai River catchment (c). (d) shows the locations of the three wells.

4.3.2 The overexploitation of groundwater resources in Beijing Plain

In general, due to the frequent drought and intensive groundwater abstraction, the groundwater level has decreased from 1995 until 2015 in most of the area. Figure 4-4a-c shows the simulated groundwater head distribution in the shallow aquifer. A cone of depression gradually developed at the No.8 Well Field near the proposed MAR site in the last 20 years. The maximum drawdown reached 50 m near the No.8 Well Field in 2014. After the pilot MAR operation at the Chaobai MAR site, the cone of depression was reduced in 2018.

The simulated groundwater head distribution in a deeper aquifer (the third aquifer from the top) is shown in Figure 4-4d-f. the cone of depression in the deep confined aquifer was caused by the over-exploitation for industrial water supply. Since the leakage of groundwater in the shallow aquifer to the confined aquifer takes time, groundwater levels in the confined aquifer are still decreasing. The short-term MAR operation has not yet

contributed to restoring the storage depletion in deeper aquifers. It will take a longer operation time before the MAR water reaches deeper aquifers.

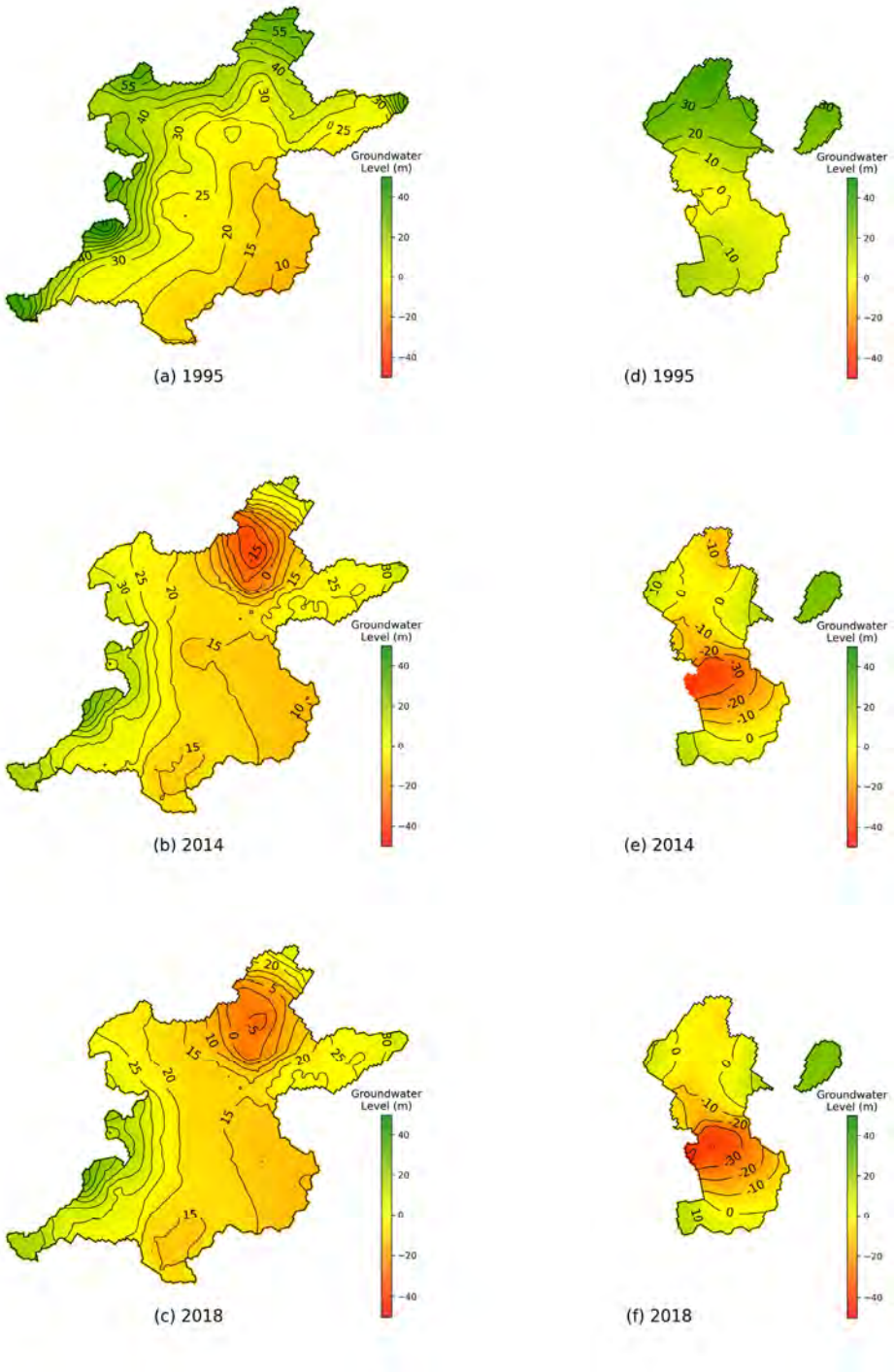

Figure 4-4 Development of cones of depression in the shallow aquifer in January of (a) 1995, (b) 2014, (c) 2018 and in the deeper confined aquifer in January of (d) 1995, (e) 2014, (f) 2018.

Figure 4-5 shows changes of major groundwater balance components and the cumulative groundwater storage change of the Beijing Plain. The majority of groundwater recharge comes from precipitation infiltration and inflow from mountainous areas which varies depending on rainfall amounts. Groundwater abstraction dominates groundwater discharge. Two major events had marked impacts on groundwater resources in the Beijing Plain. The consecutive drought from 1999 to 2010 reduced natural groundwater recharge and emergency groundwater abstraction to cope with the drought increased total groundwater abstraction. These combined effects accelerated groundwater storage depletion since 1999 shown in Figure 4-5. The cumulative storage depletion reached 12 billion m^3 in 2014. The arrival of south water to Beijing stopped further depletion of groundwater storage with the reduction of groundwater abstraction since 2015. However, without increasing groundwater recharge to replenish the aquifer, it would be difficult to recover the depleted groundwater storage in Beijing Plain. Water balance for all flow components is listed in Appendix B Figure B-1

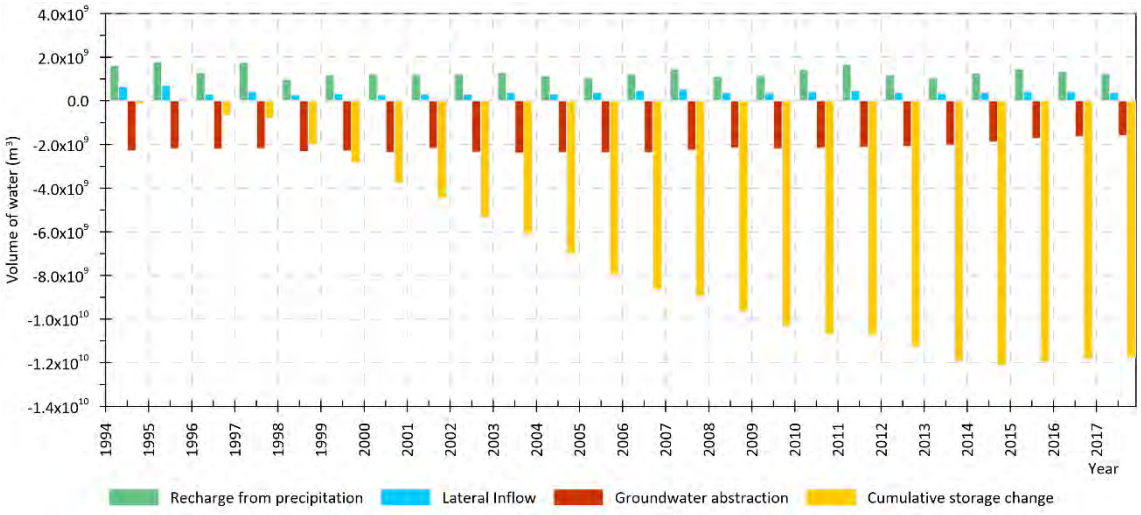

Figure 4-5 Changes of major groundwater balance components computed from the regional groundwater flow model.

4.3.3 Effects of the pilot MAR operation in Chaobai River

The pilot MAR operation was simulated by the local and site groundwater flow model from 2015-2018. Figure 4-6a-c show the computed and observed groundwater head of three observation wells near the Chaobai MAR site. The locations of these three wells are shown in Figure 4-6d. The computed heads show good consistency with the observed groundwater heads. The average residuals of the computed and observed values of these three wells are -1.1 m, -0.36 m and -1.01 m. The groundwater head recovery process after the MAR implementation has been well captured by the local groundwater flow model.

The groundwater level in the shallow aquifer responded quickly to the pilot MAR recharge. During the artificial recharge period, the groundwater level rises up significantly in the observation wells in the vicinity. After the end of each recharge period, the groundwater head was lowered due to the groundwater abstraction at the No.8 Well Field, but shows an increasing trend in general.

The decrease in the groundwater level in the Chaobai River catchment has been reversed and the groundwater storage has recovered since 2015. Both the reduction of the groundwater abstraction and the pilot MAR operation had contributions to the groundwater level increase in the Chaobai River area. The most significant increase in the groundwater level occurred near the Huairou Emergency Well Field. The head increase surrounding the MAR site has reached 10 m in these three years. The groundwater head near the MAR site increased significantly and formed a groundwater mound near the area under the infiltration pond.

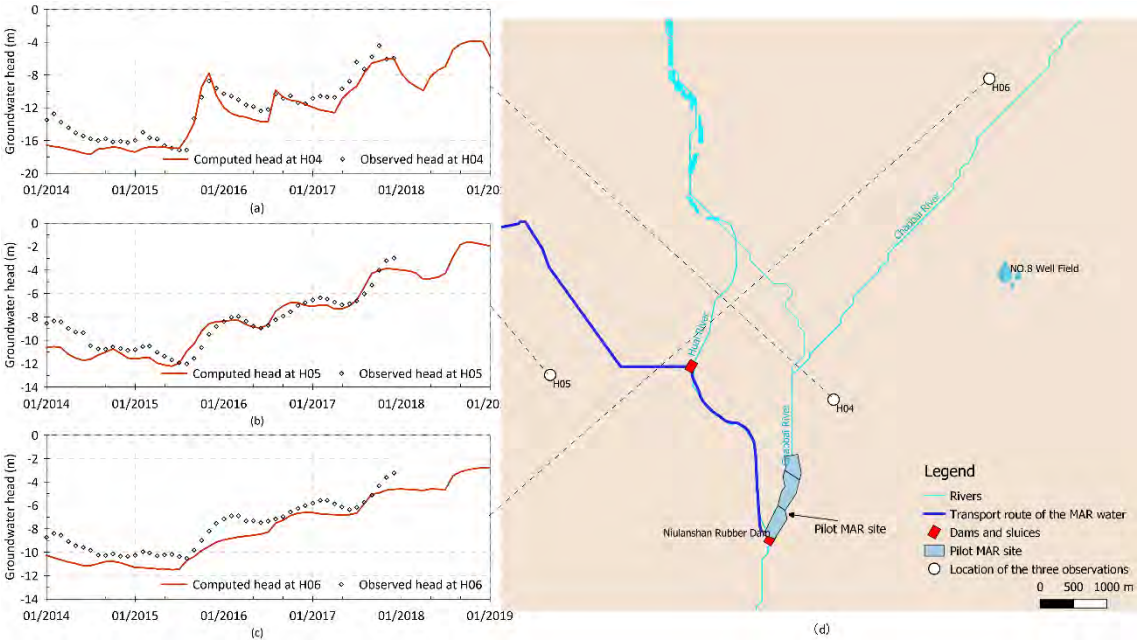

Figure 4-6 The computed and observed groundwater level series near the MAR site. (a)-(c) show the computed and observed heads at three observation wells near the MAR site. (d) shows the locations of the observation wells.

The subregional water budget of the Chaobai River catchment was computed with the Zonebudget program (ZONBUD) (Harbaugh 1990) to analyse the monthly storage change (Figure 4-7a) and cumulative storage change (Figure 4-7b). Because of the intensive groundwater exploitation in the Chaobai River catchment, the groundwater storage was depleted most of the time. The aquifer was only replenished during the rainy season. During the drought from 1999 to 2010, the aquifer storage barely recovered during the wet season. The cumulative groundwater storage depletion in the Chaobai

River catchment reached more than 3 billion m^3 (Figure 4-7b). After 2015, the aquifer received more artificial recharge with the MAR infiltration. The total recharge exceeded the total discharge, so that the groundwater storage depletion was reversed in the Chaobai River catchment.

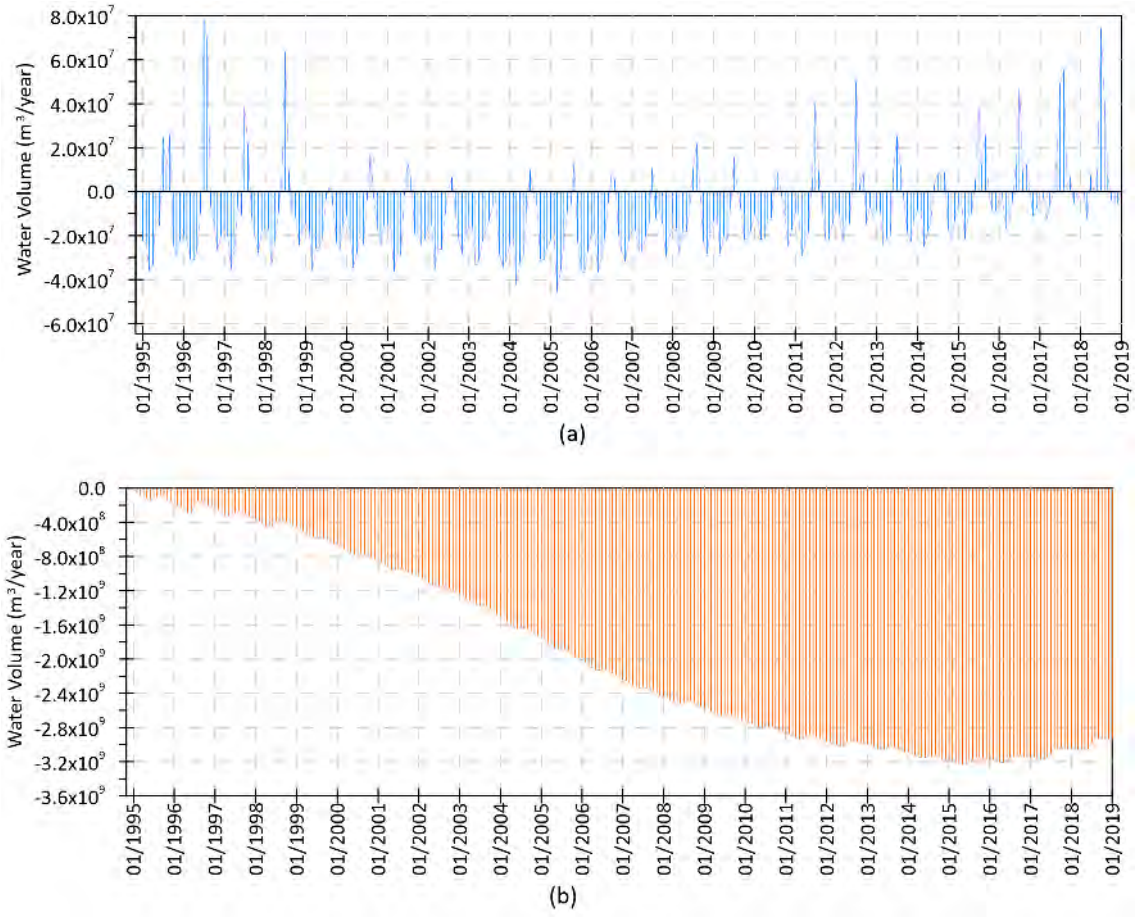

Figure 4-7 Groundwater storage change in Chaobai River Catchment. (a) Monthly groundwater storage change (b) Cumulative groundwater storage change over 1995-2018.

4.3.4 Effectiveness of the full-scale MAR operation in the Chaobai River

The simulation of the full-scale MAR operation in the Chaobai River shows that with the nine terraced infiltration ponds, the groundwater level in the Chaobai River catchment can be notably recovered. Figure 4-8 shows the predicted groundwater level change at the same 3 observation wells (well locations shown in Figure 4-6d) near the MAR site and the predicted groundwater level distribution in the Chaobai River Catchment by the year 2050. After a 15-year operation of the full-scale MAR, the groundwater system will approach a new equilibrium state and the groundwater level will be nearly stable over the

year. The minor variations in each year are caused by the seasonal change of the recharge and the suspension of the MAR operation during the winter months. Generally, the groundwater level would increase by 10 m to 20 m near the MAR site, which is very close to the ground surface. With this magnitude of groundwater level increase, the depleted aquifer will be replenished and the surface water in the infiltration ponds will have direct hydraulic connection with the groundwater. Figure 4-8d is the predicted contour map of the Beijing Plain in the year 2050. Compared with the current situation, the large cone of depression in Chaobai River catchment will be recovered. The groundwater flow direction in the north part of the plain will return to the natural condition of an alluvial fan.

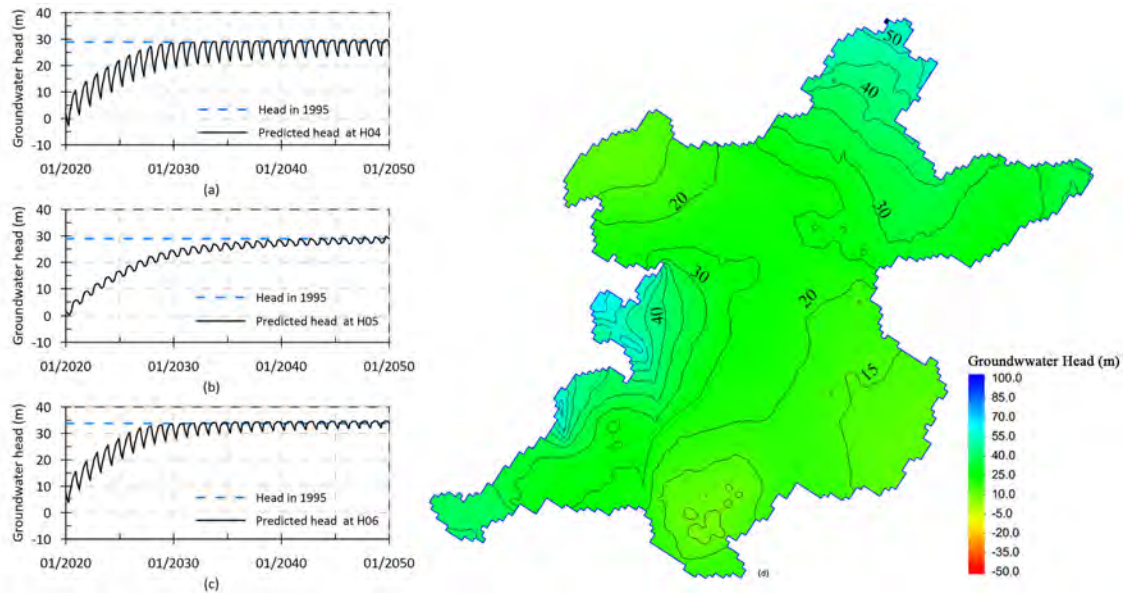

Figure 4-8 Predictions of the groundwater head change in the three observation wells near the MAR site in the year 2020-2050 and the computed groundwater contour map of the Beijing Plain in 2050.

The predicted storage change of the Chaobai River catchment is shown in Figure 4-9. In the first seven-year operation, a high MAR infiltration rate and large groundwater storage recovery can be obtained. The total MAR infiltration can reach up to 270 million m^3 per year while the groundwater abstraction in the No.8 Well Field remains at approximately 127 million m^3 per year. The average annual storage recovery in the first seven-year operation will be about 180 million m^3/year. With an increase in groundwater storage in the area, the groundwater depletion will be reversed, and the cone of depression will be recovered. With this large-scale artificial groundwater recharge, the groundwater discharge to the downstream will increase to 40 million m^3/year in 2027. However, the storage recovery will slow down sharply afterwards because the MAR infiltration rate decreases with the increase of groundwater levels after 2027. By the year 2040, the annual

MAR infiltration rate will be maintained at around 140 million m^3/year, and the discharge to the downstream area will be around 27 million m^3 every year. The system will reach a new equilibrium state in 2050 with the planned full-scale MAR operation.

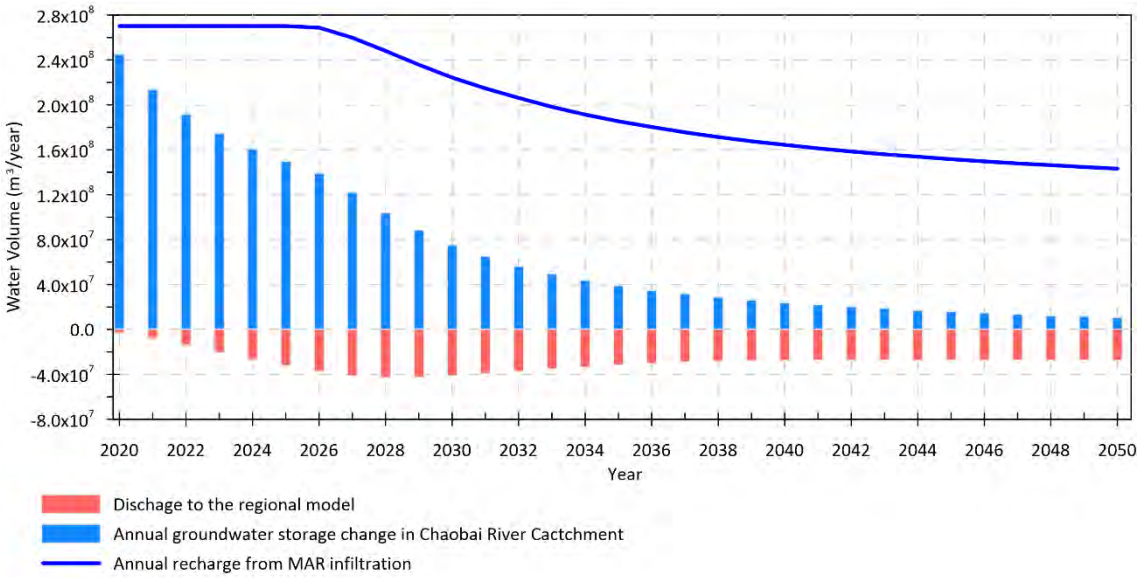

Figure 4-9 Predictions of the annual aquifer storage change and recharge from the MAR infiltration.

4.4 DISCUSSION

Numerical modelling of the groundwater availability is a useful tool for the groundwater management. It has been proved that fragmented and piecemeal arrangements are inadequate to meet the water challenge under the future change in climate and the human activities (Sophocleous 2010). An integrated groundwater model that is continually updated and refined with new data and new groundwater-related projects are very important for the decision maker to evaluate the proposed groundwater management strategies, and formulate future policy towards the sustainable groundwater development (Gleeson et al. 2010; Sophocleous 2010). In Beijing, modelling studies about the MAR implementation are mostly constructed on local scale for the demand of each specific project. For example, the groundwater modelling study for MAR in the Yongding River catchment included a model area of 888 km^2 and defined the western boundary as no flow boundary and the eastern boundary as the general head boundary (Ji et al. 2021). Flow and transport models were constructed in downstream Chaobai river in a 255 km^2 area to evaluate the impact of infiltrating reclaimed water into the riverbed. Constant head and general head boundary were applied (Jiang et al. 2022). These assumptions on boundary conditions may be adequate for the short-term simulation. However, groundwater flow dynamics could change dramatically in the region that is highly urbanised and with

intensive human activities like Beijing Plain. The assumptions on the boundary conditions on the local model would lead to inaccurate long-term prediction results.

The multi-scale groundwater flow model in Beijing Plain we present in this study can overcome the deficiencies of previous model studies. The simulation of the local-scale MAR project will not be restricted by the boundary of the local model but interlinked with the regional groundwater flow model. Moreover, combining with the solute transport model, more insight can be obtained. However, the accuracy of the tracer transport simulation can be improved with a finer grid. We compared the simulation result from a finer grid model with a coarser grid model. It turns out that increasing grid resolution can delineate tracer distribution more accurately. Thus, a multi-scale model is an optimal choice to balance the computational time and the required accuracy of the solute transport simulation. More detailed discussion can be found in Appendix C.

4.4.1 The mixing of the infiltrated water with the native groundwater during the pilot MAR test

Figure 4-10 shows the development of the mixing zone of the MAR water in different years represented by the concentration distribution. At the beginning of the MAR operation in 2015, the infiltrated water started to enter the aquifer shortly but only stayed beneath the infiltration ponds. With the formation of groundwater mound under the infiltration ponds, the infiltrated water was transported into the aquifer in all directions. A large portion of the MAR recharged water was captured by groundwater abstraction at the No.8 Well Field, which prevented the MAR water to move further to the east of the MAR site. After the 3-year artificial recharge, the mixing zone of MAR water reached 3.2 km^2 with 500 m to 700 m extent to each direction of the MAR site.

The contributions of the MAR infiltrated water to some abstraction wells are presented as breakthrough curves in Figure 4-11. The arrival time and fraction of MAR water in the well depend on the location and distance of wells from the MAR site. The abstracted groundwater in Well 01 is 100% MAR infiltrated water all the time since the beginning of the MAR operation. In Well 03 and Well 05, MAR water has become the dominant source during the recharge period. During the period without the artificial recharge, the proportion of the MAR water to the wells was reduced. In Well 07, only until the third year of the artificial recharge, a high percentage of MAR water was detected. The MAR water was not detected in other wells located the north of the infiltration pond further than Well 07.

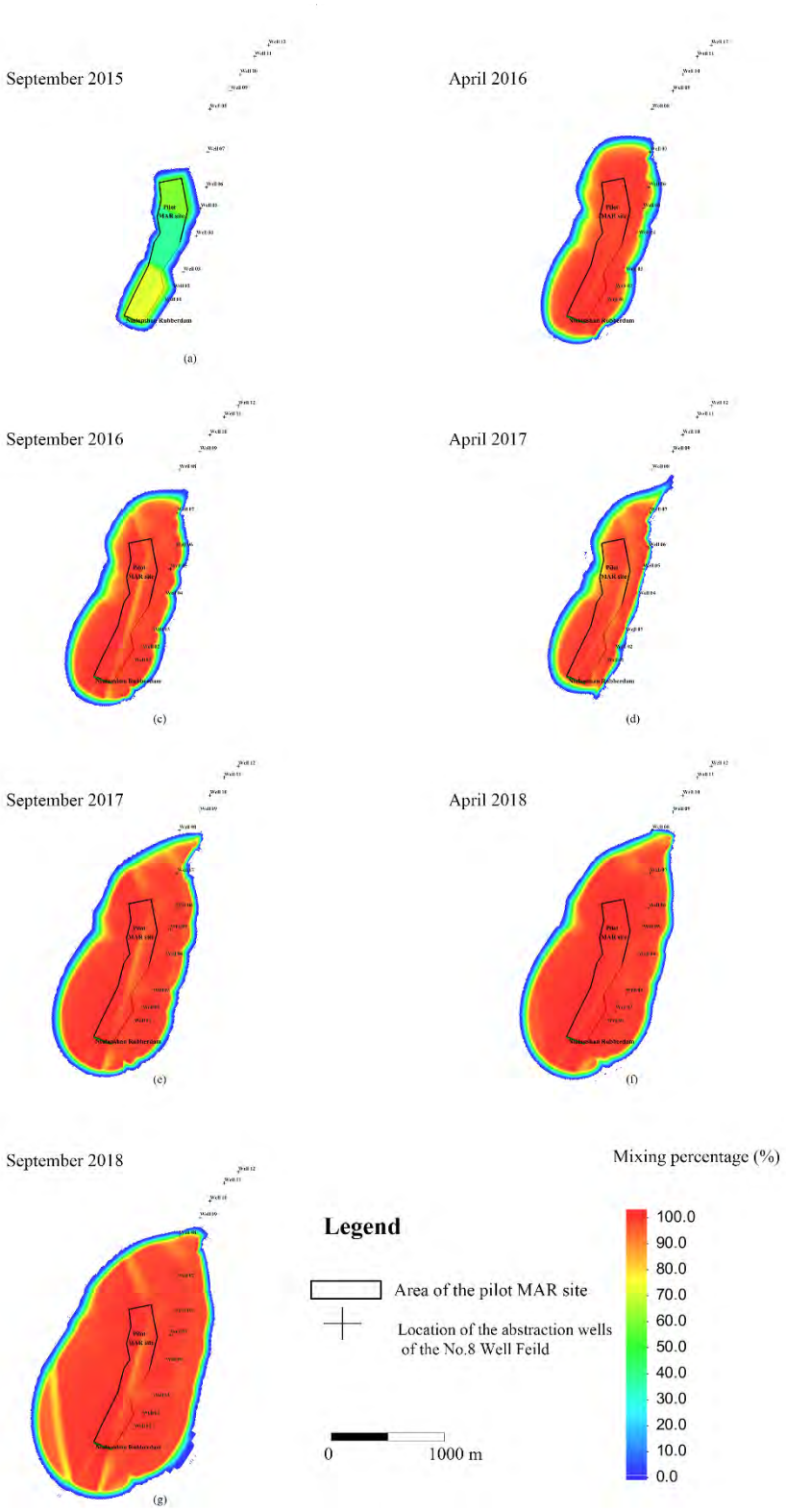

Figure 4-10 Spreading of infiltrated water and mixing percentage of the MAR water with the native groundwater near the MAR site in the shallow aquifer.

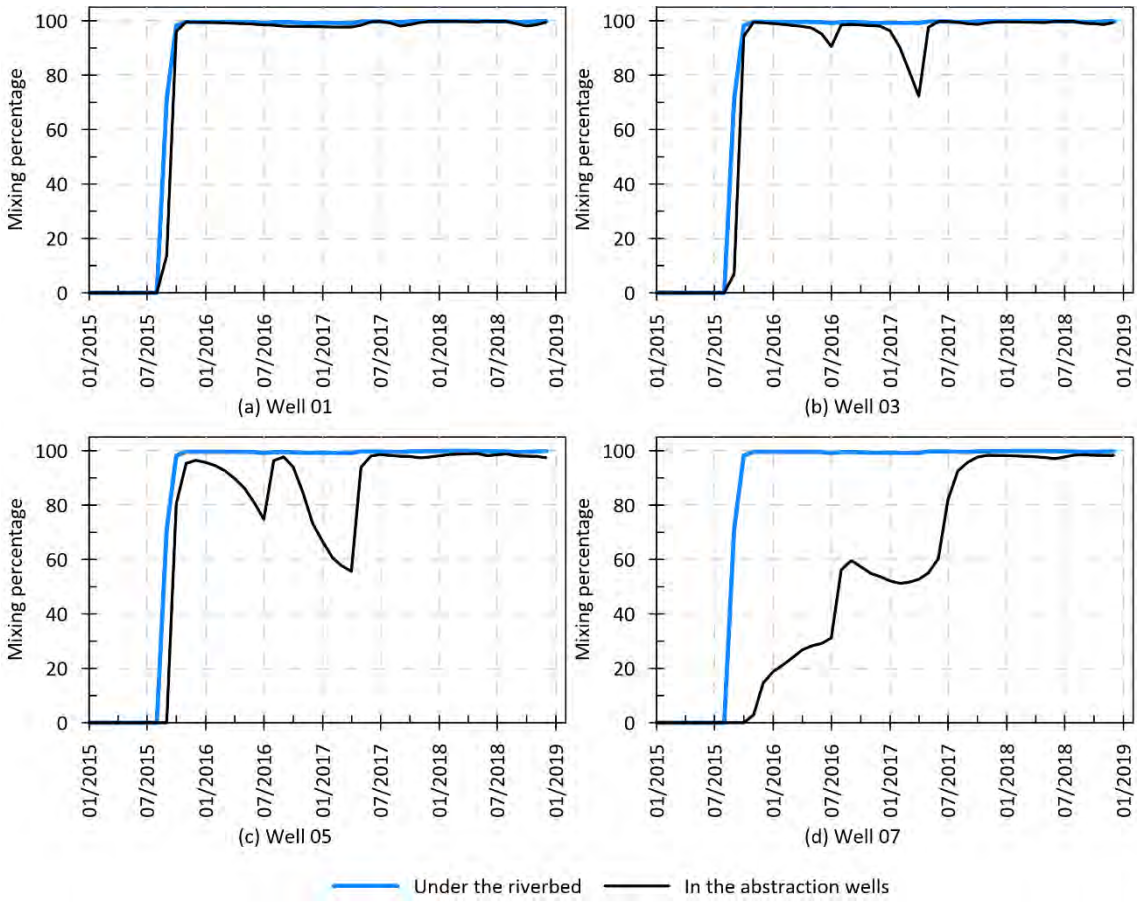

Figure 4-11 The percentage of MAR infiltrated water to each abstraction well at No.8 Well Field.

The mass balance of the solute transport model has also been analysed. The total cumulative mass entering the aquifer from the infiltration ponds and total mass captured by the abstraction wells are plotted in Figure 4-12. The ratio between these two mass volumes indicates the percentage of the MAR water abstracted by the No.8 Well Field. The graph shows at the beginning of the artificial recharge, the contribution of MAR water in the total abstraction is very limited. After three years, in total approximately 40% of the infiltrated MAR water was abstracted by the No.8 Well Field and directly served for the domestic water supply of Beijing City. The other 60% of the infiltrated water stayed in the aquifer contributing to the groundwater level recovery and storage restoration.

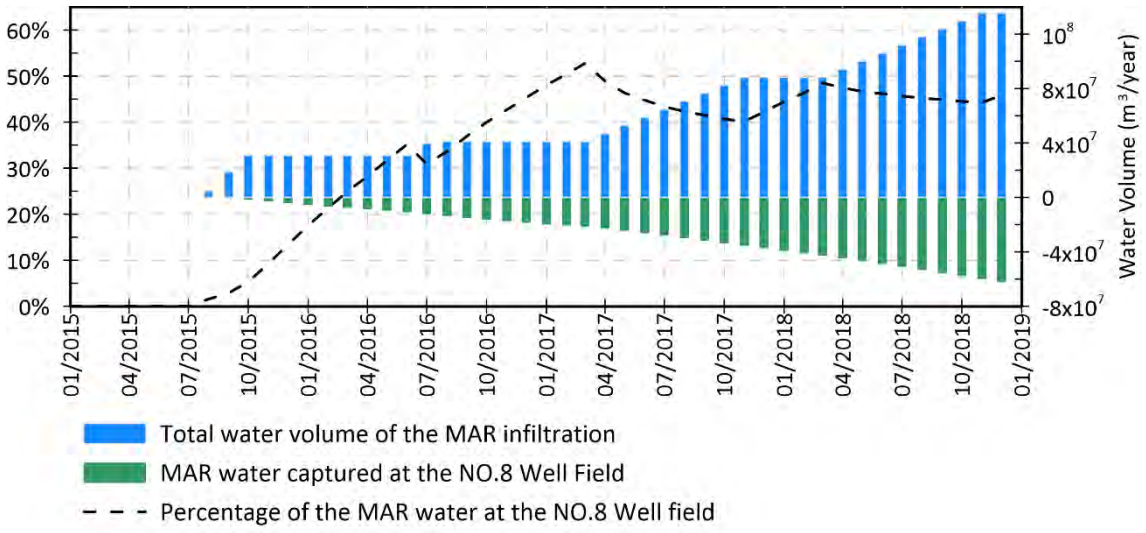

Figure 4-12 The contribution of the MAR infiltrated water to the abstraction of the NO.8 Well Field during the pilot MAR project.

4.4.2 The long-term effect of the full-scale MAR operation on the Chaobai River catchment

The mixing process of the full-scale MAR operation has also been analysed to predict the future trend (Figure 4-13). Generally, with the designed MAR scheme, the mixing zone of the MAR water and the native groundwater will keep increasing in the next 30 years. The area of the mixing zone will be developed from 27.64 km^2 in 2025 to 57.03 km^2 in 2035. However, after 2035, the development of the mixing zone becomes slower. The area of the mixing zone will be 61.86 km^2, 63.96 km^2 and 65.12 km^2 in the years 2040, 2045, and 2050, respectively. The shape of the mixing zone develops evenly in the west, north and south of the MAR site. The mixing zone has a limited extent in the east due to the continuous abstraction by the No.8 Well Field. The mixing zone can serve as the protection zone of the MAR site, which is also one of the key elements of the MAR project design. With the full-scale MAR operation, shallow groundwater levels will occur in the vicinity of the MAR site, which might cause the hazard of groundwater contamination and threatens the safety of the urban water supply. Thus, the solid waste disposal sites in the mixing zone should be surveyed and evaluated before the full-scale implementation to avoid the risk of pollution.

The mass balance from the MT3DMS model (Figure 4-14a) shows that at the beginning of the full-scale MAR operation, only 14.3% of the infiltrated MAR water was captured by the pumping wells in the No.8 Well Field. With the spreading of the MAR water in the aquifer, more MAR water will be intercepted by the No.8 Well Field. Based on the cumulative mass balance result, by the year 2050, 58% of the infiltrated water will be abstracted for the urban water supply. 42% of the infiltrated water will stay in the aquifer

formed as groundwater storage. In this 30-year operation of the system, among the 6.2 billion m^3 of water being infiltrated into the aquifer, 3.6 billion m^3 will be abstracted for the urban water supply, which accounts for 91% of the total groundwater abstraction at the No.8 Well Field. Thus, the water from the MAR project will be the major source for groundwater abstraction in the No.8 Well Field.

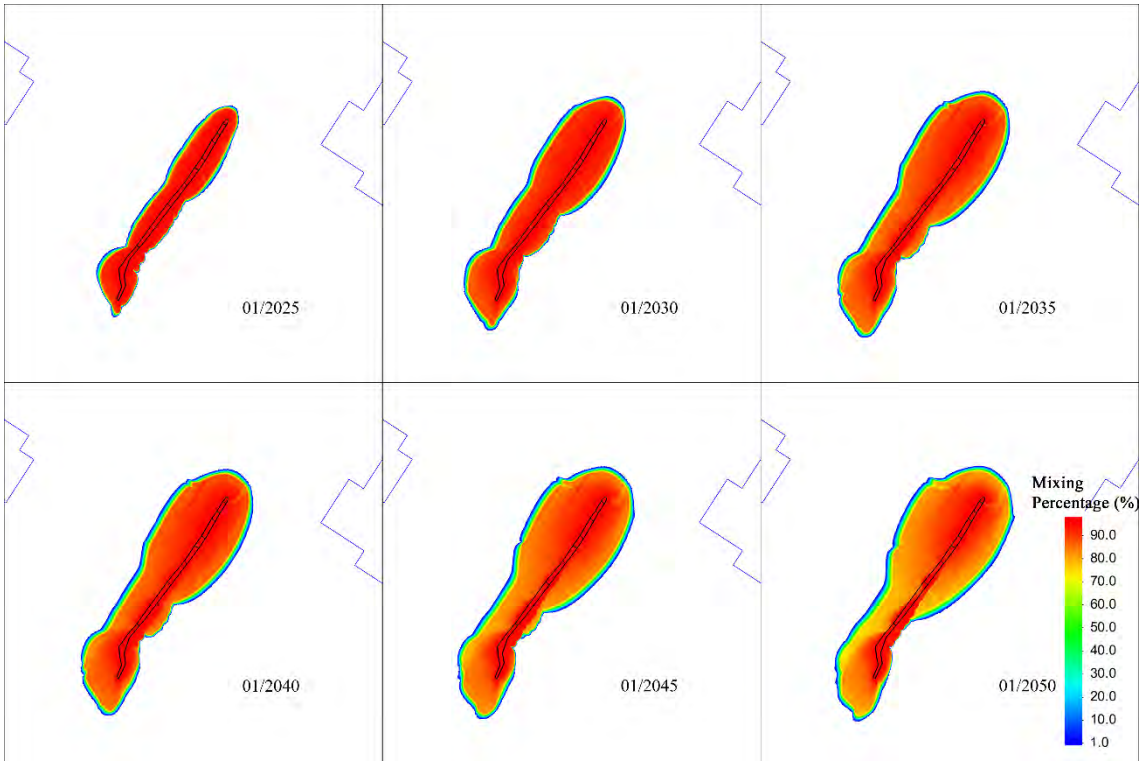

Figure 4-13 Spreading of infiltrated water and the mixing percentage of MAR water with native groundwater after the long-term full-scale MAR operation in 2025-2050.

The predicted total groundwater budget of the Chaobai River catchment is summarised in Figure 4-14b. In the early stages, due to the high infiltration from the MAR implementation, the total groundwater inflow in the Chaobai area will be up to 530 million m^3 in 2020 and gradually lower to 350 million m^3 in 2035. With the groundwater level increase in the vicinity, the total outflow of the area will only slightly increase from 285 million m^3 to 333 million m^3 due to the larger discharge to the downstream aquifer. Thus, with the current groundwater management strategy, the groundwater storage will be accumulated rapidly at first and gently level off until asymptotic to the new equilibrium stage. The groundwater depletion caused by the over-exploitation from the last decades will be gradually compensated. Up to 2050, the cumulative storage increase in the Chaobai area will reach 2.2 billion m^3. It is convinced that the sustainable groundwater development of the Chaobai River region is achievable with the combination of the MAR

implementation and groundwater management plan. However, the impact of the future climate change on the groundwater sustainability of the region still needs to be considered.

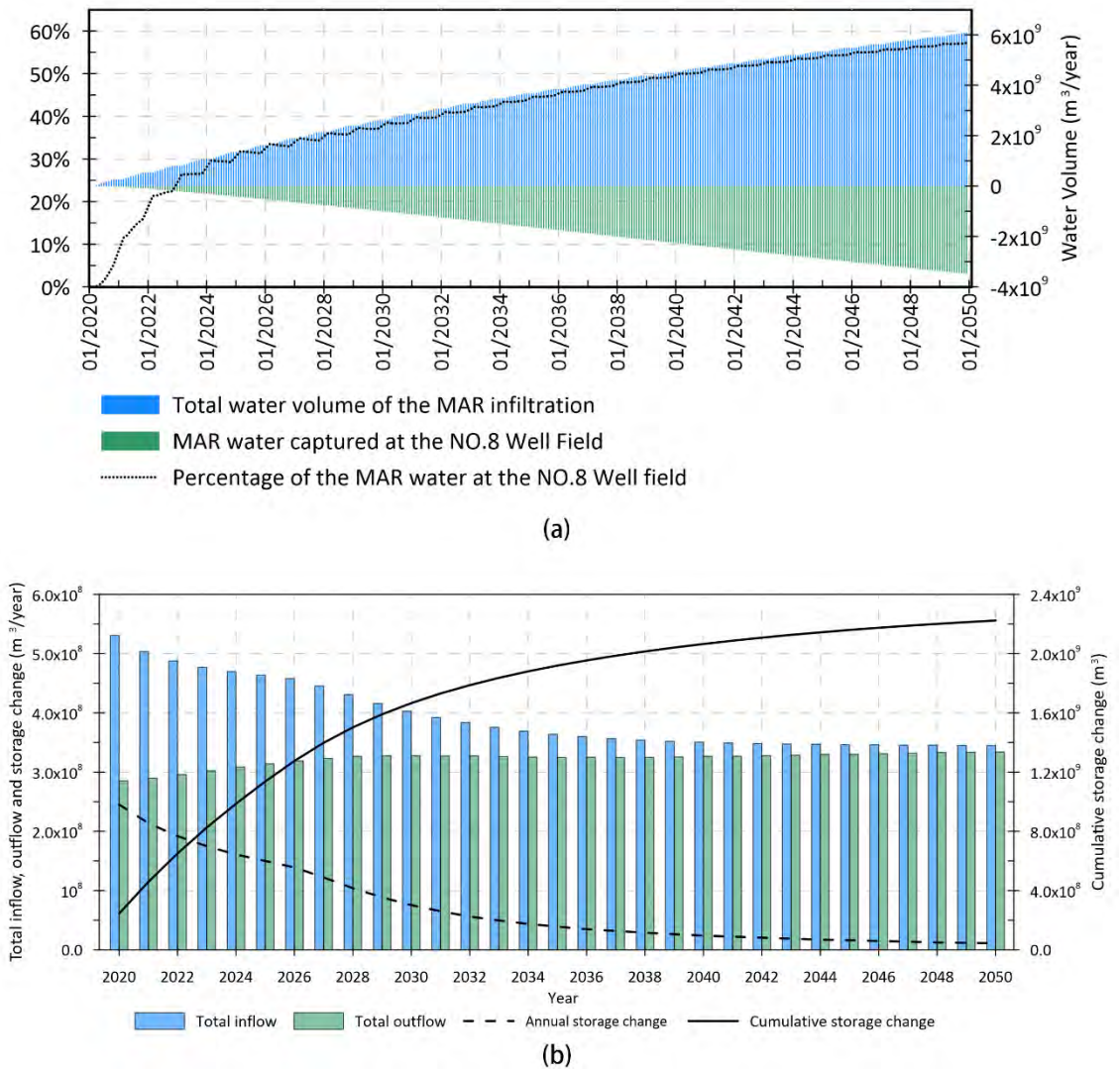

Figure 4-14 (a) The predicted mixing percentage of the MAR infiltrated water abstracted from the No.8 Well Field under the full-scale MAR scheme. (b) The predicted annual total inflow, outflow, storage change and cumulative change of storage in the Chaobai River catchment from 2020-2050.

4.4.3 The decrease of infiltration rate of long-term operation of the full-scale MAR scheme.

In the current situation, the groundwater level is approximately 30 meters lower than the bottom elevation of the infiltration ponds and the surface water is hydraulically disconnected with the groundwater. The aquifer will be recharged with the maximum

infiltration rate. However, with the increase of the groundwater level above the infiltration pond bottom, the groundwater and surface water will be hydraulically connected, and the infiltration rate will gradually decrease. By running the long-term full-scale MAR simulation, the infiltration rate of each pond can be predicted. Figure 4-15 shows the change in the infiltration rate with time for each infiltration pond. At the early stage of the full-scale MAR operation, all infiltration ponds can be operated with the maximum infiltration rate because the groundwater levels are below the bottom of the ponds. However, with the current groundwater abstraction rate and the designed MAR recharge plan, the decrease of the infiltration rate will start in 2027 when the groundwater level in the south becomes higher than the bottom elevation of the infiltration ponds. Ponds 7, 8 and 9 in the north part of the MAR site will maintain a high infiltration rate because groundwater levels remain below the pond bottom in those areas. Among the nine infiltration ponds, the largest decrease in the infiltration rate occurs in the fourth pond, which is the pond where the predicted groundwater head reaches the pond bottom earliest. The infiltration rate of other ponds in the south (ponds 1, 2 and 3) will also drop to some extent. However, because of the existence of the No.8 Well Field, the infiltrated water will be abstracted for urban water supply. This groundwater abstraction forces extra infiltration capacity for ponds 1, 2 and 3 so that the long-term infiltration rate of these ponds can be still maintained between 0.2 m/d to 0.3 m/d by the year 2050. These results show that in the early stage of the MAR operation, the most important factor to obtain high infiltration capacity is the volume of the underground space. However, to design a sustainable long-term MAR scheme, it is vital to optimize the infiltration rate to ensure the infiltrated water can spread to the aquifer to a large extent as groundwater storage or can be directly abstracted for water supply. In the recent decade, reducing groundwater abstraction in the No.8 Well Field has been advocated and implemented. However, the reduction of the groundwater abstraction will also limit the infiltration capacity of the MAR system. For a mega-city like Beijing, increasing water demand is inevitable in the future. The implementation of the MAR and the groundwater exploitation are complementary. On the one hand, the MAR provides a secure water source for the groundwater abstraction. On the other hand, a moderate level of groundwater exploitation in the area can stimulate the potential of the MAR infiltration capacity.

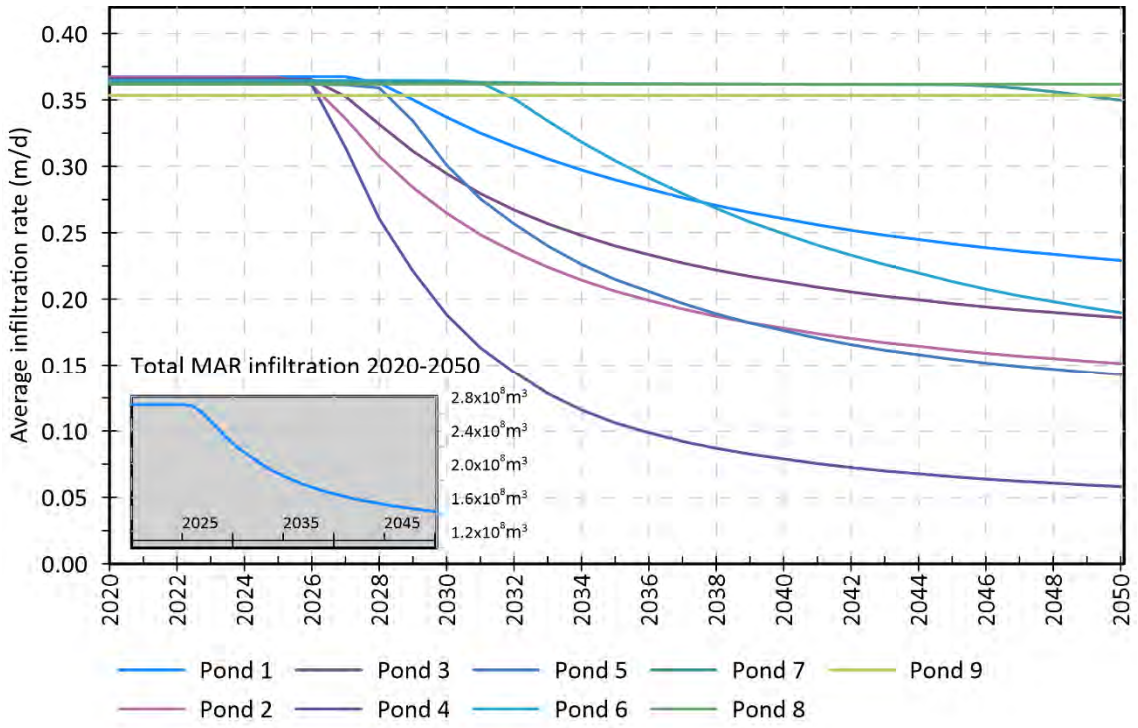

Figure 4-15 Infiltration rate of each infiltration pond from 2020 to 2050.

4.5 CONCLUSIONS

The transient simulation of the regional groundwater flow from 1995 to 2018 revealed large changes in groundwater level and storage in the Beijing Plain. The severe groundwater depletion was exacerbated by the consecutive drought from 1999 to 2010 during which natural groundwater recharge was reduced while groundwater abstraction was intensified. The South to North Water Diversion project was implemented and the south water from the Yangtze River arrived in Beijing in 2014 to substitute equivalent groundwater abstractions. Since 2015, the trend of groundwater level decline was reduced in the shallow aquifer.

The excess of the south water was also used for artificial groundwater recharge in the Chaobai River channel starting in 2015. The coupled multi-scale model simulation shows that the pilot MAR system has recharged approximately 130 million m^3 of water during 2015-2018. A water table mound was formed beneath the MAR site with a maximum recovery of groundwater levels of more than 10m. About 40% of the infiltrated water was captured by pumping wells in the No. 8 well field which contributes directly to the water supply in Beijing.

The effects of the long-term operation of the full-scale MAR were simulated with the coupled multi-scale flow and transport models from 2020 to 2050. The simulation results

show that the designed MAR scheme with 9 cascade terraced infiltration ponds in the Chaobai River catchment is very effective in restoring the depleted aquifer storage and maintaining the groundwater abstraction in the No.8 well field. After about 15 years of operation, the cone of the depression and groundwater levels will stabilize as the aquifer system approaches a new equilibrium state. By the year 2050, about 91% of the total abstraction in the No. 8 well field will come from the infiltrated water. Sustainable groundwater resources development can be achieved in the Chaobai River catchment.

The model results also show that with the increasing groundwater level beneath the infiltration ponds, the infiltration rate of several infiltration ponds will decrease. To maintain a high infiltration rate, groundwater levels beneath the ponds should be kept below the bottom of the ponds. Therefore, groundwater abstractions in the No. 8 well field should be continued with the current capacity. Other environmental problems associated with the rising water table should be investigated which is beyond the scope of this research.

This integrated modelling approach with coupled regional and locale flow and transport processes is an effective tool for designing and assessing MAR schemes. The developed model in this study will be applied to the assess effects of river leakage as a managed aquifer recharge method in the Yongding River in the Beijing Plain. The model approach adopted in this study can also be applied to the design and assessment of MAR projects in the world.

5

EFFECTS OF DOWNSTREAM ENVIRONMENTAL FLOW RELEASE ON ENHANCING THE GROUNDWATER RECHARGE AND RESTORING THE GROUNDWATER/SURFACE-WATER CONNECTIVITY IN YONGDING RIVER, BEIJING, CHINA

Corresponding paper: Liu, S., Zhou, Y., Zang, Y., McClain, M. E., & Wang, X. S. (2023). Effects of downstream environmental flow release on enhancing the groundwater recharge and restoring the groundwater/surface-water connectivity in Yongding River, Beijing, China. Hydrogeology Journal, 1-17.

ABSTRACT

The Yongding River (Beijing, China) was dry most times of the year, and groundwater storage was severely depleted. To address this issue, a river rehabilitation project was initiated. A downstream environmental flow release (EFR) project from upstream reservoirs has been implemented since 2019. This study evaluated the impact of EFR by constructing transient groundwater-flow and numerical tracer transport models to simulate the hydrogeological responses to the water release events in 2019-2020. The study identified two factors that significantly influence the river leakage rate, which are operational factors (i.e., water release rate and duration) and physical factors (i.e., hydraulic properties of the riverbed, regional hydraulic gradients, and groundwater depth) that determine the maximum water availability for groundwater recharge and maximum infiltration capacity, respectively. Predictive modelling was performed to assess the long-term effects of the proposed EFR scheme from 2021 to 2050, which showed that groundwater levels along the river will increase by 10-20 m by 2050. Groundwater storage is expected to be largely recovered and groundwater/surface-water connectivity in the middle reach of the river will be restored. This restoration will not only maintain the environmental flow for the benefit of ecosystems but also enhance groundwater recharge, promoting sustainable groundwater development in the region. Overall, this study provides valuable insights into the effectiveness of the proposed EFR scheme in achieving sustainable groundwater development in the region.

5.1 INTRODUCTION

Flow regimes in rivers globally have been altered by anthropogenic activities, including the regulation by large hydraulic infrastructures, changes in land use, and over-abstraction of water (Harwood et al. 2017). Reductions in river flow result in the degradation of ecosystems globally (Bunn and Arthington 2002; Döll et al. 2009). In order to determine flows necessary to maintain riverine habitats and ecosystem services, the science of environmental flow assessment has been established (Tharme 2003). Internationally, environmental flows are defined as “the quantity, timing, and quality of freshwater flows and levels necessary to sustain aquatic ecosystems which, in turn, support human cultures, economies, sustainable livelihoods, and well-being” (Harwood et al. 2017). Rehabilitation projects to restore drying rivers have been implemented to maintain environmental flows, restore the aquatic ecosystem and biodiversity (Amoros et al. 2005; Rolls et al. 2012; Torabi Haghighi et al. 2018), reduce water supply deficit (Ramírez-Hernández et al. 2017; Tang et al. 2018; Salem et al. 2020), improve river water quality (Tang et al. 2018), and enhance groundwater recharge (Tosline et al. 2012; Kennedy et al. 2017).

Yongding River catchment, in North China, also faces problems of drying up of the main river courses and continuous decline of groundwater levels due to the alteration of its natural flow regime (Jiang et al. 2014). Before the 1950s, flood events occurred frequently and had catastrophic impacts on the agricultural activities in Beijing Plain. Hence, to mitigate the flood risk, many reservoirs were constructed between the 1950s to 1970s. As a consequence, the river discharge was significantly reduced and the river channel downstream dried up. Water pollution was also exacerbated due to increasing discharge of industrial and domestic effluents. Large pits resulting from illicit sand mining were exposed in the downstream riverbed, which heavily altered the natural river morphology and destroyed riparian vegetation.

Moreover, the groundwater system has also been influenced by the alteration of the Yongding River flows. Yongding River was the main source of water supply to Beijing city during 1950-1970. Ever since the drying up and quality degradation of the river, groundwater has been used as an alternative source for the water supply. As a result, the groundwater level in the Yongding River area has declined dramatically since 1980. The lowering of the groundwater level also disconnected the hydraulic connectivity between the groundwater and surface water, further aggravating the drying of the Yongding riverbed downstream (Zhang and Zhang 2017).

To resolve the above-mentioned problems in the Yongding River, a river rehabilitation project has been initiated, which aims to restore the riverine ecosystem and maintain environmental flows (Shao et al. 2021). Since the completion of the Yellow River water diversion project in the upstream, regulated environmental flow releases (EFR) from the upstream reservoirs has been performed. The released water greatly increased the surface runoff in the Yongding River (Sun et al. 2021).

Most of the previous EFR-related studies focused mainly on surface hydrological processes. Groundwater responses to the EFR were neglected and lack detailed assessment. However, groundwater plays an important role in sustaining the streamflow, especially during dry periods of the year (McMahon and Nathan 2021; Lu et al. 2021). The disconnection of the hydraulic connectivity of the surface water and groundwater has effected the hyporheic zone (Hayashi and Rosenberry 2002). Thus, an integrated investigation of surface water and groundwater connectivity is necessary to the design of the EFR operation scheme (Song et al. 2020).

Numerical simulation is an effective tool for analysis of the EFR operation scheme to quantify the surface and groundwater interaction. The MODFLOW program is a commonly used model for simulating groundwater flow systems, which provides packages to simulate the groundwater/surface-water interaction at different levels (Harbaugh 2005; Niswonger and Prudic 2005; Hughes et al. 2012). The results of the groundwater model can provide quantitative information for designing the EFR operation scheme.

In this study, multi-scale transient groundwater models were constructed focusing on the western suburb area of the Beijing Plain to assess the impact of EFR on the groundwater system and surface flows of the downstream Yongding River in the Beijing Plain area. The objectives of the study were to 1) calibrate a refined transient groundwater flow model using the observations of three water release events in 2019 to 2020; 2) estimate enhanced groundwater recharge through river leakage and recovery of groundwater levels and storage; 3) delineate sections of the river where the connectivity of groundwater and surface water is restored; 4) determine influencing factors on the river leakage; and 5) predict the long-term effect of the EFR operation on the groundwater sustainability in the area.

5.2 MATERIALS AND METHODS

5.2.1 Ecological rehabilitation projects in the Yongding River catchment

Management of the Yongding River plays a vital role in controlling floods, securing the water supply, and preserving the riverine and riparian ecosystem of the city of Beijing (Jiang et al. 2014). Figure 5-1 shows a map of the Yongding River catchment. The river flows through five provinces including Inner Mongolia, Shanxi, Hebei, Beijing and Tianjin. The total catchment area is 47,000 km^2 (Figure 5-1a). The length of the main stream is 369 km, with a 2.85‰ average slope of the rivered. In total there are 267 reservoirs constructed along the river. The largest three reservoirs are Cetian, Youyi, and Guanting. The total capacity of these three reservoirs is about 3 billion m^3, and their combined surface area is 43,402 km^2. The annual average discharge above the Guanting Reservoir is around 2.08 billion m^3. With a temperate continental climate, the average annual precipitation varies between 400 and 650 mm in different parts of the catchment. However, the temporal distribution of the rainfall and surface runoff is extremely uneven. Surface runoff during the flood season (July - August) accounts for about 60% of the total runoff throughout the year. The largest annual inflow to Guanting Reservoir was recorded as 3.06 billion m^3 in 1939 and the minimum was only 374 million m^3 in 1972.

Starting from the Guanting Reservoir, the total length of the river channel in Beijing is 189 km and can be characterized into three parts (Figure 5-1b). The mountain part accounts for 108.5 km from the Guanting Reservoir to the Sanjiadian sluice, which meanders with a steep gradient. The upper plain part starts from the Sanjiadian sluice and continues to the Lugou Bridge sluice, with a length of 18.4 km. The river channel is wide and smooth with good permeability. The average width of the river channel is 300 - 500 m. The lower part of the river in the Beijing Plain is around 60 km in length, with an elevated riverbed and lower permeability. The upper part of the alluvial plain has relatively simple geology. The Quaternary deposits consist mainly of gravel and sand

with high permeability. The average thickness of the unconfined aquifer varies from 30 to 50 meters. This aquifer is underlain by bedrock characterised as a prevailing layer with significantly lower hydraulic conductivities. Figure 5-1d and 1e are two cross sections showing the hydrogeological conditions of the Beijing Plain and Yongding River.

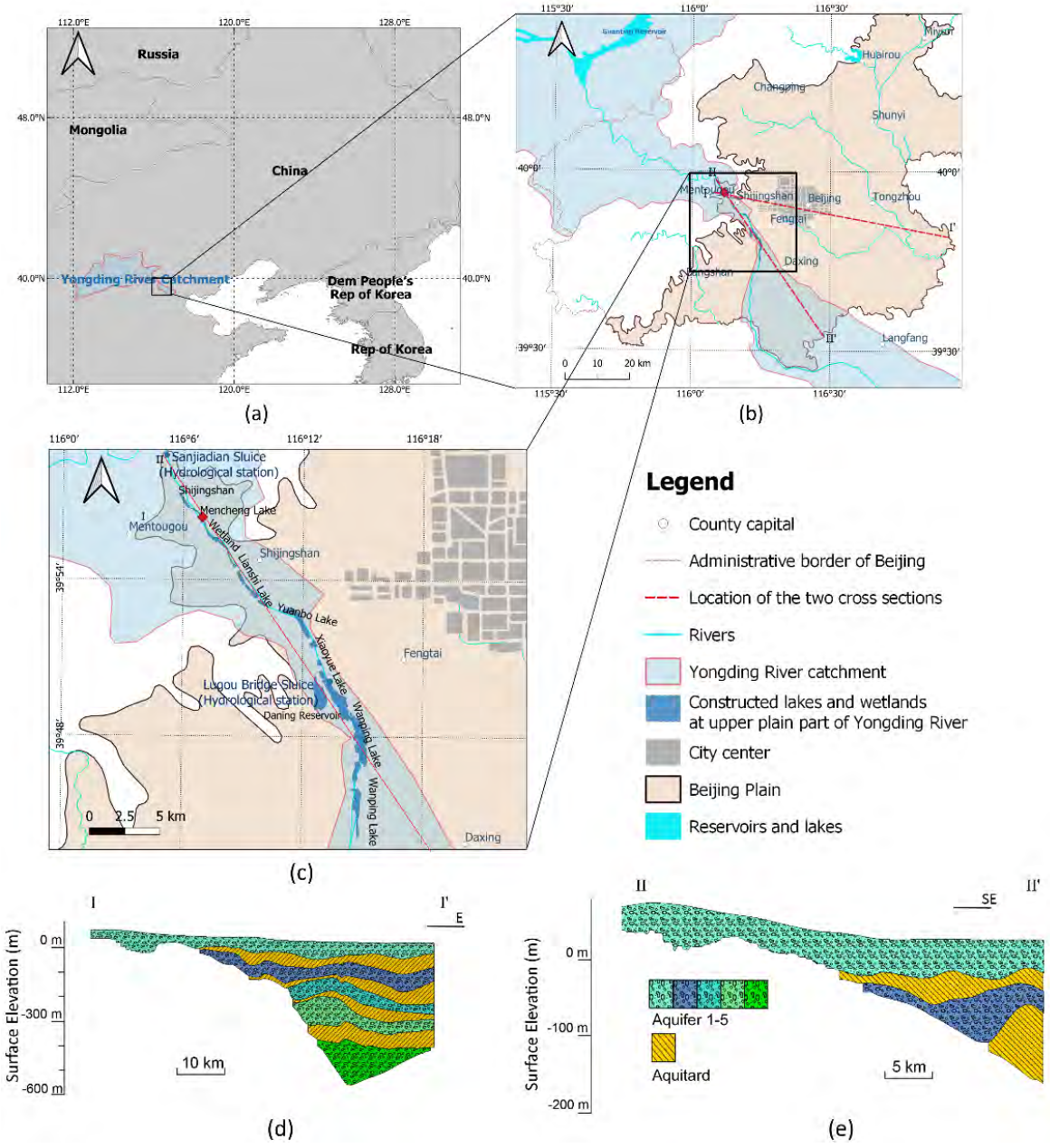

Figure 5-1 Map of the Yongding River catchment in different scales and two cross sections.

In 2009, Beijing Water Authority launched the project "Yongding River Green Ecological Corridor", aiming to rehabilitate the riverine ecosystem and maintain the environmental flow of the river (BWA 2009). The water quality of the Guanting Reservoir was improved by constructing wetlands. Riparian vegetation destroyed by the sand mining in the Beijing Plain area was restored, which helped to prevent sandstorm hazards and soil erosion of the riverbed. Large sand mining pits were converted into 4 lakes: Mencheng lake, Lianshi lake, Xiaoyue lake, and Wanping lake (Figure 5-1c). To prevent large river leakage, liners were placed on the middle part of the lake bottom, which help to maintain a minimal water level in the lake (Hu et al. 2019a). Reclaimed water from wastewater treatment plants has been discharged to the Yongding river channel to maintain river flow since 2010. The estimated river leakage to the aquifer in 2010 was only 16,500 m^3 which is negligible (Hu et al. 2018). Thus, most of the river channel remained dry and only the lakes were filled with water. In 2017, the north route of the Yellow River Diversion Project was launched. Water from the Yellow River was diverted to several reservoirs along the Yongding River, which increased the water availability to implement the EFR (Liu et al. 2016). To better recover the riverine ecosystem in the plain part of the Yongding River, a number of wetlands were constructed including Yuanbo lake (Figure 5-1c). The total storage capacity of these lakes is approximately 21 million m^3.

In 2019, the large-scale EFR from the upstream reservoirs to the Yongding River channel started on March 16th and continued for 93 days until June 16th. The total discharge from the Sanjiadian Sluice was 132 million m^3 (Ma et al. 2020). In 2020, there were two release events of shorter duration in spring and autumn. Before the flood season, 142 million m^3 of water were released during 32 days from April 21st (Zhao et al. 2020). Later on October 14th, 51 million m^3 of water were released in 22 days (Wu et al. 2021). It has been reported that with release events during 2019-2020, the riverine ecosystem in Yongding River has significantly improved (Shao et al. 2021). Besides, groundwater levels near the Yongding River channel recovered after the release events. Figure 5-2 shows the long-term historical groundwater level changes in an observation well near the Yongding River alluvial fan (location of the observation well Figure 5-1c). Due to the continuous drought from 1999 to 2010 and groundwater over-exploitation, the groundwater level decreased by more than 15 meters. Groundwater levels started to recover slightly after 2015 because of the reduced groundwater abstraction when the transferred water from the south-to-north water diversion replaced partial groundwater abstraction in the area. The groundwater level has recovered significantly with the operation of the EFR since 2019.

5.2.2 Use of groundwater flow model to compute river leakage

To understand the response of the groundwater system to the EFR and the effectiveness of the enhanced groundwater recharge in restoring groundwater depletion, a multi-scale 3D transient groundwater flow model was constructed and calibrated using MODFLOW-

2005 (Harbaugh 2005). The refined local model for the Yongding River area was constructed based on the regional model of the Beijing Plain developed in the earlier study. The regional groundwater model was constructed to simulate the monthly groundwater level changes and compute the groundwater storage change during 1995-2018 in the Beijing Plain (Liu et al. 2022b). The model only covers the Beijing Plain area (Figure 5-1b). The west and north boundaries lie along the contact between the hard rocks of the mountain areas and the alluvial deposits of the plain area. The effects of hard rock aquifers in the mountain areas were simulated by setting a lateral inflow boundary along the boundary. The model consisted of nine model layers including five aquifers and four aquitards. Table 5-1 summarizes the boundary conditions, parameter setting, sources and sinks of the regional model and specifies the package used in MODFLOW.

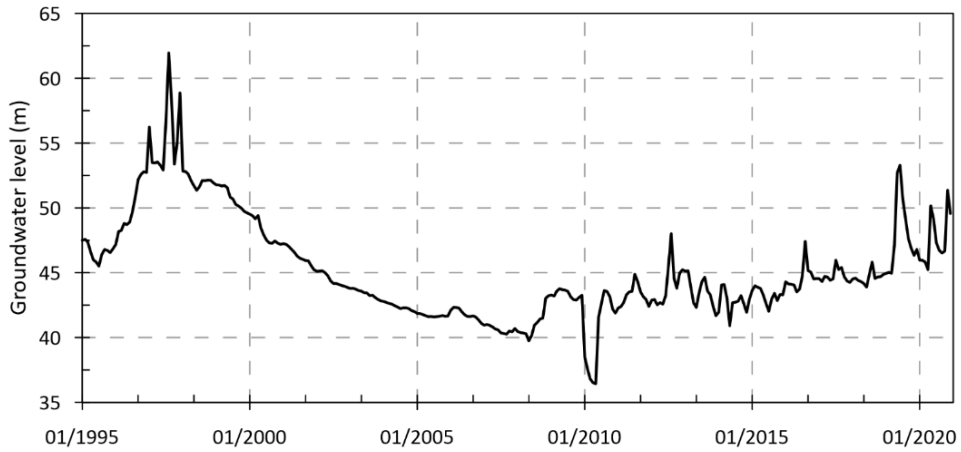

Figure 5-2 Groundwater level changes from 1995-2021 in the Yongding River alluvial

In this study, the regional model grid of 1000 m by 1000 m was refined with a local grid of 100 m by 100 m in Yongding River area (Figure 5-3a). Figure 5-3b shows the refined local model grid and lakes and wetlands along the Yongding River. In total, 19 columns and 28 rows of the regional model were refined into a local model grid of 190 columns and 290 rows, accounting for 7.6 % of the entire model domain. In the Yongding River alluvial fan, only a single layer of gravels was present (Figure 5-1d and 1e) and was simulated as unconfined aquifer with the top model layer. The model calibration period was set as three years from 2018 to 2020 when EFR was conducted. The stress period was set as daily during the EFR events and monthly for the rest of the time to save computation time. The starting head was taken from the computed groundwater heads from the regional model in January 2018.

Table 5-1 General information on the regional groundwater flow model

Feature	Model components	Conceptualization	Package in MODFLOW
Boundary conditions	Lateral inflow from mountain fronts	Specifying the inflow distributed along the boundary between mountain fronts and plain area, simulated by injection wells.	WEL
	Flow exchange through administrative borders in the south and east plain	Set as head-dependent flow boundaries, and the head and conductance were specified along the administrative border at the southern and eastern plain boundary.	GHB
Parameter settings	Hydraulic conductivity and storage coefficient	Specified by mapping parameter zones for each aquifer and aquitard based on the hydrogeological condition.	LPF
Sources	Groundwater recharge from precipitation	Calculated from the rainfall data and converted into groundwater recharge by assigning infiltration coefficients for each subregion.	RCH
	Irrigation return flow	Calculated by the reported agricultural water usage and converted into return flow during the irrigation months.	RCH
	Pipeline leakage	Estimated as a constant amount of leakage and assigned to the urban area.	RCH
	Leakage from rivers and canals	Estimated the total volume of the leakage and distributed it into different months and specified as injection wells.	WEL
	Groundwater recharge from EFRs	Specifying the surface water level and conductance of the infiltration basins/riverbed	RIV
Sinks	Groundwater abstraction for domestic, industrial, and agricultural use.	Distinguish the volume of groundwater use for different purposes and distribute the volume based on the annual Beijing water resources bulletin	WEL
	Groundwater evapotranspiration	Converted from the evaporation data from meteorological stations and specifying the maximum evaporation depth	EVT

River (RIV) package of MODFLOW was used to simulate the leakage from lakes and wetlands. Due to the channelization and lining of the river, most of the surface water leakage occurs at the constructed lakes and wetlands along the river channel. There are in total five lakes, two wetlands and a surface water reservoir, which have been conceptualized into 17 polygons based on their hydraulic properties (Figure 5-3b). Data for the RIV package include river bottom elevation (H_b), the riverbed conductance (C_{RIV}) and river head stage (H_{River}), which are listed in Table 5-2.

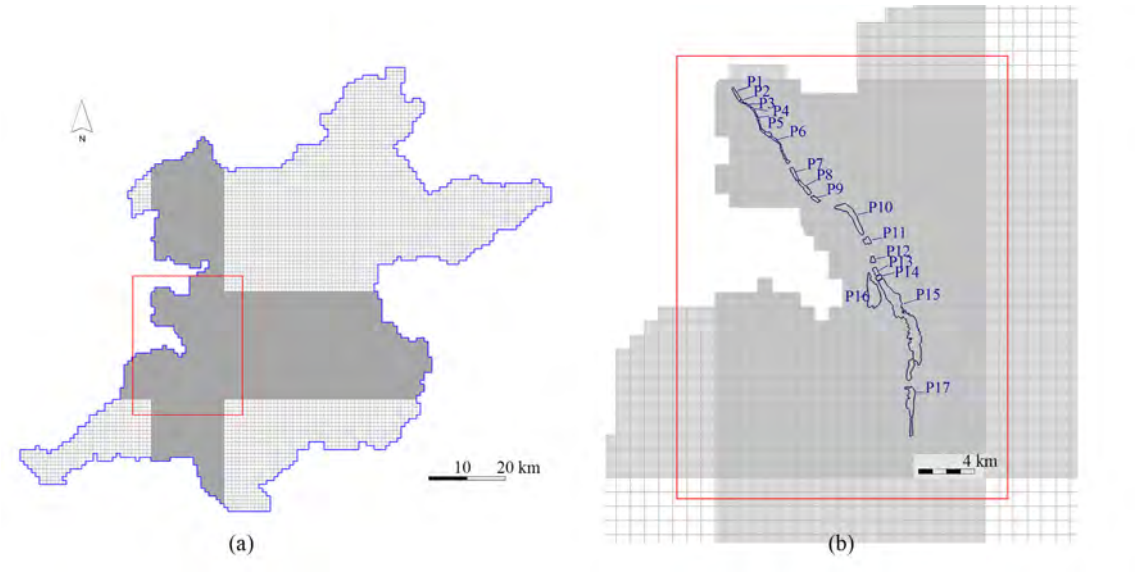

Figure 5-3 (a) Spatial discretization of the regional model and the local refinement. (b) Spatial discretization and the conceptualization of the lakes and wetland parks in Yongding River.

The river stage of each polygon was initially estimated from the total released water reported at the two hydrological stations, and the infiltration area of each polygon was slightly adjusted based on the simulated results. River conductance was assigned an initial value based on the hydrogeological conditions and calibrated by matching the computed groundwater level with the observed levels from the 46 observation wells (Figure 5-4) in the vicinity. Afterwards, the leakage rates for all lakes and wetlands were computed and the contribution of the enhanced groundwater recharge for the recovery of the aquifer system was analysed.

Table 5-2 Data for the River package: river bottom elevation (H_b), riverbed's hydraulic conductance (C_{RIV}) and the river stage (H_{River}) of each lake or wetland.

ID	Name	Area (m^2)	H_b (m)	C_{RIV} (m^2/d)	H_{River} (m)		
					2019 Spring	2020 Spring	2020 Fall
P1	Shijingshan	181,469	97	2220	100.11	100.57	99.88
P2	Yongdinglou	32,587	95	2030	97.84	98.57	97.88
P3	Mencheng Lake1	56,667	95	1830	98.95	98.57	97.88
P4	Mencheng Lake2	52,177	92	1830	95.56	96.07	94.88
P5	Mencheng Lake3	54,528	90	1720	93.57	94.17	92.88
P6	Wetland	483,850	85	1010	88.42	88.87	87.8
P7	Lianshi Lake1	218,785	75	1110	78.42	77.81	77.88
P8	Lianshi Lake2	303,206	71	1110	74.83	74.97	73.88
P9	Yuanbo Lake1	142,549	67	1320	69.63	70.97	69.84
P10	Yuanbo Lake2	1,057,740	60	1320	62.14	64.17	62.7
P11	Xiaoyue Lake1	198,250	59	911	60.14	62.37	60.7
P12	Xiaoyue Lake2	123,626	57	1320	58.14	60.37	58.7
P13	Xiaoyue Lake3	163,284	55	709	56.14	58.37	56.7
P14	Xiaoyue Lake4	119,363	55	608	56.14	58.37	56.7
P15	Wanping Lake	4,690,935	43	385	43.28	46	44.98
P16	Daning Reservoir	1,052,598	43	101	43.92	46.37	44.64
P17	Wanping Lake2	1,500,814	41	354	41.42	44.6	42.35

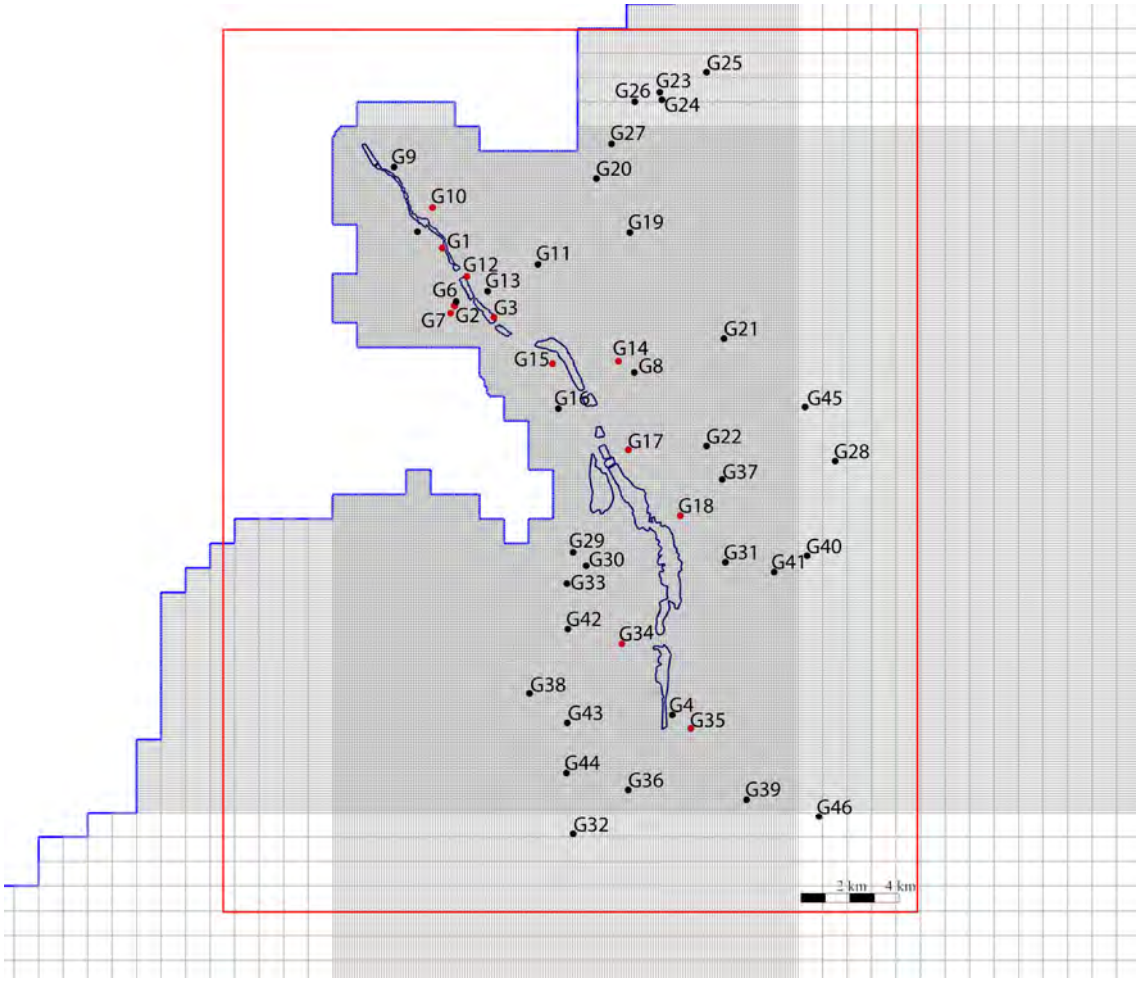

Figure 5-4 Location of the observations near the Yongding River groundwater EFR site (Beijing Water Authority 2021b)

5.2.3 Tracking the movement of the leakage water by MT3DMS

The risk of groundwater pollution from the EFR implementation should be addressed since the surface water quality has larger variation (Alam et al. 2021). Tracking of the infiltrated water and the mixing process provides information to delineate the area under risk of pollution. The movement of the infiltrated water can be tracked by a particle tracking technique. In this study, the MT3DMS program (Zheng and Wang 1999) was used to track the movement of leakage water from the river during the EFR events. A numerical tracer, with a concentration of 100 mg/L, was assigned in river polygons, while the background tracer concentration was set to 0 mg/L. Effective porosity was specified based on the soil type properties for each parameter zone. The advective transport was run to simulate tracer spreading along the river, using the MOC method. The computed tracer concentration delineates the area of spreading leakage water and the percentage of leakage water mixing with native groundwater.

5.2.4 Prediction of long-term effect on sustainable groundwater development

The EFR is implemented as a measure to maintain the environmental flow and sustain the riverine ecosystem of Yongding River. The positive side effect is enhanced groundwater recharge. Thus, the long-term effects of the EFR on the groundwater system should be assessed. The main aim of the prediction model was to quantify the contribution of the river leakage from the Yongding River channel to the groundwater storage recovery, and to investigate the potential future surface-water/groundwater interaction due to the enhanced groundwater recharge. The prediction model uses a monthly stress period and covers the period from 2021 to 2050. The initial condition was set as the computed groundwater heads in December 2020 from the current model. Groundwater abstraction remains the same as that of 2020 for future periods. Additionally, the simulation also includes the EFR in the Yongding River, which are modelled by the RIV package. The release scheme in 2019 is used in the prediction models for all the years. Other hydrologic sources and sinks of the model also remain the same as in 2020 for future stress periods. The groundwater recharge from precipitation was derived from the projected monthly precipitation of the Representative Concentration Pathways (RCP) 4.5 climate scenario of the CCLM5-0-2 Regional Climate Model. Variance-based bias correction was applied to the monthly precipitation output of the CCLM5-0-2 model before conducting further study. Since the lateral inflow from the mountains to Beijing Plain is also dependent on precipitation, it will be influenced by future precipitation variation. Therefore, the prediction model also considers the variation of lateral inflow. Water balance results from previous models indicated that the recharge from the lateral inflow contributes approximately 10% of the total inflow and 20% of the precipitation infiltration. Accordingly, the input for future lateral inflow was calculated as 20% of the projected precipitation with monthly variations. The results of the prediction model offer insight into the effects of the EFR project on the groundwater system over a long-term period.

5.3 RESULTS

5.3.1 The response of the groundwater flow system to the EFR events

Figure 5-5 shows scatter plots of computed groundwater head versus observed head for the stress periods of the two EFR events in 2020: May and November. Most of the computed heads fit the observations well. The coefficients of determination of the two stress periods are 0.874 and 0.878, respectively. The average residual errors of the two stress periods are -0.42 m and -0.71 m, while the root mean squared error (RMSE) values are 3.59 m and 2.87 m, respectively. In general, the simulated groundwater heads are slightly overestimated at the upper reach and underestimated at the lower reach. However,

the flow model was able to capture most of the peak groundwater levels in response to each EFR event. Figure 5-6 displays the time series of computed and observed groundwater heads in 12 observation wells (highlighted in red in Figure 5-4) located in the upper, middle, and lower parts of the river. Three groundwater level peaks can be captured at most of the observation wells, which correspond to the three EFR events. The trends of the computed groundwater-level change are mostly in line with the observed trends, which verifies the reliability of the simulation results.

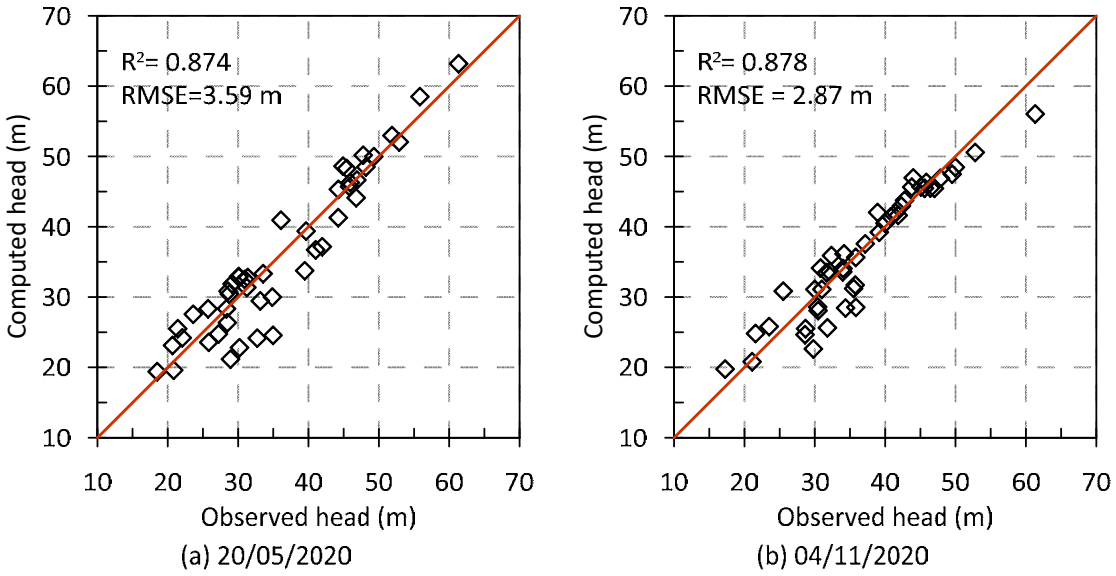

Figure 5-5 Scatter plot of the computed versus observed groundwater heads from the groundwater flow model results in May and November 2020.

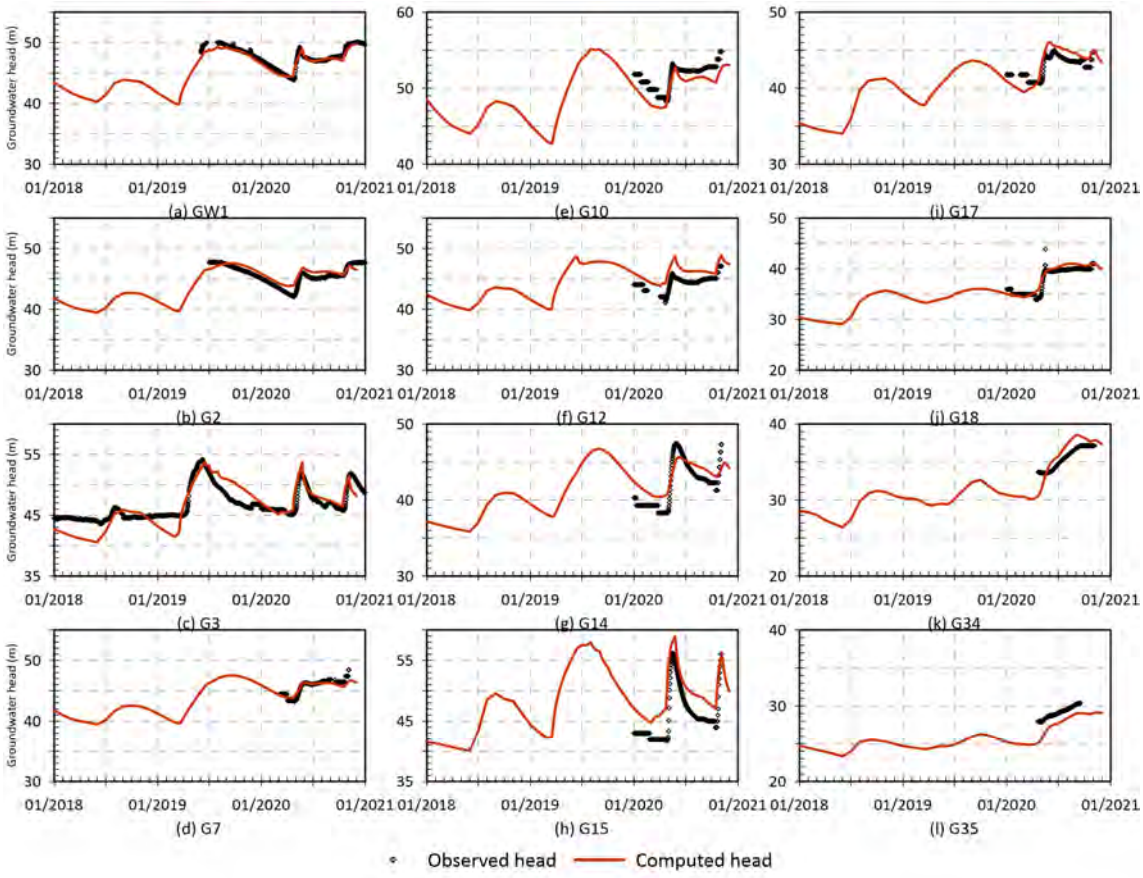

Figure 5-6 Time series of computed and observed groundwater heads in 12 observation wells distributed along the Yongding River channel.

Figure 5-7 shows maps of the groundwater level contours before and after each EFR event. The groundwater flow direction follows mainly with the topographical gradient from the west suburb region towards the south and east. In general, the patterns of the contour are similar for the three EFR events. The groundwater levels beneath the river channel increased rapidly in response to river leakage during the EFR events. However, the magnitude and the area of groundwater-level rise are slightly different.

During the EFR event in spring 2019, two groundwater mounds were formed near Mencheng Lake (P3-P5) and Lianshi Lake (P7-P8) in the upper reach (Figure 5-7b). The largest groundwater level rise reached 25 meters (Figure 5-8a). However, no significant groundwater level rise was found in the lower river reaches. After the rainy season, without receiving the river leakage from the EFR and with less natural groundwater recharge, the water mound under the riverbed dispersed and the regional groundwater level declined. During the EFR event in spring 2020 also, the groundwater level rose significantly (Figure 5-8b); the maximum increase reached 14 meters at Yuanbo Lake (P9-P10). Compared to the year 2019, groundwater level increase was found also in

Wanping Lake (P15). Three groundwater mounds were formed at Mencheng lake (P3-P5), Yuanbo Lake (P9-P10) and Wanping Lake (P15), which gradually dispersed after the end of the EFR event. After the EFR event in the fall of 2020, the rise of groundwater level occurred only in the upper and middle reaches of the river with a smaller magnitude compared with the 2020 spring event (Figure 5-8c).

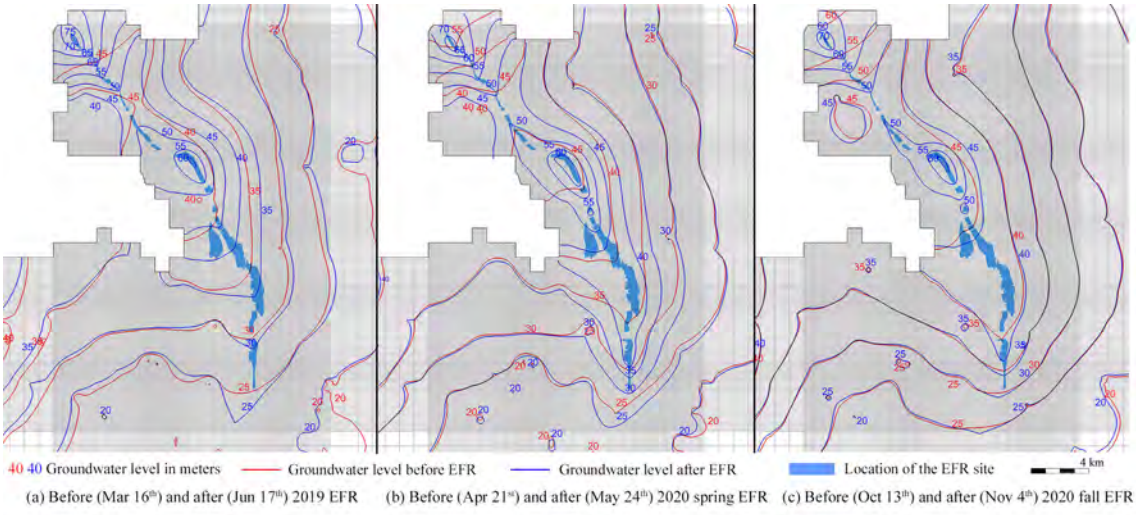

Figure 5-7 Groundwater level contour maps before and after three EFR events in Yongding River.

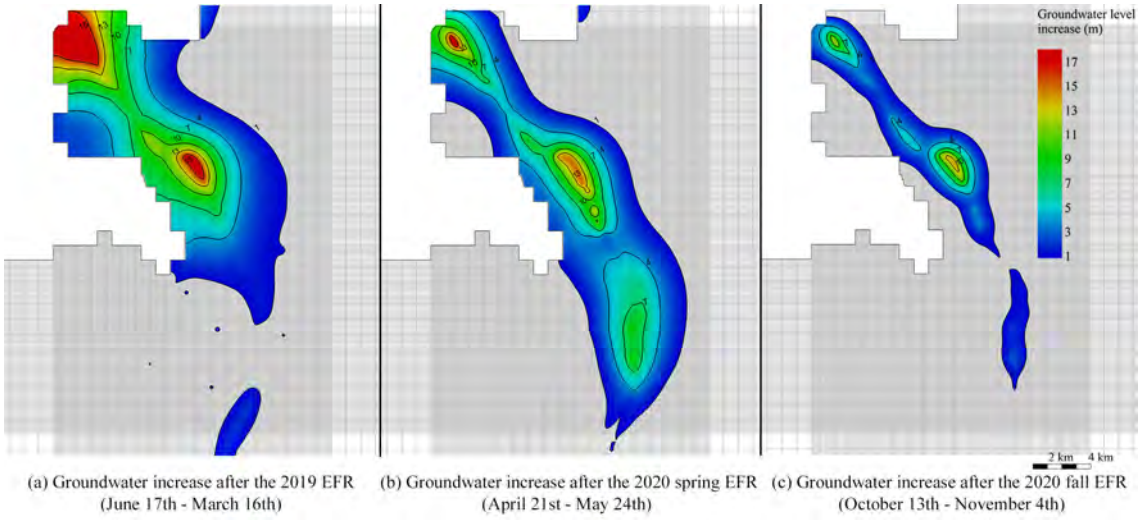

Figure 5-8 Map of the groundwater level increase along the Yongding River after each EFR event compared to the pre-event level.

5.3.2 Enhanced groundwater recharge and recovery of the groundwater storage

Table 5-3 summarises the annual groundwater budget of the local model area for 3 years. In the Yongding River area (523.6 km^2), natural recharge from precipitation and irrigation return flow contributes about one-third of the total inflow. Enhanced recharge from river leakage accounts for approximately 40-45%, and the rest comes from lateral inflow from the mountain boundary and other parts of the plain. Outflow components of the Yongding River area include groundwater abstraction, lateral flow to the downstream area of the Beijing Plain, evapotranspiration, and discharge to the river channel. Groundwater abstraction is still the major discharge, accounting for more than 75% of the total outflow in the region. The lateral flow to the other parts of the plain contributes to 20% of the total outflow. However, due to the trend of increasing groundwater levels, groundwater evapotranspiration and discharge of groundwater to the river channel increased in 2019 and 2020.

Compared to the situation in 2018, when there was no regulated EFR, the recharge through the riverbed leakage increased by 50% and 32% in 2019 and 2020, respectively. The recharge patterns of these three modelled years are also different. Figure 5-9 shows the change in infiltration rate through the riverbed with time. In 2018, most of the river leakage occurred between July and August from the stormwater released during heavy rain events. However, due to the EFR before the flood seasons in 2019 and 2020, the groundwater recharge maintained a relatively high rate during the EFR period. In 2019, 74.1% of the total river leakage (117.1 million m^3) came from the EFR period. In 2020 this percentage increased to 86.5% (120.4 million m^3).

The effect of the EFR on recovering the aquifer storage was significant. Figure 5-10 shows the groundwater storage change from 2018 to 2020 in the Yongding River region. In 2018, groundwater storage was depleted during the dry season. Groundwater storage only increased during July and September. However, positive storage change occurred from March until October 2019 and most of the months in 2020. The cumulative storage change reached 97 million m^3, which demonstrates the effectiveness of the EFR in recovering groundwater storage.

Table 5-3 Annual groundwater water balance in Yongding River area.

	Flow component	2018		2019		2020	
		Amount (10^6 m^3)	Percentage	Amount (10^6 m^3)	Percentage	Amount (10^6 m^3)	Percentage
Inflow components	Lateral boundary flow from the mountain	39.79	15.10%	40.99	11.88%	40.92	13.29%
	Natural recharge from precipitation and irrigation return flow	81.99	31.11%	115.17	33.37%	104.33	33.88%
	Recharge through the river leakage	105.08	39.87%	157.98	45.77%	139.20	45.20%
	Lateral inflow from the regional aquifer	36.70	13.93%	31.02	8.99%	23.49	7.63%
Outflow components	Abstraction	217.61	81.43%	233.89	79.05%	204.05	76.08%
	Evapotranspiration	0.07	0.03%	0.20	0.07%	0.51	0.19%
	Discharge to the river channel	0.05	0.02%	1.14	0.38%	4.84	1.81%
	Lateral outflow to the regional aquifer	49.51	18.53%	60.63	20.49%	58.79	21.92%
Annual storage change		-3.66		49.29		39.74	

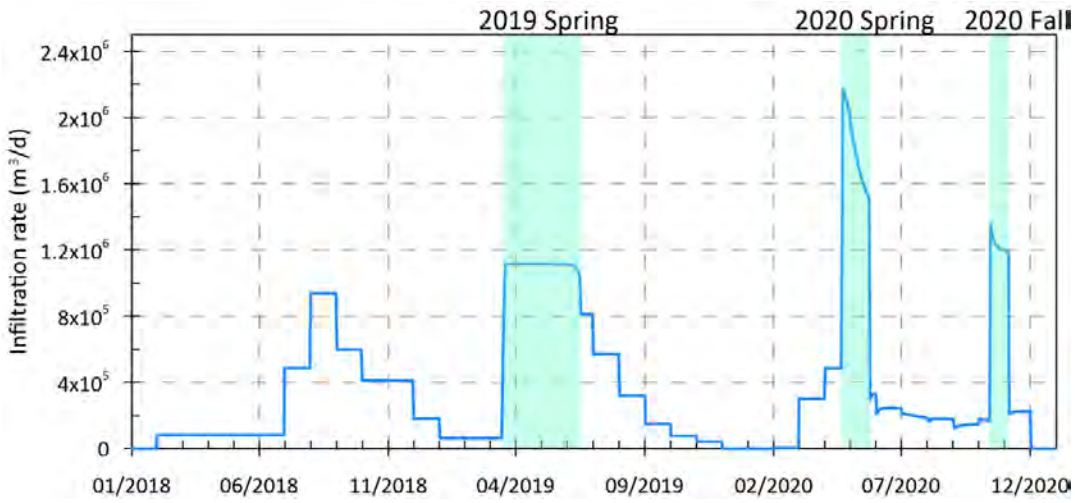

Figure 5-9 Groundwater recharge through the Yongding River leakage from 2018-2020.

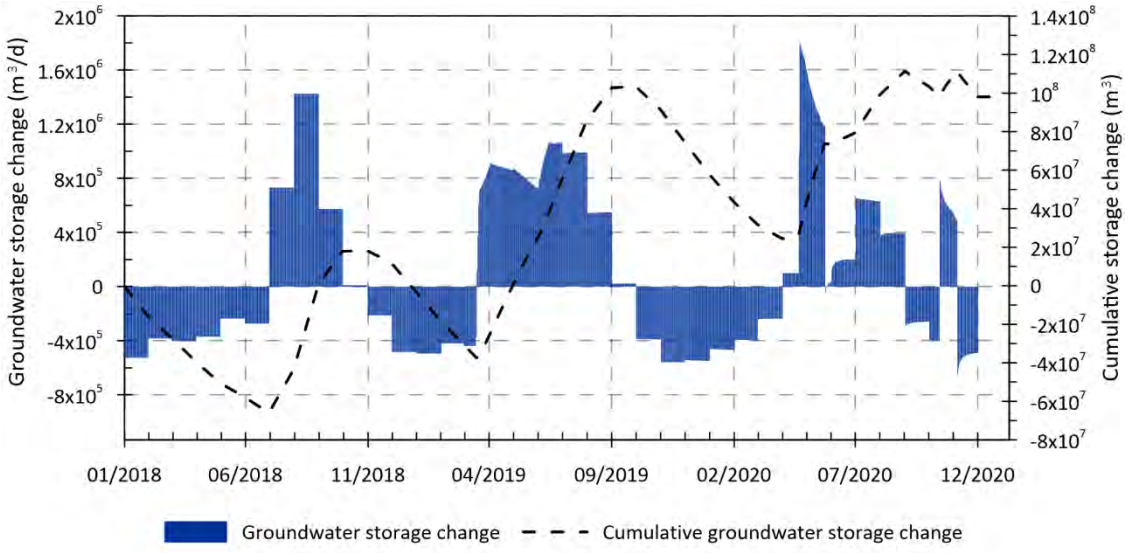

Figure 5-10 The monthly change of groundwater storage and the cumulative storage change in the Yongding River region.

5.3.3 Tracking of the leakage water and the mixing process

The result of the solute transport simulation of a numerical tracer by the MT3DMS program reveals the movement of the infiltrated water and the mixing of the infiltrated water with the native phreatic groundwater. Before the EFR events, the background concentration of the numerical tracer was 0 mg/L (Figure 5-11a). Thus, with the 100 mg/L concentration of the infiltrated water, the simulated concentration represents the mixing

percentage of the infiltrated water and ambient groundwater. As shown in Figure 5-11b, after the first EFR in 2019, the groundwater beneath the river channel at the upper stream reach was mostly replaced by the infiltrated water. However, with less infiltration at the lower stream reach, the mixing of the infiltrated and natural groundwater was also less. The infiltrated water spread to the aquifer driven by advective transport. The spreading area of the infiltrated water was limited to a 500-meter band on each side of the Yongding River channel. Before the spring EFR in 2020 (Figure 5-11c), the infiltrated water from the last year's EFR spread further into the aquifer. And with other source water (e.g., stormwater, precipitation infiltration) entering the aquifer, the percentage of infiltrated water from the EFR event reduced significantly under the riverbed. The same mixing process occurred repetitively during the two EFR events in the 2020 spring and fall, resulting in an alternately distributed high mixing and low mixing zone of the infiltrated water and the ambient groundwater at the upper reach and middle part of the EFR site (Figure 5-11d-f). The lower part of the EFR site remained at a relatively low mixing percentage throughout the EFR period, due to the low leakage rate. According to the mass balance result of the MT3DMS model, at the end of the year 2020, only 0.43% of the infiltrated water left the aquifer through groundwater abstraction and 0.59% returned to the riverbed, which is negligible. 99% of the infiltrated water stayed in the aquifer as storage without spreading far from the Yongding River channel. At the end of the year 2020, the extent of the more-than-10% mixing zone was 44.3 km^2.

Table 5-4 summarizes the average travel times of the infiltrated water for arrival at different distances, which were computed as time lags between the breakthrough curves by cross-correlation. More details can be found in Figure D-1, Appendix D. These travel times are indicative of the spreading of the infiltrated water to various distances from the river. The actual travel times from the river to these distances are longer since the travel time of infiltration through the vadose zone was not considered in the model. In general, the estimated groundwater travel times at the upper and middle reaches are similar. However, the estimated groundwater travel time is much longer in the lower reach. This spatial difference in the groundwater travel time can be explained by 1) the difference in the hydraulic characteristics of the aquifer, and 2) the difference in the spatial hydraulic gradient. With higher permeability and larger hydraulic gradient, the groundwater travel time is much faster at the upper and middle reaches, which also corresponds to the difference in mixing percentage.

At present, the mixing of infiltrated water and native groundwater occurs only in a limited area, as there is no large-scale groundwater abstraction in the vicinity. As a result, the mixing occurs only as a result of the natural hydraulic gradient. However, it is expected that with the prolonged operation of the EFR in the future, the mixing zone will expand to a larger area, and more infiltrated water will be captured by the groundwater abstraction.

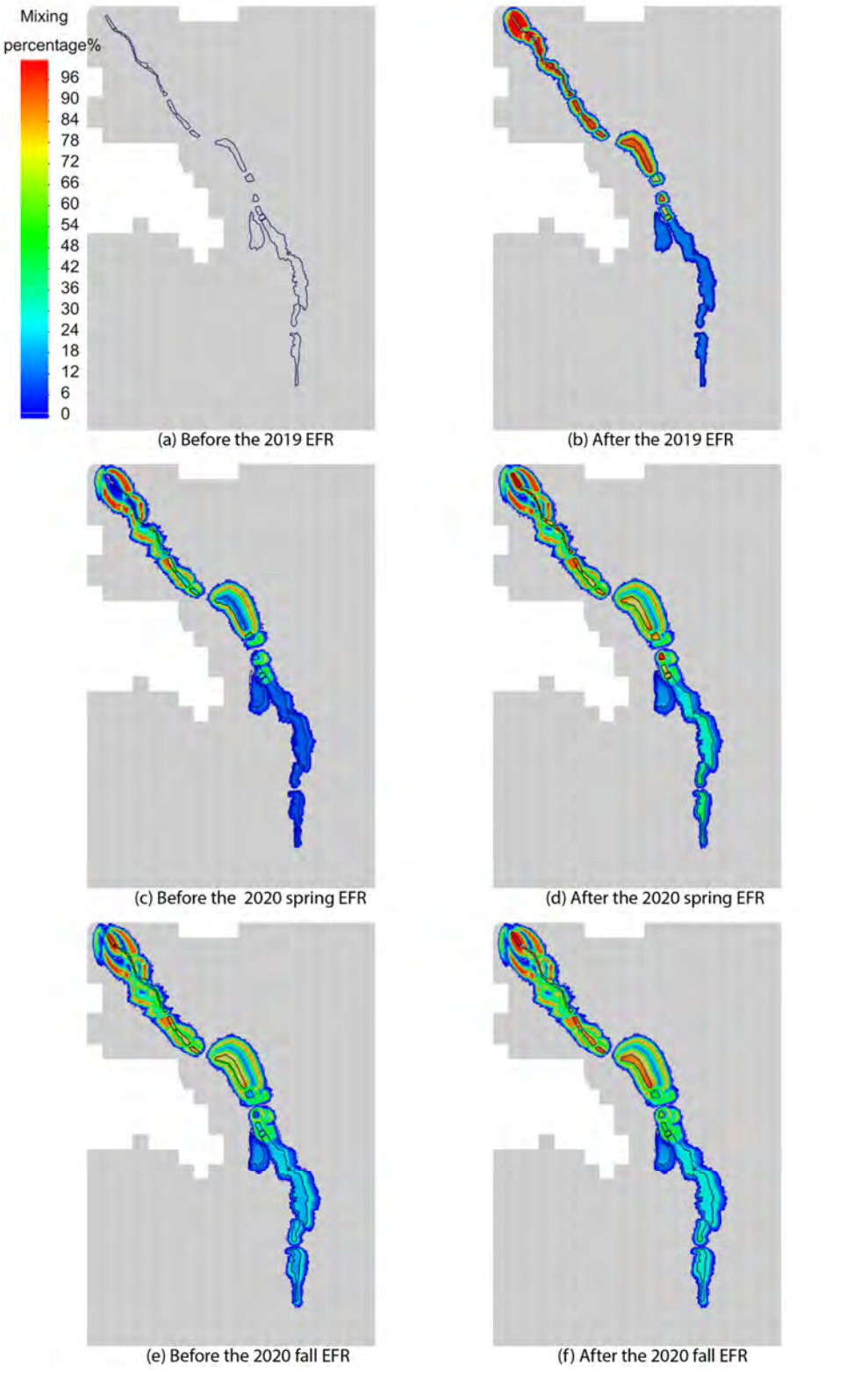

Figure 5-11 Spatial distribution of the mixing percentage of the infiltrated water and the native groundwater before and after each EFR event from 2019 to 2020 at the Yongding River EFR site.

Table 5-4 Estimated groundwater travel time based on the cross-correlation analysis results.

Location	Estimated travel time (days)		
	100 m from the river	200 m from the river	500 m from the river
Upper reach	10	49	212
Middle reach	9	36	254
Lower reach	34	122	364

5.3.4 Factors controlling the infiltration capacity of the riverbed

It is observed that during the three EFR events, the infiltration rate from river leakage also differs. Table 5-5 summarizes the estimated surface water budget of the three EFR events according to the available information. By comparing the differences of each flow component, the controlling factors that influence the groundwater recharge efficiency can be identified.

Table 5-5 Surface water budget of the three EFR events from 2019 to 2020.

	Unit	2019 Spring		2020 Spring		2020 Fall	
EFR duration	days		93		32		22
The total water release rate			1.419		4.436		2.325
Outflow downstream	$\times 10^6$	0.071	5.0%	1.109	25.0%	0.512	22.0%
Environmental flow	m^3/day	0.168	11.9%	0.489	11.0%	0.237	10.2%
Evaporation		0.048	3.4%	0.048	1.1%	0.035	1.5%
Groundwater recharge rate		1.098	77.4%	2.767	62.4%	1.486	63.9%

Firstly, operational factors, including the water release duration and water release rate, determine the water availability for the groundwater recharge. Most of the released water has been recharged to the aquifer as groundwater storage. However, by comparing the two spring EFR events in 2019 and 2020, surface water outflow to the downstream accounts for only 5% of the total amount of released water in 2019 while this percentage increased to 25% in 2020. Hence with a longer water release duration and smaller flow

rate, outflow to the downstream was reduced. Moreover, a longer release duration allows the released water to be detained longer in the recharge lakes, which prolongs the infiltration process.

Secondly, physical factors, including hydraulic properties of the riverbed and the aquifer, the regional hydraulic gradient and regional groundwater depth, control the maximum infiltration capacity. These factors also vary spatially in different river reaches.

Figure 5-12 shows the infiltration rate of nine recharge lakes located in the upper, middle, and lower reaches. The mean infiltration rate in the three EFR events was calculated as 0.10 m/d, 0.16 m/d, and 0.11 m/d, respectively. A high infiltration rate was found at the upper reach lakes (P1-P9). During the three EFR events, the infiltration rates were more than 0.5 m/d, and the maximum rate could be up to 0.8 m/d. An intermediate infiltration rate around 0.1 - 0.5 m/d was found in the middle reach. And the infiltration rate decreased significantly along the river channel. At the lower reach, the infiltration rate dropped below 0.1 m/d. Only in Lake P14, a 0.2 m/d infiltration rate was found during the 2020 spring release event. The infiltration rate of the same lake also differs in each EFR event. Generally, the highest infiltration rate was detected during the 2020 spring EFR event in most of the lakes. A constant infiltration rate can be maintained in most of the lakes at the upper and middle reaches. However, in some lakes in the lower reach, e.g., P10, P15, and P17, the infiltration rate was decreasing during the EFR events in 2020 due to the rise of the ambient groundwater level.

As a typical alluvial fan-plain hydrogeological environment, hydraulic conductivities were higher at the alluvial fan and gradually decreased along the alluvial plain, which is the main reason for the differences in the infiltration rate in the upper, middle and lower reaches.

The regional hydraulic gradients along the river determine how fast the infiltrated water can be spread into the aquifer. As can be seen from the results of the mixing process in Figure 5-11, the recharged water was not able to travel far due to the mild hydraulic gradient in the vicinity.

Besides, groundwater depth also determines the available underground space for infiltration. Figure 5-13 shows the groundwater depth before and after the EFR in 2019 and 2020. Compared with the groundwater depth at the lower reach, the groundwater depth is much deeper in the upper reach lakes. Surface water was hydraulically disconnected from the groundwater. Leakage through the riverbed was mainly driven by gravity, which allowed river leakage at a constant infiltration rate during each EFR event. However, due to the groundwater level increase, groundwater depth became much shallower before the EFR in 2020. Especially at the middle and lower reaches, groundwater levels near lakes P10, P15, P16 and P17 rose higher than the riverbed

elevation, so the infiltration rate started dropping after the beginning of the 2020 spring EFR.

Hence, it can be concluded that the permeability of the riverbed deposits, the groundwater depth and the hydraulic gradients near the streambed are three important physical factors that control the infiltration capacity during the EFR.

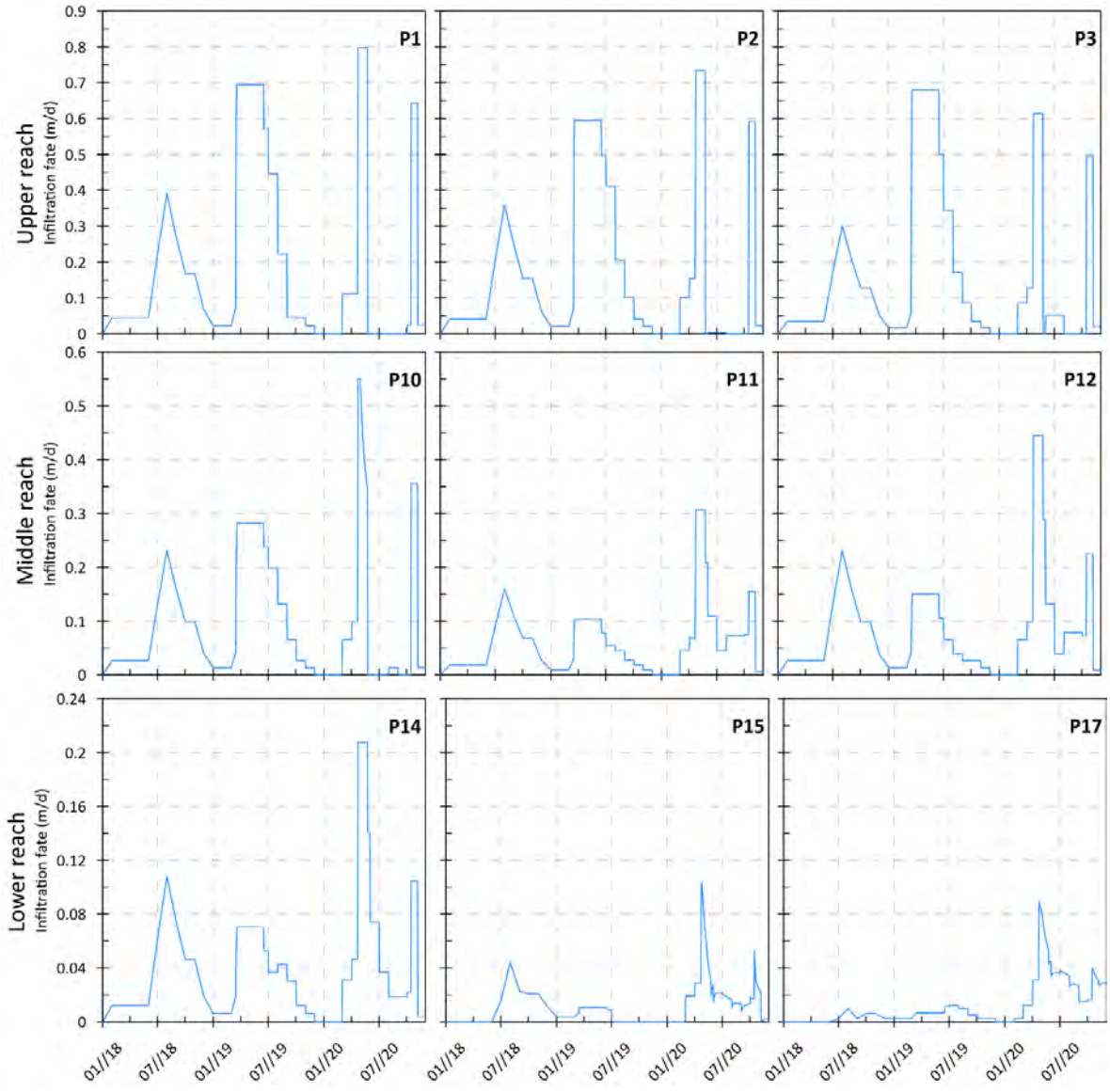

Figure 5-12 The infiltration rate of nine lakes in the upper, middle and lower reaches from 2018-2020.

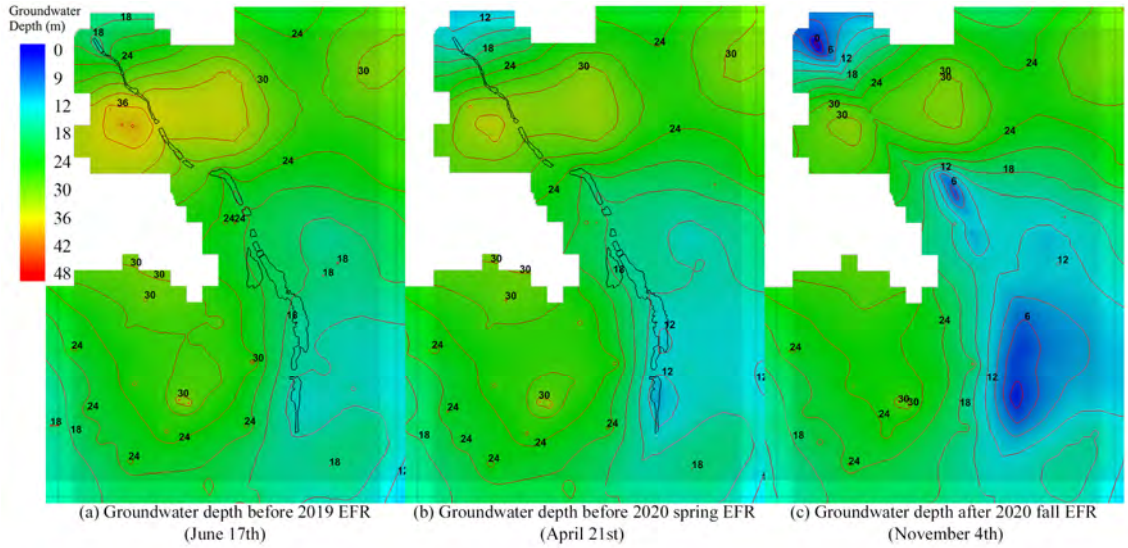

Figure 5-13 Groundwater depth before the EFR in 2019 (a), 2020 (b) and after the EFR at the end of 2020 (c).

5.4 DISCUSSION

5.4.1 Long-term effect on groundwater sustainability

In the Yongding River area, most of the EFR water ultimately percolates to the underlying aquifer of the river channel, which is considered as “surface water loss” from the perspective of surface water management. For the purpose of restoring the natural river flow regime, surface water losses should be avoided as much as possible so that the environmental flow can be sustained. However, from an integrated water management viewpoint, managed surface-water infiltration is an extra source of groundwater recharge replenishing the shallow aquifer. Thus, from the perspective of sustainable groundwater management, this enhanced groundwater recharge from the EFR increases groundwater storage, which is also a strategic resource to achieve water supply security. The concept of this innovative option for water storage has been noticed in recent years but is still under investigation (Richter et al. 2012). Thus, when it comes to the design of EFR schemes, it is meaningful to consider both the restoration of the environmental flows and the response of the groundwater system. Previous studies show that only a very small portion of the total released water could arrive at the river downstream, and most of the water will contribute to groundwater recharge (Tosline et al. 2012; Kennedy et al. 2017). Long-term EFR operation is an extra source of groundwater recharge that will gradually replenish the depleted groundwater storage and support sustainable groundwater development.

The prediction model constructed in this study predicts the groundwater levels and water budget change up to 2050. In general, groundwater heads are predicted to increase by 10-20 meters in different locations with distinct seasonal variations in the next 30 years. Long-term predicted groundwater level from 2021 to 2050 can be found in Figure D-2 of Appendix D. The high water level occurs during the EFR period annually and falls back during the dry season. The inter-annual variations can also be detected due to the variation of predicted groundwater recharge derived from the projected precipitation. Compared with the upper reach, the inter-annual fluctuation in the lower reach is relatively smaller.

With the implementation of the current EFR plan over the next 30 years, the estimated river leakage will vary from 99.9 million m^3/year to 112.6 million m^3/year. The occurrences of low river leakage are mostly in wet years with larger natural groundwater recharge from precipitation. When the aquifer receives more natural recharge, the groundwater level near the river channel will rise beyond the river bottom elevation and the river leakage rate will be reduced. Hence, with the groundwater level rise, the infiltration through river leakage will be less. The mean river leakage is predicted to be 106.1 million m^3/year from 2020 to 2050, which is larger than the recharge from precipitation infiltration. Moreover, this extra source of groundwater recharge will mitigate the groundwater storage depletion accumulated over the last two decades. Groundwater storage change in 2020-2050 will fluctuate between 0.87 million m^3 and -0.42 million m^3 under the influence of the precipitation infiltration variation. The groundwater balance will reach a new equilibrium state, which can accomplish a healthy groundwater development in this region. A detailed groundwater balance chart can be found in Figure D-3 of Appendix D.

5.4.2 Restoration of groundwater-surface water connectivity

Although it is predicted that the groundwater system in the Yongding River region will reach a new steady state in the next 30 years, the predicted result shows that the groundwater and surface water system will remain disconnected. Groundwater levels will be higher than the riverbed bottom only in the middle reach so that the groundwater and river become connected hydraulically Furthermore, the formation of a hyporheic zone beneath and adjacent to the streambed could provide soil water for the growth of riparian vegetation, which improves the groundwater-dependent ecosystem (Conant et al. 2019). However, the upper reach of the river channel will remain a permanently disconnected stream.

The restoration of the stream-aquifer connectivity can be achieved by several measures. Under the condition of adequate water availability from the upstream reservoirs, measures that increase the riverbed permeability, prolong the water release duration and increase the water release rate will enhance sufficient leakage and reconnect the surface water with the groundwater system. Thus, removing the liner that is currently installed at the river

bottom to increase the riverbed permeability can be easily implemented compared with the other measures. The numerical model developed in this study can be used to evaluate the effect of the proposed measure by adapting the model settings accordingly.

This study tested a scenario assuming that the hydraulic conductance of all the lakes will be 1.5 higher than the current situation after removing the geomembrane liner at the river bottom, while the wetland remains the same. A small increase of the river conductance was used in consideration of possible clogging of the lake bottom during long-term operation. The configuration of the river stage and river bottom using the RIV package and other sources and sinks remains unchanged in the prediction model. By mapping out the area with higher groundwater level than the river bottom, the area with connected stream can be delineated (details can be found in Figure D-4 of Appendix D). Result shows the current extent of the connected stream, which only accounts for 22.2% of the total river channel and is mainly at the middle reach. However, with higher hydraulic conductance, the extent of the connected stream increases to 34% of the total river channel.

Moreover, during long-term operations, it is important to remain aware of the risk of clogging caused by the formation of a bioactive layer at the river bottom. The accumulation of this layer during low flow periods can impede the effectiveness of environmental flow release, by reducing water flow, and it can pose potential risks to groundwater quality. To address this issue, regular monitoring and maintenance of the river channel may be necessary to prevent the build-up of a bioactive layer.

5.5 CONCLUSIONS

To maintain the environmental flow and improve the riverine ecosystem, EFR have been implemented in the Yongding River area in Beijing, China. Released water from the upstream reservoirs replenishes river flow in the Beijing Plain. Transient groundwater flow and numerical tracer transport models were used to assess the observed EFR events in 2019-2020 and predict the effects of long-term operation of the EFR in 2021-2050. The results show that during the three EFR events from 2019 to 2020, groundwater levels increased significantly near the Yongding River channel. Groundwater storage increased by 97 million m^3 at the end of 2020. It was found that the river leakage rate was controlled by two main factors. Operational factors control the water availability for the groundwater recharge and physical factors determine the maximum infiltration capacity. With long-term operation of the proposed EFR scheme from 2021-2050, groundwater levels along the Yongding River are predicted to rise by 10-20 meters. The enhanced river leakage will contribute significantly to groundwater sustainability in the region. The groundwater system will be able to reach a new equilibrium state in this region. The middle reach of the river channel will be reconnected with the groundwater hydraulically, which benefits the recovery of groundwater-dependent ecosystems.

6

TOWARDS SUSTAINABLE GROUNDWATER DEVELOPMENT WITH EFFECTIVE MEASURES UNDER FUTURE CLIMATE CHANGE IN BEIJING PLAIN

Corresponding paper: Liu, S., Zhou, Y., Eiman, F., McClain, M. E., & Wang, X. S. (2024). Towards sustainable groundwater development with effective measures under future climate change in Beijing Plain, China. Journal of Hydrology, 130951.

ABSTRACT

To cope with the groundwater depletion problem and achieve sustainable groundwater development, groundwater conservation measures and managed aquifer recharge (MAR) have been implemented worldwide. However, knowledge gaps exit how does the aquifer system respond to these interventions differently and if these interventions are adequate to lead to long-term sustainable groundwater development under future climate change. In Beijing Plain, two measures have been implemented: reduction of groundwater abstraction by substituting groundwater abstraction with transferred surface water and implementation of managed aquifer recharge (MAR) in two major rivers. This study aims to assess how do the shallow and deep aquifers respond to these measures and if these measures can lead to long-term sustainable groundwater development in Beijing Plain under future climate change. A 3-D transient groundwater flow model was calibrated and used to simulate groundwater level and budget changes from 2021 to 2050. The monthly groundwater recharge was estimated using the projected monthly precipitation from three downscaled regional climate models under two scenarios (RCP4.5 and RCP8.5). The results show that declines in groundwater head and storage can be reversed with the combined two measures, thereby contributing to achieve sustainable groundwater development. The reduction of abstractions is a deciding measure to reverse the trend of groundwater depletion, especially in the deep confined aquifers, while large scale MAR schemes can restore the cones of depressions in shallow aquifers and maintain the groundwater abstraction. Climate variation has large impacts on groundwater resources, especially, consecutive dry years can cause rapid groundwater storage depletion. The projected monthly precipitation from 2021 to 2050 is not significantly different from the past. Therefore, the projected future precipitation has minor impacts on groundwater resources in the next 30 years. The findings from the study will support the Beijing municipality to maintain the tight control on groundwater abstraction and to implement large-scale MAR schemes in two rivers. This successful example will encourage managers of other heavily exploited aquifers to take similar measures to achieve sustainable groundwater development.

6.1 INTRODUCTION

Ever since 20th century, groundwater exploitation has been booming due to the flourishing of socio-economic development and population growth globally (van der Gun 2012). Especially in arid and semi-arid regions, groundwater is a reliable water supply source that is more resilient to climatic variability, especially during drought periods (Edmunds 2003; Cuthbert et al. 2019). Groundwater withdrawal increased 15% per decade globally between 1960 to 2010 to meet the demand for all kinds of anthropogenic activities (Wada and Bierkens 2014). Consequently, the abstraction rate has exceeded the groundwater

renewal rate. The estimate of global groundwater depletion ranges between 100 and 200 km³/year, constituting approximately 15 to 25% of the world's total groundwater withdrawals (UN-water 2022). Particularly, regions such as Central Asia, USA, North China and Middle East, face the most severe groundwater depletion issues (Konikow and Kendy 2005; Wada 2016; Zhao et al. 2019; Ashraf et al. 2021).

Researchers and policymakers have recognized the urgent need to develop effective strategies for remediating and restoring depleted aquifers (Liu et al. 2001, 2022a). One crucial aspect of aquifer management involves reducing groundwater abstraction to minimize the stress on aquifers (Deines et al. 2019; Van et al. 2023). By enhancing the efficiency of water usage and implementing strict regulations to limit groundwater extraction, a sustainable development can be achieved. However, limiting groundwater use alone may not be sufficient to fully restore depleted aquifers. This is where MAR techniques come into play (Bouwer 2002; Dillon et al. 2009). MAR involves artificially recharging aquifers by diverting excess surface water or treated wastewater to infiltration basins, injection wells, or other engineered structures. MAR has been applied globally at different operation scales (IGRAC 2007). The combined efforts of optimizing the water supply structure and implementing MAR techniques hold significant potential for addressing the challenges of over-exploited aquifers. These approaches not only provide immediate relief by mitigating extraction pressure on aquifers but also contribute to the long-term sustainability of groundwater resources (UNESCO 2021). Numerical modelling is a powerful tool to evaluate the effectiveness of mitigation measures (Konikow and Kendy 2005; Maliva et al. 2009; Ringleb et al. 2016). Numerical modelling provides a quantitative approach to assess and analyse the recovery of groundwater storage and groundwater levels with the implementation of MARs and groundwater conservation policies (Valley et al. 2005; Vandenbohede et al. 2008; Xanke et al. 2016).

Apart from the impact of human activities on the groundwater system, the influence of climate change has also been recognized and emphasized in recent years (IAH 2016). A common method to investigate the potential impact of climate change on groundwater is coupling downscaled General Circulation Model (GCM) climate projections with the hydrological models (Epting et al., 2022; 2023; Gemitzi et al., 2017; Green, 2016; Pulido-Velazquez et al., 2015). The downscaling of the GCM output can be achieved by two approaches: dynamic downscaling and statistical downscaling. Dynamic downscaling reproduces the Regional Climate model (RCM) by taking GCM data as boundary conditions and employs some physical principles considering the interactions of atmosphere, land water and social economics (Xu et al. 2019). Statistical downscaling, on the other hand, corrects the RCM or GCM data by applying statistical analysis of the historical climate data and the RCM/GCM model data. Amanambu et al. (2020) summarized a generalized conceptual framework of modelling the future impacts of climate change on groundwater. Typically, downscaled GCM/RCM data were used as

inputs to hydrological models to future predictions. Many studies have been conducted using this methodology in different types of climatic zones, which has expanded our understanding of the interplay between climate and groundwater systems. Most of the modelling scales fall between small (10^2-10^3 km^2) to medium (10^3-10^4 km^2). Although the uncertainty in prediction is still a major challenge, research results show deviated future trends in groundwater recharge, groundwater storage and groundwater levels in different climate regions. For instance, studies have reported a decrease in groundwater recharge and storage in humid tropical regions (Alam et al. 2019; Klaas et al. 2020; Patil et al. 2020) as well as semi-arid and arid tropical regions (Herrera-Pantoja and Hiscock 2015; Goodarzi et al. 2016; Ghazavi and Ebrahimi 2019). Predictions in temperate zones show more uncertainty, with the majority of studies concluding in a decrease in groundwater recharge and storage, but some research has also reported an increase of recharge and storage (Tillman et al. 2016; Niraula et al. 2017; Ou et al. 2018; Rasmussen et al. 2023).

The climate change and groundwater over-exploitation create challenges for sustainable groundwater management, particularly in regions with severely depleted aquifers. In the Indus basin, achieving sustainable development requires a focus on reducing water consumption, which can be accomplished through the improvement of irrigation techniques and the optimization of cropping patterns (Muzammil et al. 2023). Similarly, in California's Central Valley, groundwater is heavily over-exploited due to huge groundwater pumping for irrigation during consecutive droughts over two decades (Konikow 2015; Liu et al. 2022a). To combat the threat of groundwater depletion and other related hazards, the Sustainable Groundwater Management Act (SGMA) was enacted, dedicating to manage the groundwater use at a sustainable level by implementing a better water allocation scheme (Alam et al. 2019). Similarly, in the U.S. Central High Plains aquifer, to stop the trend of groundwater level decline, with a bottom-up approach, farmers were empowered to work together with the local officials to make future water conservation plans. Assessment of these measures found that the water use in Kansas state decreased 31% over the first five-year period (Deines et al. 2019). In the North China Plain, the depletion rate of groundwater has been quantified and mapped (Cao et al. 2013). Several measures have been considered, including the implementation of MAR, increasing water use efficiency, and implementing inter-basin water transfer schemes. These global examples highlight the strong commitment of scientists, governments, and local communities to ensure the sustainability of groundwater for future generations.

However, knowledge gap exits if the present groundwater conservation measures and MAR could lead to long-term sustainable groundwater development under future climate change. Little is known how do the shallow and deep aquifers respond to these interventions differently. There are few studies dealing with joint assessment of

groundwater conservation polices and future climate change on the long-term groundwater sustainability.

Beijing is one of the few successful cases that is moving rapidly towards sustainable groundwater development. Two drastic measures have been planned and implemented. The first measure is substituting a large amount of groundwater abstraction with transferred surface water from the South-to-North transfer scheme (Liu and Zheng 2002). The second measure is enhancing groundwater recharge by implementing MAR in two major rivers (Zhou et al. 2012). Observed groundwater levels have shown that the declining trend of groundwater levels in the last two decades has been reversed and an increase in groundwater levels has been observed in shallow aquifers (Long et al. 2020). Are these two measures sufficient to achieve sustainable groundwater development? Will future climate change compromise these measures? This study aims to assess the sustainability of groundwater development in Beijing Plain under the implementation of these two measures under future climate change. The specific objectives are: 1) to develop a 3-D transient groundwater flow simulation model using MODFLOW model including pilot MARs in two rivers from 1995 to 2020; 2) to calibrate and validate three downscaled climate models for monthly precipitation projections; 3) to develop a groundwater prediction model including operational MARs from two rivers and updated recharge with the biased correction of the projected monthly rainfall from 2021 to 2050; 4) to predict changes of groundwater level and storage under three climate models and to assess sustainability of future groundwater development.

6.2 MATERIALS AND METHODS

6.2.1 Study area

Beijing City (39°28´N - 41°05´N, 115°25´E -117°30´E), the capital of China, functions as the political, cultural, diplomatic, and educational centre of the nation. The total area of the municipality is 16,410 km^2 with 38% of plain area and 62% of mountainous area(Figure 6-1). The plain area of Beijing gently decreases from 100 m above mean sea level at the foot of the mountains in the north and west to 20m in the southeast. Beijing has a continental type of climate with hot, humid summers and cold and dry winters. The average monthly temperature varies from -2.9℃ (in January) to 26.9℃ (in July). The average annual precipitation from 1959-2020 is 573 mm. With uneven temporal precipitation distribution, 75% of the rainfall occurs during the rainy season (June-August). The annual precipitation from 1959-2020 is shown in Figure 6-2. In general, the annual rainfall shows a decreasing trend in the last 60 years.

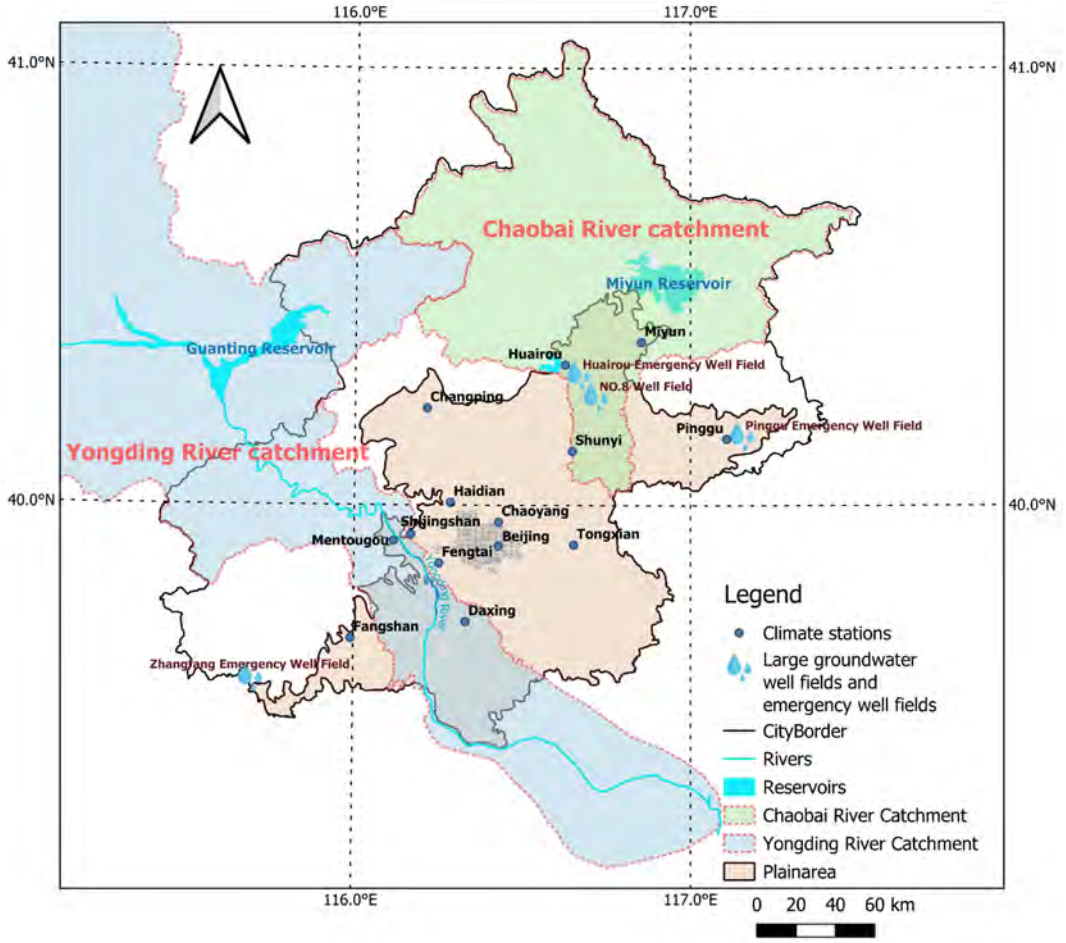

Figure 6-1 Map of Beijing City, Beijing Plain, main groundwater well fields and two main river catchments.

In the last several decades, Beijing has become a mega city with rapid urban development. In 2020, the total population in Beijing reached 21.9 million. However, the water shortage problem largely restrained the city's sustainable development. The city's average per capita water resource was only 118 m^3 in 2020 (Beijing Water Authority 2021a), which is far below the international water shortage limit standard (1000 m^3 per capita) (WWAP 2012). Figure 6-3 shows the water supply sources of Beijing from 1999-2020. Before the large-scale use of reclaimed water and the implementation of the South-to-North (S2N) water transfer project, groundwater accounted for more than 60% of the urban water supply. Since 1999, the city experienced a continuous 10-year drought period with an average of only 480 mm/year of precipitation. The decrease in rainfall and surface runoff resulted in the drying up of the main rivers and less water supply from the surface reservoirs. To meet the huge water demand, emergency well fields were put into operation to increase groundwater supply. Consequently, the groundwater was heavily over-exploited, and the groundwater storage was depleted. Moreover, groundwater depletion

also brought other environmental problems to the region including water quality deterioration, riverine ecosystem deterioration, and land subsidence (Li et al. 2015; Hu et al. 2019b) .

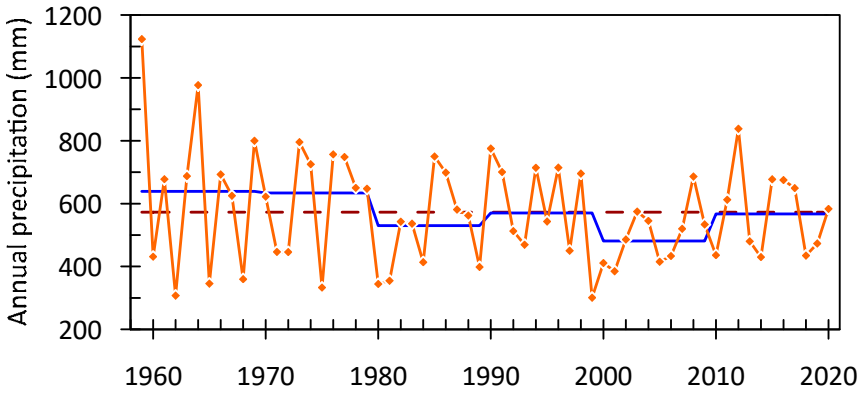

Figure 6-2 Historical annual precipitation data from 1959-2020 in Beijing, blue line indicates the step changes of annual precipitation, red dashed line plots the average annual precipitation from 14 stations.

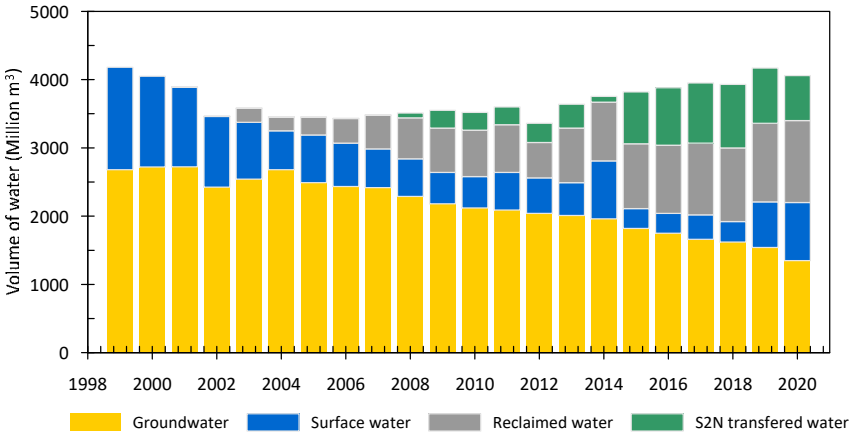

Figure 6-3 Water supply sources in Beijing from 1999 - 2020.

6.2.2 Effective measures to achieve sustainability.

To cope with the water scarcity problem, the Central Route of the South to North (S2N) Water Transfer project was initiated in 2003. The Central Route diverts Yangzte River water to Beijing and other neighbouring provinces along a 1267 km constructed canal. The Central Route S2N Water transfer became operational in 2015. Beijing receives approximately 1.0 billion m^3 of transferred water annually. The transferred water has become a new alternative water source for the urban water supply and alleviated the water shortage problem in the city. Thus, groundwater abstraction has been reduced from more than 2 billion m^3 per year to 1.5 billion m^3 per year in Beijing since 2015. The operation

of emergency well fields was suspended. Pumping wells for industrial water supply from deep confined aquifers were shut down. Moreover, some of the transferred water was used for recharging the aquifer. The MAR project was piloted in 2015 in the Chaobai River and found to be feasible. Due to the over-abstraction at the No.8 Well Field and the Huairou Emergency Well Field (Figure 6-1) during the drought period from 1999-2009, a large cone of depression was formed near the Chaobai River, which provided adequate underground space for recharging and storing the transferred water from the S2N Water Transfer Project. A large-scale MAR is planned to convert the 12 km river channel into 9 terraced infiltration basins for artificial recharge (Figure 6-4, right). Details of the design can be found in Liu et al., (2022). The estimated annual recharge capacity is about 290 million m^3 for the large-scale MAR operation.

To cope with the degraded surface water bodies and the degraded riverine ecosystem, an environmental flow release (EFR) project was also implemented in the Yongding River Catchment. In 2009, Beijing Water Authority initiated the "Yongding River Green Ecological Corridor" project, aiming to restore the environmental flow and improve the ecosystem. The original Yongding River channel was constructed with several lakes and wetlands. Water diverted from the Yellow River Diversion Project was released from the upstream reservoirs before the flood season to both mitigate the flood risk and maintain the environmental flow in the Yongding River (Figure 6-4). Due to the high permeability of the riverbed and surrounding aquifer, the released water also enhances the groundwater recharge through the river leakage. The pilot project was launched in 2019 and 2020. The results show that the released water is able to sustain the river flow and also restore the groundwater storage in this region (Liu et al. 2023).

In general, with extra water resources from the regional water transfer projects, the water supply structure of the city is in a transition. The percentage of groundwater use for the urban water supply reduced significantly from 52% in 2014 to 33% in 2020 (Figure 6-3). Together with the implementation of the MAR in Chaobai River and EWR in Yongding River, the groundwater depletion caused by the over-exploitation in the past is expected to be gradually recovered and sustainable groundwater development may be achieved in the future.

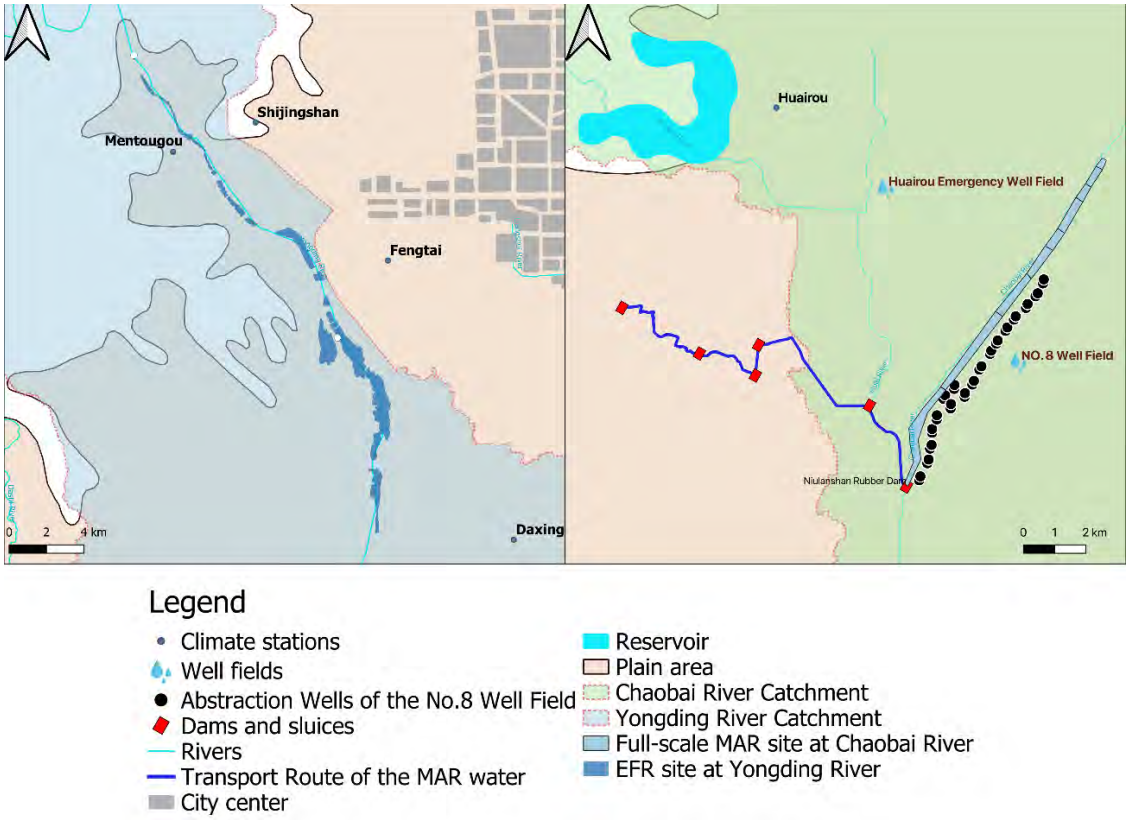

Figure 6-4 Locations of MAR project in Chaobai River (right) and EFR project in Yongding River (left).

6.2.3 Evaluating the impact of future climate change on the groundwater system

- **Selection of the RCM models and scenarios.**

The infiltration from rainfall and the lateral inflow from the mountain are the major sources for recharging the shallow aquifer in Beijing Plain. The lateral inflow consists of two components. The first one is subsurface inflow from hard rock aquifer in the mountainous areas into the alluvial plains. The second one is the infiltration of runoff from hillslopes during the rains. Natural recharge from two rivers is limited. The Chaobai River is dry since the Miyun Reservoir upstream stores surface water and is one of the main sources of surface water supply for Beijing City. The Yongding river is also regulated by reservoirs upstream. Leakage from EFR provides artificial groundwater recharge. The spatial and temporal variability in precipitation patterns directly affect the distribution and volume of groundwater recharge. Thus, to predict the future groundwater level and storage change in Beijing Plain, the groundwater recharge estimated from the projection of the future precipitation is essential.

This study used the projected future precipitation generated by Regional Climate Models (RCMs) from the Coordinated Regional Climate Downscaling Experiment (CORDEX) project (Remedio et al. 2019). The CORDEX project was initiated by the World Climate Research Program (WCRP) to coordinate the downscaling of Coupled Model Intercomparison Project (CMIP5) simulation results produced in support of Intergovernmental Panel on Climate Change (IPCC) assessments, which contain more than twenty RCMs. In total 13 domains are defined in the CORDEX project including the East Asia domain. Selection of the climate model is crucial in conducting impact studies as large differences and uncertainties have been observed among various RCMs and their driving models (the GCM model behind the RCM model). In this study, four RCMs have been initially selected for analysis (Hereafter referred to as M1, M2, M3 and M4). Details of these four RCMs can be found in Table 6-1. All selected RCMs could provide monthly precipitation data at a resolution of 0.44° (~50 km) for the historical period from 1951 to 2006, and for the future period under different Representative Concentration Pathway (RCP) scenarios. In this study, RCP 4.5 and RCP 8.5 scenarios are selected. RCP 4.5 scenario is a moderate estimation, which assumes the greenhouse gas emission will reach the peak in the mid-21st century and then decline. While RCP 8.5 assumes continuous increase of greenhouse gas emissions throughout the century. These RCP scenarios provide the potential impacts of different greenhouse gas emission pathways on the future precipitation patterns, which indirectly influence the groundwater recharge from the precipitation infiltration.

Table 6-1 Information of the selected RCM models.

Model ID	M1	M2	M3	M4
RCM model	CCLM5-0-2	CCLM5-0-2	CCLM5-0-2	HIRHAM5
Institute	Helmholtz-Zentrum Geesthacht	Helmholtz-Zentrum Geesthacht	Helmholtz-Zentrum Geesthacht	Danish Meteorological Institute
Driven GCM model	MPI-M-MPI-ESM-LR	ICHEC-EC-EARTH	CNRM-CERFACS-CNRM-CM5	ICHEC-EC-EARTH
Spatial resolution	0.44°			
Temporal resolution	Daily/Monthly			
Driving GCM scenarios	Historical, RCP 4.5, and RCP 8.5			
Model Ensemble	r1i1p1	r12i1p1	r1i1p1	r3i1p1
Application	(Voldoire et al. 2013; Chen et al. 2020; Awad et al. 2021; Zhuo et al. 2022)			

- **Bias correction of the projected precipitation data.**

Although RCMs provide dynamically downscaled outputs that consider atmospheric processes and heterogenous land topography at the regional level, there are still systematic biases against observational data. To evaluate the performance of the four RCM models, the observed precipitation data from 14 meteorological stations were compared with the model projections. The comparison results for three stations are presented in Figure 6-5, and results for the other stations can be found in Appendix E. M4 model produced consistently extremely low monthly precipitations comparing to measured precipitations in Beijing plain in the validation period from 1950 to 2006 (Figure 6-5d). Therefore, M4 model was discarded from further analysis. For the other three RCM models, large discrepancies were also detected between the observations and projections, particularly during the wet period of the year, with rainfall in summer months being highly underestimated. To address this issue, bias correction methods were applied to the monthly precipitation output of the RCMs before conducting further study. The correction assumed that the discrepancy between the model output and observed data is constant over time, and it was formulated as:

$$P'_{cor} = T_{BC}(P'_M) \qquad 6\text{-}1$$

where P'_{cor} is the corrected precipitation for the future period, and P'_M is the projected precipitation from the RCM model for the corresponding future period. T_{BC} is the statistical transformation function that compensates for the discrepancy between the projected and observed data.

In the calibration phase, 30 years of data (1961-1990) comprised of observed monthly precipitation and RCM monthly precipitation outputs were used to derive the statistical transformation function. The validation phase consisted of 15 years of data (1991-2005). In this study, we tested both the mean-based and variance-based transformation methods, which are calculated as:

$$P_{cor} = P_M \frac{\mu_O}{\mu_M} \qquad \text{(Mean-based Transformation)} \qquad 6\text{-}2$$

$$P_{cor} = \frac{P_M - \mu_M}{\sigma_M} \times \sigma_O + \mu_O \qquad \text{(Variance-based Transformation)} \qquad 6\text{-}3$$

Where P_{cor} and P_M are the corrected precipitation and projected precipitation from the RCM model for the calibration and validation period. μ_O and μ_M are the monthly average of the observed and projected precipitation of the calibration and validation period. σ_O and σ_M are the monthly standard deviation of the observed and projected precipitation of the calibration and validation period. The corrected precipitation data of the validation period were compared with the observations to select an optimal method for the bias-correction of the future period.

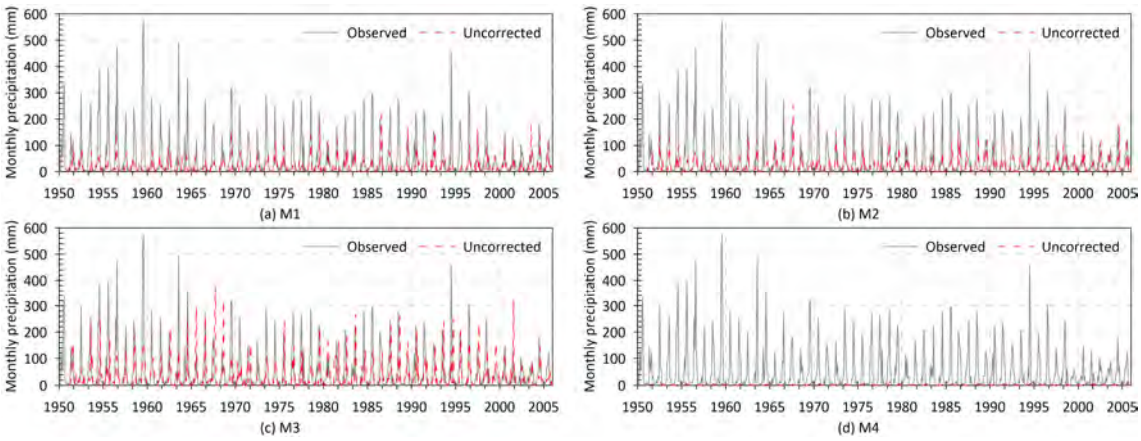

Figure 6-5 Raw precipitation data predicted by four RCM models (a)-(d) against the observed historical precipitation data for Beijing station.

The average of the bias-corrected precipitation data of the 14 stations from the three RCMs were used to estimate the groundwater recharge to 2050 for both RCP 4.5 and RCP 8.5 scenarios. These data were then utilized as precipitation infiltration in groundwater models. To accomplish this, the Beijing Plain area was divided into 74 recharge zones using polygons. Infiltration coefficients were assigned to each polygon based on hydrogeological settings of the plain and lithology of the unsaturated zone in the particular area. The infiltration coefficients range from 0.15 to 0.35 and to avoid unrealistically high infiltration rates, a threshold of 6 mm/day was set based on the maximum infiltration capacity of the top layer soil. Further information can be found in Appendix E.

6.2.4 Construction of the transient groundwater flow model

In this study, the transient groundwater flow model was constructed with the MODFLOW 2005 program. Transient groundwater flow models developed by Liu et al., (2022) and Liu et al., (2023) were combined to form a transient simulation model for this study. This new model was checked with monthly groundwater level measurements from 1995 to 2020. The performance of the new model is comparable with the model calibration of Liu et al. (2022; 2023). A brief summary of the model structure is given here. The model comprises nine model layers including five aquifers and four aquitards with a grid resolution of 1000 m. The extent and elevation of each model layer are determined by the interpolated geological borehole data. Lateral flow from the mountain is simulated as inflow boundary represented by injection wells using the Well (WEL) package at the western and northern model boundaries. The administrative border at the eastern and southern model boundaries are set as head-dependent flow boundaries by the General Head Boundary (GHB) package. The conductance value was estimated with the aquifer thickness and hydraulic conductivity values. The model includes six types of sources and

sinks. Precipitation infiltration, irrigation return flow and pipeline leakage were simulated using the Recharge (RCH) package. Evapotranspiration (EVT) package was used to simulate groundwater evaporation. Groundwater abstraction for agriculture, domestic and township water supply and industry was simulated using the WEL package. The pilot MAR in Chaobai River and EFR in Yongding River were simulated with the River (RIV) package. The model was run monthly from 1995 to 2020 to compute groundwater levels and water budget components. The computed groundwater levels were compared with the measured groundwater heads at observation wells.

The prediction model covers a time period from 2021-2050 with a monthly stress period. The initial condition was inputted from the computed groundwater heads in December 2020 from the simulation model. For the GHB package, reference heads at the boundary were kept the same as the computed heads in December 2020 across the future prediction period (2021-2050). The historical monthly mean evapotranspiration rates were used in the EVT package for the prediction model. Groundwater abstraction for the year 2020 was held 1.57 billion m^3/year constantly for the future periods. The implementation of the large-scale MAR (Figure 6-4) in the Chaobai River and the EFR in the Yongding River were also included in the simulation, which were simulated using the RIV package. The river stages for the nine infiltration ponds in the Chaobai River were computed based on the elevation of pond bottom and designed water depth for the prediction model(Liu et al., 2022). For the Yongding River, the computed river stages in 19 polygons according to the water release in 2019 were used for the prediction model (Liu et al. 2023). Recharge from precipitation and lateral inflow from the mountain were adapted from the projected precipitation.

Three prediction models were constructed: a model using the average monthly precipitation (hereafter referred to as Pav), one using the projected precipitation from the RCP4.5 scenarios (hereafter referred to as Prcp45) and one using the projected precipitation from with RCP8.5 scenarios (hereafter referred to as Prcp85). The groundwater recharge from the precipitation was derived from the monthly precipitation and the projected monthly precipitation of both climate scenarios. Apart from the groundwater recharge from the precipitation, lateral inflow from the mountains to the Beijing Plain will also be influenced by the future climate change since it is dependent on the precipitation. Thus, the variation of the lateral inflow was also considered in the prediction model.

6.3 RESULTS

6.3.1 Calibration and validation of the projected precipitation series

The projected precipitation series from the RCM data were bias corrected by mean and variance-based correction methods. Figure 6-6 illustrates the corrected precipitation data from the three RCMs for Beijing and Huairou stations, while additional data for the remaining stations can be found in Appendix F The data accuracy was significantly improved after performing the bias-correction by both methods.

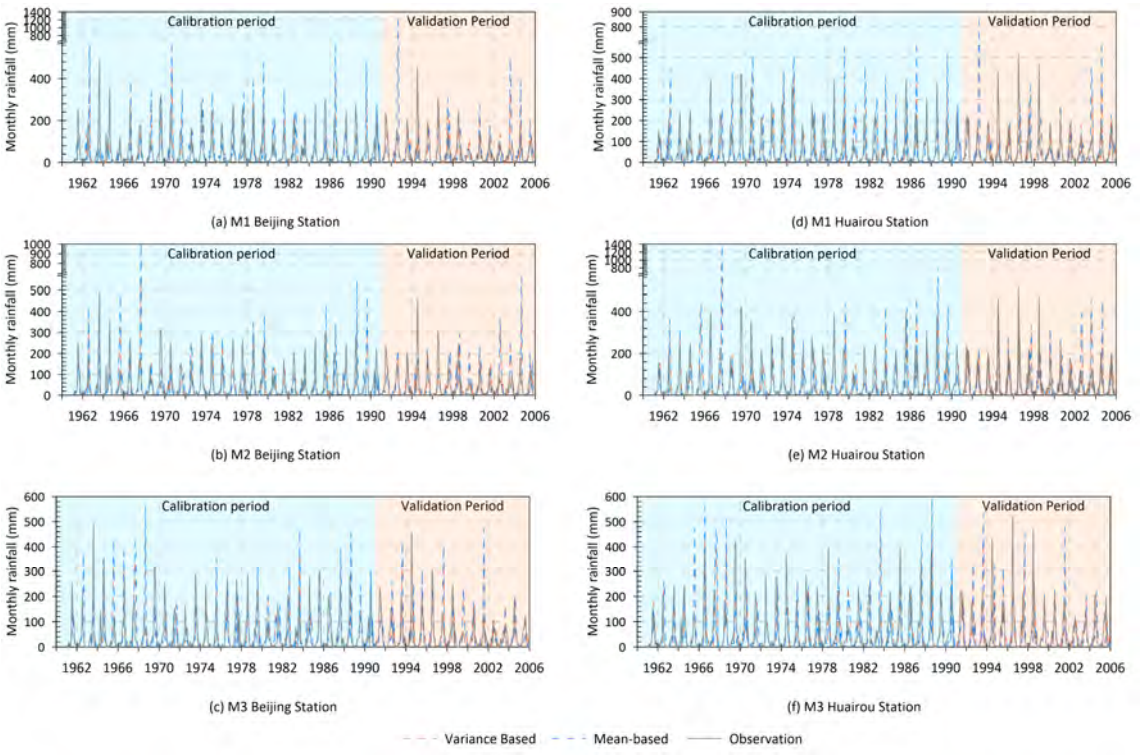

Figure 6-6 Comparison of the variance based and mean based bias-corrected precipitation data with the observation.

Statistics of the difference between the bias-corrected and observed monthly precipitations was shown in Table 6-2 using the Beijing station as an example. In general, the standard deviations of residuals from variance-based bias correction were found to be smaller in all stations. As a result, the variance-based bias correction method was chosen to predict and correct the monthly precipitation from 2006 to 2050, for RCP 4.5 and RCP 8.5 scenarios.

Table 6-2 Statistics of the differences between the observed and bias-corrected monthly precipitation for Beijing station from the period of 1961-2005.

	Mean-based corrected precipitation (mm/month)		Variance-based corrected precipitation (mm/month)	
	Calibration	Validation	Calibration	Validation
Mean	0.47	3.20	0.52	4.08
Median	1.28	1.06	1.51	2.47
Standard Deviation	53.24	64.33	46.74	54.75
Kurtosis	16.12	17.79	16.30	14.33
Skewness	-1.23	0.70	-1.72	-0.17

Figure 6-7 shows the predicted precipitation data by averaging the three RCMs for Beijing station and Huairou Station. Compared to the historical period, more extreme rainfall during the summer months is predicted expecially in RCP 8.5 scenarios. However, the average annual precipitation for all 14 stations is 512 mm and 544 mm for RCP 4.5 and RCP 8.5 scenarios, respectively, which is 12% and 6.5% lower than the historical precipitation (Table 6-3). Student t-test has been performed to detect if there is significant difference between the historical and future precipitation. However, there is no significant trend of decrease in precipitation for both scenarios. Nevertheless, it is noted that RCP 4.5 scenarios predict several consecutive wet and dry years. After 2038, there are a few years with precipitation larger than the long-term average value. While wet and dry years are distributed more evenly in the RCP 8.5 scenarios.

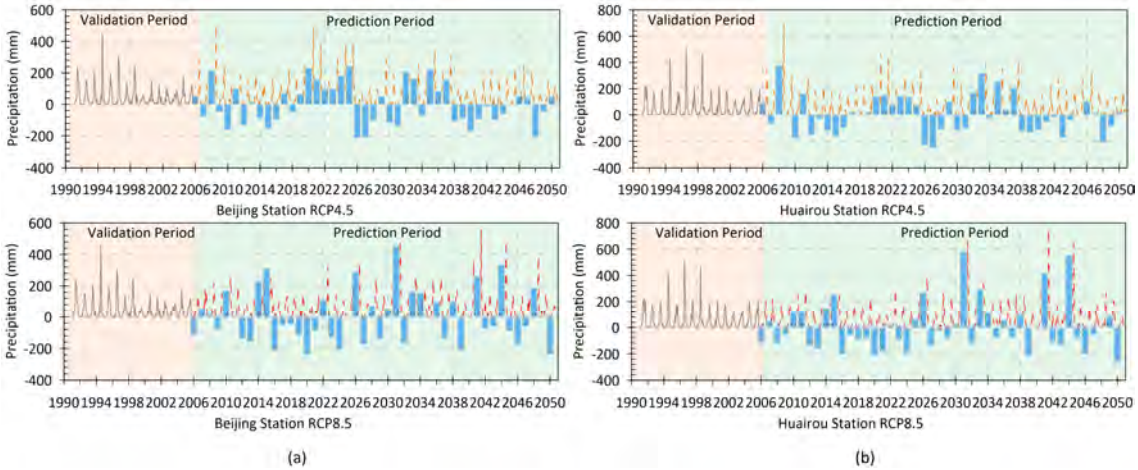

Figure 6-7 Projected precipitation data from the bias-corrected precipitation from the three RCMs for (a) Beijing Station (b) Huairou Station. Line plots are the monthly projected precipitation, and the bar chart depicts the difference between the annual precipitation and the average precipitation from 2006-2050.

Table 6-3 Comparison of the historical annual precipitation with the prediction.

Station	Historical annual precipitation (mm)	RCP 4.5 projected precipitation (mm)	RCP 8.5 projected precipitation (mm)
Beijing	597	486	523
Changping	537	471	493
Chaoyang	579	507	530
Daxing	537	470	507
Fangshan	557	496	542
Fengtai	569	496	537
Haidian	566	522	555
Huairou	649	572	601
Mentougou	600	517	561
Miyun	638	567	586
Pinggu	627	549	572
Shijingshan	541	514	551
Shunyi	592	516	541
Tongzhou	555	487	521
Average	**582**	**512**	**544**

6.3.2 Effects of three future climate scenarios

The spatial and temporal distribution of groundwater heads and groundwater budgets of the three scenario models were compared to analyze the aquifer response to future climate change and human activities. The Pav model used the historical mean monthly precipitation as input and Prcp45/Prcp85 models applied the projected monthly precipitation as inputs.

Figure 6-8 compares the groundwater level contour map in year 2021 and 2050 for the shallow unconfined aquifer (model layer 1) and the deep confined aquifer (model layer 5) for the Prcp45 model. Results in Prcp85 and Pav models are not shown here due to the high resemblance of the contour map results of the three models. Details can be found in Appendix G. Figure 6-9 plots predicted groundwater level series from five selected areas. It can be seen that the cone of the depression in the shallow unconfined aquifer in the Chaobai River area (northeast) will be recovered completely by 2050 with MAR in the Chaobai River (Figure 6-8b). The increase of groundwater level is significant from below 0 m to 24 meters in 15 years and gradually reach a new equilibrium state (Figure 6-9, H01). In Yongding River area, groundwater levels in the shallow aquifer are also increased with the EFR implementation in the Yongding River. The predicted groundwater levels at H02 and H04 will increase by 6 to 10 m. However, the cone of depression in the deep confined aquifer remains by 2050 (Figure 6-8d). The predicted groundwater heads in the middle confined aquifer (H03_m) and the deep confined aquifer (H03_d) in the Tongzhou area will increase with a slower pace. In this area, multi-aquifers are separated by the clay and silty confining layers. These deep aquifers were over-

exploited for industrial water supply over decades. The reduction of deep aquifer abstraction since 2015 results in slow recovery of groundwater levels. However, the only source water to recover the depleted storage is the vertical leakage from the shallow aquifer. Due to the existence of the low permeable layers, the renewal rate of the groundwater in deep aquifer is much slower than the unconfined aquifer. Thus, without other measures implemented, the recovery of the deep aquifer depletion may take much longer time.

In general, the Prcp45 model predicts lower groundwater level increase comparing to the Prcp85 model for all locations. Especially, the Prcp45 model predicts a decrease of groundwater levels after 2038. This is caused because the RCP 4.5 scenario predicts lower precipitation after 2038 (Figure 6-7), therefore, results in less recharge after 2038 (Figure 6-10a).

Groundwater balance analysis provides a quantitative assessment of groundwater resources in Beijing Plain for the future. Figure 6-10a shows the projected annual groundwater recharge from the natural precipitation infiltration, which is the major recharge component. In general, the Prcp45 model predicted lower groundwater recharge comparing to the Prcp85 model. Especially, the predicted groundwater recharge by the Prcp45 model is lower than the historical average (Pav) after 2038. In the Prcp45 model, the average annual precipitation infiltration in the next 30 years is 1.09 billion m^3. The minimum and maximum recharge will be 6.74 million m^3 and 1.57 billion m^3 in 2027 and 2033 respectively. In the Prcp85 model, the average annual precipitation infiltration in the next 30 years is 1.18 billion m^3. The minimum and maximum recharge will be 6.84 million m^3 and 2.21 billion m^3 in 2050 and 2031, respectively. It can be concluded that under the RCP 8.5 scenario, there will be an average of 8% more precipitation infiltration compared with the RCP 4.5 scenario and extreme dry and wet years are likely to occur more frequently in the RCP 8.5 scenario.

Other water balance components of the Prcp45 and Prcp85 models are compared in Figure 6-10b. The lateral inflow from the mountains is also an important source of groundwater recharge. Average lateral inflow from the mountains in the Prcp45 model will be only 286 million m^3/year, which will be lower than the Pav model all the time from 2020 to 2050. In the Prcp85 model, average annual lateral inflow is 294 million m^3/year, which is 3% higher than the Prcp45 model.

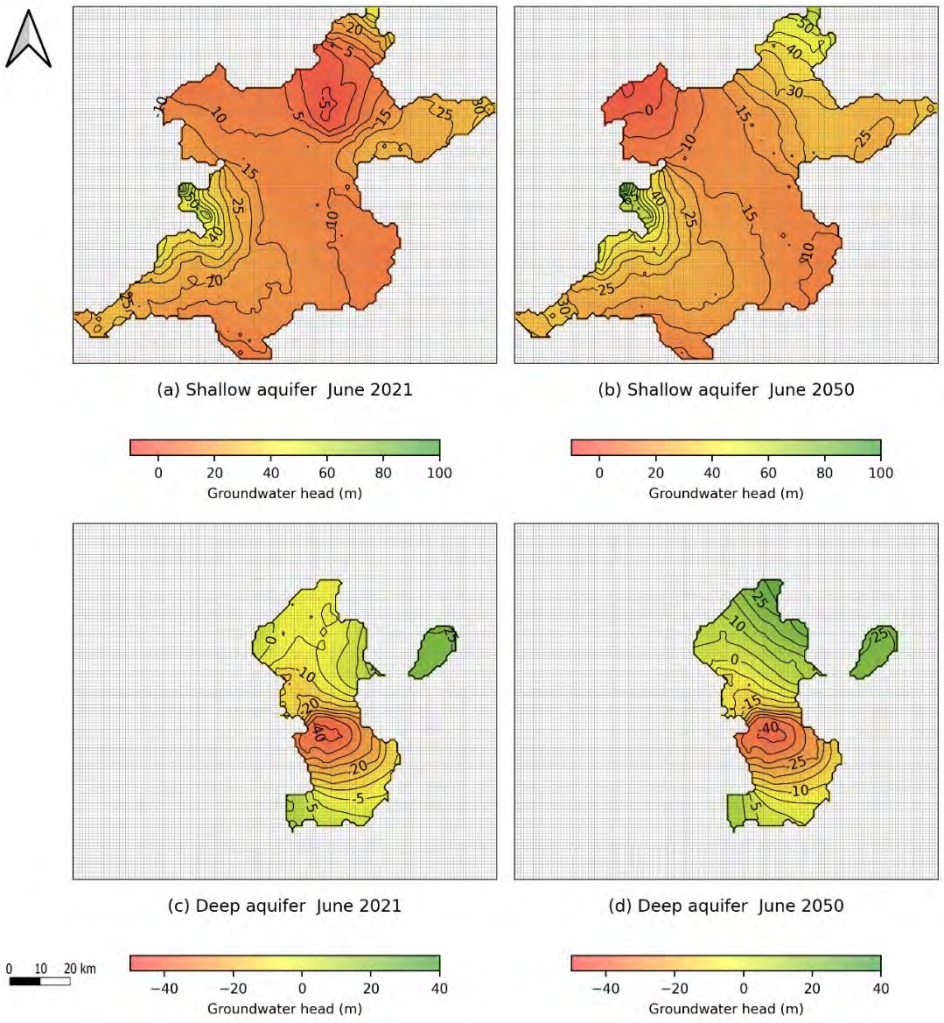

Figure 6-8 Groundwater level contour maps of the shallow aquifer (a-b) and deep aquifer (c-d) at the beginning and end of the simulation period predicted by Prcp45 model.

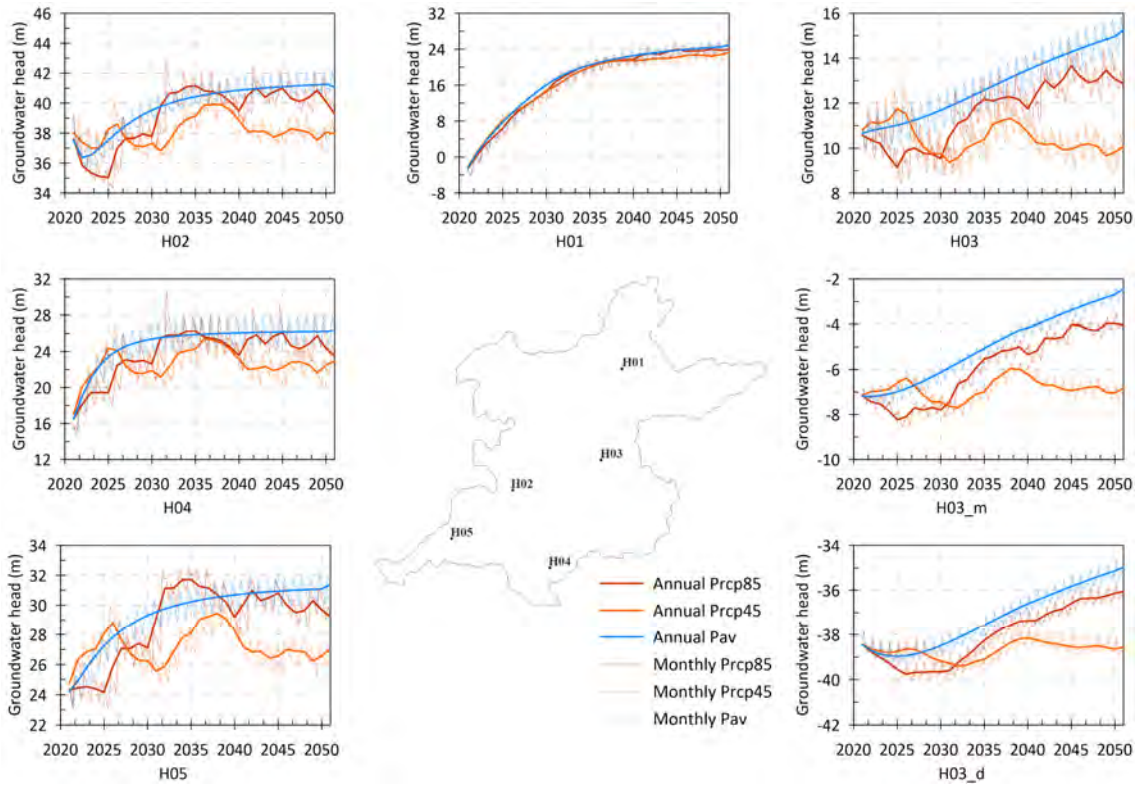

Figure 6-9 Predicted groundwater level at different locations and aquifers from 2020-2050 by the three prediction models. Solid lines stand for the annual average groundwater levels. Dashed lines show the monthly fluctuations.

Table 4 lists the average amount and percentage of all flow components for each scenario. As can be seen, groundwater abstraction is the major discharge component that accounts for more than 90% of the total outflow. Historically, the annual groundwater abstraction in Beijing Plain has declined from 2.4 billion m^3 in 2004 to 1.5 billion m^3 in the recent years, which is still the dominant groundwater discharge component. Natural recharge from precipitation accounts for about 60%, lateral inflow from the mountain accounts for about 14%, and artificial recharge from the MAR and EFR accounts for about 17%. The total average annual groundwater recharge summing up from the precipitation infiltration and lateral inflow from the mountains will be 1.38 and 1.47 billion m^3 predicted by the Prcp45 and Prcp85 models. The natural groundwater recharge alone cannot meet the 1.5 billion m^3 annual groundwater abstraction. Therefore, MAR is necessary. With a combined artificial recharge of 0.34 billion m^3 from two major rivers, the total groundwater recharge exceeds the total abstraction, so groundwater storage gradually increases and sustainable development can be achieved.

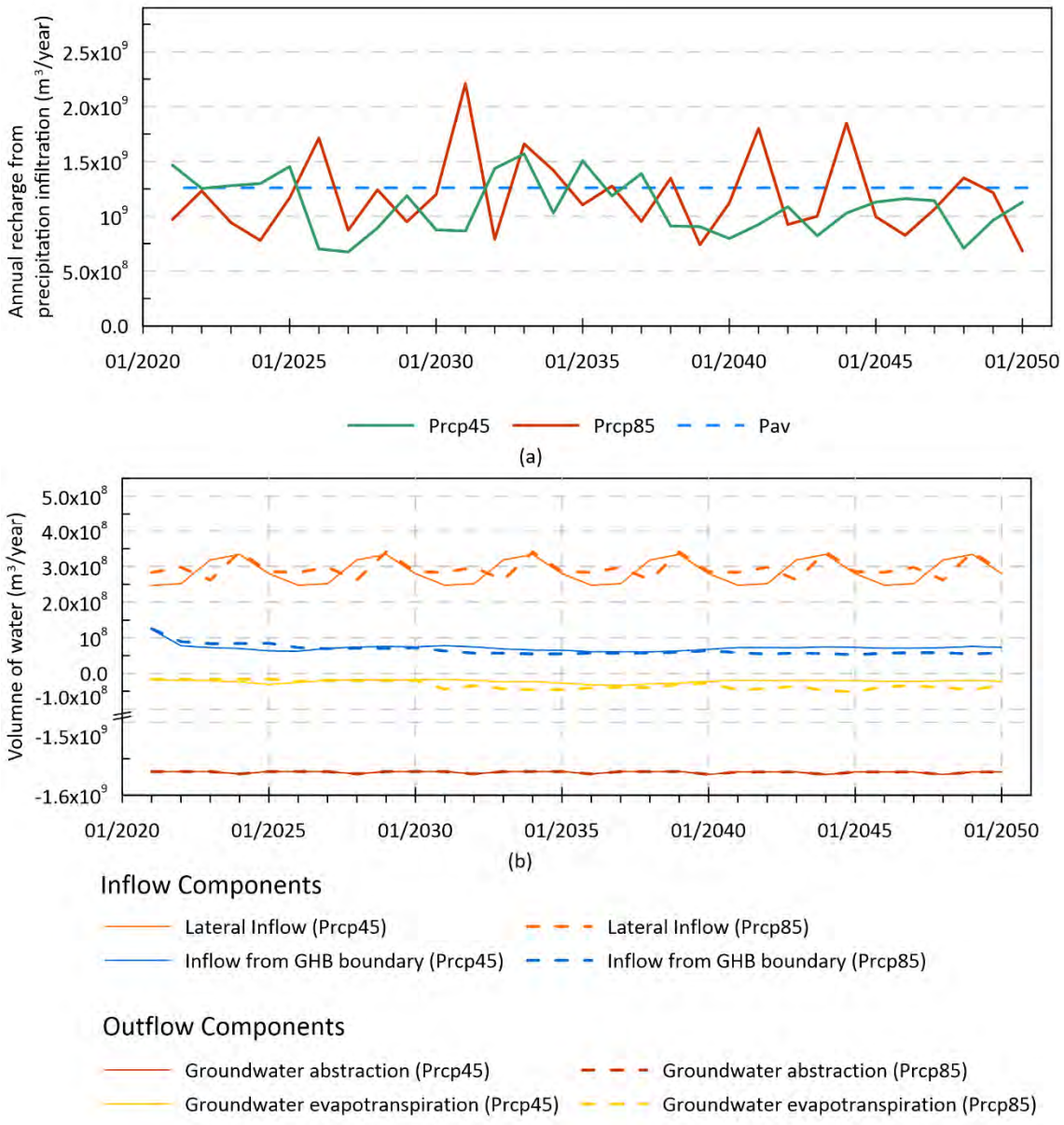

Figure 6-10 Annual groundwater recharge from (a) precipitation infiltration and (b) lateral inflow from the mountain from 2021-2050 predicted by the three prediction models.

Table 6-4 Average amount and percentage of each flow component for each prediction model.

Flow components	Pavp model		Prcp45 model		Prcp85 model	
	Amount(m^3/year) and percentage					
Natural groundwater recharge	1.26×10^9	63.4%	1.04×10^9	57.6%	1.14×10^9	60.7%
Lateral inflow from the mountains	326×10^6	14.4%	292×10^6	16.2%	299×10^6	16.0%
Infiltration from MAR and EFR	286×10^6	17.2%	308×10^6	17.1%	285×10^6	15.2%
Head dependent inflow	50.6×10^6	2.5%	73.2×10^6	4.1%	56.4×10^6	3%
Groundwater abstraction	1.57×10^9	91.9%	1.57×10^9	94.4%	1.57×10^9	92.7%
Groundwater discharge to surface water	56.9×10^6	3.3%	42.7×10^6	2.6%	57.6×10^6	3.4%
Groundwater evapotranspiration	57.6×10^6	3.4%	20.8×10^6	1.3%	41.3×10^6	2.4%
Head dependent outflow	72.8×10^6	4.3%	40.3×10^6	2.4%	52.1×10^6	3.6%
Change of storage	166×10^6		38.0×10^6		52.1×10^6	

6.3.3 Effects of the managed aquifer recharge

The amount of artificial groundwater recharge from the MAR implementation in Chaobai River and the EFR project in Yongding River was calculated for the Prcp45 and Prcp85 models (Figure 6-11). The average annual artificial groundwater recharge simulated by the Prcp45 model is 350 million m^3, which is 11 million m^3 higher than the Prcp85 model (339 million m^3). This difference is caused by the computed higher groundwater level from the Prcp85 model near the Chaobai and Yongding River channels (Figure 6-9: H01 and H02). Higher groundwater levels reduce the hydraulic gradient between the surface water and groundwater, resulting in less recharge through the river leakage, which also explains the decrease of total recharge from MAR and EFR with the increase of groundwater levels in the next 30 years. In 2021, both models predict more than 420 million m^3 total artificial recharge. The artificial recharge declines to 317 million m^3 and 311 million m^3 in 2040 for the Prcp45 and Prcp85 models and remain relatively stable as they reach a new equilibrium state. The recharge from the MAR and EFR accounts for 62% and 38% of the total artificial recharge, respectively. Figure 6-8 shows that the cone of depression in the Chaobai River area (Figure 6-8a) is effectively recovered with the MAR operation (Figure 6-8b). Similar effects occur in the Yongding River area with the EFR operation.

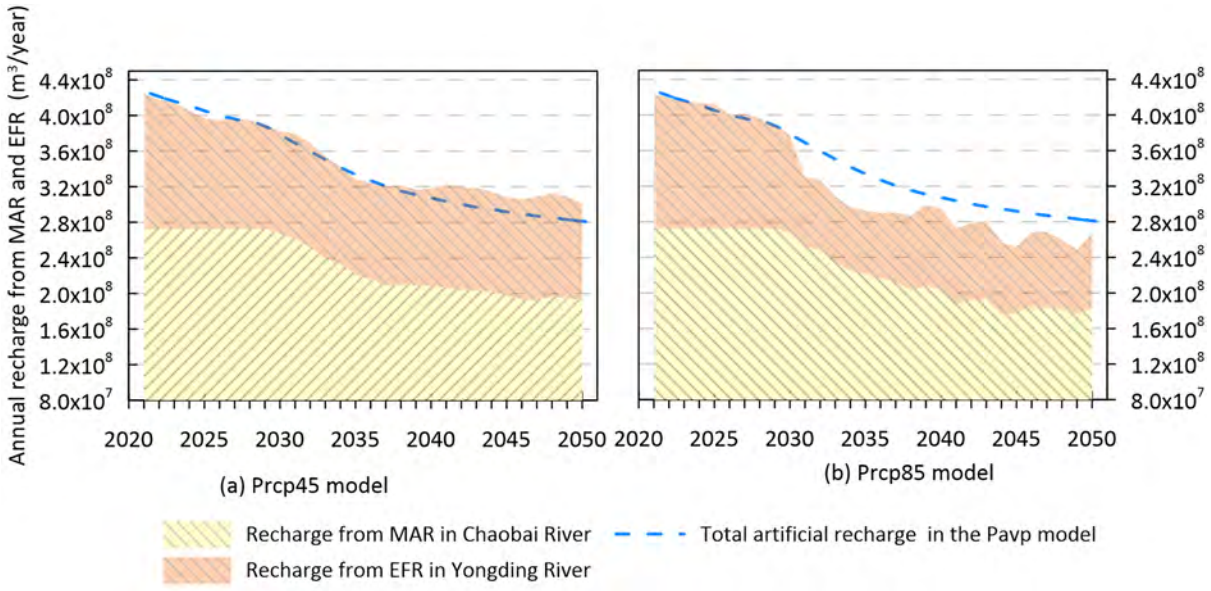

Figure 6-11 Artificial recharge from the MAR and EFR project in Chaobai and Yongding River predicted by the Prcp45 and Prcp85 model.

6.3.4 The recovery of the groundwater storage in the near future

The changes in groundwater storage for the Prcp45 and Prcp85 models are also calculated and depicted in Figure 6-12a. Storage change indicates the storage recovery when it is positive and storage depletion when it is negative. The impact of future climate change on the groundwater system can be clearly seen by comparing the two climate scenario models with the Pav model, which uses the average historical precipitation. Larger variations are found in the Prcp85 model. In the next 30 years simulation, there are 15 years and 18 years with positive groundwater storage change. Strong correlations are found between the year with groundwater storage recovery and the wet year predicted by the future climate scenarios. The average annual storage changes of the Prcp45 and Prcp85 models are 137 million and 186 million m^3, respectively. From the cumulative storage change plotted in Figure 6-12b, we clearly see that the groundwater storage will recover significantly in the first 15 years of simulation and then gradually approaches stationary values. This is a clear indication that the groundwater system is approaching a new equilibrium so that groundwater development becomes sustainable. The predicted total groundwater recovery until 2050 will be 4.14 and 5.58 billion under the RCP 4.5 and RCP 8.5 scenarios, respectively. However, it is noted the storage recovery will mostly occur in the shallow aquifer. In the deep confined aquifer, only a very limited amount of storage can be recovered after 2035.

s

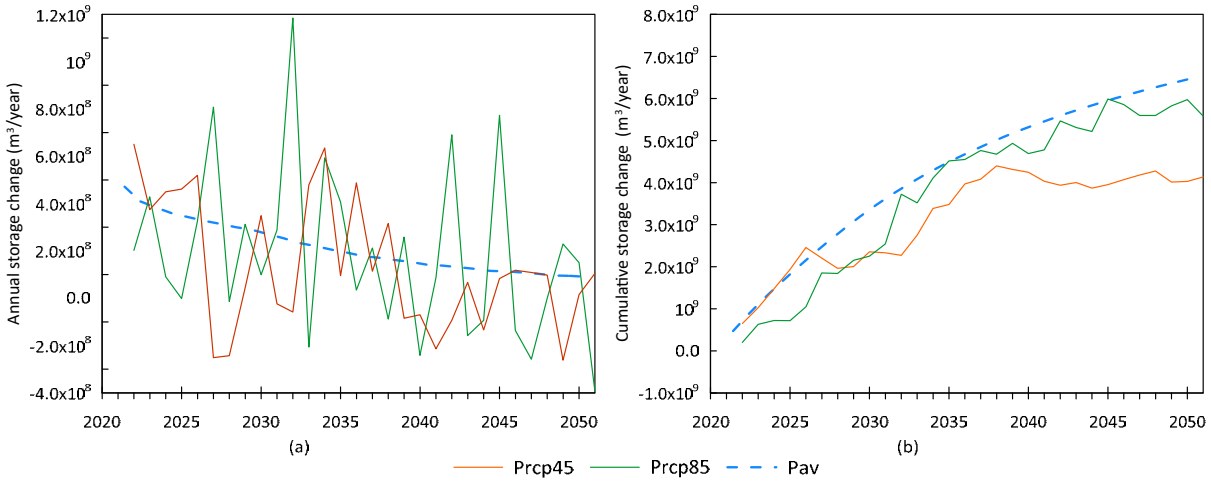

Figure 6-12 Annual groundwater storage change (a) and cumulative storage change (b) predicted by the Prcp45 and Prcp85 model from 2021 to 2050.

6.4 DISCUSSION

6.4.1 Climate and human impacts on groundwater sustainability in Beijing Plain

The impacts of future climate change on the groundwater system, particularly groundwater recharge have been widely recognized, and many modelling studies investigated this aspect in recent years (Goderniaux et al. 2009; Jackson et al. 2011; Crosbie et al. 2013; Chang et al. 2015; Zhou et al. 2020). Based on our simulation results, future climate change has minor impacts on groundwater resources in Beijing Plain. The variation of the wet and dry years predicted by the RCP8.5 scenario only results in inter-annual groundwater storage change with limited effect. Nevertheless, the model results from the RCP 4.5 scenario show continues groundwater storage depletion (Figure 6-12, Prcp45) during seven consecutive dry years after 2038 (Figure 6-7b). Other climate change models need to be investigated to ascertain the results of the impact.

Measures undertaken by Beijing municipality have addressed various key factors to guide the city towards groundwater sustainability.

The most important measure was the reduction of groundwater abstraction by substituting groundwater supply with the transferred surface water (about 1.0 billion m^3/year), which is a deciding measure to reverse the trend of groundwater depletion in Beijing Plain. Especially in deep confined aquifers, shutdown of pumping wells for industrial water supply effectively stopped rapid groundwater level decline. However, the recovery of

groundwater level and storage in the deep confined aquifers will still take a longer time because leakage from shallow aquifers is the only recharge and limited.

Additionally, large-scale MARs in two major rivers are very effective to close the gap of groundwater balance and contribute to sustainable development. These two measures combined can effectively restore the depleted groundwater storage and gradually contribute to a sustainable development by 2050. Furthermore, artificial recharge from MAR operations can restore the cone of the depression and become the main source of water for maintaining groundwater abstraction in the Chaobai River area, accounting for over 50% of total groundwater abstraction (Liu et al., 2022). The EFR project in Yongding River not only benefits the riparian ecosystem (Zhai et al. 2022), but also enhances groundwater recharge through river leakage which balances the recharge and abstraction in this area (Liu et al., 2023).

While the long-term groundwater management strategies described above indicate a positive trajectory towards more sustainable groundwater usage in Beijing Plain, it is important to acknowledge that the assessment of groundwater sustainability should consider multiple dimensions. As highlighted by Llamas et al. (2006), apart from the hydrological and groundwater-dependent ecological perspectives, institutional, economic, and social constraints were not considered in this study. Therefore, further investigation is necessary to comprehensively understand and address these additional aspects of groundwater sustainability.

6.4.2 Uncertainties and limitations

Uncertainties and limitations in this study need to be addressed from two perspectives.

Firstly, there are uncertainties associated with the climate model projection and bias correction method. In this study, there are large discrepancies between the precipitation projected by the RCM models and measured precipitation at meteorological stations. Additionally, the bias correction method employed in this study introduces its own uncertainties, as different methods may have varying assumptions and limitations. For future research on the impact of climate change on groundwater recharge, it is recommended to incorporate multiple GCMs and employ different bias correction methods to minimize uncertainties.

Secondly, uncertainties and limitations of the groundwater prediction model consist of three primary components: simplification of the simulation of precipitation infiltration, simulation of groundwater evapotranspiration (EVT), and the simplification of projected groundwater withdrawal scenarios that do not consider socio-economic factors. In the model settings, precipitation infiltration is treated as an instantaneous process at monthly time scale, thereby not accounting for the delayed recharge dynamics through the unsaturated zone. In the deep-water table area, infiltration water may take a number of

months to reach the water table. Unsaturated zone model should be used to investigate the delayed recharge process and compute monthly groundwater recharge as a cumulative effect of previous monthly precipitations. In the climate change prediction model, impact of future change of EVT was not considered. According to the projected temperature increase, the maximum EVT flux will increase. Especially, groundwater level depth will become shallower due to the implementation of groundwater conservation polices. Therefore, it is necessary to investigate impacts of EVT on groundwater resources in consideration of future temperature increase and groundwater level rise. In regard to the projected scenarios of future groundwater withdrawal, the current model assumes that total abstraction rate will remain constant at the current level. However, as reported by Wu et al. (2022), an increase in temperature by one degree is projected to result in an additional 177 million m^3 of domestic water consumption in Beijing, an aspect that was not taken into account in the prediction model. Temperature variations also have the potential to impact agricultural water usage, particularly in regions where groundwater serves as the primary source for irrigation. Temperature increase opens a new direction for groundwater development in connection with the MAR: not only as resources, but also as geothermal energy (Epting et al. 2023). Furthermore, the design of future scenarios should be integrated with the long-term development plans of Beijing municipality in order to provide a more accurate estimation of future groundwater usage.

6.4.3 Concerns of rising water table

A rising water table close to the surface may have negative impacts on the underground infrastructure in urban areas, induced groundwater pollution from unprotected solid waste disposal sites, sceptic tanks, and agriculture source, and soil salinization. Long et al. (2020) projected an average water table depth of 10 m by 2030. In our prediction model, the predicted water table depth varies in between 5 m in the southeast plain area and above 25 m in the west and north high elevation areas by 2050. In Beijing urban area, the predicted water table depth is about 15 m by 2050. Li et al. (2022) has reported the increase of NO3-N during the high water level period in Daxing District, southeast area of Beijing Plain. Thus, future strategies for urban groundwater management in the region should progressively adapt, with an increased emphasis on identifying and addressing the impacts of rising groundwater levels.

6.5 Conclusions

Groundwater use in Beijing Plain has increased greatly due to rapid socio-economic development and consequently groundwater reserves have been heavily depleted since the 1980s. Severe negative impacts forced Beijing municipality to take drastic measures to reverse the trend. The first measure was the reduction of groundwater abstraction by

substituting urban and industrial groundwater supply with transferred surface water from the south-to-north water transfer scheme since 2015. The second measure was the increase of groundwater recharge by implementing MARs in two major rivers. Pilot infiltration basin has been constructed in Chaobai River and operated since 2015. EFR in Yongding River has been conducted since 2019. Rising groundwater levels in these two areas have been observed in recent years. This study aimed to assess if the combined two measures can lead to long-term sustainable groundwater development in Beijing Plain.

First, a 3-D transient groundwater flow simulation model was developed and checked with historical groundwater level measurement from 1995 to 2020. The simulation model is capable to simulate trends of groundwater level and budget changes. Second, monthly rainfalls projected from three downscaled regional climate models under two scenarios (RCP4.5 and RCP8.5) were calibrated and validated with 30 years and 15 years measured monthly rainfalls from 14 meteorological stations, respectively. The average monthly rainfalls from the three models with the variance-based bias-correction statistically represent measured rainfalls very well in 45 years. Therefore, monthly groundwater recharge and lateral inflow were updated with the average monthly rainfalls from the three models under two scenarios from 2021 to 2050. Third, a transient groundwater flow prediction model was constructed with the estimated recharge and lateral inflow from 2021 to 2050. The prediction model used the reduced abstraction at the level of year 2020 and included a planned large-scale MAR in Chaobai River and EFR in Yongding River. Fourth, the prediction model was used to simulate the effects of the combined measures of abstraction reduction and artificial recharge from 2021 to 2050. From the analysis of the predicted groundwater levels and water budget, conclusions can be drawn. When groundwater abstraction is controlled at the current level (about 1.5 billion m^3/year), implementation of large-scale MARs in Chaobai and Yongding Rivers can lead to long-term sustainable groundwater development in Beijing plain. Reduction of groundwater abstraction for urban and industrial water supply is a deciding factor to reverse the trend of groundwater level decline, especially in deep confined aquifers. MARs in two major rivers are effective in restoring cones of depression in shallow aquifers and maintaining groundwater abstraction in these areas. Climate variation has large impacts on groundwater resources, especially, consecutive dry years can cause rapid groundwater storage depletion. The projected monthly precipitation from 2021 to 2050 is not significantly different from the past. Therefore, the projected future precipitation has minor impacts on groundwater resources in the next 30 years.

The findings of this study provide science-based information for Beijing municipality to strictly control groundwater abstractions and implement large-scale groundwater recharge schemes in Chaobai and Yongding rivers. Furthermore, methods used in this study can be applied in other regions facing similar challenges and opportunities for

sustainable groundwater management, making it a valuable contribution to the global scientific community.

7

CONCLUSIONS AND FUTURE RESEARCH

7.1 CONCLUSIONS

This research has developed a comprehensive modelling framework for assessing the effects of managed aquifer recharge at local scale in connection to groundwater flow at regional scale. An integrated groundwater model for Beijing Plain was constructed and can be continuously updated and refined with new data and new groundwater-related simulations. The results of the research provided science-based recommendations to formulate policies towards the sustainable groundwater development. Several conclusions can be drawn from this this study.

(1) Various conceptualizations of models can be created by integrating the same hydrogeological information. However, relying solely on testing statistical or information criteria may not be adequate to determine the optimal conceptual model. The selection of an appropriate conceptual model should also consider whether the constructed model can effectively achieve the desired modelling objectives. This involves a thorough assessment of the model's ability to accurately capture the fundamental characteristics of the system under study and to generate the desired outputs or predictions with precision. Comparison of multiple alternative models can significantly improve the likelihood of developing a robust and reliable model that aligns with the intended purpose and provides valuable insights for groundwater resources planning and management. In the case of Beijing Plain, while a simplified quasi-3D model may be sufficient for regional groundwater resources planning and management, a multiple aquifer-aquitard conceptual model offers greater accuracy for conducting particle tracking and contaminant transport simulations. Truncation of aquifers and aquitards with the basement should be performed to determine exact spatial distribution of each layer.

(2) A regional-scale groundwater model provides general flow pattern and overall water budget. A local-scale model is necessary for detailed simulation of important local phenomena such as managed aquifer recharge through infiltration basins and enhanced river leakage. Interactions between the regional and local models must be accounted. Therefore, a coupled regional and local model is required to design and assess the managed aquifer recharge schemes. This can be achieved by inserting a locally refined model in the regional model. Three methods can be used. The comparative assessment of the three model refinement methods found that the CGR method, despite its shortcomings, is capable of constructing coupled regional and local models for various simulations. The USG method, with its flexibility and adaptability, can construct multi-scale models fitting to diverse hydrogeological features and processes but requires more time and effort in the initial stages for model construction. The LGR method has limited applications due to the lack of a corresponding transport model code and unresolved interfacing problems with the regional model. The selection of a model refinement method should take into account the specific requirements of the local model, the complexity of the hydrogeological conditions, the flow and transport processes to be simulated.

(3) A thorough understanding of historical changes of groundwater levels in response to human activities and climate variability is the basis for better future predictions. Therefore, a long-term transient groundwater flow model should be constructed and calibrated. For Beijing Plain, a long-term monthly transient flow model from 1995 to 2020 was constructed and calibrated. This model reveals that groundwater was continuously overexploited in Beijing Plain until 2014. The rapid decline of groundwater levels and storage depletion was caused by intensified groundwater abstraction to combat drought during the consecutive drought periods. Severe drought from 1999 to 2010 not only reduced groundwater recharge, but also triggered emergency water supply with groundwater as only the source. Since 2015, emergency well fields ceased operation, a quarter of groundwater supply was substituted with transferred water from the South-to-North Water Diversion project, so that the amount of groundwater abstraction was reduced below the natural recharge. Since then, the trend of groundwater level decline and storage depletion was reversed.

(4) The No.8 well field located along the Chaobai River provides important urban water supply for the east area of Beijing City. Long-term overexploitation created a large cone of depression in the area. To sustain the well field, managed aquifer recharge was piloted since 2015. The transient simulation results reveal that the implementation of the MAR system in Chaobai River has effectively recovered groundwater depletion and reversed the trend of groundwater level decline in the area. Furthermore, the full-scale MAR operation could sustainably support the majority of the groundwater abstraction at the No.8 Well Field in the future, which secures the urban water supply. However, the model results also show that as groundwater levels rise beneath the infiltration ponds, the infiltration rate may decrease. Therefore, to maintain a high infiltration rate, groundwater levels beneath the ponds should be kept below the bottom of the ponds, necessitating the continuation of groundwater abstractions at the current capacity.

(5) Under natural conditions, leakage from Yongding River provides significant groundwater recharge in the west suburb of the Beijing Plain. The river became dry most times every year due to dam constructions upstream. From 2019, environmental flow release (EFR) from upstream reservoirs kept river flow for a number of months. EFR may have a positive effect on groundwater recharge. From the groundwater flow and solute transport simulation of the EFR in Yongding River, it can be concluded that EFR operation has enhanced the groundwater recharge and maintained the river flow. The long-term EFR operation will significantly contribute to groundwater sustainability in the region and could restore the connection of the river channel with the groundwater in the middle reach. A new equilibrium state for the groundwater system will be reached to sustain groundwater-dependent ecosystems in Yongding River. Furthermore, the river leakage rate is controlled by several operational factors of the EFR and physical factors of the river channel properties, which can be managed and controlled in accordance to balance the need of enhancing groundwater recharge or sustaining the environmental flow.

(6) Measures taken in Beijing to address groundwater depletion by substituting urban and industrial groundwater supply with transferred surface water and implementing MAR in major rivers have shown potential for sustainable groundwater development in the future. In particular, reduction of groundwater abstraction is very effective to reverse the trend of groundwater decline, especially in deep confined aquifers. The managed aquifer recharge through infiltration basins and river leakage can sustain important well fields for urban water supply. Climate change is projected to have minor effects. However, consecutive dry years may lead to short-term depletion of groundwater storage in the future. A drought response policy is required.

Lessons and experiences of groundwater abstraction in the Beijing Plain from overexploitation towards sustainable development can be helpful for other major cities that are dependent on groundwater. The integrated model simulations in this research illustrated the history of groundwater overexploitation and provided science-based evidence to assess the present and future impacts of measures taken by Beijing municipality towards sustainable development of groundwater resources. The comprehensive modelling framework developed in this research can be applied in similar settings worldwide, providing a valuable contribution towards sustainable groundwater management strategies.

7.2 APPLICATION OF THE MODELLING FRAMEWORK

The modelling framework developed in this research for Beijing Plain has the potential to be continuously refined and extended to adapt to future groundwater management strategies or new MAR designs and operations. Data used in this research including the meteorological data, groundwater monitoring data, water consumption data from different sectors, should be continuously collected to ensure that the model simulation can be regularly updated with the most current data, maintaining its status as a reliable tool for decision makers. Furthermore, the involvement of more government agencies and stakeholders is essential to enhance this modelling framework. By engaging additional organizations, their expertise and data resources can be utilized to improve the model. Different government departments can express their specific needs and utilize the modelling framework to simulate various socioeconomic and climate scenarios that align with their respective goals, ultimately facilitating more informed decision-making and policy development.

Beyond its application at the current spatial scale, the modelling framework has the potential for broader use in larger-scale groundwater management projects. For instance, it could serve as a foundation for an integrated groundwater management plan encompassing the entire North China Plain. This expanded application could provide valuable insights into sustainable groundwater development strategies on a regional scale.

In summary, the modelling framework developed for the Beijing Plain represents a dynamic and adaptable tool for future groundwater management. Through continuous data integration, collaboration with government agencies, and potential expansion to larger scales, this framework stands as a valuable asset aiming for the sustainable groundwater management not only in Beijing but also in other regions facing similar challenges.

7.3 LIMITATIONS OF THE MODELLING FRAMEWORK

While our modelling framework has allowed for a thorough assessment of the impacts of MAR implementation on the groundwater system of the Beijing Plain, it still possesses certain limitations.

Firstly, there are limitations related to the data utilized in the model. Due to the lack of surface water data, the representation of surface water bodies within the model is somewhat oversimplified. Although hydrogeological data near the MAR sites are relatively comprehensive, in some other areas, such as the Changping region in the northwest of the plain, there is a lack of deep borehole data reaching the bedrock layer. This resulted in uncertainties in the interpretation of aquifer layers in that region, which, while not significantly impacting our study, do affect the accuracy of regional groundwater level simulations.

Secondly, our current model only encompasses groundwater flow simulations and primarily focuses on the recovery of groundwater depletion through MAR implementation. Environmental concerns related to groundwater quality have not been included. While the water quality of MAR source water is generally better than the native groundwater, the mixing of these two different water qualities and the water quality change along the movement of the infiltration process remains an important research topic. Unfortunately, due to challenges in obtaining water quality data, this aspect was not analysed in our study.

7.4 FUTURE RESEARCH

The findings of this research provide an important basis for further studies related to groundwater management, particularly in the context of MAR systems. Here are five directions for future research:

Conducting research on risk analysis of rising groundwater level in the highly urbanized area in Beijing.

It is observed from the groundwater level monitoring data and the model prediction that the groundwater level has been rising and will continue to rise in most parts of Beijing. It is essential to redirect attention from recovering groundwater storage to recognizing the

potential hazards posed by rising groundwater levels and shallow groundwater depths, especially in highly urbanized areas. Data related to Beijing's urban underground infrastructure, including water supply systems, sewage networks, and subway tunnels should be collected. These data could be integrated with groundwater level predicted by the model, to identify areas vulnerable to future high groundwater levels. Proactive monitoring and precautionary measures should be implemented at the identified area.

Implementing Heat and Isotope Tracer Tests for Enhanced Understanding of Water Movement

Further studies could employ tracer tests to improve the understanding of water movement from managed aquifer recharge systems (infiltration basins and rivers) into aquifer systems. Tracers such as heat and isotopes can be used to track the flow paths of recharged water in the subsurface, enabling more precise quantification of recharge rates and the delineation of mixing zones. Moreover, tracer tests can provide valuable data for calibrating and validating the numerical simulation results.

Evaluating the Role of the Unsaturated Zone in Managed Aquifer Recharge

The current model settings overlook the infiltration process of MAR water in the vadose zone, which is an important aspect to consider. The unsaturated zone plays a significant role in MAR systems and can have a substantial impact on the recharge process. Therefore, future research should focus on investigating the hydraulic properties of the unsaturated zone and their influence on infiltration rates, deep percolation, and changes in water quality during recharge. One approach to incorporate unsaturated flow processes is by adding the Unsaturated Zone Flow (UZF) package of the MODFLOW program (Niswonger et al. 2006) to the simulation. Additionally, coupling the groundwater model with other hydrological models, such as the HYDRUS (Hydrological transport model for Unsaturated Soil) model (Beegum et al. 2018), could also be considered. However, it is important to note that implementing these models would require additional soil parameters, which can be obtained through the collection of additional monitoring data.

Developing Advanced Monitoring Systems for Effective Management of MAR Operations

A comprehensive and reliable monitoring system is essential for the successful long-term operation and management of MAR systems. Future work should also focus on the design and implementation of monitoring networks that can effectively capture spatial and temporal changes in groundwater levels and water quality. To accurately simulate the heat transport and the unsaturated zone flow process, it is also important to monitor the

groundwater and surface water temperature. Collection of isotope data at key locations is also crucial for a comprehensive understanding of the MAR system.

In addition, data from the monitoring system could also be combined with other data sources, such as remote sensing and airborne data. Integration of these diverse datasets can provide a more holistic understanding of the hydrological processes and dynamics of the MAR system.

Model Improvement

Although the models used in this research have been proved sufficient to fulfil the modelling objectives, with the development of the new modelling programs and modelling tools there is always room for improving the model construction. A possible pathway is to convert the groundwater flow model from MODFLOW-2005 into MODFLOW 6 (Hughes et al. 2017). MODFLOW 6 offers two types of hydrologic models: the Groundwater flow (GWF) model and the Groundwater Transport (GWT) model. The GWF model utilizes the control-volume finite-difference (CVFD) approach, which has demonstrated to have better flexibility of grid generation. This flexibility is particularly beneficial for coupling the regional and local groundwater flow model.

With the new capability of the MODFLOW 6, it is possible to expand the current model domain to include the Karst aquifer in the mountainous area located in the west of Beijing Plain with a more flexible mesh scheme. By incorporating the karst aquifer into the model lateral inflow from the mountainous area can be accounted and the accuracy of model simulations and predictions can be further improved.

Conducting Post-Audit Analysis for Model Predictions

A post-audit involves comparing model predictions with observed data that were not available or used during model calibration. This process can provide a robust test of the model's predictive performance and can identify areas where the model may need improvements. Post-audits could be conducted after several years of operation of the MAR systems in the Beijing Plain to assess the long-term accuracy of the model predictions.

These research directions mentioned above could enhance our understanding of MAR systems and contribute to the further development of sustainable groundwater management strategies in the Beijing Plain and similar regions.

REFERENCES

Abbo H, Gev I (2008) Numerical model as a predictive analysis tool for rehabilitation and conservation of the Israeli coastal aquifer: example of the Shafdan sewage reclamation project. Desalination 226:47–55

Aeschbach-Hertig W, Gleeson T (2012) Regional strategies for the accelerating global problem of groundwater depletion. Nat Geosci 5:853–861. https://doi.org/10.1038/ngeo1617

Akaike H (1973) Information theory and the maximum likelihood principle. In: 2nd International Symposium on Information Theory

Akaike H (1974) A New Look at the Statistical Model Identification. IEEE Trans Automat Contr. https://doi.org/10.1109/TAC.1974.1100705

Alam S, Borthakur A, Ravi S, et al (2021) Managed aquifer recharge implementation criteria to achieve water sustainability. Sci Total Environ 768:144992. https://doi.org/https://doi.org/10.1016/j.scitotenv.2021.144992

Alam S, Gebremichael M, Li R, et al (2019) Climate change impacts on groundwater storage in the Central Valley, California. Clim Change 157:387–406. https://doi.org/10.1007/s10584-019-02585-5

Alberti L, Colombo L, Formentin G (2018) Null-space Monte Carlo particle tracking to assess groundwater PCE (Tetrachloroethene) diffuse pollution in north-eastern Milan functional urban area. Sci Total Environ. https://doi.org/10.1016/j.scitotenv.2017.11.253

Amanambu AC, Obarein OA, Mossa J, et al (2020) Groundwater system and climate change: Present status and future considerations. J Hydrol 589:125163. https://doi.org/10.1016/j.jhydrol.2020.125163

Amoros C, Elger A, Dufour S, et al (2005) Flood scouring and groundwater supply in rehabilitated side-channels of the Rhône River, France. Arch fur Hydrobiol 155:147–167. https://doi.org/10.1127/lr/15/2003/147

Anderson MP, Woessner WW, Hunt RJ (2015) Modeling Purpose and Conceptual Model. In: Anderson MP, Woessner WW, Hunt RJ (eds) Applied Groundwater Modeling (Second Edition). Academic Press, San Diego, pp 27–67

Aphale O, Tonjes DJ (2017) Multimodel Validity Assessment of Groundwater Flow Simulation Models Using Area Metric Approach. Groundwater 55:219–226. https://doi.org/10.1111/gwat.12470

Appels WM, Bogaart PW, van der Zee SEATM (2017) Feedbacks Between Shallow Groundwater Dynamics and Surface Topography on Runoff Generation in Flat Fields. Water Resour Res. https://doi.org/10.1002/2017WR020727

AQSIQ, SAC (2017) Standard for Groundwater Quality. China

Aquaveo (2017) GMS (Groundwater Modeling System) , Version 10.4, Reference Mannual

Aquaveo (2019) GMS - Groundwater Modeling System 10.4 Tutorials. https://www.aquaveo.com/software/gms-learning-tutorials

Ashraf S, Nazemi A, AghaKouchak A (2021) Anthropogenic drought dominates groundwater depletion in Iran. Sci Rep 11:9135. https://doi.org/10.1038/s41598-021-88522-y

Awad A, Luo W, Zou J (2021) DRAINMOD simulation of paddy field drainage strategies and adaptation to future climate change in lower reaches of the Yangtze river basin*. Irrig Drain 70:819–831. https://doi.org/https://doi.org/10.1002/ird.2564

Bahar T, Oxarango L, Castebrunet H, et al (2021) 3D modelling of solute transport and mixing during managed aquifer recharge with an infiltration basin. J Contam Hydrol 237:103758. https://doi.org/https://doi.org/10.1016/j.jconhyd.2020.103758

Barber ME, Hossain A, Covert JJ, Gregory GJ (2009) Augmentation of seasonal low stream flows by artificial recharge in the Spokane Valley-Rathdrum Prairie aquifer of Idaho and Washington, USA. Hydrogeol J 17:1459–1470. https://doi.org/10.1007/s10040-009-0467-6

Basharat M (2019) Chapter 16 - Water Management in the Indus Basin in Pakistan: Challenges and Opportunities. In: Khan SI, Adams TEBT-IRB (eds). Elsevier, pp 375–388

Beegum S, Šimůnek J, Szymkiewicz A, et al (2018) Updating the Coupling Algorithm between HYDRUS and MODFLOW in the HYDRUS Package for MODFLOW. Vadose Zo J 17:180034. https://doi.org/https://doi.org/10.2136/vzj2018.02.0034

Beijing Water Authority (2019) Beijing Water Resources Bulletin. http://swj.beijing.gov.cn/zwgk/szygb/. Accessed 1 Dec 2020

Beijing Water Authority (2021a) Beijing Water Resources Bulletin (1986-2020). In: Beijing Water Auth. http://swj.beijing.gov.cn/zwgk/szygb/. Accessed 2 Nov 2021

Beijing Water Authority (2021b) Detailed information of the Water release event of the Yongding River. http://nsbd.swj.beijing.gov.cn:8088/uacp/pageview/bjsw/main. Accessed 1 Mar 2021

Beven K, Binley A (1992) The future of distributed models: Model calibration and uncertainty prediction. Hydrol Process 6:279–298. https://doi.org/10.1002/hyp.3360060305

Beven KJ (2018) On hypothesis testing in hydrology: Why falsification of models is still a really good idea. Wiley Interdiscip Rev Water 5:. https://doi.org/10.1002/wat2.1278

Bouwer H (2002) Artificial recharge of groundwater: Hydrogeology and engineering. Hydrogeol J 10:121–142. https://doi.org/10.1007/s10040-001-0182-4

Božović Đ, Polomčić D, Bajić D, Ratković J (2020) Hydrodynamic analysis of radial collector well ageing at Belgrade well field. J Hydrol 582:124463. https://doi.org/10.1016/j.jhydrol.2019.124463

Bredehoeft J (2005) The conceptualization model problem—surprise. Hydrogeol J 13:37–46. https://doi.org/10.1007/s10040-004-0430-5

Bunn SE, Arthington AH (2002) Basic Principles and Ecological Consequences of Altered Flow Regimes for Aquatic Biodiversity. Environ Manage 30:492–507. https://doi.org/10.1007/s00267-002-2737-0

BWA (2009) Green Yongding River: the construction plan for an ecological corridor. Beijing, China (in Chinese). Beijing, China

Cao G, Zheng C, Scanlon BR, et al (2013) Use of flow modeling to assess sustainability of groundwater resources in the North China Plain. Water Resour Res 49:159–175. https://doi.org/https://doi.org/10.1029/2012WR011899

Cao X, Zhai Y, Li M, et al (2022) The suitability assessment of groundwater recharge by leakage of the Yongding River. Hydrogeol Eng Geol 49:20–29. https://doi.org/10.16030/j.cnki.issn.1000-3665.202107069

Chang J, Wang G, Mao T (2015) Simulation and prediction of suprapermafrost groundwater level variation in response to climate change using a neural network model. J Hydrol 529:1211–1220. https://doi.org/10.1016/j.jhydrol.2015.09.038

Charlesworth PB, Narayan KA, Bristow KL, et al (2020) The Burdekin Delta—Australia's oldest artificial recharge scheme. In: Management of Aquifer Recharge for Sustainability: Proceedings of the 4th International Symposium on Artificial Recharge of Groundwater, Adelaide, September 2002, 1st Editio. CRC Press, pp 347–352

Chen BB, Gong HL, Li XJ, et al (2011) Spatial-temporal characteristics of land subsidence corresponding to dynamic groundwater funnel in Beijing Municipality, China. Chinese Geogr Sci 21:753–764. https://doi.org/10.1007/s11769-011-0509-6

Chen H, Wang S, Zhu J, Zhang B (2020) Projected Changes in Abrupt Shifts Between Dry and Wet Extremes Over China Through an Ensemble of Regional Climate Model Simulations. J Geophys Res Atmos 125:e2020JD033894. https://doi.org/https://doi.org/10.1029/2020JD033894

Conant B, Robinson CE, Hinton MJ, Russell HAJ (2019) A framework for conceptualizing groundwater-surface water interactions and identifying potential impacts on water quality, water quantity, and ecosystems. J Hydrol 574:609–627. https://doi.org/https://doi.org/10.1016/j.jhydrol.2019.04.050

Craig JR, Ramadhan M, Muffels C (2020) A Particle Tracking Algorithm for Arbitrary Unstructured Grids. Groundwater 58:19–26. https://doi.org/https://doi.org/10.1111/gwat.12894

Crosbie RS, Scanlon BR, Mpelasoka FS, et al (2013) Potential climate change effects on groundwater recharge in the High Plains Aquifer, USA. Water Resour Res 49:3936–3951. https://doi.org/https://doi.org/10.1002/wrcr.20292

Cuthbert MO, Taylor RG, Favreau G, et al (2019) Observed controls on resilience of groundwater to climate variability in sub-Saharan Africa. Nature 572:230–234. https://doi.org/10.1038/s41586-019-1441-7

de Graaf IEM, van Beek RLPH, Gleeson T, et al (2017) A global-scale two-layer transient groundwater model: Development and application to groundwater depletion. Adv Water Resour 102:53–67.

https://doi.org/https://doi.org/10.1016/j.advwatres.2017.01.011

Deines JM, Kendall AD, Butler JJ, Hyndman DW (2019) Quantifying irrigation adaptation strategies in response to stakeholder-driven groundwater management in the US High Plains Aquifer. Environ Res Lett 14:44014. https://doi.org/10.1088/1748-9326/aafe39

Dillon P (2005) Future management of aquifer recharge. Hydrogeol J 13:313–316. https://doi.org/10.1007/s10040-004-0413-6

Dillon PJ, Pavelic P, Page D, et al (2009) Managed aquifer recharge: An Introduction. National Water Commission, Canberra

Doherty J (2010) PEST: Model-Independent Parameter Estimation, User Manual: 5th Edition

Döll P, Fiedler K, Zhang J (2009) Global-scale analysis of river flow alterations due to water withdrawals and reservoirs. Hydrol Earth Syst Sci 13:2413–2432. https://doi.org/10.5194/hess-13-2413-2009

Ebraheem AM, Riad S, Wycisk P, Sefelnasr AM (2004) A local-scale groundwater flow model for groundwater resources management in Dakhla Oasis, SW Egypt. Hydrogeol J 12:714–722. https://doi.org/10.1007/s10040-004-0359-8

Edmunds WM (2003) Renewable and non-renewable groundwater in semi-arid and arid regions. In: Alsharhan AS, Wood WWBT-D in WS (eds) Water Resources Perspectives: Evaluation, Management and Policy. Elsevier, pp 265–280

Elshall AS, Tsai FTC (2014) Constructive epistemic modeling of groundwater flow with geological structure and boundary condition uncertainty under the Bayesian paradigm. J Hydrol 517:105–119. https://doi.org/https://doi.org/10.1016/j.jhydrol.2014.05.027

Emiliano PC, Vivanco MJF, de Menezes FS (2014) Information criteria: How do they behave in different models? Comput Stat Data Anal 69:141–153. https://doi.org/https://doi.org/10.1016/j.csda.2013.07.032

Enemark T, Peeters LJM, Mallants D, Batelaan O (2019) Hydrogeological conceptual model building and testing: A review. J Hydrol 569:310–329

Epting J, Råman Vinnå L, Piccolroaz S, et al (2022) Impacts of climate change on Swiss alluvial aquifers – A quantitative forecast focused on natural and artificial groundwater recharge by surface water infiltration. J Hydrol X 17:100140. https://doi.org/https://doi.org/10.1016/j.hydroa.2022.100140

Epting J, Vinnå, Råman L, Affolter A, et al (2023) Climate change adaptation and mitigation measures for alluvial aquifers - Solution approaches based on the thermal exploitation of managed aquifer (MAR) and surface water recharge (MSWR). Water Res 238:119988. https://doi.org/https://doi.org/10.1016/j.watres.2023.119988

Eshtawi T, Evers M, Tischbein B (2015) Potential impacts of urban area expansion on groundwater level in the Gaza Strip: A spatial-temporal assessment. Arab J Geosci. https://doi.org/10.1007/s12517-015-1971-8

Evans P, Arunakumaren J (2012) Groundwater Management in Bribie Island Fo Urban

Expansion. Achiev Groundw Supply Sustain Reliab through Manag Aquifer Recharg Proc 7th Int Symp Manag Aquifer Recharg 381–388

Famiglietti JS (2014) The global groundwater crisis. Nat Clim Chang 4:945–948. https://doi.org/10.1038/nclimate2425

Feinstein DT, Dunning CP, Juckem PF, et al (2010) Application of the Local Grid Refinement package to an inset model simulating the interactions of lakes, wells, and shallow groundwater, northwestern Waukesha County, Wisconsin. Reston, VA

Feinstein DT, Fienen MN, Reeves HW, Langevin CD (2016) A Semi-Structured MODFLOW-USG Model to Evaluate Local Water Sources to Wells for Decision Support. Groundwater. https://doi.org/Hydrodynamic analysis of radial collector well ageing at Belgrade well field

Foglia L, Mehl SW, Hill MC, et al (2007) Testing alternative ground water models using cross-validation and other methods. Groundwater 45:627–641. https://doi.org/10.1111/j.1745-6584.2007.00341.x

Foglia L, Mehl SW, Hill MC, Burlando P (2013) Evaluating model structure adequacy: The case of the Maggia Valley groundwater system, southern Switzerland. Water Resour Res 49:260–282

Forghani A, Peralta RC (2017) Transport modeling and multivariate adaptive regression splines for evaluating performance of ASR systems in freshwater aquifers. J Hydrol. https://doi.org/10.1016/j.jhydrol.2017.08.012

Gale I (2005) Strategies for Managed Aquifer Recharge (MAR) in semi-arid areas. UNESCO

Ganot Y, Holtzman R, Weisbrod N, et al (2018) Managed aquifer recharge with reverse-osmosis desalinated seawater: modeling the spreading in groundwater using stable water isotopes. Hydrol Earth Syst Sci 22:6323–6333. https://doi.org/10.5194/hess-22-6323-2018

Ganot Y, Holtzman R, Weisbrod N, et al (2017) Monitoring and modeling infiltration–recharge dynamics of managed aquifer recharge with desalinated seawater. Hydrol Earth Syst Sci 21:4479

Gao Y, Yu M (2018) Assessment of the economic impact of South-to-North Water Diversion Project on industrial sectors in Beijing. J Econ Struct 7:4. https://doi.org/10.1186/s40008-018-0104-4

Gedeon M, Mallants D (2012) Sensitivity Analysis of a Combined Groundwater Flow and Solute Transport Model Using Local-Grid Refinement: A Case Study. Math Geosci 44:881–899. https://doi.org/10.1007/s11004-012-9416-3

Gemitzi A, Ajami H, Richnow H-H (2017) Developing empirical monthly groundwater recharge equations based on modeling and remote sensing data – Modeling future groundwater recharge to predict potential climate change impacts. J Hydrol 546:1–13. https://doi.org/https://doi.org/10.1016/j.jhydrol.2017.01.005

Ghayoumian J, Ghermezcheshme B, Feiznia S, Noroozi AA (2005) Integrating GIS and DSS for identification of suitable areas for artificial recharge, case study Meimeh

Basin, Isfahan, Iran. Environ Geol 47:493–500. https://doi.org/10.1007/s00254-004-1169-y

Ghazavi R, Ebrahimi H (2019) Predicting the impacts of climate change on groundwater recharge in an arid environment using modeling approach. Int J Clim Chang Strateg Manag 11:88–99. https://doi.org/10.1108/IJCCSM-04-2017-0085

Gleeson T, VanderSteen J, Sophocleous MA, et al (2010) Groundwater sustainability strategies. Nat Geosci 3:378–379. https://doi.org/10.1038/ngeo881

Goderniaux P, Brouyère S, Fowler HJ, et al (2009) Large scale surface-subsurface hydrological model to assess climate change impacts on groundwater reserves. J Hydrol 373:122–138. https://doi.org/10.1016/j.jhydrol.2009.04.017

Gonzalez D, Janardhanan S, Pagendam DE, Gladish DW (2020) Probabilistic groundwater flow, particle tracking and uncertainty analysis for environmental receptor vulnerability assessment of a coal seam gas project. Water (Switzerland). https://doi.org/10.3390/w12113177

Goodarzi M, Abedi-Koupai J, Heidarpour M, Safavi HR (2016) Evaluation of the Effects of Climate Change on Groundwater Recharge Using a Hybrid Method. Water Resour Manag 30:133–148. https://doi.org/10.1007/s11269-015-1150-4

Green TR (2016) Linking Climate Change and Groundwater. In: Jakeman AJ, Barreteau O, Hunt RJ, et al. (eds) Integrated Groundwater Management: Concepts, Approaches and Challenges. Springer International Publishing, Cham, pp 97–141

Guo W, Maliva R, Missimer T (2010) Recovery efficiency assessment of an ASR well using groundwater models

Han J (2007) Transient modelling of groundwater flow in Beijing Plain. UNESCO-IHE Institete for Water Education

Hao Q, Shao J, Cui Y, Xie Z (2014) Applicability of artificial recharge of groundwater in the Yongding River alluvial fan in Beijing through numerical simulation. J Earth Sci. https://doi.org/10.1007/s12583-014-0442-6

Harbaugh AW (2005) MODFLOW-2005, the US Geological Survey modular ground-water model: the ground-water flow process. US Department of the Interior, US Geological Survey Reston

Harbaugh AW (1990) A computer program for calculating subregional water budgets using results from the US Geological Survey modular three-dimensional finite-difference ground-water flow model. US Geological Survey

Harbaugh BAW, Banta ER, Hill MC, Mcdonald MG (2000) MODFLOW-2000 , The U .S . Geological Survey modular graound-water model — User guide to modularization concepts and the ground-water flow process. US Geol Surv 130

Harwood A, Johnson S, Richter B, et al (2017) Listen to the river: Lessons from a global review of environmental flow success stories. Woking,UK

Hashemi H, Berndtsson R, Persson M (2015) Artificial recharge by floodwater spreading estimated by water balances and groundwater modelling in arid Iran. Hydrol Sci Journal-Journal Des Sci Hydrol 60:336–350.

https://doi.org/10.1080/02626667.2014.881485

Hassan AE, Bekhit HM, Chapman JB (2009) Using Markov Chain Monte Carlo to quantify parameter uncertainty and its effect on predictions of a groundwater flow model. Environ Model Softw. https://doi.org/10.1016/j.envsoft.2008.11.002

Hayashi M, Rosenberry DO (2002) Effects of Ground Water Exchange on the Hydrology and Ecology of Surface Water. Groundwater 40:309–316. https://doi.org/https://doi.org/10.1111/j.1745-6584.2002.tb02659.x

Hayes P, Nicol C, La Croix AD, et al (2020) Enhancing geological and hydrogeological understanding of the Precipice Sandstone aquifer of the Surat Basin, Great Artesian Basin, Australia, through model inversion of managed aquifer recharge datasets. Hydrogeol J. https://doi.org/10.1007/s10040-019-02079-9

Herrera-Pantoja M, Hiscock KM (2015) Projected impacts of climate change on water availability indicators in a semi-arid region of central Mexico. Environ Sci Policy 54:81–89. https://doi.org/https://doi.org/10.1016/j.envsci.2015.06.020

Hill MC, Tiedeman CR (2006) Effective groundwater model calibration: with analysis of data, sensitivities, predictions, and uncertainty. Hoboken, New Jersey: John Wiley and Sons

Hoard CJ (2010) Implementation of local grid refinement (LGR) for the Lake Michigan Basin regional groundwater-flow model

Howard KWF, Gelo KK (2001) Intensive groundwater use in urban areas: the case of megacities. In: Intensive use of groundwater challenges and opportunities

Hsieh H-H, Lee C-H, Ting C-S, Chen J-W (2010) Infiltration mechanism simulation of artificial groundwater recharge: a case study at Pingtung Plain, Taiwan. Environ Earth Sci 60:1353–1360. https://doi.org/10.1007/s12665-009-0194-2

Hu H, Mao X, Yang Q (2019a) Development of a groundwater fl ow and reactive solute transport model in the Yongding River alluvial fan , China. 13:371–384

Hu H, Mao X, Yang Q (2018) Impacts of Yongding River Ecological Restoration on the Groundwater Environment: Scenario Prediction. Vadose Zo J 17:180121. https://doi.org/10.2136/vzj2018.06.0121

Hu L, Dai K, Xing C, et al (2019b) Land subsidence in Beijing and its relationship with geological faults revealed by Sentinel-1 InSAR observations. Int J Appl Earth Obs Geoinf 82:101886. https://doi.org/https://doi.org/10.1016/j.jag.2019.05.019

Huang J, Christ JA, Goltz MN (2008) An Assembly Model for Simulation of Large-Scale Ground Water Flow and Transport. Groundwater 46:882–892. https://doi.org/10.1111/j.1745-6584.2008.00484.x

Huang PS, Chiu YC (2018) A simulation-optimization model for seawater intrusion management at Pingtung Coastal Area, Taiwan. Water (Switzerland). https://doi.org/10.3390/w10030251

Hughes J., Langevin C., Chartier K., White JT (2012) Documentation of the Surface-Water Routing (SWR1) Process for Modeling Surface-Water Flow with the U.S. Geological Survey Modular Groundwater Model (MODFLOW–2005), 6th edn. U.S.

Geological Survey Techniques and Methods

Hughes JD, Langevin CD, Banta ER (2017) Documentation for the MODFLOW 6 framework. Reston, VA

IAH (2016) Global Change & Groundwater

IGRAC (2007) Global MAR Inventory Report

Izbicki JA, Flint AL, Stamos CL (2008) Artificial recharge through a thick, heterogeneous unsaturated zone. Ground Water 46:475–488. https://doi.org/10.1111/j.1745-6584.2007.00406.x

Jackson CR, Meister R, Prudhomme C (2011) Modelling the effects of climate change and its uncertainty on UK Chalk groundwater resources from an ensemble of global climate model projections. J Hydrol 399:12–28. https://doi.org/10.1016/j.jhydrol.2010.12.028

Jarraya Horriche F, Benabdallah S (2020) Assessing Aquifer Water Level and Salinity for a Managed Artificial Recharge Site Using Reclaimed Water. Water 12

Ji Z, Cui Y, Zhang S, et al (2021) Evaluation of the impact of ecological water supplement on groundwater restoration based on numerical simulation: A case study in the section of yongding river, beijing plain. Water (Switzerland) 13:. https://doi.org/10.3390/w13213059

Jia X, Hou D, Wang L, et al (2020) The development of groundwater research in the past 40 years: A burgeoning trend in groundwater depletion and sustainable management. J Hydrol 587:125006. https://doi.org/10.1016/j.jhydrol.2020.125006

Jiang B, Wong CP, Lu F, et al (2014) Drivers of drying on the Yongding River in Beijing. J Hydrol 519:69–79. https://doi.org/10.1016/j.jhydrol.2014.06.033

Jiang R, Han D, Song X, Zheng F (2022) Numerical modeling of changes in groundwater storage and nitrate load in the unconfined aquifer near a river receiving reclaimed water. Environ Sci Pollut Res. https://doi.org/10.1007/s11356-022-18597-1

Karimov AK, Smakhtin V, Mavlonov A, et al (2015) Managed Aquifer Recharge: Potential Component of Water Management in the Syrdarya River Basin. J Hydrol Eng 20:1–12. https://doi.org/10.1061/(asce)he.1943-5584.0001046

Kashyap RL (1982) Optimal Choice of AR and MA Parts in Autoregressive Moving Average Models. IEEE Trans Pattern Anal Mach Intell. https://doi.org/10.1109/TPAMI.1982.4767213

Kennedy J, Rodríguez-Burgueño JE, Ramírez-Hernández J (2017) Groundwater response to the 2014 pulse flow in the Colorado River Delta. Ecol Eng 106:715–724. https://doi.org/10.1016/j.ecoleng.2016.10.072

Khan S, Abbas A, Blackwell J, et al (2007) Hydrogeological assessment of serial biological concentration of salts to manage saline drainage. Agric Water Manag 92:64–72. https://doi.org/10.1016/j.agwat.2007.05.011

Klaas DKSY, Imteaz MA, Sudiayem I, et al (2020) Assessing climate changes impacts on tropical karst catchment: Implications on groundwater resource sustainability and management strategies. J Hydrol 582:124426.

https://doi.org/https://doi.org/10.1016/j.jhydrol.2019.124426

Kloppmann W, Aharoni A, Chikurel H, et al (2012) Use of groundwater models for prediction and optimisation of the behaviour of MAR sites. In: Kazner C, Wintgens T, Dillon P (eds) Water reclamation technologies for safe managed aquifer recharge. IWA Publishing London, pp 311–349

Konikow LF (2015) Long-Term Groundwater Depletion in the United States. Groundwater 53:2–9. https://doi.org/https://doi.org/10.1111/gwat.12306

Konikow LF, Kendy E (2005) Groundwater depletion: A global problem. Hydrogeol J 13:317–320. https://doi.org/10.1007/s10040-004-0411-8

Lacher LJ, Turner DS, Gungle B, et al (2014) Application of Hydrologic Tools and Monitoring to Support Managed Aquifer Recharge Decision Making in the Upper San Pedro River, Arizona, USA. Water 6:3495–3527. https://doi.org/10.3390/w6113495

Lautz LK, Siegel DI (2006) Modeling surface and ground water mixing in the hyporheic zone using MODFLOW and MT3D. Adv Water Resour 29:1618–1633. https://doi.org/10.1016/j.advwatres.2005.12.003

Leake SA (1998) Assignment of boundary conditions in embedded ground water flow models. Ground Water 36:621–625. https://doi.org/10.1111/j.1745-6584.1998.tb02836.x

Leake SA, Claar D V. (1999) Procedures and computer programs for telescopic mesh refinement using MODFLOW

Li C, Men B, Yin S, et al (2022) Research into the Optimal Regulation of the Groundwater Table and Quality in the Southern Plain of Beijing Using Geographic Information Systems Data and Machine Learning Algorithms. ISPRS Int. J. Geo-Information 11

Li ZP, Liu JR, Sun Y, et al (2015) Considerations on the coordinated city development with groundwater resources in Beijing. In: Water Resources and Environment. CRC Press, pp 277–283

Lin G, Zheng X (2008) Simulation of Recovery Options of Brackish Water Aquifer in the Dagu River Area, China. In: 2008 2nd International Conference on Bioinformatics and Biomedical Engineering. pp 2966–2969

Liu C, Yu J, Kendy E (2001) Groundwater exploitation and its impact on the environment in the North China Plain. Water Int 26:265–272. https://doi.org/10.1080/02508060108686913

Liu C, Zheng H (2002) South-to-north water transfer schemes for China. Int J Water Resour Dev 18:453–471. https://doi.org/10.1080/0790062022000006934

Liu H-J, Hsu N-S, Lee TH (2009) Simultaneous identification of parameter, initial condition, and boundary condition in groundwater modelling. Hydrol Process 23:2358–2367. https://doi.org/https://doi.org/10.1002/hyp.7344

Liu M, Lin A, Gu J, et al (2016) Evaluation on Water Quality of North Water Delivery Line of Water Diversion Project from Yellow River to Beijing (in Chinese). J Water Resour Res 05:510–515. https://doi.org/10.12677/jwrr.2016.55059

Liu P-W, Famiglietti JS, Purdy AJ, et al (2022a) Groundwater depletion in California's Central Valley accelerates during megadrought. Nat Commun 13:7825. https://doi.org/10.1038/s41467-022-35582-x

Liu S, Zhou Y, Luo W, et al (2022b) A numerical assessment on the managed aquifer recharge to achieve sustainable groundwater development in Chaobai River area, Beijing, China. J Hydrol 613:128392. https://doi.org/https://doi.org/10.1016/j.jhydrol.2022.128392

Liu S, Zhou Y, Tang C, et al (2021a) Assessment of alternative groundwater flow models for Beijing Plain, China. J Hydrol 596:126065. https://doi.org/https://doi.org/10.1016/j.jhydrol.2021.126065

Liu S, Zhou Y, Xie M, et al (2021b) Comparative Assessment of Methods for Coupling Regional and Local Groundwater Flow Models: A Case Study in the Beijing Plain, China. Water 13

Liu S, Zhou Y, Zang Y, et al (2023) Effects of downstream environmental flow release on enhancing the groundwater recharge and restoring the groundwater/surface-water connectivity in Yongding River, Beijing, China. Hydrogeol J. https://doi.org/10.1007/s10040-023-02675-w

Llamas MR, Martinez-Santos P, De la Hera A (2006) The manifold dimensions of groundwater sustainability: An overview. In: International Symposium on Groundwater Sustainability. Alicante, Spain, pp 105–116

Long D, Yang W, Scanlon BR, et al (2020) South-to-North Water Diversion stabilizing Beijing's groundwater levels. Nat Commun 11:. https://doi.org/10.1038/s41467-020-17428-6

Lu M, Rogiers B, Beerten K, et al (2021) Exploring river–aquifer interactions and hydrological system response using baseflow separation, impulse response modelling and time series analysis in three temperate lowland catchments. Hydrol Earth Syst Sci Discuss 2021:1–45. https://doi.org/10.5194/hess-2021-422

Lux M, Szanyi J, Tóth TM (2016) Evaluation and optimization of multi-lateral wells using MODFLOW unstructured grids. Open Geosci. https://doi.org/10.1515/geo-2016-0004

Ma X, Yang Y, Hu G, et al (2020) The impact of eological water supplement of Yongding River on groundwater recharge (in Chinese). Beijing Water 22–27. https://doi.org/10.19671/j.1673.2020.04.005

Maliva RG, Clayton EA, Missimer TM (2009) Application of advanced borehole geophysical logging to managed aquifer recharge investigations. Hydrogeol J 17:1547–1556. https://doi.org/10.1007/s10040-009-0437-z

Maliva RG, Herrmann R, Coulibaly K, Guo WX (2015) Advanced aquifer characterization for optimization of managed aquifer recharge. Environ Earth Sci 73:7759–7767. https://doi.org/10.1007/s12665-014-3167-z

Martinez GF, Gupta H V (2011) Hydrologic consistency as a basis for assessing complexity of monthly water balance models for the continental United States. Water Resour Res 47:. https://doi.org/10.1029/2011WR011229

Masetti M, Pedretti D, Sorichetta A, et al (2016) Impact of a Storm-Water Infiltration Basin on the Recharge Dynamics in a Highly Permeable Aquifer. Water Resour Manag 30:149–165. https://doi.org/10.1007/s11269-015-1151-3

Masetti M, Pettinato S, Nghiem S V, et al (2018) Combining COSMO-SkyMed satellites data and numerical modeling for the dynamic management of artificial recharge basins. J Hydrol 567:41–50. https://doi.org/https://doi.org/10.1016/j.jhydrol.2018.09.067

Mazzoni A, Heggy E, Scabbia G (2018) Forecasting water budget deficits and groundwater depletion in the main fossil aquifer systems in North Africa and the Arabian Peninsula. Glob Environ Chang 53:157–173. https://doi.org/https://doi.org/10.1016/j.gloenvcha.2018.09.009

McMahon TA, Nathan RJ (2021) Baseflow and transmission loss: A review. WIREs Water 8:e1527. https://doi.org/https://doi.org/10.1002/wat2.1527

Megdal SB (2018) Invisible water: the importance of good groundwater governance and management. npj Clean Water 1:15. https://doi.org/10.1038/s41545-018-0015-9

Mehl S, Hill MC, Leake SA (2006) Comparison of Local Grid Refinement Methods for MODFLOW. Groundwater 44:792–796. https://doi.org/10.1111/j.1745-6584.2006.00192.x

Mehl SW, Hill MC (2006) MODFLOW-2005, the US Geological Survey modular ground-water model-documentation of shared node local grid refinement (LGR) and the boundary flow and head (BFH) package

Memari SS, Bedekar VS, Clement TP (2020) Laboratory and Numerical Investigation of Saltwater Intrusion Processes in a Circular Island Aquifer. Water Resour Res. https://doi.org/10.1029/2019WR025325

Michael HA, Khan MR (2016) Impacts of physical and chemical aquifer heterogeneity on basin-scale solute transport: Vulnerability of deep groundwater to arsenic contamination in Bangladesh. Adv Water Resour. https://doi.org/10.1016/j.advwatres.2016.10.010

Mirlas V, Antonenko V, Kulagin V, Kuldeeva E (2015) Assessing artificial groundwater recharge on irrigated land using the MODFLOW model. Earth Sci Res 4:. https://doi.org/10.5539/esr.v4n2p16

Moeck C, Molson J, Schirmer M (2020) Pathline Density Distributions in a Null-Space Monte Carlo Approach to Assess Groundwater Pathways. Groundwater. https://doi.org/10.1111/gwat.12900

Moel PJ, Verberk JQJC, Van Dijk JC (2006) Drinking water: principles and practices. World Scientific Singapore

Muzammil M, Zahid A, Farooq U, et al (2023) Climate change adaptation strategies for sustainable water management in the Indus basin of Pakistan. Sci Total Environ 878:163143. https://doi.org/https://doi.org/10.1016/j.scitotenv.2023.163143

Namjou P, Pattle AD (2002) Hydrogeological feasibility of disposal of treated effluent in coastal dunes near Auckland, New Zealand. In: Management of Aquifer Recharge

for Sustainability: Proceedings of the 4th International Symposium on Artificial Recharge of Groundwater. CRC Press., Adelaide, p 5

Nan T, Shao JL, Cui YL (2016) Column test-based features analysis of clogging in artificial recharge of groundwater in Beijing. J Groundw Sci Eng 4:88–95

Neuman SP, Wierenga PJ (2003) A comprehensive strategy of hydrogeologic modeling and uncertainty analysis for nuclear facilities and sites. University of Arizona. Report NUREG/CR-6805

Neumann I, Barker J, MacDonald D, Gale I (2004) Numerical approaches for approximating technical effectivessness of artificial recharge structures

Niraula R, Meixner T, Dominguez F, et al (2017) How Might Recharge Change Under Projected Climate Change in the Western U.S.? Geophys Res Lett 44:10,407-410,418. https://doi.org/https://doi.org/10.1002/2017GL075421

Niswonger RG, Morway ED, Triana E, Huntington JL (2017) Managed aquifer recharge through off-season irrigation in agricultural regions. Water Resour Res 53:6970–6992. https://doi.org/10.1002/2017WR020458

Niswonger RG, Prudic DE (2005) Documentation of the Streamflow-Routing (SFR2) Package to Include Unsaturated Flow Beneath Streams—A Modification to SFR1. US Geol Surv

Niswonger RG, Prudic DE, Regan SR (2006) Documentation of the Unsaturated-Zone Flow (UZF1) Package for Modeling Unsaturated Flow Between the Land Surface and the Water Table with MODFLOW-2005. US Geol Surv Tech Methods 71

Olsthoorn TN, Mosch MJM (2002) Fifty years of artificial recharge in the Amsterdam Dune area. In: Management of Aquifer Recharge for Sustainability: Proceedings of the 4th International Symposium on Artificial Recharge of Groundwater, Adelaide, September 2002, 1st Editio. CRC Press, pp 29–33

Ou G, Munoz-Arriola F, Uden DR, et al (2018) Climate change implications for irrigation and groundwater in the Republican River Basin, USA. Clim Change 151:303–316. https://doi.org/10.1007/s10584-018-2278-z

Panday S, Langevin CD, Niswonger RG, et al (2013) MODFLOW–USG version 1: an unstructured grid version of MODFLOW for simulating groundwater flow and tightly coupled processes using a control volume finite-difference formulation. US Geological Survey

Patil NS, Chetan NL, Nataraja M, Suthar S (2020) Climate change scenarios and its effect on groundwater level in the Hiranyakeshi watershed. Groundw Sustain Dev 10:100323. https://doi.org/10.1016/j.gsd.2019.100323

Pliakas F, Petalas C, Diamantis I, Kallioras A (2005) Modeling of groundwater artificial recharge by reactivating an old stream bed. Water Resour Manag 19:279–294. https://doi.org/10.1007/s11269-005-3472-0

Poeter EP, Hill MC (2007) MMA, a computer code for multi-model analysis. United States Geological Survey-Nevada, Henderson, Nevada

Poeter EP, Hill MC, Lu D, et al (2014) UCODE_2014, with new capabilities to define

parameters unique to predictions, calculate w eights using simulated values, estimate parameters w ith SVD, evaluate uncertainty with MCMC, and more. Integrated Groundwater Modeling Center (IGWMC), of the Colorado School of Mines

Pollock DW (1994) User's Guide for MODPATH/MODPATH-PLOT, Version 3: A particle tracking post-processing package for MODFLOW, the U.S. Geological Survey finite-difference ground-water flow model. Open-File Rep 94-464 0–249. https://doi.org/94-464

Pulido-Velazquez D, García-Aróstegui JL, Molina J-L, Pulido-Velazquez M (2015) Assessment of future groundwater recharge in semi-arid regions under climate change scenarios (Serral-Salinas aquifer, SE Spain). Could increased rainfall variability increase the recharge rate? Hydrol Process 29:828–844. https://doi.org/https://doi.org/10.1002/hyp.10191

Pyne RDG (1995) Groundwater recharge and wells: a guide to aquifer storage recovery, 1st Editio. CRC press

Rahman M, Rusteberg B, Uddin M, et al (2013) An integrated study of spatial multicriteria analysis and mathematical modelling for managed aquifer recharge site suitability mapping and site ranking at Northern Gaza coastal aquifer. J Environ Manage 124:25–39. https://doi.org/10.1016/j.jenvman.2013.03.023

Ramírez-Hernández J, Rodríguez-Burgueño JE, Kendy E, et al (2017) Hydrological response to an environmental flood: Pulse flow 2014 on the Colorado River Delta. Ecol Eng 106:633–644. https://doi.org/10.1016/j.ecoleng.2017.03.003

Rasmussen P, Kidmose J, Kallesøe AJ, et al (2023) Evaluation of adaptation measures to counteract rising groundwater levels in urban areas in response to climate change. Hydrogeol J 31:35–52. https://doi.org/10.1007/s10040-022-02573-7

Remedio AR, Teichmann C, Buntemeyer L, et al (2019) Evaluation of New CORDEX Simulations Using an Updated Köppen–Trewartha Climate Classification. Atmosphere (Basel). 10

Richter BD, Davis MM, Apse C, Konrad C (2012) A PRESUMPTIVE STANDARD FOR ENVIRONMENTAL FLOW PROTECTION. River Res Appl 28:1312–1321. https://doi.org/https://doi.org/10.1002/rra.1511

Ringleb J, Sallwey J, Stefan C (2016) Assessment of Managed Aquifer Recharge through Modeling—A Review. Water 8:579. https://doi.org/https://doi.org/10.3390/w8120579

Rojas R, Feyen L, Dassargues A (2008) Conceptual model uncertainty in groundwater modeling: Combining generalized likelihood uncertainty estimation and Bayesian model averaging. Water Resour Res 44:. https://doi.org/10.1029/2008WR006908

Rojas R, Kahunde S, Peeters L, et al (2010) Application of a multimodel approach to account for conceptual model and scenario uncertainties in groundwater modelling. J Hydrol 394:416–435

Rolls RJ, Boulton AJ, Growns IO, et al (2012) Effects of an experimental environmental flow release on the diet of fish in a regulated coastal Australian river. Hydrobiologia 686:195–212. https://doi.org/10.1007/s10750-012-1012-5

Ronayne MJ, Roudebush JA, Stednick JD (2017) Analysis of managed aquifer recharge for retiming streamflow in an alluvial river. J Hydrol 544:373–382. https://doi.org/10.1016/j.jhydrol.2016.11.054

Russo TA, Fisher AT, Lockwood BS (2015) Assessment of Managed Aquifer Recharge Site Suitability Using a GIS and Modeling. Groundwater 53:389–400. https://doi.org/10.1111/gwat.12213

Salem A, Dezső J, El-Rawy M, Lóczy D (2020) Hydrological Modeling to Assess the Efficiency of Groundwater Replenishment through Natural Reservoirs in the Hungarian Drava River Floodplain. Water 12

Sashikkumar MC, Selvam S, Kalyanasundaram VL, Johnny JC (2017) GIS based groundwater modeling study to assess the effect of artificial recharge: A case study from Kodaganar river basin, Dindigul district, Tamil Nadu. J Geol Soc India 89:57–64. https://doi.org/10.1007/s12594-017-0558-2

Sbai MA (2020) Unstructured Gridding for MODFLOW from Prior Groundwater Flow Models: A New Paradigm. Groundwater. https://doi.org/10.1111/gwat.13025

Scanlon BR, Faunt CC, Longuevergne L, et al (2012) Groundwater depletion and sustainability of irrigation in the US High Plains and Central Valley. Proc Natl Acad Sci U S A 109:9320–9325. https://doi.org/10.1073/pnas.1200311109

Schenk J, Poeter E, Navidi W (2018) The influence of Fisher Information in KIC model selection

Schöniger A, Wöhling T, Samaniego L, Nowak W (2014) Model selection on solid ground: Rigorous comparison of nine ways to evaluate Bayesian model evidence. Water Resour Res 50:9484–9513. https://doi.org/10.1002/2014wr016062

Schwarz G (1978) Estimating the Dimension of a Model. Ann Stat 6:461–464. https://doi.org/10.1214/aos/1176344136

Shafii M, Tolson BA (2015) Optimizing hydrological consistency by incorporating hydrological signatures into model calibration objectives. Water Resour Res 51:3796–3814. https://doi.org/10.1002/2014wr016520

Shao H, Liu J, Liu P, et al (2021) Study on allocation scheme of ecological water supply in Beijing section of Yongdinghe River. Water Resour Hydropower Eng 52:62–72. https://doi.org/10. 13928 /j. cnki. wrahe. 2021. 07. 007

Soleimani S, Van Geel PJ, Isgor OB, Mostafa MB (2009) Modeling of biological clogging in unsaturated porous media. J Contam Hydrol 106:39–50. https://doi.org/https://doi.org/10.1016/j.jconhyd.2008.12.007

Song J, Yang Y, Sun X, et al (2020) Basin-scale multi-objective simulation-optimization modeling for conjunctive use of surface water and groundwater in northwest China. Hydrol Earth Syst Sci 24:2323–2341. https://doi.org/10.5194/hess-24-2323-2020

Sophocleous M (2010) Review: groundwater management practices, challenges, and innovations in the High Plains aquifer, USA—lessons and recommended actions. Hydrogeol J 18:559–575. https://doi.org/10.1007/s10040-009-0540-1

Sreekanth J, Moore C (2018) Novel patch modelling method for efficient simulation and

prediction uncertainty analysis of multi-scale groundwater flow and transport processes. J Hydrol 559:122–135. https://doi.org/https://doi.org/10.1016/j.jhydrol.2018.02.028

Sugiura N (1978) Further Analysis of the Data by Anaike' S Information Criterion and the Finite Corrections. Commun Stat - Theory Methods 7:13–26. https://doi.org/10.1080/03610927808827599

Sun J, Donn MJ, Gerber P, et al (2020) Assessing and Managing Large-Scale Geochemical Impacts From Groundwater Replenishment With Highly Treated Reclaimed Wastewater. Water Resour Res 56:e2020WR028066. https://doi.org/https://doi.org/10.1029/2020WR028066

Sun R, Pan X, Wang J, et al (2021) An analysis and evaluation of ecological water replenishment benefit of Yongding River (Beijing Section). China Rural Water Hydropower 6:19–24

Tang C, Yi Y, Yang Z, et al (2018) Effects of ecological flow release patterns on water quality and ecological restoration of a large shallow lake. J Clean Prod 174:577–590. https://doi.org/10.1016/j.jclepro.2017.10.338

Teatini P, Comerlati A, Carvalho T, et al (2015) Artificial recharge of the phreatic aquifer in the upper Friuli plain, Italy, by a large infiltration basin. Environ Earth Sci 73:2579–2593. https://doi.org/10.1007/s12665-014-3207-8

Tharme RE (2003) A global perspective on environmental flow assessment: Emerging trends in the development and application of environmental flow methodologies for rivers. River Res Appl 19:397–441. https://doi.org/10.1002/rra.736

Tillman FD, Gangopadhyay S, Pruitt T (2016) Changes in groundwater recharge under projected climate in the upper Colorado River basin. Geophys Res Lett 43:6968–6974. https://doi.org/10.1002/2016GL069714

Torabi Haghighi A, Fazel N, Hekmatzadeh AA, Klöve B (2018) Analysis of Effective Environmental Flow Release Strategies for Lake Urmia Restoration. Water Resour Manag 32:3595–3609. https://doi.org/10.1007/s11269-018-2008-3

Tosline D, Prudhom B, Falcon D, et al (2012) Enhanced Recharge Demonstration Project , Increasing Treated Effluent Recharge Rates in the Santa Cruz River , Tucson , Arizona

UN-water (2022) The United Nations World Water Development Report 2022: groundwater: making the invisible visible; executive summary. UNESCO

UNESCO (2005) Strategies for Managed Aquifer Recharge (MAR) in semi-arid areas. United Nations Educational, Scientific, and Cultural Organization (UNESCO), Paris, France

UNESCO (2021) Managing aquifer recharge: a showcase for resilience and sustainability. United Nations Educational, Scientific and Cultural Organization, Paris

Valley S, Landini F, Pranzini G, et al (2005) Transient flow modelling of an overexploited aquifer and simulation of artificial recharge measures. ISMAR5 388–394

van der Gun J (2012) Groundwater and global change: trends, opportunities and

challenges. UNESCO, Paris

Van TD, Zhou Y, Stigter TY, et al (2023) Sustainable groundwater development in the coastal Tra Vinh province in Vietnam under saltwater intrusion and climate change. Hydrogeol J 31:731–749. https://doi.org/10.1007/s10040-023-02607-8

Vandenbohede A, Houtte E, Lebbe L (2008) Groundwater flow in the vicinity of two artificial recharge ponds in the Belgian coastal dunes. Hydrogeol J 16:1669–1681. https://doi.org/10.1007/s10040-008-0326-x

Vandenbohede A, Wallis I, Van Houtte E, Van Ranst E (2013) Hydrogeochemical transport modeling of the infiltration of tertiary treated wastewater in a dune area, Belgium. Hydrogeol J 21:1307–1321. https://doi.org/10.1007/s10040-013-1008-x

Vaux H (2011) Groundwater under stress: the importance of management. Environ Earth Sci 62:19–23. https://doi.org/10.1007/s12665-010-0490-x

Vilhelmsen TN, Christensen S, Mehl SW (2012) Evaluation of MODFLOW-LGR in Connection with a Synthetic Regional-Scale Model. Groundwater 50:118–132. https://doi.org/10.1111/j.1745-6584.2011.00826.x

Voldoire A, Sanchez-Gomez E, Salas y Mélia D, et al (2013) The CNRM-CM5.1 global climate model: description and basic evaluation. Clim Dyn 40:2091–2121. https://doi.org/10.1007/s00382-011-1259-y

Wada Y (2016) Modeling Groundwater Depletion at Regional and Global Scales: Present State and Future Prospects. Surv Geophys 37:419–451. https://doi.org/10.1007/s10712-015-9347-x

Wada Y, Beek LPH Van, Kempen CM Van, et al (2010) Global depletion of groundwater resources. 37:1–5. https://doi.org/10.1029/2010GL044571

Wada Y, Bierkens MFP (2014) Sustainability of global water use: Past reconstruction and future projections. Environ Res Lett 9:. https://doi.org/10.1088/1748-9326/9/10/104003

Ward J, Simmons C, Dillon P, Pavelic P (2009) Integrated assessment of lateral flow, density effects and dispersion in aquifer storage and recovery. J Hydrol - J HYDROL 370:83–99. https://doi.org/10.1016/j.jhydrol.2009.02.055

Webber M, Crow-Miller B, Rogers S (2017) The South–North Water Transfer Project: remaking the geography of China. Reg Stud 51:370–382. https://doi.org/10.1080/00343404.2016.1265647

Wei D (2005) Beijing water resources and the south to north water diversion project. Can J Civ Eng 32:159–163. https://doi.org/10.1139/l04-113

Wheater HS, Mathias SA, Li X (2010) Groundwater modelling in arid and semi-arid areas. Cambridge University Press

Wu H, Long B, Pan Z, et al (2022) Response of Domestic Water in Beijing to Climate Change. Water (Switzerland) 14:. https://doi.org/10.3390/w14091487

Wu H, Wang M, Li S, et al (2021) Preliminary analysis on the loss of winter ecological water supplement in Guanting gorge of Yongding River. Beijing Water. https://doi.org/10.19671/j.1673-4637.2021.06.002

Wu J, Zeng X (2013) Review of the uncertainty analysis of groundwater numerical simulation. Chinese Sci Bull 58:3044–3052. https://doi.org/0.1007/s11434-013-5950-8

WWAP (World Water Assessment Programme) (2012) The United Nations World Water Development Report 4: Managing Water under Uncertainty and Risk (Vol. 1), Knowledge Base (Vol. 2) and Facing the Challenges (Vol. 3). UNESCO, Paris

Xanke J, Jourde H, Liesch T, Goldscheider N (2016) Numerical long-term assessment of managed aquifer recharge from a reservoir into a karst aquifer in Jordan. J Hydrol 540:603–614. https://doi.org/10.1016/j.jhydrol.2016.06.058

Xu C, Sun Y, Shi B, et al (2022) Study on the Processes Influencing and Importance of Ecological Water Replenishment for Groundwater Resources: A Case Study in Yongding River. Water 14

Xu Z, Han Y, Yang Z (2019) Dynamical downscaling of regional climate: A review of methods and limitations. Sci China Earth Sci 62:365–375. https://doi.org/10.1007/s11430-018-9261-5

Yang H, Zehnder A (2001) China's regional water scarcity and implications for grain supply and trade. Environ Plan A 33:79–95. https://doi.org/10.1068/a3352

Yang S, Tsai FT-C (2020) Understanding impacts of groundwater dynamics on flooding and levees in Greater New Orleans. J Hydrol Reg Stud 32:100740. https://doi.org/https://doi.org/10.1016/j.ejrh.2020.100740

Yao X (2014) Preliminary Analysis of the Conditions for Constructing an Underground Reservoir in Beijing (in Chinese). Water Resour Plan Des 29–32. https://doi.org/10.3969/j.issn.1672-2469.2014.03.011

Yaraghi N, Ronkanen A kaisa, Darabi H, et al (2019) Impact of managed aquifer recharge structure on river flow regimes in arid and semi-arid climates. Sci Total Environ 675:429–438. https://doi.org/10.1016/j.scitotenv.2019.04.253

Ye M, Meyer PD, Neuman SP (2008) On model selection criteria in multimodel analysis. Water Resour Res. https://doi.org/10.1029/2008WR006803

Ye M, Pohlmann KF, Chapman JB, et al (2010) A model-averaging method for assessing groundwater conceptual model uncertainty. Groundwater 48:716–728

Zeelie S (2002) OMDEL dam and recharge ponds to enhance recharge in the Namib Desert. In: Management of aquifer recharge for sustainability. CRC Press, pp 387–392

Zeng J, Zha Y, Zhang Y, et al (2017) On the sub-model errors of a generalized one-way coupling scheme for linking models at different scales. Adv Water Resour 109:69–83. https://doi.org/https://doi.org/10.1016/j.advwatres.2017.09.005

Zhai L, Cheng S, Sang H, et al (2022) Remote sensing evaluation of ecological restoration engineering effect: A case study of the Yongding River Watershed, China. Ecol Eng 182:106724. https://doi.org/https://doi.org/10.1016/j.ecoleng.2022.106724

Zhang A, Bureau BG and MRE and D, Geology BI of H and E (2008) Beijing groundwater(Chinese Edition). China Land Press Pub, Beijing, China

Zhang H, Xu Y, Kanyerere T (2020) A review of the managed aquifer recharge: Historical development, current situation and perspectives. Phys Chem Earth 118–119:102887. https://doi.org/10.1016/j.pce.2020.102887

Zhang L, Zhang L (2017) The ecological Environment Succession and Management of Yongding River in Beijing. J Beijing Union Univ (Humanities Soc Sci 15:118–124

Zhang Y, Gong H, Gu Z, et al (2014) Characterization of land subsidence induced by groundwater withdrawals in the plain of Beijing city, China. Hydrogeol J 22:397–409. https://doi.org/10.1007/s10040-013-1069-x

Zhang Y, Sun Y, Wang X (2013) Introduction of the Artificial Recharge of Beijing groundwater (In chinese). City Geol 8:51–53

Zhao Q, Zhang B, Yao Y, et al (2019) Geodetic and hydrological measurements reveal the recent acceleration of groundwater depletion in North China Plain. J Hydrol 575:1065–1072. https://doi.org/https://doi.org/10.1016/j.jhydrol.2019.06.016

Zhao X, Wang Y, Zhang X, et al (2020) Analysis and research on ecological water supplement hydrologic monitoring of Yongding River in the spring of 2020 (in Chinese). Beijing Water 18–22. https://doi.org/10.19671/j.1673-4637.2020.04.004

Zheng C, Wang PP (1999) MT3DMS: a modular three-dimensional multispecies transport model for simulation of advection, dispersion, and chemical reactions of contaminants in groundwater systems; documentation and user's guide. Environmental Laboratory (US)

Zhou P, Wang G, Duan R (2020) Impacts of long-term climate change on the groundwater flow dynamics in a regional groundwater system: Case modeling study in Alashan, China. J Hydrol 590:125557. https://doi.org/10.1016/j.jhydrol.2020.125557

Zhou Y, Herath HMPSD (2017) Evaluation of alternative conceptual models for groundwater modelling. Geosci Front 8:437–443. https://doi.org/https://doi.org/10.1016/j.gsf.2016.02.002

Zhou Y, Li W (2011) A review of regional groundwater flow modeling. Geosci Front 2:205–214

Zhou Y, Olsthoorn T, Liu P (2021) Good Practice for Managed Aquifer Recharge with Infiltration Basins. China Electric Power Press, Beijing

Zhou Y, Wang L, Liu J, et al (2012) Options of sustainable groundwater development in Beijing Plain, China. Phys Chem Earth 47–48:99–113. https://doi.org/10.1016/j.pce.2011.09.001

Zhou YX, Dong DW, Liu JR, Li WP (2013) Upgrading a regional groundwater level monitoring network for Beijing Plain, China. Geosci Front 4:127–138. https://doi.org/10.1016/j.gsf.2012.03.008

Zhu L, Gong H, Li X, et al (2015) Land subsidence due to groundwater withdrawal in the northern Beijing plain, China. Eng Geol 193:243–255. https://doi.org/10.1016/j.enggeo.2015.04.020

Zhuo C, Junhong G, Wei L, et al (2022) Changes in wind energy potential over China using a regional climate model ensemble. Renew Sustain Energy Rev 159:112219.

https://doi.org/https://doi.org/10.1016/j.rser.2022.112219

ANNEXES

APPENDIX A ADDITIONAL INFORMATION OF THE STEADY STATE MODEL CONSTRUCTION AND CALIBRATION

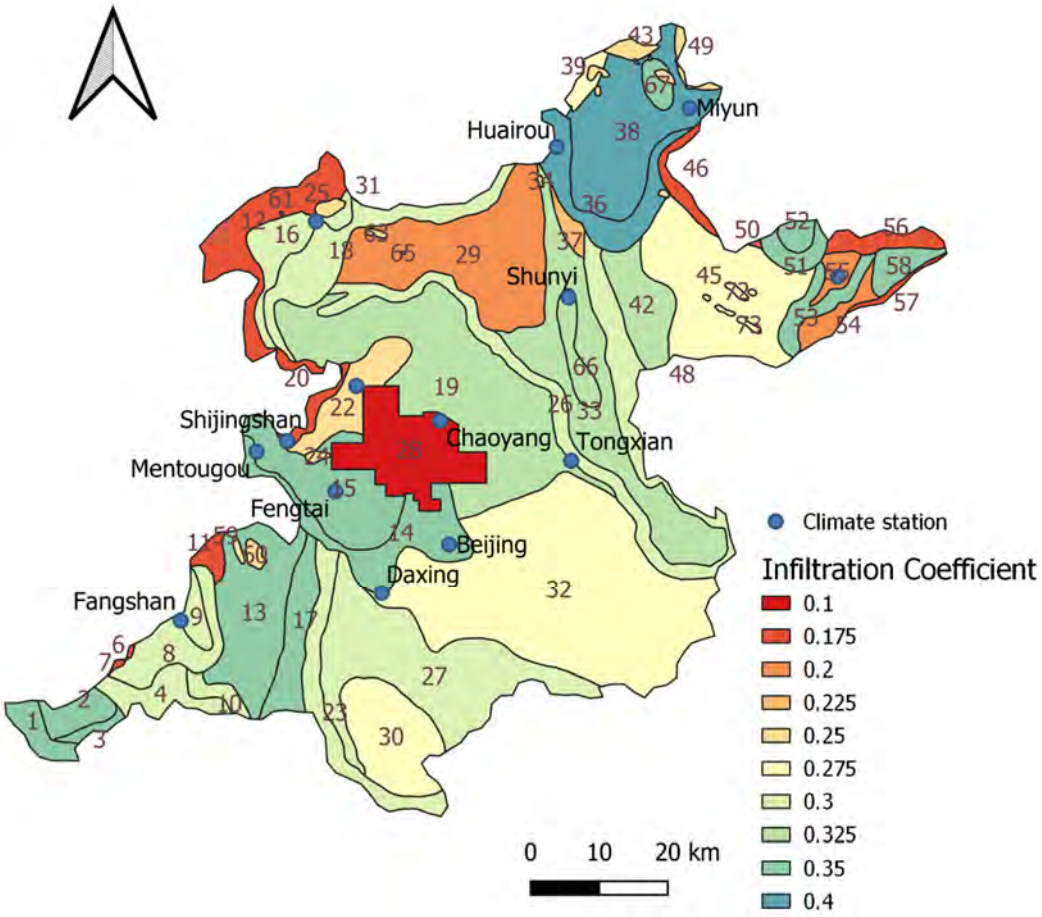

Figure A-1 Map of recharge coefficient for calculating the groundwater recharge from precipitation.

Table A.1. Information of the RIV package setting to simulate the pilot scale MAR operation.

Zone number	Area (m^2)	Pond bottom elevation (m)	Hydraulic conductance (m^2/d)
Zone 1	88,981	31.55	
Zone 2	102,378	31.90	368 for all ponds
Zone 3	65,309	31.31	

The hydraulic conductivities, storage coefficients are specified as homogeneous parameter zones by LFP package in MODFLOW. The parameter zonation is shown in Figure A-2. The zone ID contains two parts connected by "-". First digit stands for the model layer, followed by a number specifying the zone number. Detailed parameter values are listed in Table A-2.

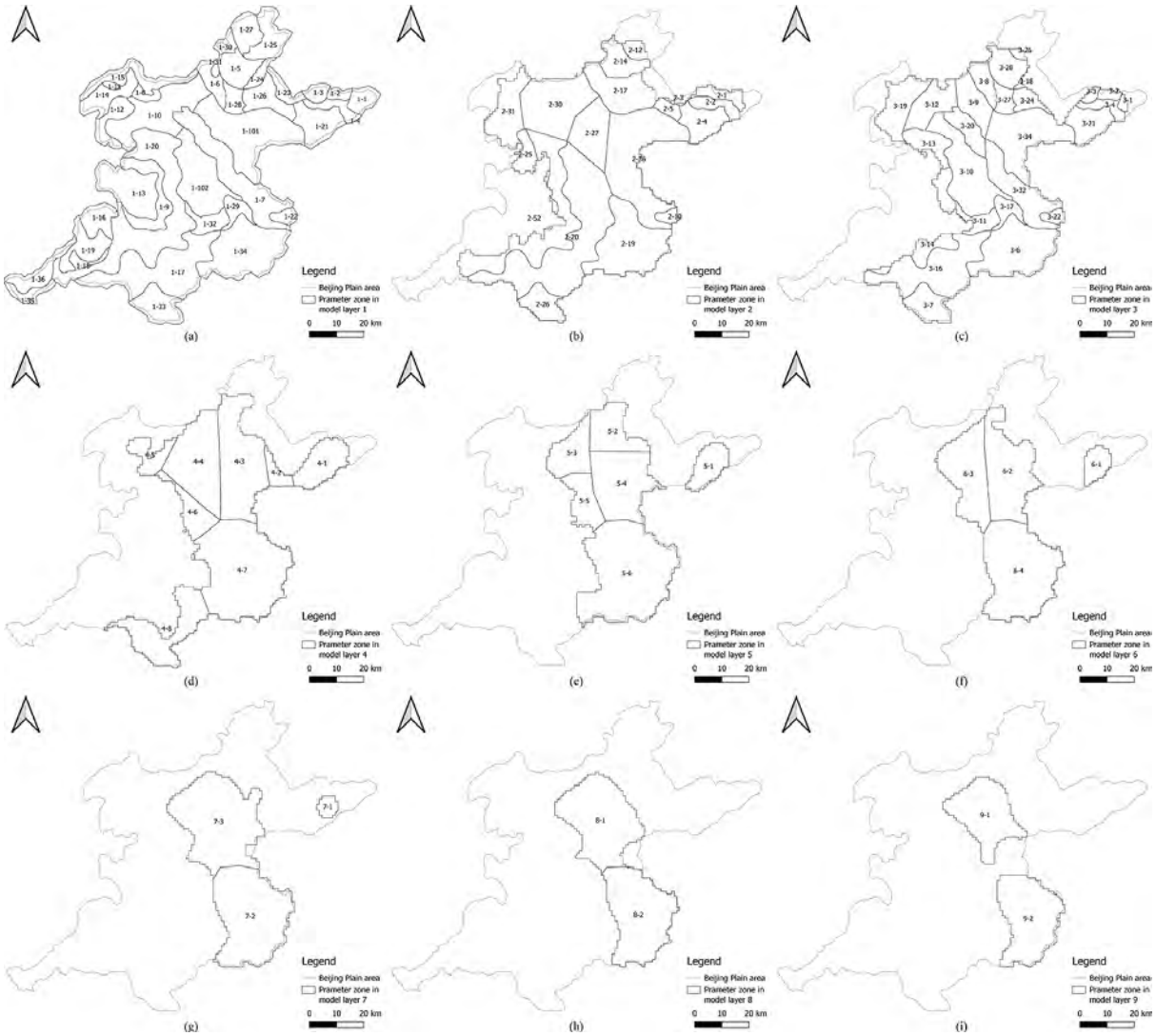

Figure.A-2 Spatial distribution of the parameter zones for the hydraulic conductivity and storage coefficient. From (a) to (i) are the model parameter zones for model layer 1 to 9.

Table A-2. Horizontal, vertical hydraulic conductivity and Storage coefficient specified for each parameter zone.

Model layer	Zone ID	Horizontal hydraulic conductivity (m/d)	Vertical hydraulic conductivity (m/d)	Storage coefficient (1/m)	Model layer	Zone ID	Horizontal hydraulic conductivity (m/d)	Vertical hydraulic conductivity (m/d)	Storage coefficient (1/m)
1	1- 1	19.394	9.2535	0.003	3	3- 1	28.622	1.4343	5.00×10^{-6}
1	1- 10	12.133	2.1952	0.0006	3	3- 10	150	6.825	2.50×10^{-5}
1	1- 101	75.592	4.0757	0.0025	3	3- 11	20	4.5226	2.50×10^{-5}
1	1- 102	42.577	16.225	0.006	3	3- 12	20.093	1.88	2.00×10^{-6}
1	1- 11	100	5	0.0015	3	3- 13	10.75	10.833	6.00×10^{-6}
1	1- 12	50	1	0.001	3	3- 14	31.423	15.548	1.30×10^{-5}
1	1- 13	225	0.5	0.0025	3	3- 16	31	2.25	1.30×10^{-5}
1	1- 14	84.764	3.8234	0.002	3	3- 17	97.868	3.0463	2.50×10^{-5}
1	1- 15	80	8	0.0015	3	3- 18	25	2.8775	3.00×10^{-6}
1	1- 16	80	8	0.001	3	3- 19	105	3.1657	3.00×10^{-6}
1	1- 17	239.04	4.7459	0.0015	3	3- 2	60	7.3988	2.50×10^{-5}
1	1- 18	125.49	10.457	0.00125	3	3- 20	55.451	2.9276	3.00×10^{-6}
1	1- 19	120	8	0.0015	3	3- 21	5	1.4953	1.30×10^{-5}
1	1- 2	120	7.4937	0.003	3	3- 22	46.094	2.4997	1.30×10^{-5}
1	1- 20	354.6	10.905	0.0015	3	3- 24	25	10.379	3.00×10^{-6}
1	1- 21	35.986	15	0.003	3	3- 26	100	0.1	3.00×10^{-6}
1	1- 22	48.156	4.4821	0.0015	3	3- 27	7.39	2.4324	1.30×10^{-5}

Model layer	Zone ID	Horizontal hydraulic conductivity (m/d)	Vertical hydraulic conductivity (m/d)	Storage coefficient (1/m)	Model layer	Zone ID	Horizontal hydraulic conductivity (m/d)	Vertical hydraulic conductivity (m/d)	Storage coefficient (1/m)
1	1- 23	160	15.722	0.0025	3	3- 28	54.528	5	6.00×10^{-6}
1	1- 24	71.165	20.296	0.0025	3	3- 3	12.409	2.6743	3.00×10^{-6}
1	1- 25	83.167	0.1	0.003	3	3- 32	30	8.9567	2.50×10^{-5}
1	1- 26	60	5.2824	0.003	3	3- 34	20	2.9151	2.50×10^{-5}
1	1- 27	56.113	2.3276	0.0015	3	3- 4	50	5	1.30×10^{-5}
1	1- 28	100	6.595	0.001	3	3- 6	27.142	2.25	3.00×10^{-6}
1	1- 29	50	10	0.001	3	3- 7	6.691	3.9994	1.30×10^{-5}
1	1- 3	51.754	4.8786	0.003	3	3- 8	2.55	0.0208	1.30×10^{-5}
1	1- 30	100	1	0.003	3	3- 9	0.162	0.0116	3.00×10^{-6}
1	1- 31	83.245	7.618	0.003	4	4- 1	0.347	0.01	1.25×10^{-2}
1	1- 32	80	5	0.0008	4	4- 2	0.146	0.001	1.25×10^{-2}
1	1- 33	11.582	5.1751	0.0015	4	4- 3	1	0.15	1.50×10^{-4}
1	1- 34	7.883	2.7012	0.0006	4	4- 4	0.109	0.0026	1.50×10^{-4}
1	1- 35	300.24	10	0.0025	4	4- 5	0.026	0.0001	1.50×10^{-4}
1	1- 36	80	6.6039	0.0035	4	4- 6	0.41	0.002	1.50×10^{-4}
1	1- 4	24.24	1.8273	0.001	4	4- 7	36.614	0.9801	1.50×10^{-4}
1	1- 5	79.826	1.4963	0.0015	4	4- 8	12.457	3	1.50×10^{-4}
1	1- 6	27.768	5.2	0.00175	5	5- 1	20	3	2.50×10^{-5}

Model layer	Zone ID	Horizontal hydraulic conductivity (m/d)	Vertical hydraulic conductivity (m/d)	Storage coefficient (1/m)	Model layer	Zone ID	Horizontal hydraulic conductivity (m/d)	Vertical hydraulic conductivity (m/d)	Storage coefficient (1/m)
1	1- 7	51.25	6.75	0.0018	5	5- 2	11.925	0.0338	2.50×10^{-5}
1	1- 8	5.85	1.5211	0.0025	5	5- 3	16	1	2.50×10^{-5}
1	1- 9	1.25	0.75	0.0025	5	5- 4	12	0.0195	2.50×10^{-5}
2	2- 1	0.296	0.075	1.50×10^{-4}	5	5- 5	1.36	0.025	2.50×10^{-5}
2	2- 10	5.625	0.2813	1.50×10^{-4}	5	5- 6	1	0.003	2.50×10^{-5}
2	2- 12	1.375	0.0553	1.50×10^{-4}	6	6- 1	1.136	0.003	1.50×10^{-4}
2	2- 14	1.025	0.0025	5.00×10^{-6}	6	6- 2	1.063	0.003	1.50×10^{-4}
2	2- 17	14.11	2.1042	3.00×10^{-6}	6	6- 3	4	10	1.50×10^{-4}
2	2- 19	15	5	1.50×10^{-4}	6	6- 4	4	0.6	1.50×10^{-4}
2	2- 2	10	0.8	1.50×10^{-4}	7	7- 1	1	2	2.50×10^{-5}
2	2- 20	0.1	0.0005	1.50×10^{-4}	7	7- 2	15	3	2.50×10^{-5}
2	2- 25	0.1	0.001	5.00×10^{-6}	7	7- 3	75	5	2.50×10^{-5}
2	2- 26	5.699	3.0755	5.00×10^{-6}	8	8-1	0.5	0.05	1.50×10^{-4}
2	2- 27	1.123	0.0031	3.00×10^{-6}	8	8-2	0.5	0.01	1.50×10^{-4}
2	2- 3	0.1	0.0003	1.50×10^{-4}	9	9-1	5	2	2.50×10^{-5}
2	2- 30	1.07	0.0024	1.50×10^{-4}	9	9-2	5	0.5	2.50×10^{-5}
2	2- 31	1.125	0.0063	1.50×10^{-4}					
2	2- 36	0.1	0.0006	1.50×10^{-4}					

Model layer	Zone ID	Horizontal hydraulic conductivity (m/d)	Vertical hydraulic conductivity (m/d)	Storage coefficient (1/m)	Model layer	Zone ID	Horizontal hydraulic conductivity (m/d)	Vertical hydraulic conductivity (m/d)	Storage coefficient (1/m)
2	2- 4	1	0.0063	1.50×10^{-4}					
2	2- 5	310.5	8.9766	5.00×10^{-6}					

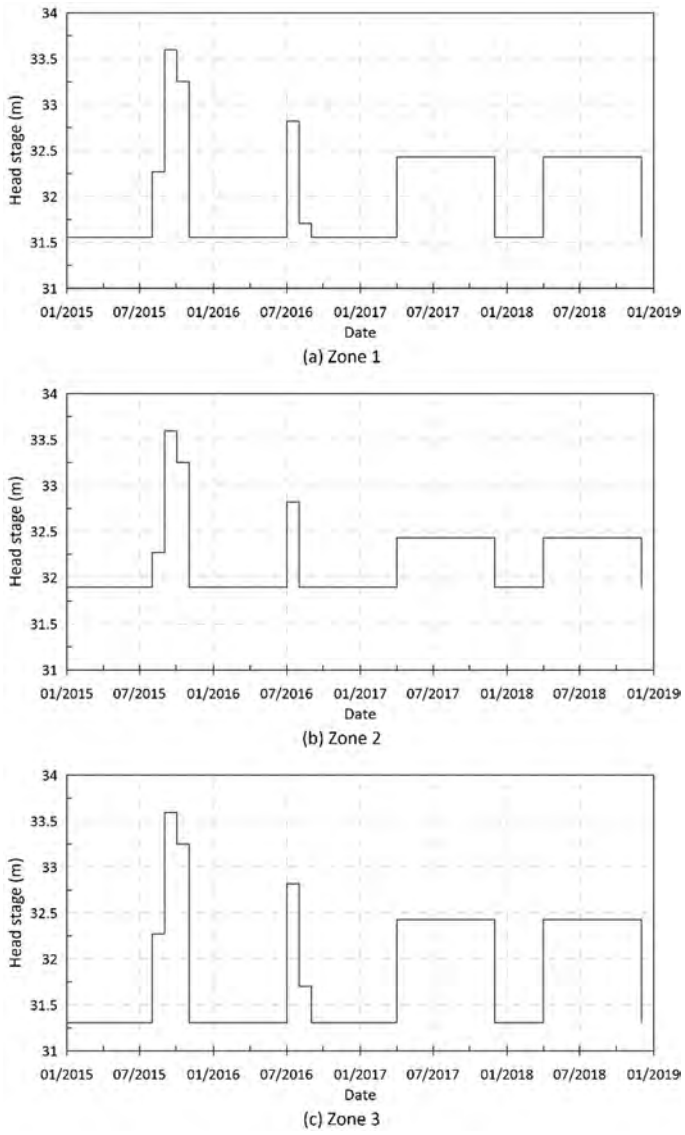

Figure A-3 Head stage change for the three polygons for the RIV package.

The transient regional groundwater flow model was calibrated by minimizing the residuals of the computed and observed groundwater head by trial and error. Figure A-4 displays scatter plots of the computed and observed groundwater level in January of the years 1995, 2000, 2005, 2010 in which large number of observed groundwater levels are available. In general, computed heads and observed heads fall around the diagonal line with large scatters. The coefficients of determination of the computed and observed groundwater levels for all years are above 0.65, which is acceptable for the regional groundwater model to be coupled with the local MAR model in this study.

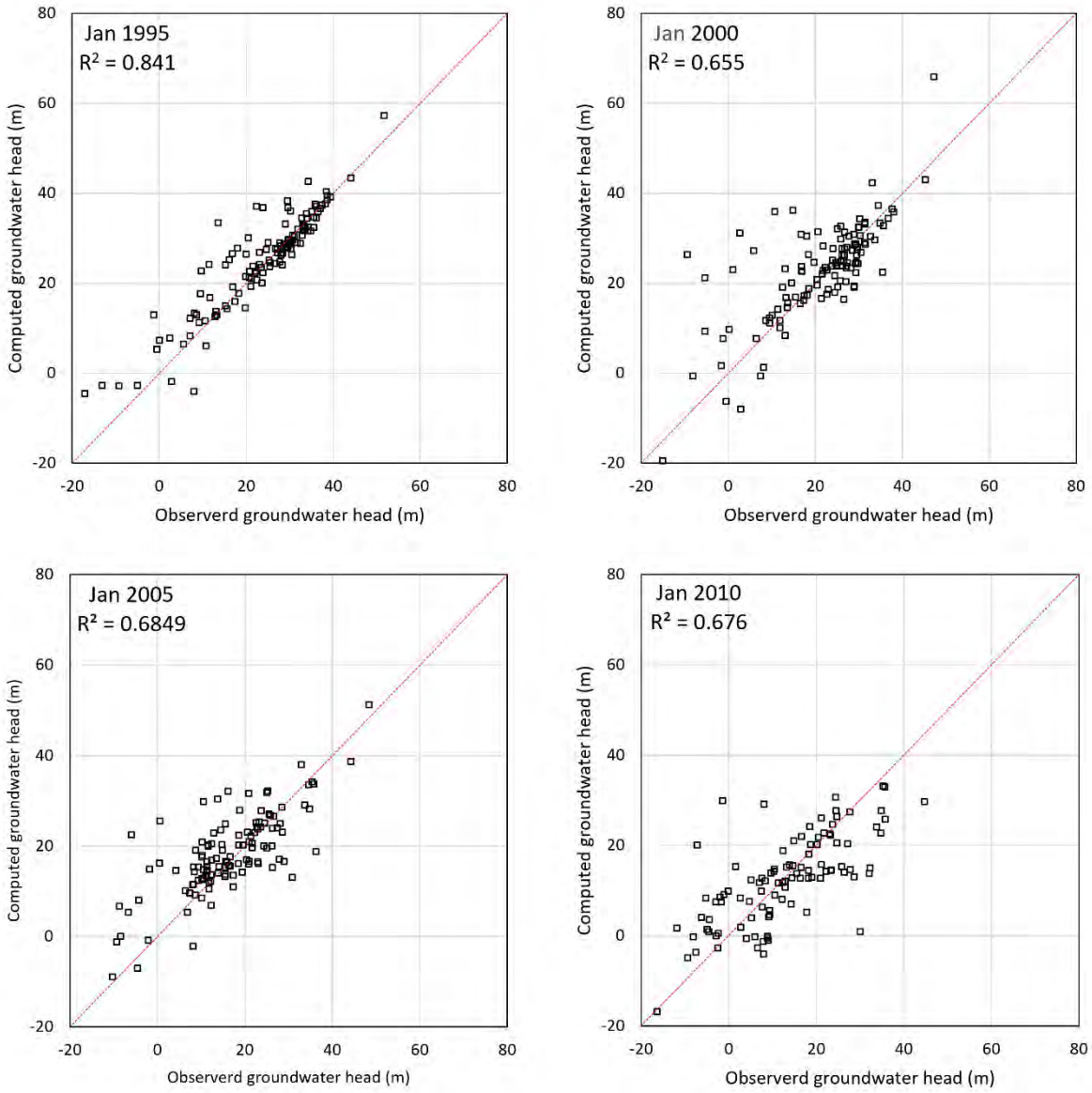

Figure A-4 The scatter plot of the computed and observed groundwater head of the regional flow model in the years 1995, 2000, 2005, and 2010.

APPENDIX B WATER BUDGET FOR ALL FLOW COMPONENTS FOR REGIONAL GROUNDWATER FLOW MODEL.

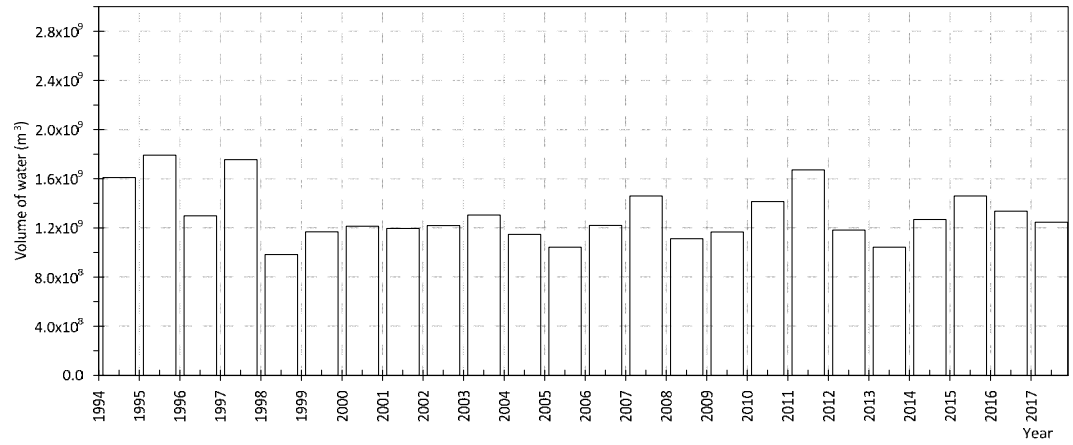

(a) Recharge from precipitation infiltration, irrigation return flow, and pipe leakage .

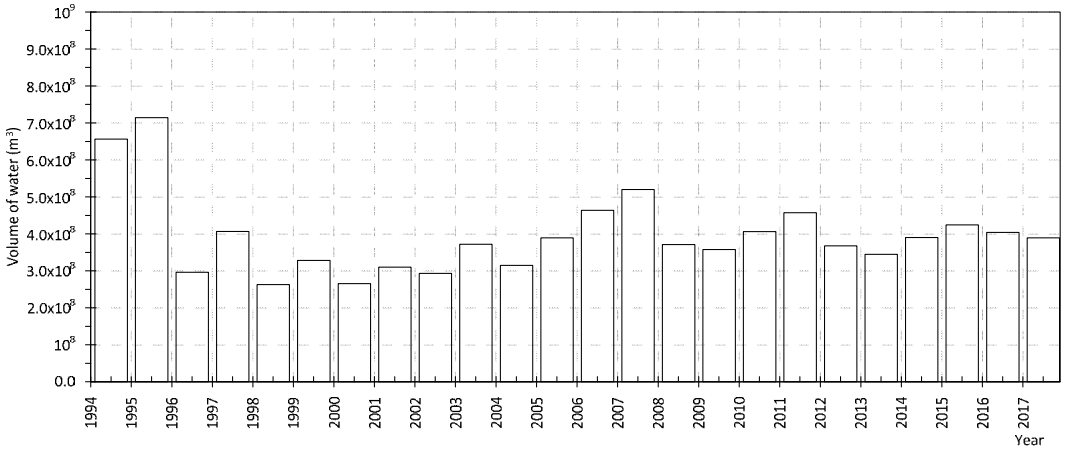

(b) Lateral inflow from the mountain.

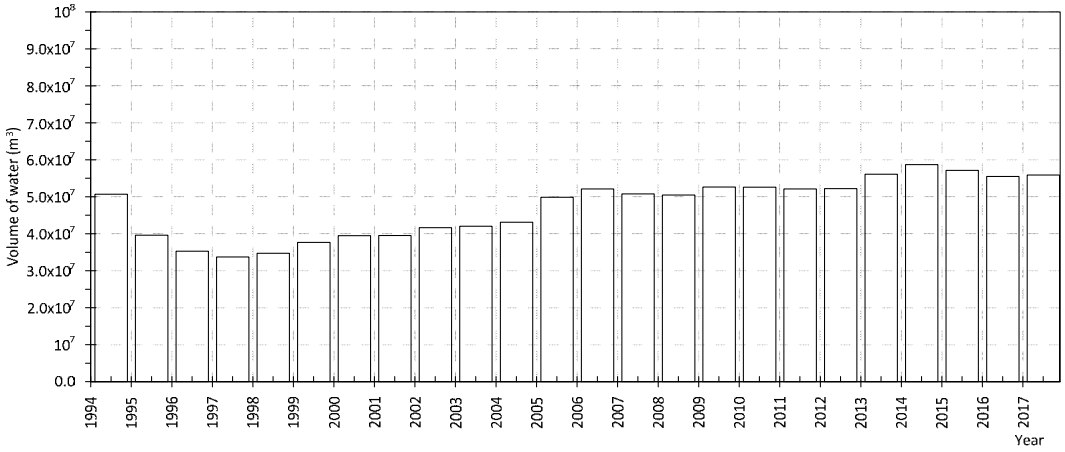

(c) Inflow from the general head boundary.

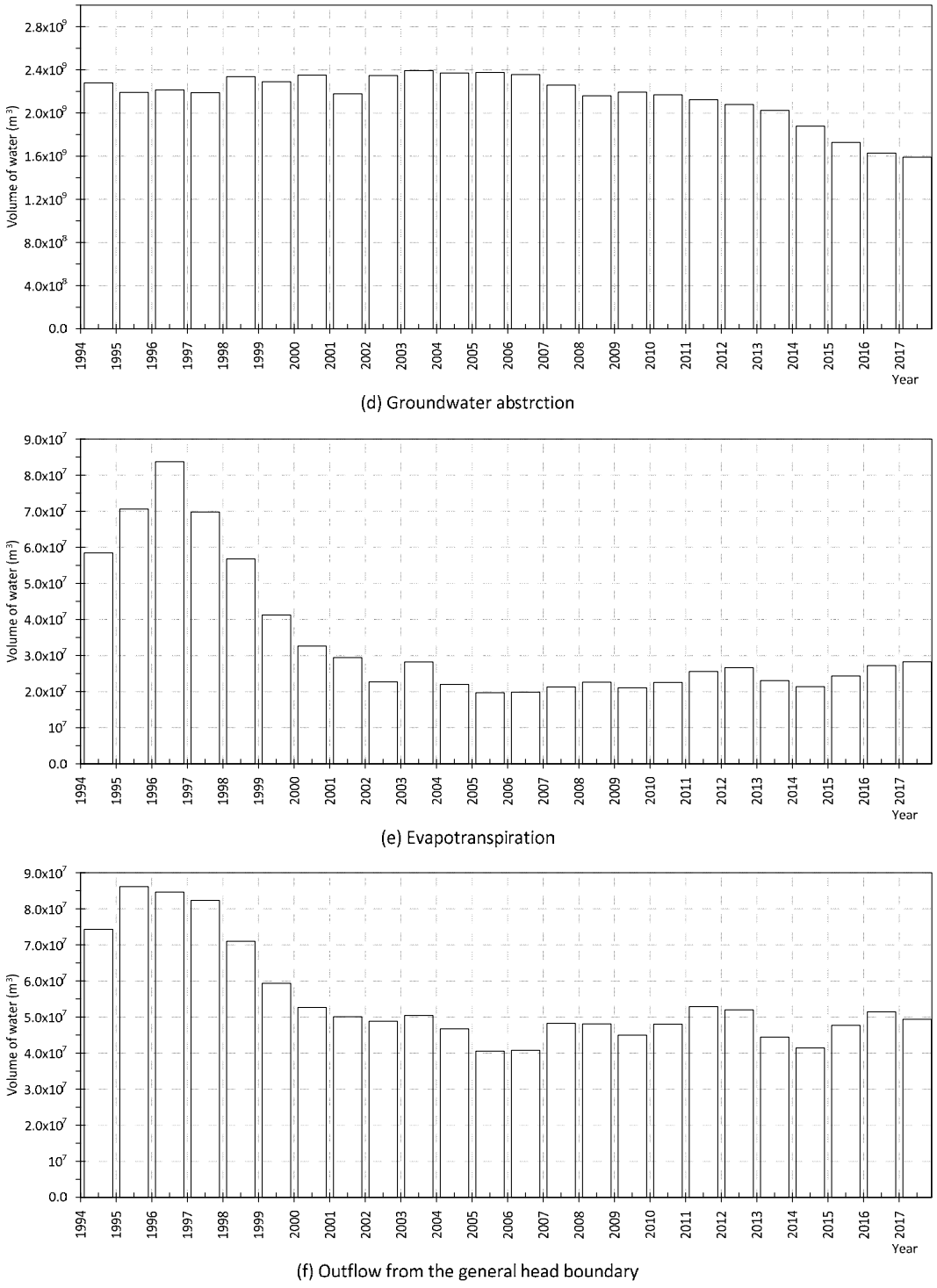

Figure B-1. Water budget for the regional flow model. (a)-(c) are the inflow components. (d)-(f) are the outflow components.

APPENDIX C EFFECT OF THE MESH SIZE ON THE SIMULATION RESULTS

The effects of the grid size of the local model on the simulation of transport of the infiltrated water were investigated in this study. A local model with a 100 m grid size and the other with a 20 m grid size were used to simulate pilot MAR operation. The simulated mixing zone of the pilot MAR operation in December 2018 is shown in Figure C-1. The main differences between the finer grid and coarser grid are: (a) the distribution area of the infiltrated water is larger predicted with the coarser grid model than the finer grid model; (b) The coarser grid model computed the larger transition zone around the MAR site than the finer grid model.

These differences are caused by numerical dispersion error in the model. The coarser grid model used also larger transport steps (1.82 days) resulting in larger numerical dispersion. The finer grid model uses a smaller transport step (0.58 days) so that the numerical dispersion is reduced. Therefore, the accuracy of the tracer transport simulation from the finer grid model is much higher than the coarser grid model. In order to delineate the distribution area of the infiltrated water and compute mixing percent of infiltrated water to the pumping wells accurately, the finer grid model is required. However, the finer grid model is computationally demanding with a larger number of grid cells combined with larger number of transport steps. As a compromise, a multi-scale model was created in this study: a coarser grid of 100m for the local model and a finer grid of 20m for the site model. These two models were imbedded in the regional model with a grid of 1000m.

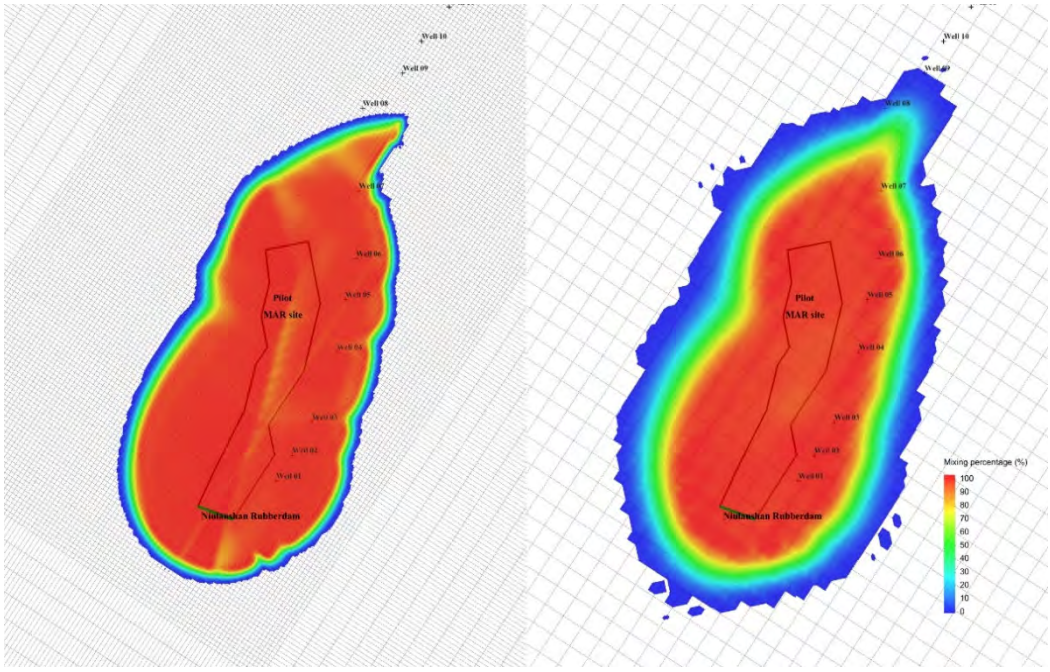

Figure C-1. The comparison of the mixing zones simulated by finer grid (left) and coarser grid (right).

APPENDIX D ADDITIONAL MODEL RESULTS OF THE YONGDING EFR SIMULATION

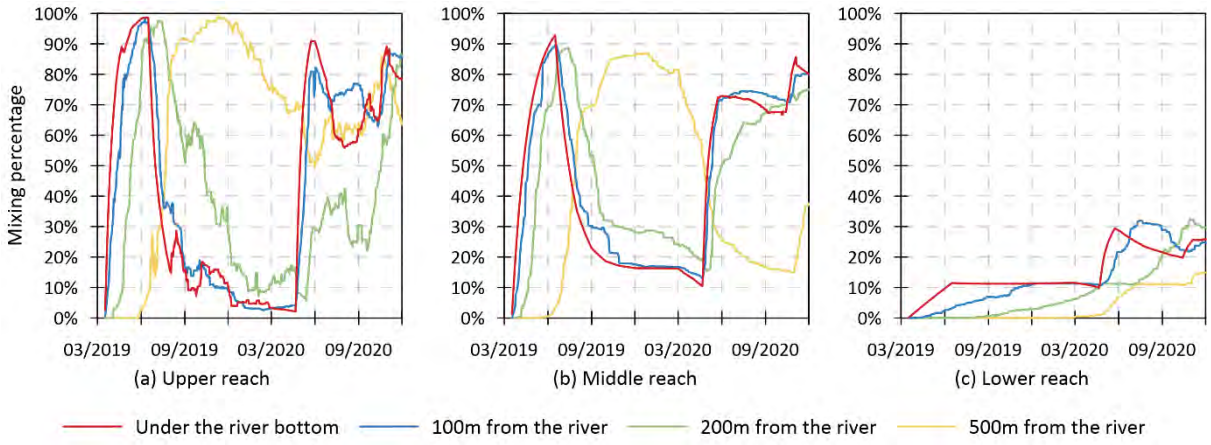

Figure D-1. The breakthrough curves of the infiltrated water at different distances from the river channel in the upper reach (a), middle reach (b) and lower reach (c) of the Yongding River.

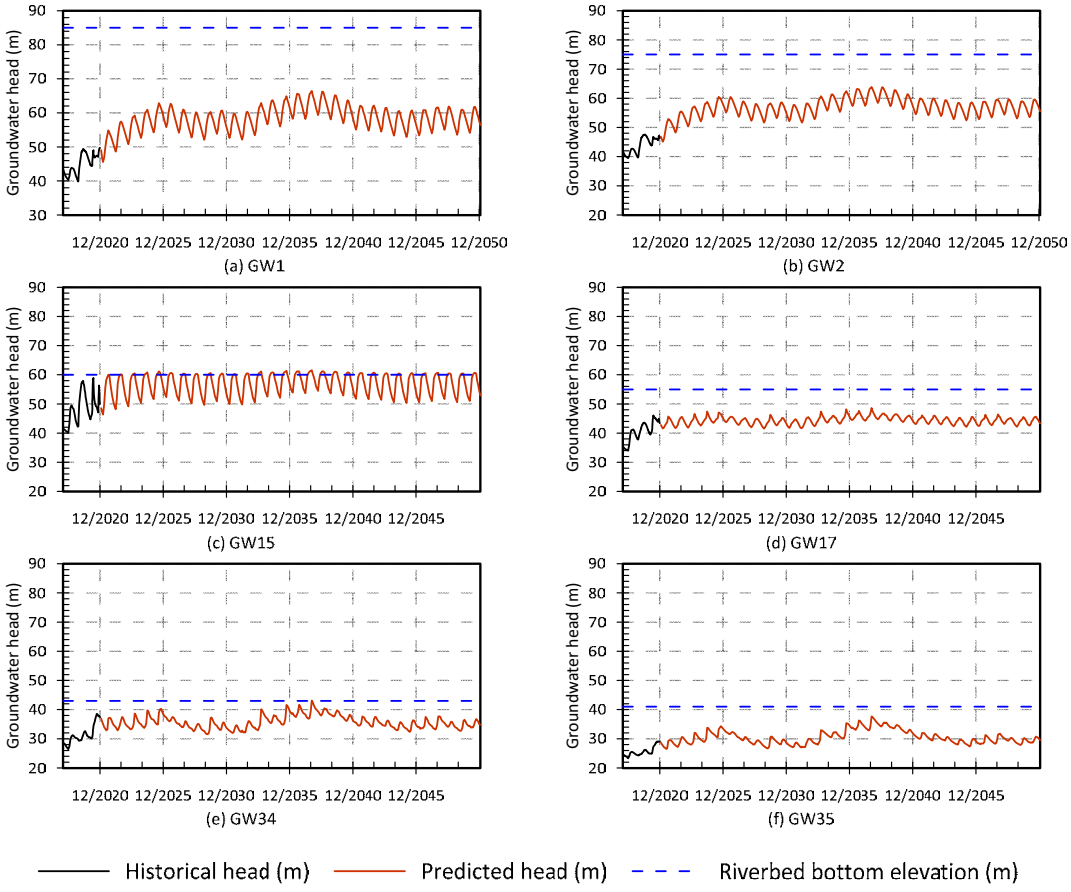

Figure D-2 Predicted groundwater levels close to the river channels from 2021-2050.

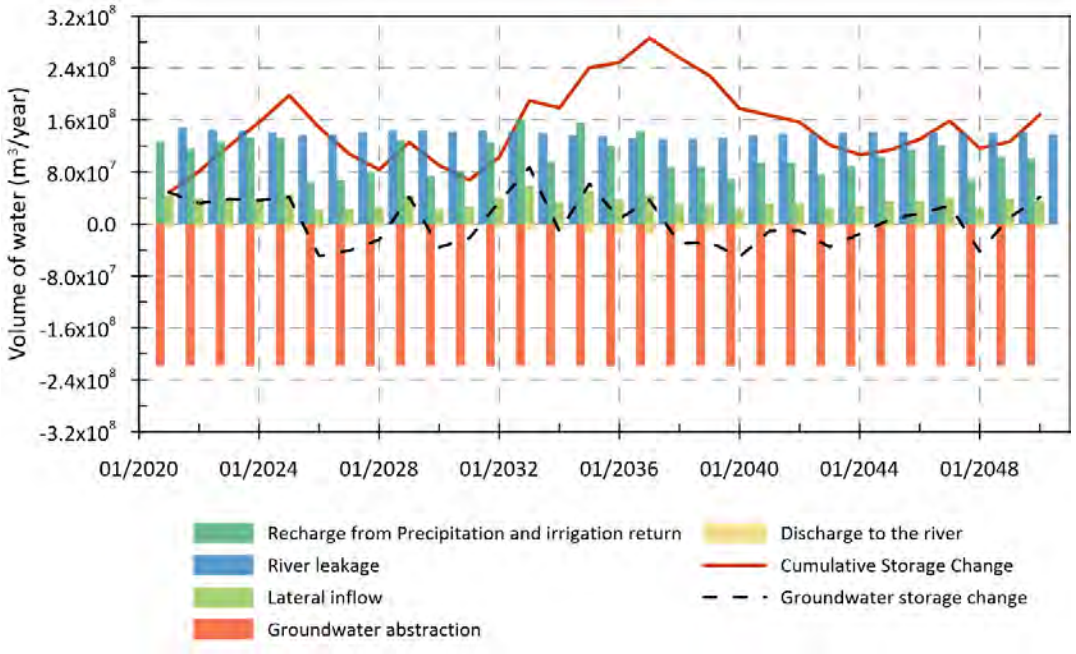

Figure D-3. The predicted groundwater balance components in the Yongding River region.

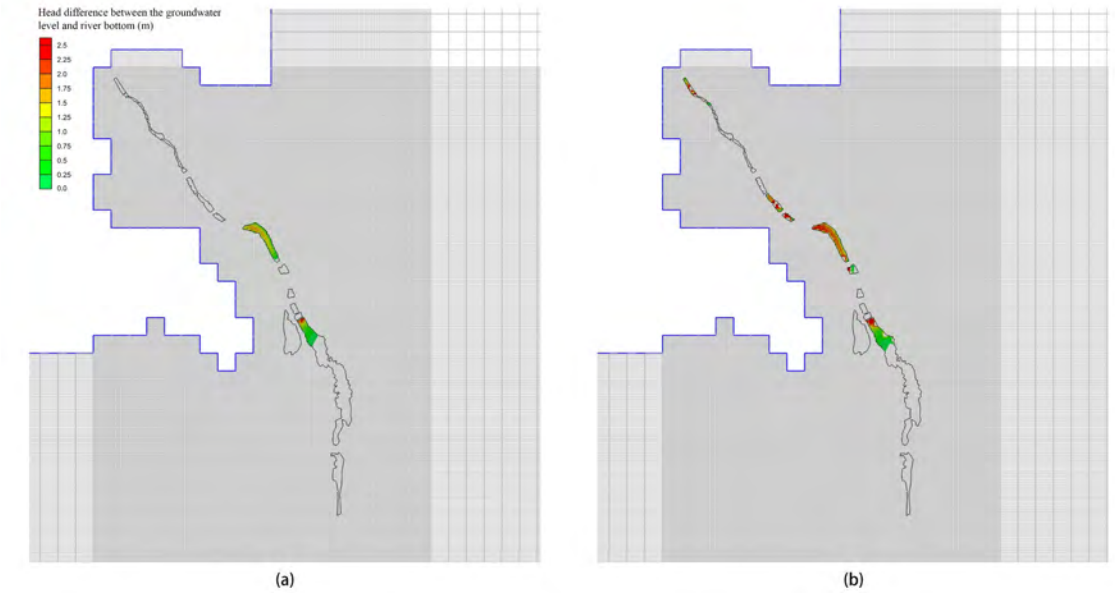

Figure D-4. Comparison of the mapping of the connected stream under the current riverbed permeability (a) and 1.5 higher river hydraulic conductance for all lakes (b).

APPENDIX E COMPARISON OF THE HISTORICAL PRECIPITATION AND THE RCM PREDICTED PRECIPITATION DATA

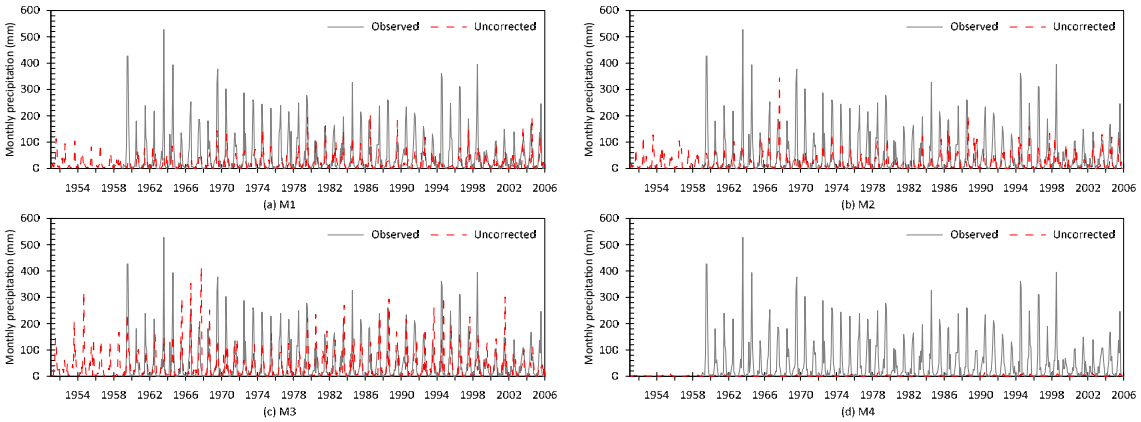

(a) Chaoyang Station

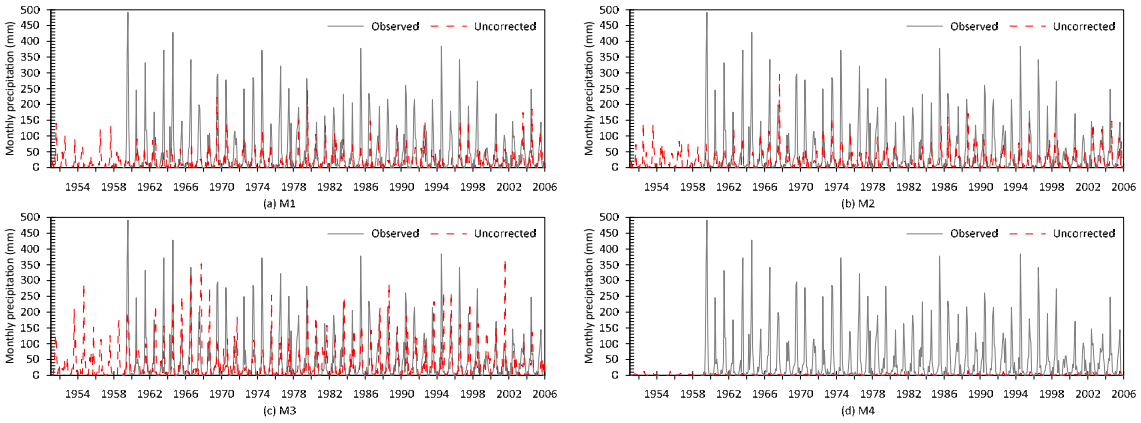

(b) Fengtai Station

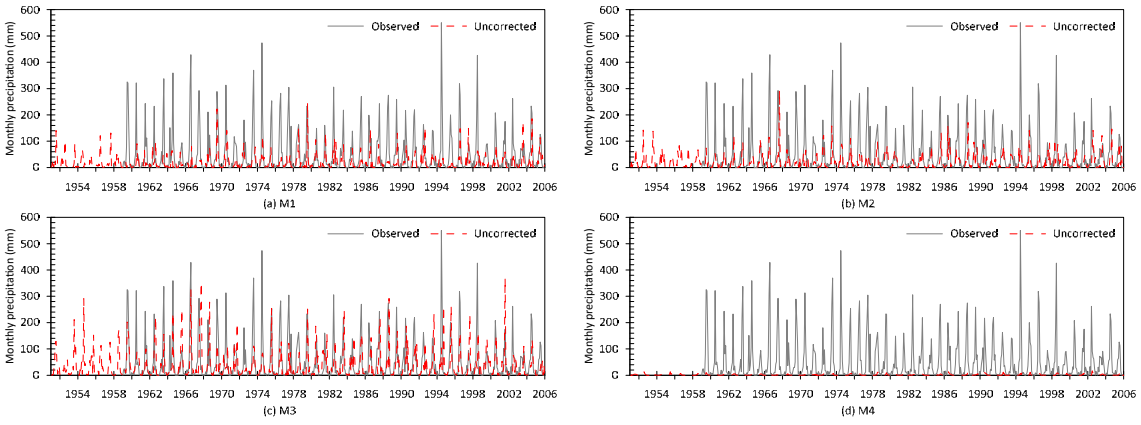

(c) Mentougou Station

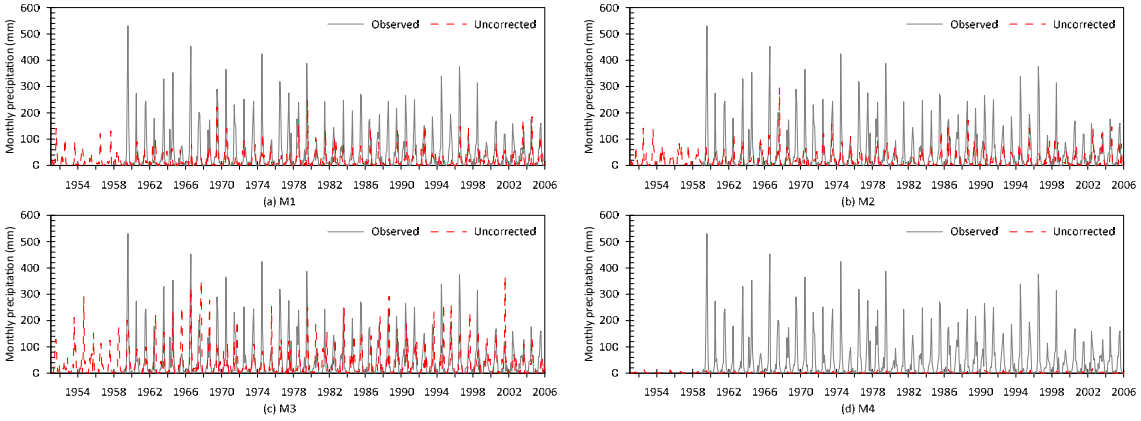

(d) Fangshan Station

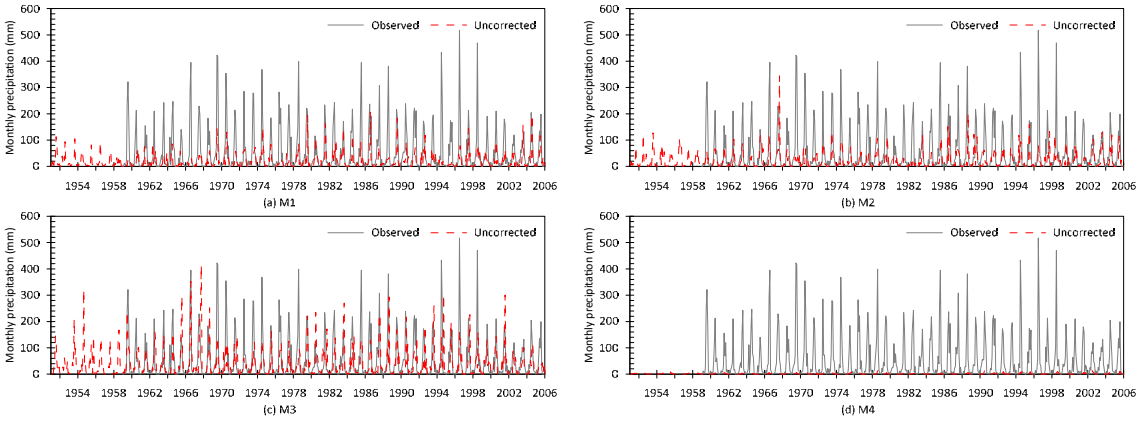

(e) Huairou Station

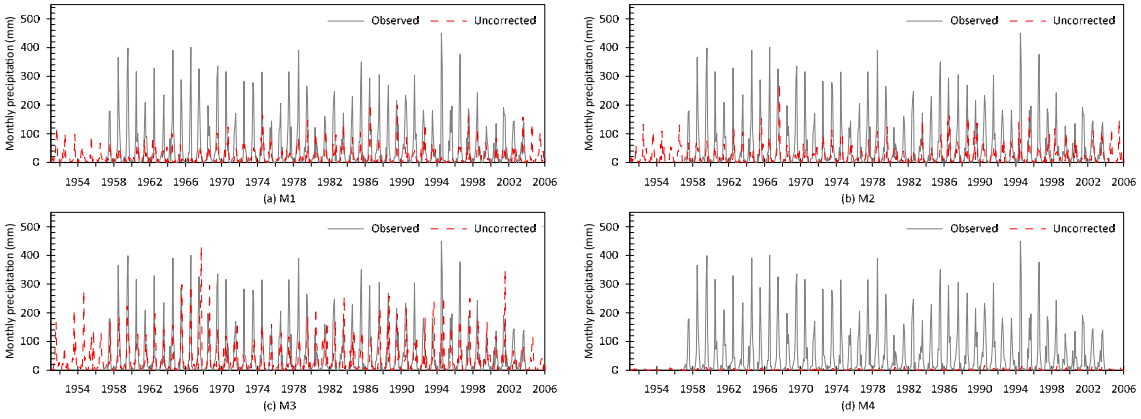

(f) Miyun Station

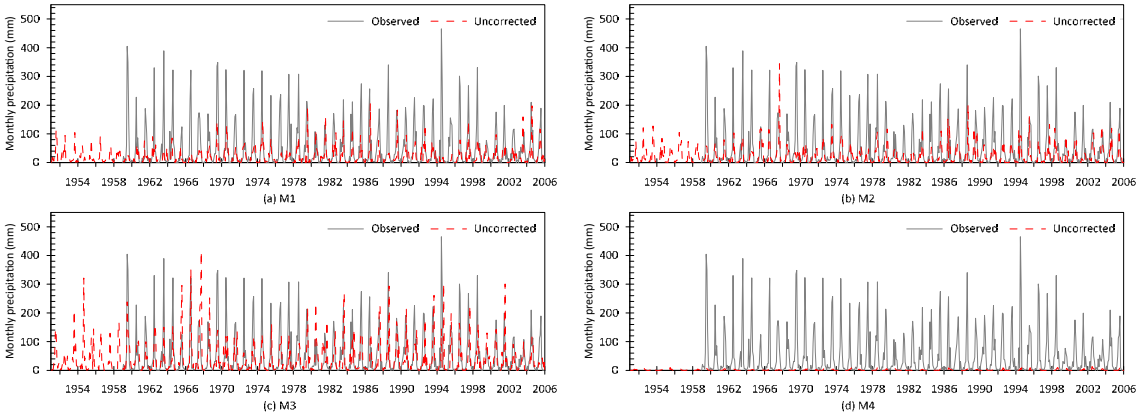

(f) Shunyi Station

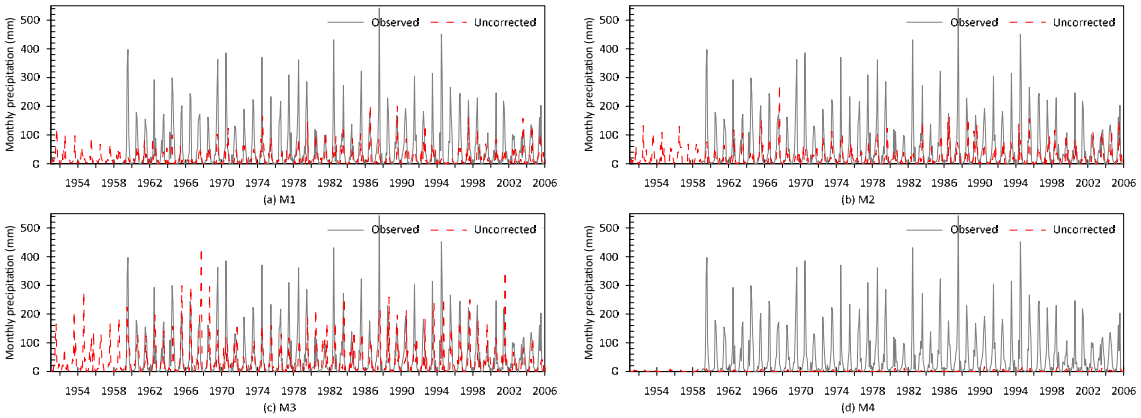

(g) Pinggu Station

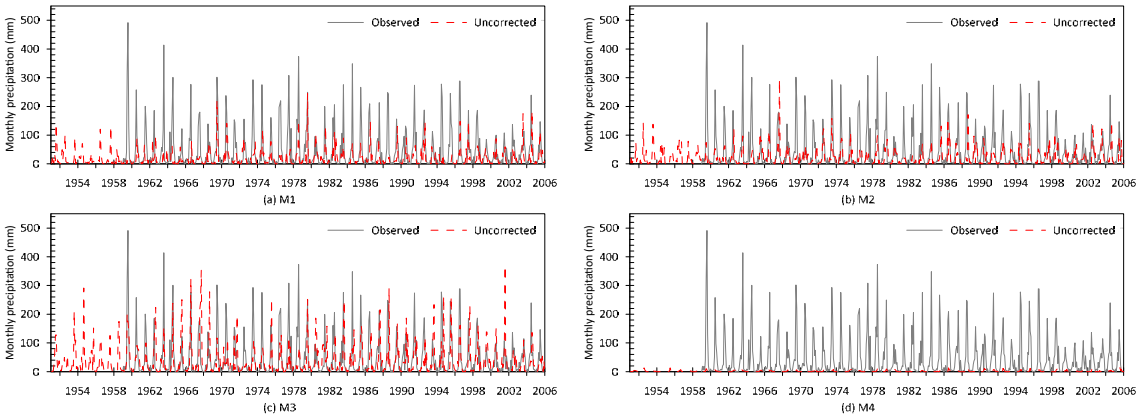

(h) Daxing Station

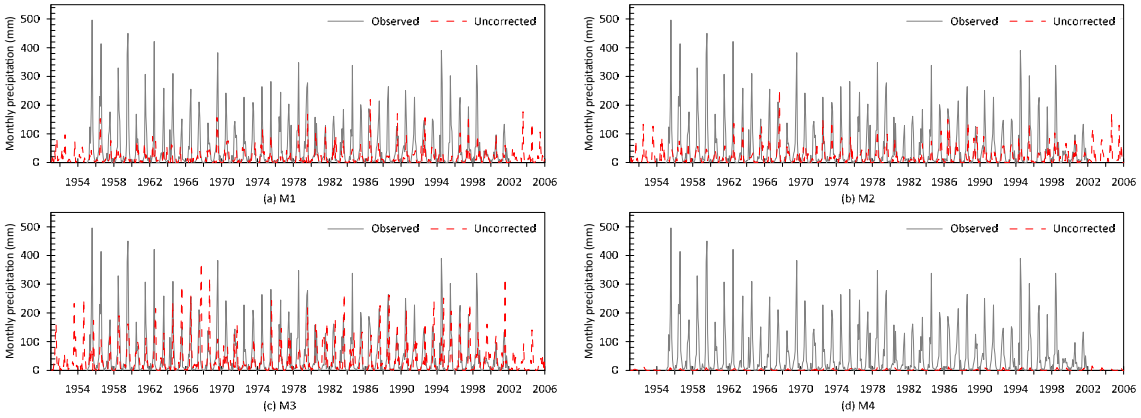

(i) Tongzhou Station

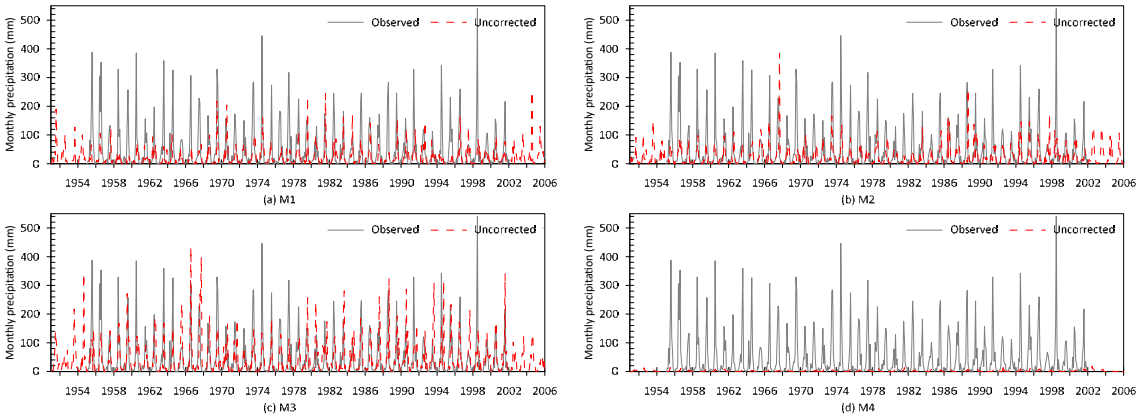

(j) Changping Station

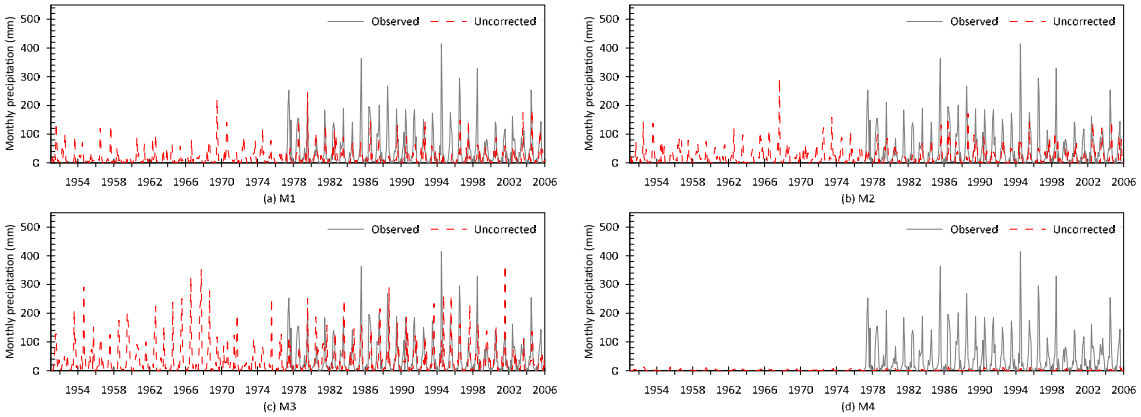

(k) Shijingshan Station

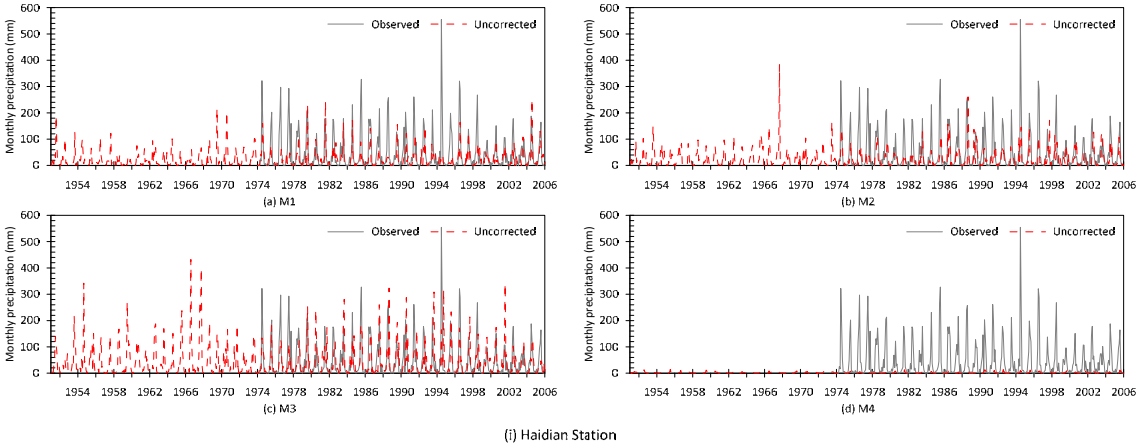

Figure E-1. Comparison of the monthly precipitation observed at each meteorological station and predicted by four RCM models.

APPENDIX F BIAS-CORRECTED PRECIPITATION DATA FOR EACH METEOROLOGICAL STATION

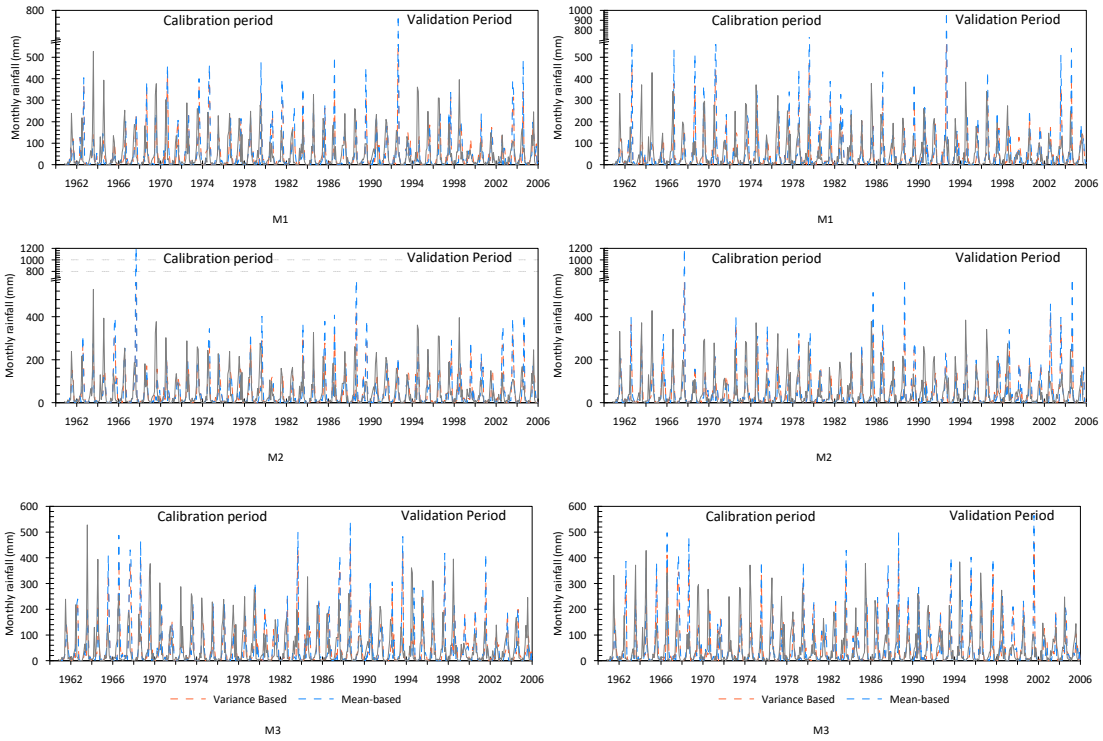

(a) Chaoyang Station

(b) Fengtai Station

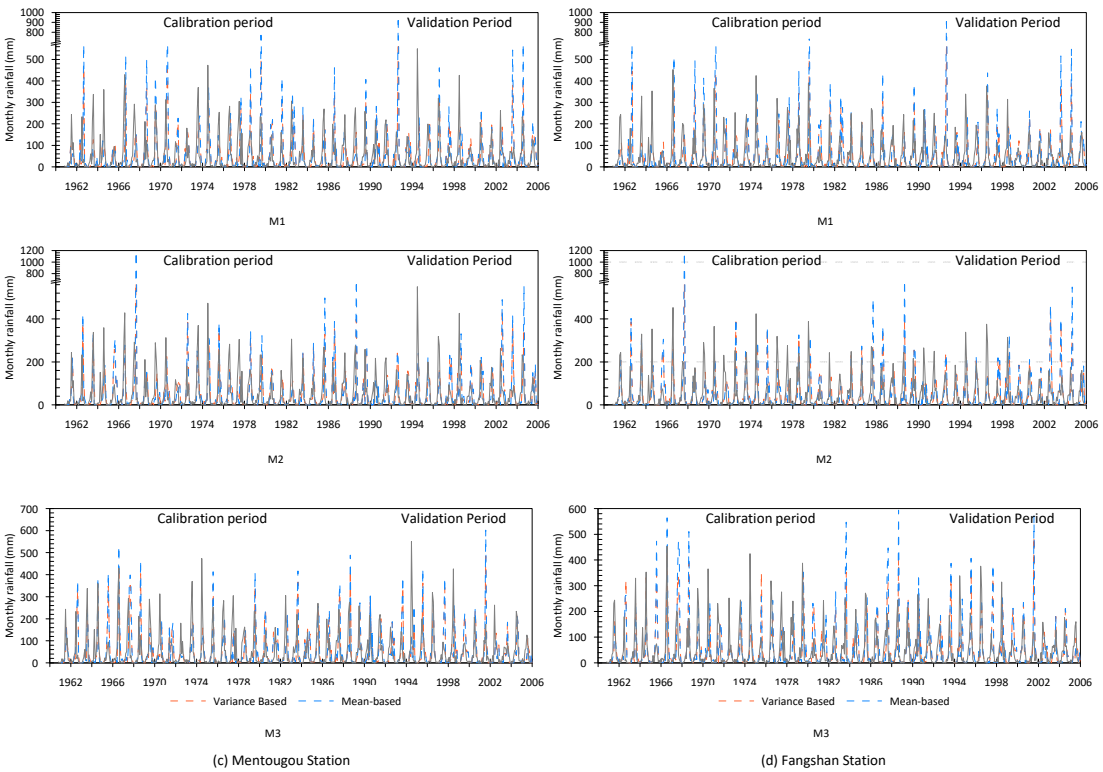

(c) Mentougou Station

(d) Fangshan Station

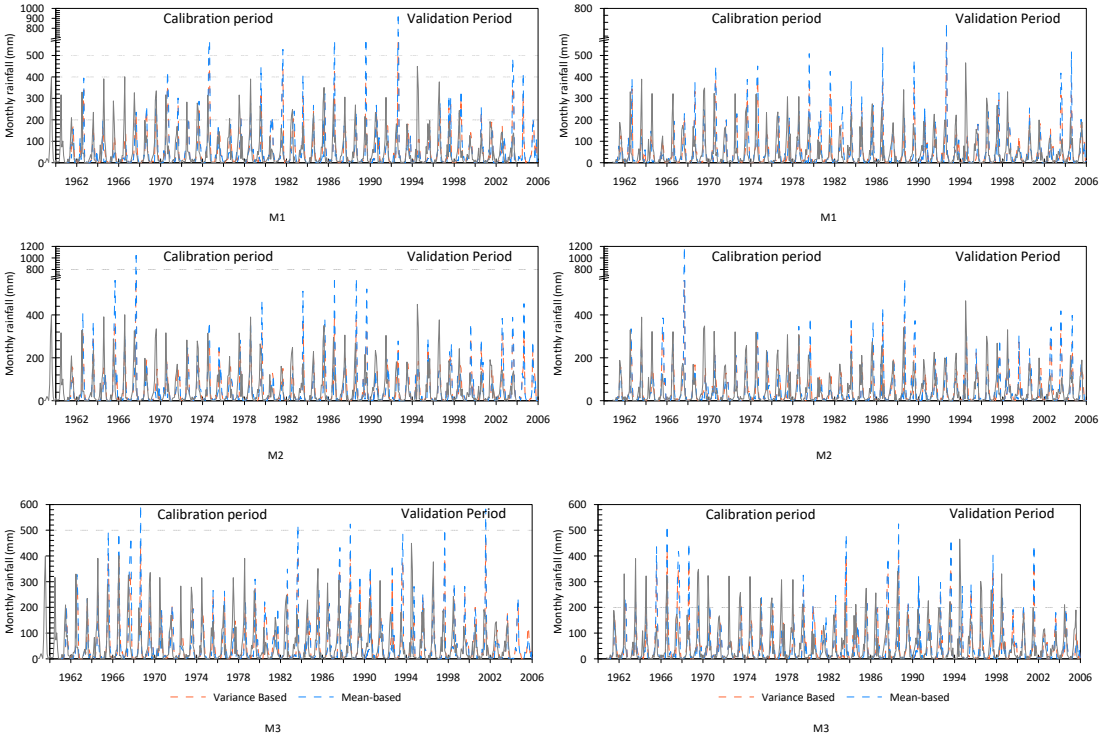

(e) Miyun Station

(f) Shunyi Station

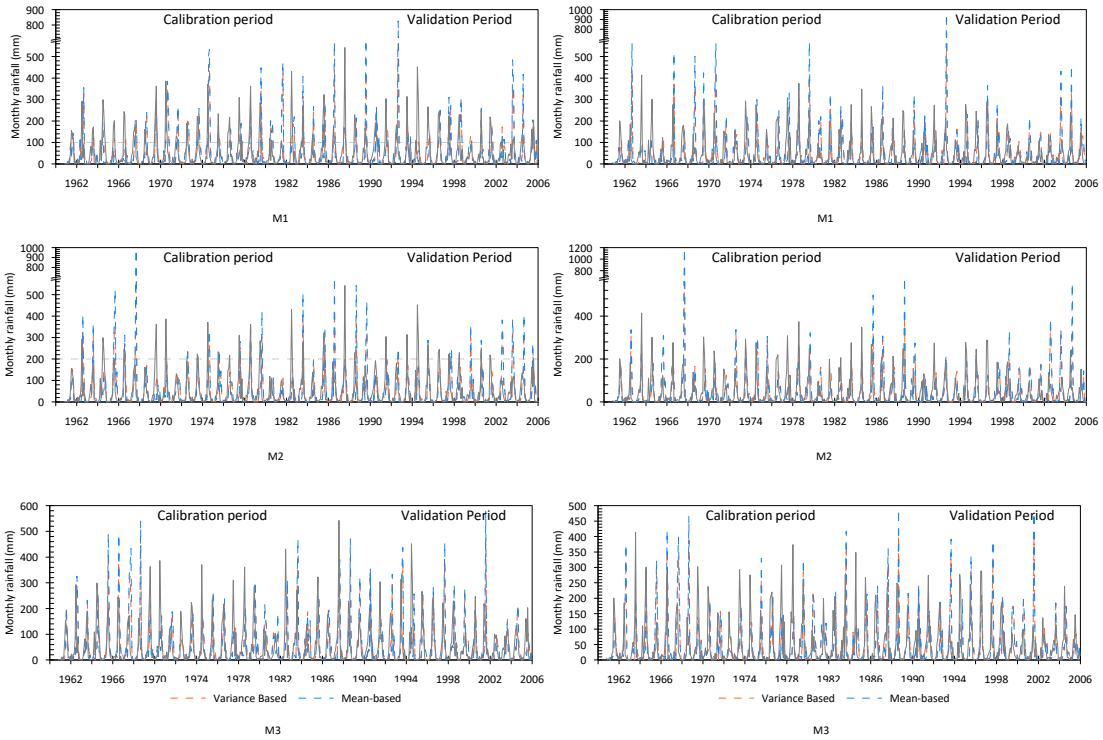

(g) Pinggu Station

(h) Daxing Station

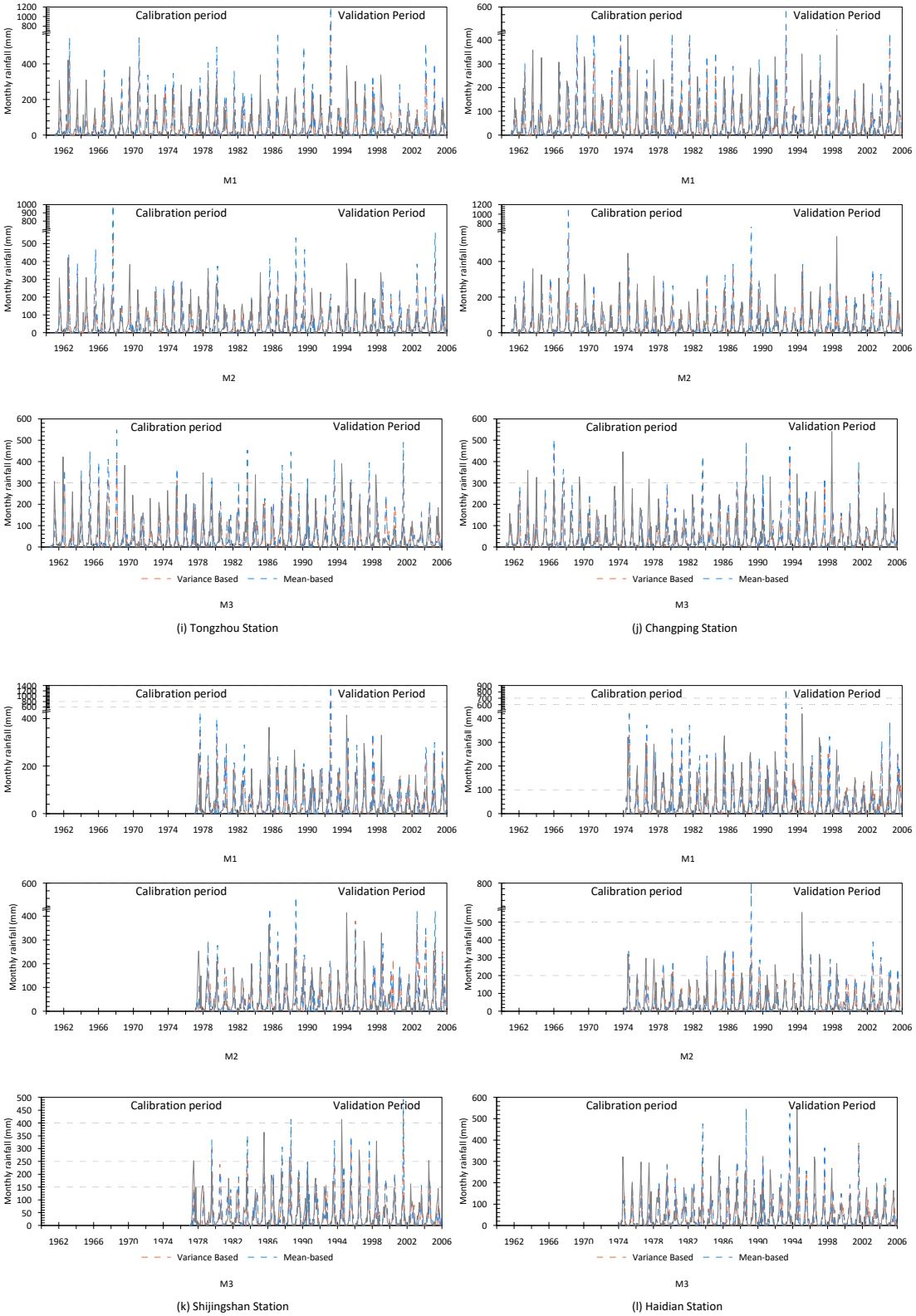

Figure F-1 Bias-corrected precipitation data for each meteorological station

Table F-1. Statistics of the differences between the observed and bias-corrected monthly precipitation for each station from the period of 1961-2005.

Chaoyang Station	Mean-based corrected precipitation (mm/month)		Variance-based corrected precipitation (mm/month)	
	Calibration	Validation	Calibration	Validation
Mean	1.00	1.12	-1.45	0.03
Median	1.53	1.84	1.03	1.44
Standard Deviation	58.57	50.52	62.54	56.19
Kurtosis	17.28	18.10	7.42	6.58
Skewness	-0.44	-1.68	-0.14	-0.12
Fengtai Station	Mean-based corrected precipitation (mm/month)		Variance-based corrected precipitation (mm/month)	
	Calibration	Validation	Calibration	Validation
Mean	0.95	1.04	2.11	2.93
Median	1.39	1.86	0.79	1.75
Standard Deviation	55.36	47.13	59.42	51.14
Kurtosis	9.04	7.27	9.23	5.84
Skewness	0.14	-0.73	0.69	0.16
Mentougou Station	Mean-based corrected precipitation (mm/month)		Variance-based corrected precipitation (mm/month)	
	Calibration	Validation	Calibration	Validation
Mean	0.27	0.36	2.80	3.46
Median	1.17	1.39	1.50	2.17
Standard Deviation	59.79	52.78	66.06	58.80
Kurtosis	6.17	4.92	17.59	15.95
Skewness	0.18	-0.31	-0.85	-1.41

Fangshan Station	Mean-based corrected precipitation (mm/month)		Variance-based corrected precipitation (mm/month)	
	Calibration	Validation	Calibration	Validation
Mean	0.92	0.98	2.68	3.46
Median	1.41	1.59	1.31	1.57
Standard Deviation	57.01	51.00	56.30	48.51
Kurtosis	8.22	6.70	8.04	5.57
Skewness	-0.19	-0.63	0.81	0.35
Huairou Station	Mean-based corrected precipitation (mm/month)		Variance-based corrected precipitation (mm/month)	
	Calibration	Validation	Calibration	Validation
Mean	0.50	0.55	-0.59	1.14
Median	1.05	1.23	1.51	2.09
Standard Deviation	59.06	49.52	67.51	59.72
Kurtosis	6.09	6.74	8.44	8.96
Skewness	0.15	-0.77	-0.45	-0.93
Miyun Station	Mean-based corrected precipitation (mm/month)		Variance-based corrected precipitation (mm/month)	
	Calibration	Validation	Calibration	Validation
Mean	-0.47	-0.43	-0.42	1.58
Median	0.80	1.18	1.27	1.64
Standard Deviation	69.87	56.13	65.55	55.66
Kurtosis	9.49	6.18	15.18	12.23
Skewness	0.63	-0.09	1.12	0.68
Shunyi Station	Mean-based corrected precipitation (mm/month)		Variance-based corrected precipitation (mm/month)	

	Calibration	Validation	Calibration	Validation
Mean	0.49	0.56	-1.71	-0.22
Median	1.29	1.43	1.21	1.63
Standard Deviation	58.09	49.16	58.63	51.39
Kurtosis	7.91	6.89	11.38	11.13
Skewness	0.36	-0.43	-0.47	-0.65
Pinggu Station	Mean-based corrected precipitation (mm/month)		Variance-based corrected precipitation (mm/month)	
	Calibration	Validation	Calibration	Validation
Mean	0.64	0.69	-1.05	0.58
Median	1.53	1.81	0.90	1.27
Standard Deviation	53.64	45.98	68.69	59.70
Kurtosis	8.40	7.37	10.97	9.80
Skewness	0.12	-0.81	-0.02	-0.07
Daxing Station	Mean-based corrected precipitation (mm/month)		Variance-based corrected precipitation (mm/month)	
	Calibration	Validation	Calibration	Validation
Mean	0.05	0.13	2.99	3.74
Median	1.62	1.94	1.25	1.78
Standard Deviation	52.98	45.87	53.73	47.50
Kurtosis	10.53	8.11	5.78	3.27
Skewness	-0.01	-0.96	0.64	0.28
Tongzhou Station	Mean-based corrected precipitation (mm/month)		Variance-based corrected precipitation (mm/month)	
	Calibration	Validation	Calibration	Validation

Mean	0.71	0.77	2.99	3.90
Median	1.38	2.00	1.84	1.81
Standard Deviation	51.02	43.28	65.95	55.77
Kurtosis	5.89	4.57	11.77	8.43
Skewness	0.02	-0.76	0.74	-0.09
Changping Station	Mean-based corrected precipitation (mm/month)		Variance-based corrected precipitation (mm/month)	
	Calibration	Validation	Calibration	Validation
Mean	-0.39	-0.31	1.04	2.29
Median	1.01	1.25	0.92	1.13
Standard Deviation	53.30	46.89	55.16	52.81
Kurtosis	10.58	9.93	12.59	14.52
Skewness	0.01	-0.94	-1.45	-1.72
Haidian Station	Mean-based corrected precipitation (mm/month)		Variance-based corrected precipitation (mm/month)	
	Calibration	Validation	Calibration	Validation
Mean	0.81	0.89	2.05	4.27
Median	1.09	1.04	1.58	2.35
Standard Deviation	55.38	49.41	60.22	56.74
Kurtosis	7.06	5.32	18.87	18.08
Skewness	-0.12	-0.68	-1.31	-2.00
Shijingshan Station	Mean-based corrected precipitation (mm/month)		Variance-based corrected precipitation (mm/month)	
	Calibration	Validation	Calibration	Validation
Mean	0.32	0.44	4.89	5.81

Median	0.82	1.22	2.97	2.77
Standard Deviation	54.40	49.35	55.37	49.06
Kurtosis	6.56	5.35	19.76	11.19
Skewness	-0.11	-0.62	1.25	-0.39

APPENDIX G GROUNDWATER CONTOUR MAP FOR PRCP85 MODEL

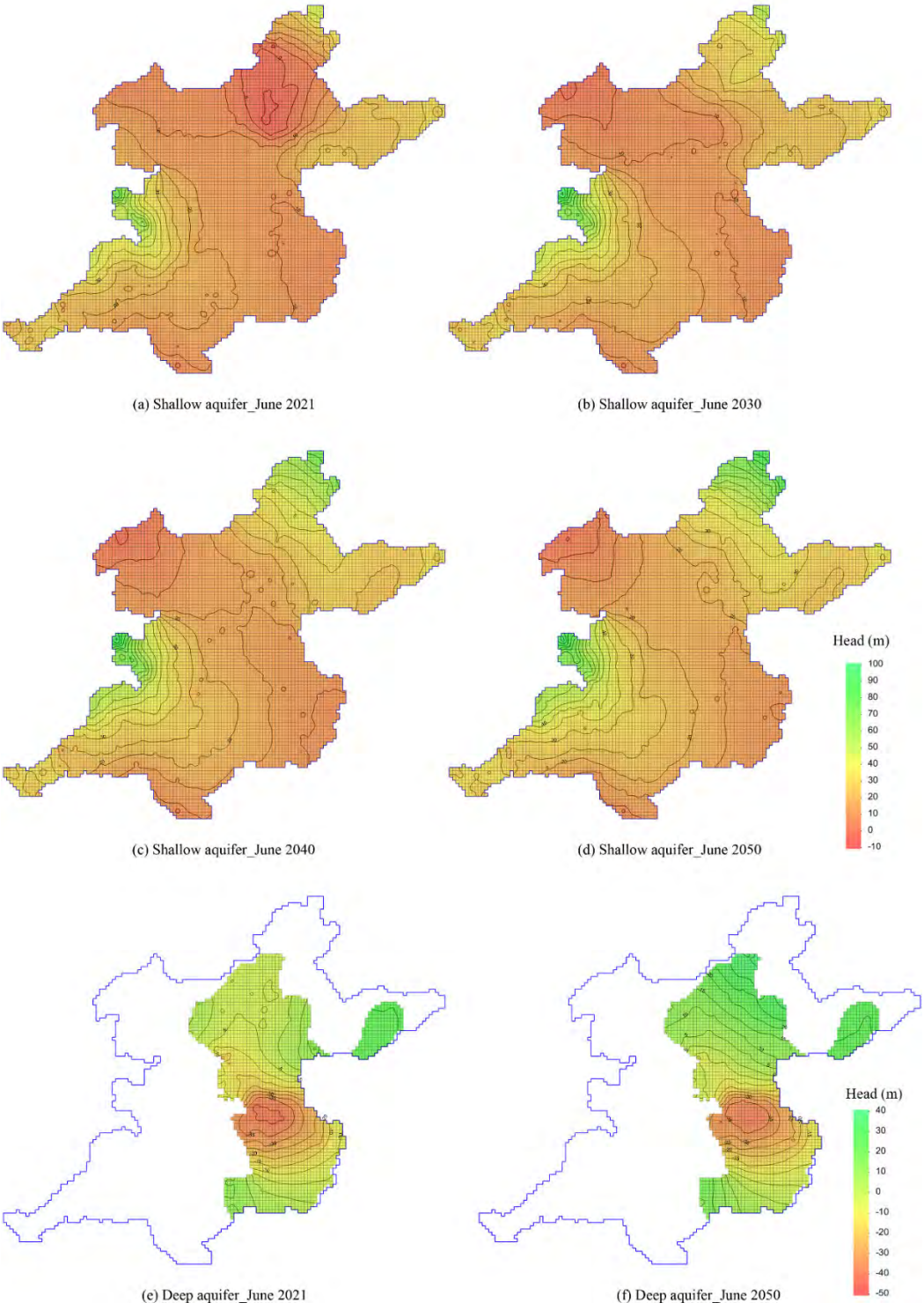

Figure G-1 Groundwater contour map for Prcp85 model

LIST OF ACRONYMS

3D	Three dimensional
AIC	Akaike information criteria
AICc	Corrected Akaike information criteria
AM1	Alternative Model 1
AM2	Alternative Model 2
AM3	Alternative Model 3
ASR	Aquifer Storage and Recovery
BIC	Bayesian Information Criterion
CCLM5-0-2	Climate Limited-area Modelling Community (CLM-Community) version 5-0-2
CGR	Conventional Grid Refinement
CMIP5	Coupled Model Intercomparison Project
CORDEX	Coordinated Regional Climate Downscaling Experiment
CSS	Composite scaled sensitivity
DEM	Digital Elevation Model
DSS	Dimensionless scaled sensitivity
EFR	Environmental Flow Release
ET	Evaporation
EVT	Evapotranspiration package of MODFLOW
GCM	General Circulation Model

GHB	General Head Boundary package of MODFLOW
GLUE	Generalized Likelihood Uncertain Estimation
GMS	Groundwater Modelling System
GUI	Graphic User Interface
IC	Information Criteria
IGRAC	International Groundwater Resources Assessment Center
IPCC	Intergovernmental Panel on Climate Change
Kh	Horizontal hydraulic conductivity
KIC	Kashyap Information Criterion
Kv	Vertical hydraulic conductivity
LGR	Local Grid Refinement
LPF	Layer Property Flow package of MODFLOW
MAR	Managed Aquifer Recharge
ME	Mean error
MOC	Method of Characteristics
MODFLOW	Modular Finite-Difference Flow Model
MODPATH	A Particle-Tracking Model for MODFLOW
Mod-PATH3DU	Particle tracking code for calculating the three-dimensional flow pathlines of purely advective solute particles
MT3DMS	Modular Three-Dimensional Multispecies Transport Model
NCP	North China Plain
NPE	Number of process model parameters
Pav	Model with average historical precipitation input

PEST	Model-Independent Parameter Estimation and Uncertainty Analysis
PHT3D	A reactive multicomponent transport model for saturated porous media
Prcp45	Model with precipitation input projected under RCP 4.5 scenario
Prcp85	Model with precipitation input projected under RCP 4.5 scenario
RCH	Recharge package of MODFLOW
RCM	Regional Climate Model
RCP	Representative Concentration Pathways
RIV	River package for MODFLOW
RMSE	Root mean squared errors
RT3D	Software package for simulating three-dimensional, multi-species, reactive transport of chemical compounds (solutes) in groundwater
S2N	South to North
SEAWAT	Computer Program for Simulation of Three-Dimensional Variable-Density Ground-Water Flow and Transport
SGMA	Sustainable Groundwater Management Act
SRF2	Streamflow-Routing Package of MODFLOW
SWSR	Sum of weighted squared residuals
TMR	Telescopic Mesh Refinement
UCODE	Computer code for universal inverse modeling
USG	Unstructured Grid

WCRP	World Climate Research Program
WEL	Well package of MODFLOW
ZONBUD	Zone Budget program

LIST OF TABLES

LIST OF FIGURES

ABOUT THE AUTHOR

Sida Liu was born in 1992 in Beijing, China. She obtained her B.Sc. in Groundwater Science and Engineering from the School of Water Resources and Environment at China University of Geoscience, Beijing, in 2014. Following her undergraduate studies, she pursued a master's degree in Hydrology and Water Resources in 2016 from the IHE Delft Institute for Water Education in the Netherlands. In 2017, Sida started on her doctoral research at the department of Water Resources and Ecosystems within the same institute. Her research specialization focused on the numerical modelling of Managed Aquifer Recharge systems.

Journals publications

Liu, S., Zhou, Y., Eiman, F., McClain, M. E., & Wang, X. S. (2024). Towards sustainable groundwater development with effective measures under future climate change in Beijing Plain, China. Journal of Hydrology, 130951.

Liu, S., Zhou, Y., Zang, Y., McClain, M. E., & Wang, X. S. (2023). Effects of downstream environmental flow release on enhancing the groundwater recharge and restoring the groundwater/surface-water connectivity in Yongding River, Beijing, China. Hydrogeology Journal, 1-17.

Li, J., Zhou, Y., Wang, W., **Liu, S**., Li, Y., & Wu, P. (2022). Response of hydrogeological processes in a regional groundwater system to environmental changes: A modeling study of Yinchuan Basin, China. Journal of Hydrology, 615, 128619.

Liu, S., Zhou, Y., Luo, W., Wang, F., McClain, M. E., & Wang, X. S. (2022). A numerical assessment on the managed aquifer recharge to achieve sustainable groundwater development in Chaobai River area, Beijing, China. Journal of Hydrology, 613, 128392.

Liu, S., Zhou, Y., Xie, M., McClain, M. E., & Wang, X. S. (2021). Comparative Assessment of Methods for Coupling Regional and Local Groundwater Flow Models: A Case Study in the Beijing Plain, China. Water, 13(16), 2229.

Liu, S., Zhou, Y., Tang, C., McClain, M., & Wang, X. S. (2021). Assessment of alternative groundwater flow models for Beijing Plain, China. Journal of Hydrology, 596, 126065.

Liu, S., Zhou, Y., Kamps, P., Smits, F., & Olsthoorn, T. (2019). Effect of temperature variations on the travel time of infiltrating water in the Amsterdam Water Supply Dunes (the Netherlands). Hydrogeology Journal, 27(6), 2199-2209.

Conference presentations and posters

Liu, S., Zhou, Y., Eiman, F., McClain, M., & Wang, X. S. (2023). Achieving Sustainable Groundwater Development with Effective Measures in Beijing Plain, China (No. EGU23-6556). Copernicus Meetings. [poster presentation]

Liu, S., Zhou, Y., Zang, Y., McClain, M. E., Enhancing groundwater recharge while maintaining environmental flow in the Yongding River, Beijing, China, International Conference "Groundwater, key to the Sustainable Development Goals". Paris, May 18-20th, 2022 [oral presentation]

Liu, S., Zhou, Y., Tang, C., McClain, M. E., Evaluation of two alternative groundwater flow models for Beijing Plain, China, 47th IAH Congress, 2021, Brazil [oral presentation]

Netherlands Research School for the
Socio-Economic and Natural Sciences of the Environment

D I P L O M A

for specialised PhD training

The Netherlands research school for the
Socio-Economic and Natural Sciences of the Environment
(SENSE) declares that

Liu Sida

born on the 8th of June in Beijing, China

has successfully fulfilled all requirements of the
educational PhD programme of SENSE.

Delft, the 25th of April 2024

Chair of the SENSE board

Prof. dr. Martin Wassen

The SENSE Director

Prof. Philipp Pattberg

The SENSE Research School has been accredited by the Royal Netherlands Academy of Arts and Sciences (KNAW)

KONINKLIJKE NEDERLANDSE
AKADEMIE VAN WETENSCHAPPEN

The SENSE Research School declares that **Liu Sida** has successfully fulfilled all requirements of the educational PhD programme of SENSE with a work load of 35,7 EC, including the following activities:

SENSE PhD Courses

- Environmental research in context (2017)
- Research in context activity: IHE Delft PhD symposium (2019)

Other PhD and Advanced MSc Courses

- Visual methods for water communication, IHE Delft (2018)
- Bayesian Statistics: from concept to data analysis, University of California (2019)
- MODFLOW 6 and FloPy, Australian Water School, Australia (2022)
- PhD Start-up course, TU Delft (2017)
- Scientific text processing with LaTeX, TU Delft (2017)
- Problem-solving & decision making in research, TU Delft (2017)
- Becoming a Creative Researcher in Academia, TU Delft (2017)
- Making an impact with Open Science, TU Delft (2017)
- Speedreading and mind mapping, TU Delft (2017)
- Achieving your goals and performing successfully in your PhD, TU Delft (2017)
- Using creativity to maximize productivity and innovation in your PhD, TU Delft (2017)
- Self-Presentation 2: storyline structure and presentation slides, TU Delft (2017)

Management and Didactic Skills Training

- Supervising MSc student with thesis entitled 'Assessment of Managed Aquifer Recharge Scheme in Chaobai River, Beijing, China '(2021)

Oral Presentations

- *Multi-Modeling of Managed Aquifer Recharge (MAR) System*. IHE Delft PhD symposium, 2-3 October 2017, Delft, The Netherlands
- *Enhancing groundwater recharge while maintaining environmental flow in the Yongding River, Beijing, China.* Groundwater, key to the sustainable development goals Paris 2022, 19 May 2022, Paris, France
- *Evaluation of alternative groundwater flow models for Beijing Plain, China.* 47th IAH Congress Brazil 2021, 22 August 2021, Online
- *Yongding River Catchment, China - Assessing the impact of Managed Aquifer Recharge on the groundwater system by numerical modelling.* IHE Delft Alumni Online Seminar on Groundwater, 14 March 2022, Online
- *Achieving Sustainable Groundwater Development with Effective Measures in Beijing Plain, China.* EGU General Assembly 2023, 28 April 2023, Vienna, Austria

SENSE coordinator PhD education

Dr. ir. Peter Vermeulen

IHE DELFT
Institute for Water Education
under the auspices of UNESCO

TU Delft Delft University of Technology

This study explores the challenge of groundwater depletion in the Beijing Plain, a problem exacerbated by rapid socio-economic expansion and unsustainable groundwater abstraction. The core of this research is the development and application of multi-scale numerical groundwater flow and transport models to rigorously evaluate the measures implemented by the Beijing municipality. These measures include the strategic reduction of groundwater abstraction and the adoption of innovative water management practices such as Managed Aquifer Recharge (MAR) and Environmental Flow Release (EFR) operations. Through the development of various hydrogeological conceptual models and a number of multi-scale flow and transport models, the study has successfully simulated groundwater storage depletion in the past and assessed the long-term sustainability of groundwater resources, taking into account the impact of current measures and future climate changes. The findings highlight the crucial role of MAR operations in restoring depleted groundwater storage in the shallow aquifer and the essential need for reducing abstraction in the deep confined aquifers. This research not only supports the sustainable groundwater management strategy in Beijing but also provides a valuable framework for other urban areas worldwide facing similar challenges of groundwater depletion.

This book is printed on paper from sustainably managed forests and controlled sources

9 789073 445598